ANALYTICA CHIMICA ACTA

International monthly devoted to all branches of analytical chemistry
Revue mensuelle internationale consacrée à tous les domaines de la chimie analytique
Internationale Monatsschrift fur alle Gebiete der analytischen Chemie

ELSEVIER SCIENTIFIC PUBLISHING COMPANY

AMSTERDAM

✓*Anal. Chim. Acta*, Vol. 74, No. 2, 225–466, February 1975

Published monthly

Completing Volume 74

Publication Schedule for 1975

Vol. **74**, No. **1**	January 1975	
Vol. **74**, No. **2**	February 1975	**(completing Vol. 74)**
Vol. **75**, No. **1**	March 1975	
Vol. **75**, No. **2**	April 1975	**(completing Vol. 75)**
Vol. **76**, No. **1**	May 1975	
Vol. **76**, No. **2**	June 1975	**(completing Vol. 76)**
Vol. **77**, No. **1**	July 1975	
Vol. **77**, No. **2**	August 1975	**(completing Vol. 77)**
Vol. **78**, No. **1**	September 1975	
Vol. **78**, No. **2**	October 1975	**(completing Vol. 78)**
Vol. **79**, No. **1**	November 1975	
Vol. **79**, No. **2**	December 1975	**(completing Vol. 79)**

Subscription price: Dfl. 570.00 plus Dfl. 54.00 postage; US$ 249.60 inclusive of postage. Subscribers in the U.S.A. and Canada receive their copies by airmail. Additional charges for airmail to other countries are available on request. For advertising rates apply to the publishers.

Subscriptions should be sent to:
Elsevier Scientific Publishing Company, P.O. Box 211, Amsterdam, The Netherlands.

GENERAL INFORMATION

Languages

Papers will be published in English, French or German.

Submission of papers

Papers should be sent to:

PROF. PHILIP W. WEST,
Coates Chemical Laboratories,
College of Chemistry and Physics,
Louisiana State University,
Baton Rouge 3,
La. 70803 (U.S.A.)

or to:

DR. A. M. G. MACDONALD,
Department of Chemistry,
The University,
P.O. Box 363
Birmingham B15 2TT (Great Britain)

Reprints

Fifty reprints will be supplied free of charge. Additional reprints (minimum 100) can be ordered at quoted prices. They must be ordered on order forms which are sent together with the proofs.

PRINTED IN THE NETHERLANDS

Inorganica Chimica Acta

Incorporating Inorganica Chimica Acta Rewiews

MONTHLY frequency provides rapid publication of contributions

LETTERS SECTION offers quick and concise information on important research developments in the field of inorganic chemistry

Scope of the Journal

Inorganica Chimica Acta, an international MONTHLY publication, provides a medium for original, high-level scientific contributions dealing with developments in inorganic chemistry from classic inorganic and coordination compounds to organometallic and bio-inorganic systems.

Subjects covered include

Synthesis, characterization and reactivity of coordination compounds

Synthesis and reactivity of organometallic compounds

Metals in biological systems

Metals in homogeneous catalysis

Metals in organic chemistry

Kinetics, reaction mechanisms, reaction intermediates and stereoselectivity

MO calculations — LCAO-CNDO — etc.

ESR, ESCA, NMR, PES and magnetic studies

Electron transfer, catalysis

Raman, IR, UV and CD spectra

X-ray and Neutron diffraction, Mössbauer spectra

Optimal Substance Separation with Pre-packed Columns

Analytica Chimica Acta, 74 (1975) 225–245

AUTOMATIC MULTI-SAMPLE SIMULTANEOUS MULTI-ELEMENT ANALYSIS WITH A H.F. PLASMA TORCH AND DIRECT READING SPECTROMETER

S. GREENFIELD, I. LL. JONES, H. MCD. MCGEACHIN and P. B. SMITH

Albright and Wilson Ltd., Industrial Chemicals Division, P.O. Box 80, Oldbury, Warley, West Midlands, B69 4LN (England)

(Received 12th August 1974)

The use of inductively coupled plasmas as excitation sources for trace metals was first reported by Greenfield *et al.*[1] in 1964. Shortly afterwards, Wendt and Fassel[2] reported their independent studies using the plasma. These two papers followed Reed's pioneering work[3] in this field of high-frequency plasma generation, although the credit for the original investigation into inductively coupled plasmas should go to Babat[4] who, in 1946, published a paper on electrodeless discharges in high-frequency magnetic fields.

Since 1964 a rapidly increasing volume of papers has appeared dealing with investigations into these plasmas. Most of these have been largely concerned with simple theoretical and experimental investigations of plasma parameters and some preliminary studies of the feasibility of plasmas as spectrochemical sources. Little has been published to indicate that the technique has progressed to the stage of being a routine analytical method of great versatility.

Since our first patent application[5] was made in 1963, a high-frequency plasma torch has been used, in these laboratories, with increasing success, for day to day analysis of a wide variety of sample types with greatly differing concentration ranges. Thus our experiences may be of value to those whose interests lie in practical analysis.

The general approach was to concentrate on those aspects of design necessary to produce a stable plasma which was easily started and would not be extinguished when an aerosol of high solute content was injected through it. Success has been such that only minor changes have been made to the system despite testing of many variations, some original and some following the suggestions of others.

For the last four years the system has been coupled to a 30-channel direct-reading spectrometer with fully automatic sequential sampling, exposure and read-out. The read-out is processed by an off-line computer. With this equipment simultaneous multi-element analysis can be done at both trace and assay levels on each exposure.

The equipment requires minimal setting up, and this may be done by relatively unskilled personnel, after which it requires no supervision, so that the operator is free to continue with sample preparation. This saving in manpower more than off-sets the cost of the equipment which, because of the direct-reading spectrometer, is high. In this laboratory, however, the plasma source

replaces two conventional source units which do not possess its precision and freedom from matrix effects, and the complete system has made redundant two atomic absorptiometers which do not possess its simultaneous multi-element facility.

In the sections which follow the equipment is described with comments on the aspects considered important, or otherwise. Finally, various examples of the equipment's versatility are given.

THE HIGH-FREQUENCY GENERATOR

The generator employed for analytical work is the Radyne Delapena plasma generator model RD150/H, of 15 kW output at 7 MHz, controlled by a Hirst 30 K.V.A. saturable reactor, Mk. Vl.B, and is shown schematically in Fig. 1. It is of the free running type where the basic frequency of the oscillator is fixed by the values of the components in the tank circuit. These in turn are modified by any changes in plasma impedance and in the coupling of the plasma to the work coil. A 2.4-KW, 36-MHz generator has also been used in experimental studies.

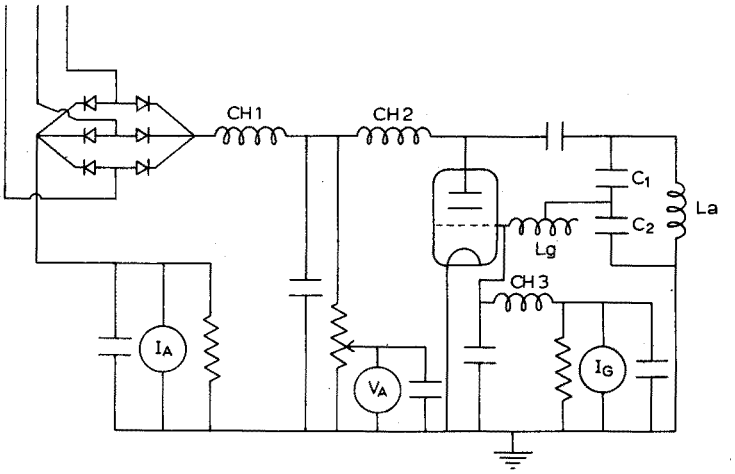

Fig. 1. Circuit diagram of the RD 150/H Generator. The three-phase supply comes from a saturable reactor.

A method[6] which used calorimetric measurements on a dummy load of copper and iron, gave results which indicated that the efficiency of power transfer is probably about 50%. The loads were altered until they gave readings of anode voltage, anode current and grid current which corresponded to values obtainable with a plasma. In view of the greatly different conductivities of metals and a plasma, it is possible that the value of 50% may not be very accurate for power transfer to a plasma.

The output part of the circuit of Fig. 1 can be simplified to that shown in Fig. 2. The resonant frequency f of the tuned circuit of Fig. 2 is given by

$$(2\pi f)^2 \simeq \omega^2 = \frac{1}{LC} - \frac{R^2}{L^2} \qquad (1)$$

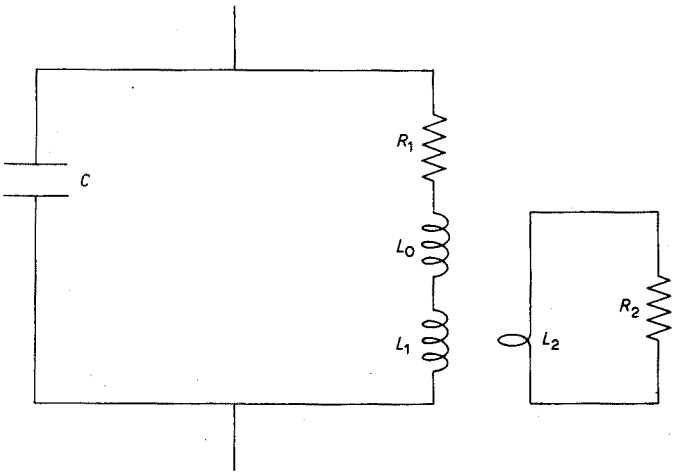

Fig. 2. Simplified anode circuit of the generator.

where L is the sum of the inductance of the work coil, L_1, and the residual inductance, L_0. In the circuit used $L=1$ H, corresponding to $L_1=0.32$ μH and $L_0=0.68$ μH, and $C=500$ pF so that $\omega^2=10^{12}(2000-R^2)$. However, R is unlikely to be greater than a few ohms (see below) so that the term in R^2 can be ignored, and therefore:

$$\omega^2 = 1/LC \tag{2}$$

The work coil (whose dimensions are length $l_1=1.3$ cm, and radius $b=1.875$ cm) can be considered as the primary of a transformer, the secondary of which is the plasma. The secondary can be thought of as a single turn, co-axial with the work coil, possessing inductance L_2 and resistance R_2. For the present purpose, it is assumed to be a cylinder of radius a and length l_2, and—arbitrarily but plausibly—its dazzlingly bright region, which is usually sharply defined, is used to estimate the dimensions of the electrically conducting part. The formula, applicable for a long solenoid with N turns, $L=(4\pi^2a^2N^2/l)\cdot 10^{-9}$ H, is used to give an order of magnitude for the inductance; for a single turn and $l_2=2$ cm, the inductive component of the impedance is found to be $\omega L_2=0.88\ a^2$ ohm. The resistance is estimated by considering an annulus of outer radius a and thickness d, and d is assumed to be the skin depth (*i.e.* the distance in which the induced current is reduced to $1/e^{\text{th}}$ of its surface value). The length of the current path has a mean value which can be approximated by $2\pi a$ and the cross-section is $l_2 d$. Then $R_2=2\pi a/\sigma l_2 d$ where σ is the conductivity of the plasma. Since $d=10^5/2\pi\sqrt{10f\sigma}$ cm at frequency f, the resistance $R_2=(4\pi^2 a/l_2\sqrt{10f/\sigma})\cdot 10^{-5}$ ohm, and the ratio x of the resistive to the inductive component of the impedance is given by

$$x = \frac{R_2}{\omega L_2} \approx \frac{10^4}{2a\sqrt{f\sigma}} \tag{3}$$

For an argon plasma at 10000°K, $\sigma\approx 30$ mho/cm. For the system at this temperature, $R_2\approx 0.3\ a$ ohm. For a radius of 1 cm, the ratio x is about 0.34, and

it should be noted for subsequent use that R_2 is not negligible in comparison with ωL_2.

If the impedance of the primary of a transformer is Z_1 when the secondary is open-circuited, its effective impedance Z when that of the secondary is Z_2 is given by $Z=Z_1+\omega^2M^2/Z_2$, where M is the mutual inductance.

Thus

$$Z = R_1+j\omega L_1 + \frac{\omega^2M^2}{R_2+j\omega L_2}$$

R_1, the inherent resistance of the primary is usually negligible. Then

$$Z = \frac{\omega^2M^2R_2}{R_2^2+\omega^2L_2^2} + j\omega L_1\left(1-\frac{\omega^2M^2L_2/L_1}{R_2^2+\omega^2L_2^2}\right)$$

From the definition of mutual inductance as the number of flux linkages produced in one winding of N_2 turns by unit current in the other, of N_1 turns and length l_1, we can take as an approximation $M=(4\pi^2a^2N_1N_2/l_1)\cdot 10^{-9}$ H. Then if the radius of the coil is b and $N_2=1$,

$$Z = \frac{R_2N_1^2}{1+x^2}\cdot\frac{l_2^2}{l_1^2} + j\omega L_1\left(1-\frac{a^2/b^2}{1+x^2}\cdot\frac{l_2}{l_1}\right) \tag{4}$$

and if the values suggested above are used, for a radius of 1 cm the effective resistance R of the primary is about $0.6N_1^2$. In these applications N_1 is typically 2 or 3, giving estimates for R of 2.4 or 5.4 ohm; this is the justification for ignoring the term R^2/L^2 in eqn. (1).

The resultant inductance can be estimated from eqn. (4). The coarsest approximation (I), which might be reasonable for a metal cylinder in a long coil, is to take $L_1'=L_1(1-l_2a^2/l_1b^2)$. However, R_2 is not negligible in comparison with ωL_2 (see above); the next approximation (II) is to assume that frequency and conductivity remain constant, and to use eqn. (3) to estimate the denominator in eqn. (4). The values of inductance obtained can be added to L_0 to calculate the resonant frequencies of the primary circuit for different plasma radii, and these can be compared with experimental values obtained with a digital frequency meter. The results are shown in Fig. 3 and it is seen that neither approximation is satisfactory; since both come from formulae which are appropriate for very long coils, this is hardly surprising.

The effect on inductance of surrounding a short coil by a cylindrical conducting screen has been investigated by Bogle[7]. His semi-empirical findings were applied to our system where the conducting cylinder (the plasma) is now inside the coil. There are again two approximations, the validity of the simpler depending on $R_2 \ll \omega L_2$ as before. Bogle's simpler expression is

$$\frac{\Delta L_1}{L_1} = \frac{l_1/g}{l_1/g+1.55}\cdot\frac{b^2}{a^2}$$

where l_1 is the length of the coil (in our case 1.3 cm), a the radius of the screen, b the radius of the coil (1.875 cm) and g their separation $(a-b)$. This can be re-written

$$\frac{\Delta L_1}{L_1} = \frac{1}{a^2/b^2[1+1.55c(a/b-1)]}$$

where c is the ratio of the radius of the coil to its length. For present purposes a and b can be interchanged since the cylinder, being inside the coil, has the smaller radius; the formula then becomes:

$$\frac{\Delta L_1}{L_1} = \frac{1}{(b^2/a^2)[1+1.55c(b/a-1)]}$$

This expression, which is a function only of the dimensions of coil and plasma, and in particular is independent of the plasma conductivity, is not expected to be valid unless $x^2 \ll 1$ which, as has been seen, is not the case for our plasma. The correction is, as before, to divide $\Delta L_1/L_1$ by $1+x^2$. The ratio x is a function of frequency and conductivity; in applying the correction we have taken both to be constant although the frequency must change with the inductance. The error introduced is not likely to be large.

The curves given by Bogle's formula are also plotted (III, IV) in Fig. 3. The agreement between the experimental points and the curve corrected for con-

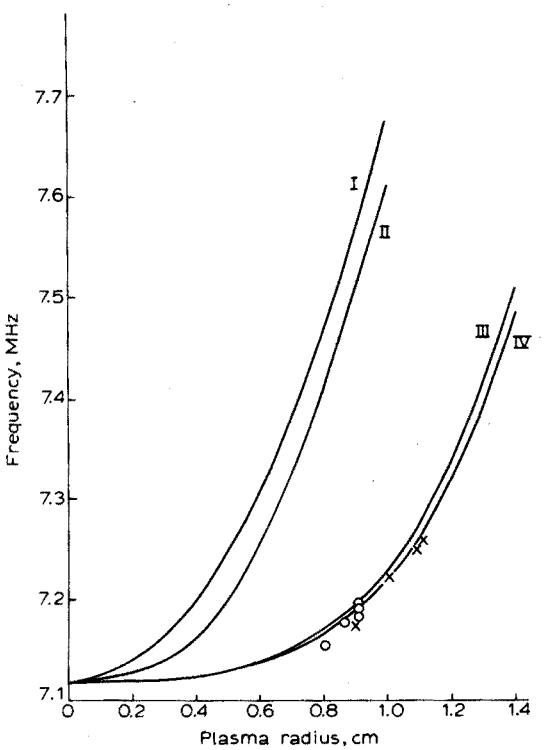

Fig. 3. Dependence of frequency on plasma radius a. I and II are calculated from the simplest formula appropriate for a long coil. III and IV are calculated from Bogle's formula. II and IV incorporate corrections for the conductivity of the plasma. Experimental points are shown, with argon (○) and nitrogen (×) as the outer gas stream.

ductivity is very good. This suggests that the approach is valid and that, since Bogle's curves lie close together, the frequency is not very sensitive to variations in conductivity even when the criterion $x^2 \ll 1$ is not fulfilled.

Although it is not negligible, the resistance of the plasma remains at least very nearly constant under the usual working conditions. This is inferred from the experimental fact that the great majority of calibration curves proved to be linear, so that the temperature can be assumed to remain constant when test materials are introduced in different amounts. The most likely way to achieve this is by the dissipation of constant power, which in turn implies the likelihood of constant resistance. To obtain linear calibrations would require fortuitous cancellation of different effects if the resistance of the plasma were not very nearly constant. The reason for this constancy may be the great dilution of the test materials in the plasma gas or that they may concentrate in the central channel of the plasma while the electrical coupling is concentrated in the outside skin depth.

Since variations in conductivity are expected to be small, and since frequency changes should be insensitive to changes in conductivity, changes in frequency due to the introduction of samples of different kinds should be small, provided that the plasma radius does not change. This was confirmed by measurements with a digital frequency meter when aerosols of concentrated hydrochloric, perchloric, sulphuric and nitric acids, of 50% phosphoric acid and of acetic acid were supplied to the plasma at powers of 5.5 KW and 2 KW. The changes in frequency from the nominal value of 7 MHz at the high power were all less than 1 KHz, and at low power less than 1.5 KHz, except with acetic acid when a change of 7.3 KHz was observed. This larger change is typical of those found with organic solvents, which make the plasma appear more diffuse, and its radius difficult to define. It is possible, therefore, that the large change is due to a change in radius. Another

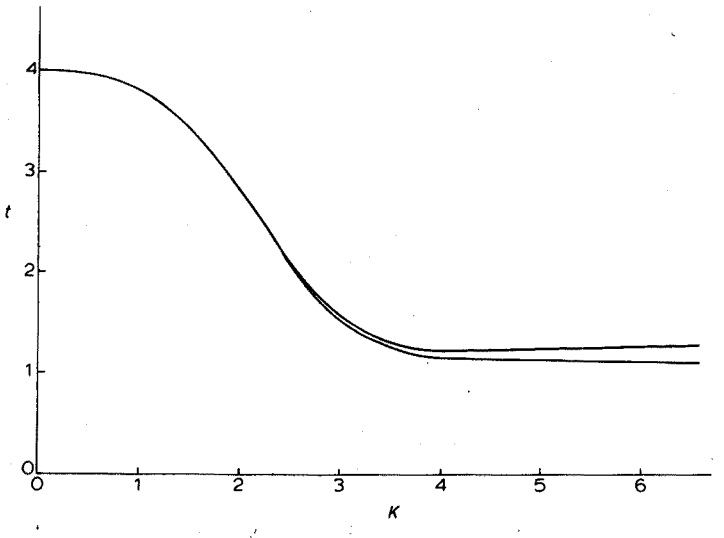

Fig. 4. The exponent t in the relation between power P and plasma radius a, $P \propto a^t$, plotted as a function of the coupling parameter K. The upper curve is for a system where the frequency is allowed to float, the lower for a fixed-frequency system.

possible explanation is that the low surface tension of organic solvents changes the flow paths taken by the particles of the aerosol from the injector, and that the vapours may penetrate the outer part of the plasma more than aqueous aerosols, causing a larger change in electrical conductivity in the outer region. The largest frequency change of all, about 100 KHz, occurs when the discharge is started.

With a free running oscillator there are no problems of tuning, since the oscillations will follow the resonant frequency of the only tuned circuit. However, the power delivered to the plasma is a function of frequency[8],

$$P = AI^2a^2\omega Q \tag{5}$$

where P is the power dissipated per unit length, A is a constant, I the current in the work coil, a the plasma radius and Q a flux integral which can be evaluated as a function of K, a coupling parameter defined by $K = a(\mu_0\sigma\omega)^{\frac{1}{2}}$ where σ is the conductivity and $\mu_0(=4\pi\cdot 10^{-9})$ the permeability of free space. If we take $\sigma = 30$ mho/cm, $f = 7$ MHz, and a in the range 0.7–1.0 cm, K has values in the range 3–4.

If a and I are constant, but ω is allowed to change, perhaps by variations in plasma conductivity,

$$\frac{dP}{P} = \frac{d\omega}{\omega} + \frac{dQ}{Q} = \frac{d\omega}{\omega}\left(1 + \frac{\omega}{Q}\cdot\frac{dK}{d\omega}\cdot\frac{dQ}{dK}\right)$$

$$= \frac{d\omega}{\omega}\left(1 + \frac{1}{2}\cdot\frac{K}{Q}\cdot\frac{dQ}{dK}\right) = \frac{s\,d\omega}{\omega}$$

This implies that the power dissipated is proportional to the s^{th} power of the frequency; s is not a constant, but varies with K. From calculations of Q and dQ/dK, it has been found that s varies from 2 to 0.5. The latter value is obtained for values of $K > 8$, and hence for large values of a, σ or ω, and corresponds to the approximation $P \propto \omega^{\frac{1}{2}}$ frequently used in calculations of induction heating in metals. In Fig. 4, the lower curve shows $2s$ as a function of K; for the type of plasma used, s is expected to lie in the range 0.6–0.8; in no case can it exceed 2. With the frequency changes under usual conditions being perhaps 0.01%, power fluctuations of not more than 0.02% are therefore expected if the plasma radius and coil current are constant.

Suppose now the plasma radius a varies but that I is held constant. This causes variations in inductance and hence in frequency (much larger than those due to variable conductivity which we can now ignore), in K (through both a and ω) and hence in Q. From eqn. (5)

$$\frac{dP}{P} = \frac{2da}{a} + \frac{d\omega}{\omega} + \frac{dQ}{Q}$$

If the relations $\omega = 1/(LC)^{\frac{1}{2}}$ and $L = L_0 + L_1\,(1 - a^2/b^2)$, are used then:

$$\frac{dP}{P} = \left[2 + \frac{1}{(b^2/a^2)(L_0/L_1 + 1) - 1}\right] s\cdot\frac{da}{a} = t\cdot\frac{da}{a}$$

where, again $s = 1 + \frac{1}{2}\cdot K/Q\cdot dQ/dK$

In the system used, b, the radius of the work coil, is 1.85 cm, L_0 is 0.68 μH, and L_1 is 0.32 μH. The plasma radius usually lies in the range 0.7 cm to 1.0 cm. Under these conditions, the term in brackets takes values from 2.05 to 2.10, so that the second term in the brackets has comparatively little effect; the small value of this term is the justification for using a poor approximation for L. This term arises through variations in frequency; if the frequency is held constant it vanishes so that $t=2s$. Values of t are plotted as a function of K in Fig. 4 for both the cases of constant frequency, and floating frequency for the typical values of the system; the differences for the relevant range of K (roughly 3 to 4) are seen to be small.

This means that the advantage of a fixed frequency over a floating frequency is only marginal if the plasma radius varies but the current in the work coil is constant. This advantage would be gained by using a crystal-controlled oscillator. However, since a change in plasma radius alters the effective inductance of the coil, the resonant circuit will no longer be tuned to the frequency of the crystal, and this mistuning will cause changes in the current in the coil. The magnitude of these changes depends on the circuit parameters, but the resulting fluctuations in power are likely to outweigh the small improvement gained. It is for this reason that a free-running oscillator is preferred.

POWER AND FREQUENCY

There are four advantages to be gained by working with a fairly high power, at least 5 KW dissipated in the plasma; these are greater sensitivity, frequent improvement in precision, elimination of band spectra, and elimination of chemical interferences.

The intensity of a line is proportional to the number of atoms excited to the appropriate upper level, and this is given by Boltzmann's equation if local thermodynamic equilibrium (L.T.E.) is assumed,

$$\frac{N_i}{N} = \frac{g_i}{Z(T)} \exp\left[-\frac{E_i}{kT}\right]$$

where N_i/N is the fraction of the atoms of the given element in the i^{th} excited state, whose energy is E_i and whose statistical weight is g_i. $Z(T)$ is the partition function for the element, and increases continuously with temperature T, while the exponential term approaches unity as T becomes large. N_i therefore increases with T only up to a certain value (called the norm temperature by German writers) and then decreases. A norm temperature also exists even if the plasma is not in L.T.E. Provided, therefore, that the temperature of the source is less than the norm temperature (which for most lines exceeds 10000°K), the sensitivity will increase with temperature and so with power. This has been confirmed in practice[9]. The advantage of greater sensitivity can be utilized in two ways: a line with a high excitation energy or low transition probability, which might be unobservable at low power, can be measured; alternatively, an acceptably large signal can be obtained without excessive amplification for a more easily excited line. This second case frequently leads to improved precision, particularly if obsolescent electronics have to be used as they are in the present case.

Molecules and radicals give rise to band spectra which can result in high and troublesome backgrounds. Analyte atoms can take part in the formation of refractory radicals, giving rise to chemical interferences so that the intensity of an analyte line is not independent of the composition of the sample matrix. A sufficiently high gas temperature will ensure that dissociation is complete so that both these effects are eliminated. However, a very high temperature will cause a high background of continuum radiation (bremsstrahlung and recombination radiation) which is associated with high electron density; the dazzling appearance of the plasma fireball is due to this. The background falls off very quickly with distance from the fireball. In practice, the part of the tail-flame used as a source for spectral analysis is fairly free from continuum radiation and, in addition, chemical interferences and most band spectra appear to be absent. Thus it seems possible in practice to find positions in the tail-flame which are cool enough for the continuum to be tolerably low, but yet hot enough, or sufficiently close to a hot enough region upstream, for the recombination of atoms into radicals to be frequently negligible. However, this is only possible when a fairly high power is available, for gas temperatures of perhaps 10000°K and upwards may be required in the fireball to ensure dissociation.

It is not easy to predict with confidence the optimal frequency at which to work. At low frequencies the skin depth is large so that the power is dissipated over a large volume; a high-power generator is therefore required to maintain the discharge. At high frequencies the plasma can be maintained by a generator of lower power. However, as indicated above, there are significant advantages in using a high power even if the plasma can be operated at a lower power. Since it is much easier and cheaper to obtain high powers at lower frequencies, the optimal frequency is probably quite low, perhaps in the range 5–10 MHz; for a plasma of conductivity 30 mho cm^{-1}, the corresponding range of skin depth is about 0.4–0.3 cm. The frequency used here for analytical work is about 7 MHz. In practice, high power is considered to be more important than the frequency chosen, provided that the frequency is high enough for the skin depth to be substantially smaller than the plasma radius.

THE PLASMA TORCH

A plasma can be produced, with a single laminar gas flow of argon, by induction heating in any quartz tube, placed within the work-coils of an h.f. generator operating at a suitable power and frequency. An ellipsoidal plasma is obtained into which it is almost impossible to inject an aerosol without blowing out the plasma. The introduction of a second gas stream flattens the base of the ellipsoidal plasma, enabling an aerosol to be injected through it. This results in an annular plasma, with the analyte atoms passing through a central tunnel[1,10]. Experience has indicated that such a configuration gives greater sensitivity than is obtained if the analyte atoms pass either round the outside of the plasma, or through it. This has led to the design of a torch, shown in Fig. 5, which was adopted after much experimentation with different designs.

The aim was to design a torch which would provide a stable, easily lit plasma into which an aerosol could be easily injected. It is desirable that the

torch should be readily fabricated in small quantities and that replacement torches should all give similar performance; a design whose behaviour depends critically on small changes in dimensions is not recommended.

Investigations covered both laminar and tangential flow in torches with a single tube; in torches with two tubes, some with the two gas streams independent and some with a shared control; and in demountable tubes. The effects of changing the dimensions were also studied.

The drawbacks of single-tube torches have already been mentioned. Two-tube torches with shared control of the gas streams are attractive, because of reduction of the number of variables and the consequent simplification of the apparatus; however, the loss of flexibility led to a critical dependence on dimensions. A demountable torch with a water-cooled metal base initially suffered from high-frequency loading into the base and the cooling water, and in spite of ameliorative measures, this problem could not be completely and convincingly overcome.

The torch described in Fig. 5 is the most satisfactory of those studied in terms of stability and ease of operation. The only dimension which appears to be at all critical is the bore of the injector, which must be accurately 2.0 ± 0.1 mm. Small changes in any other dimensions can be compensated by changing gas flows. One factor which seems very important for stability is the concentricity of the work-coil and the tubes of the torch.

While theoretical ideas provided useful guidelines, their application was not always practically successful. Mironer and Hushfar[11] predicted that the most

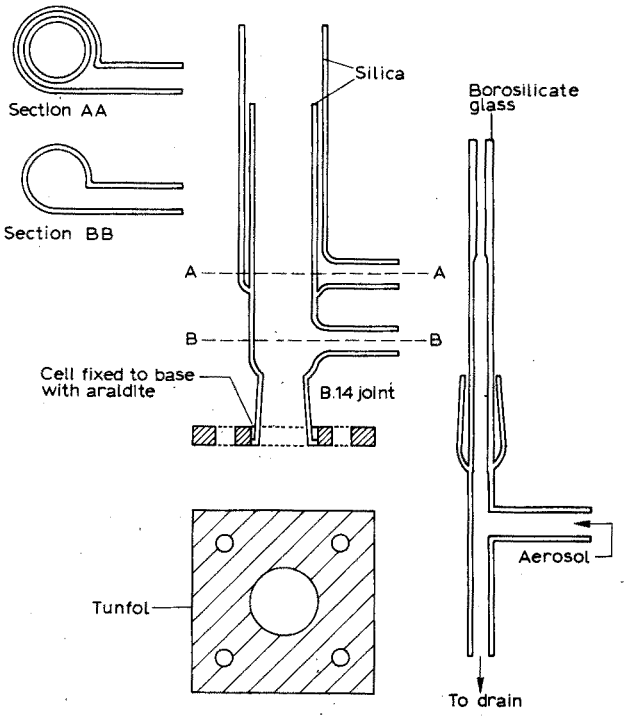

Fig. 5. The plasma torch.

efficient coupling between work-coil and plasma should occur when the ratio of plasma radius to skin depth is about 2.25. This suggested that with an assumed temperature of 10000°K and a frequency of 36 MHz, an efficiently coupled plasma could be contained in a tube as narrow as 0.5-cm diameter. In only one of a series of cells of approximately this size was it found possible to maintain a plasma, so that operation seemed to depend critically on dimensions, and in addition the plasma was unstable and difficult to work with. Most of our work in the search for stability and ease of operation was conducted on a trial-and-error basis.

The torch consists of three concentric tubes. The two outer tubes are made from silica and are used to contain the plasma. The inner tube can be of borosilicate glass and is used to inject an aerosol through the plasma once it has been formed. The top of the torch is concentric with the work-coil of the h.f. generator.

Argon gas is fed tangentially into the central silica tube at between 10 and 35 $l\ min^{-1}$, the h.f. field is applied by the work-coil and some free electrons are produced by a Tesla coil. Once the gas ionizes and so becomes conducting, a current is induced, and a plasma formed. There is no difficulty in doing this if about 2 KW can be supplied by the coil.

Once the plasma is struck, nitrogen gas at the rate of 20–70 $l\ min^{-1}$ is introduced quickly into the outer silica tube to stabilize the plasma and keep it off the walls. A hole is then punched through the flattened base of the plasma by the introduction, through the injector, of an aerosol in argon gas, at the rate of 2–3 $l\ min^{-1}$. The aerosol entering the torch passes through a tunnel of plasma and a long tail-flame results; it is this tail-flame which is used as a spectroscopic source.

Gases such as oxygen and hydrogen can also be used to surround the plasma. In the case of a polyatomic gas, a thermal pinch is applied to the plasma; dissociation of the gas absorbs energy, the outside of the plasma becomes cooler and hence less conducting, and a smaller, more intense plasma results. A substantial reduction in the continuum radiation was found when a polyatomic gas (particularly nitrogen) was used as the outer stream. This had a marked effect in lowering the limit of detection.

The torch has tangential gas entries since it was thought[3] that the vortex created by tangential flow would recycle some of the plasma and so maintain it. However, as has already been said, a laminar gas flow torch will function, and two-stream versions have their advocates[2]. The plasma must, in this case, be maintained by ionization of the on-coming gas through random electron collisions. There seems little to choose between laminar or tangential flow. However, experience has indicated that two gas flows, either tangential or laminar, are essential for the production of a stable well-formed plasma into which aerosols can be easily injected.

It has been stated[10] that higher frequencies favour the formation of a toroidal plasma and facilitate the introduction of sample through the tunnel so formed. This might be expected from considerations of skin depth, which decreases as frequency increases; thus if the plasma radius remains constant, the central tunnel would become larger with increase in frequency. It is doubtful whether the

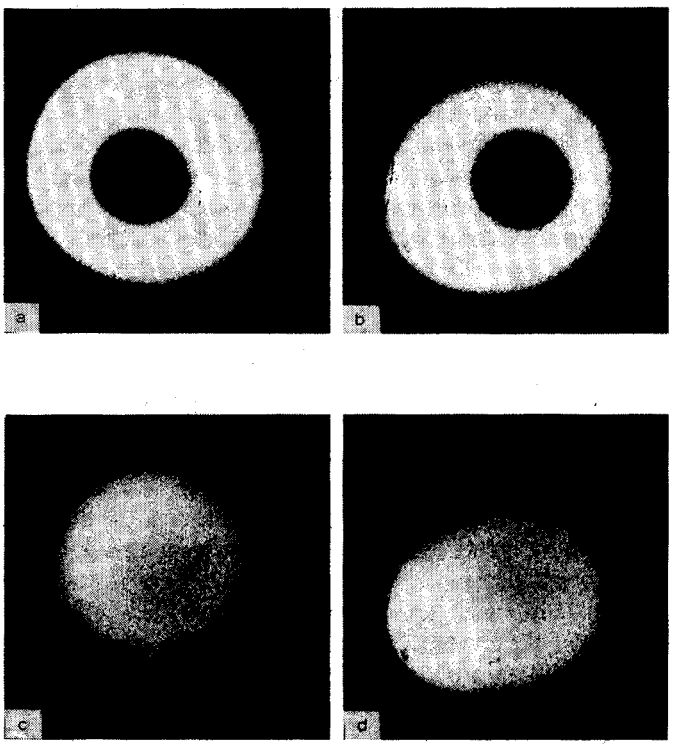

Fig. 6. View along the axis of four plasmas. (a) 7 MHz, with injector. (b) 36 MHz, with injector. (c) 7 MHz, without injector. (d) 36 MHz, without injector. The eccentricity of the 36 MHz plasma is due to its being horizontal.

plasma radius would remain constant with change in frequency, however, and Fig. 6, which shows photographs looking down the axis of the plasmas produced at two frequencies with and without an injector gas flow, demonstrates that the tunnel effect is more a function of injector gas flow than skin depth. There is little difference in the plasmas at different frequencies and the injector gas flow produces the tunnel in both.

NEBULIZERS

Initially, various forms of pneumatic direct injectors were used; these can transfer large quantities of material to the plasma. Their construction is entirely of glass, however, and they are too delicate for routine use. These were followed by various indirect pneumatic nebulizers, which were simpler to use and gave results of equal or better precision. Various desolvation systems were investigated; these gave better sensitivity but not precision, and occasionally suffered from memory effects. A spinning disc nebulizer was studied but this again showed no clear advantage. A modified Unicam SP 900 nebulizer is used, which seemed some years ago to give the best results of the nebulizers suitable for automatic operation which were investigated. It may well be that some present-day pneumatic nebulizers would prove superior.

A successful ultrasonic nebulizer with desolvation was also developed. However, as this had to be washed out after each sample, it was useful only for single samples and not in the automatic mode employed in routine work.

For everyday operation, the samples and standards, which are in liquid (usually aqueous) form, are loaded, interleaved by water washes, on the turntable of a modified Technicon auto-sampler and nebulized with a Unicam SP 900 pneumatic nebulizer. The loading pattern is shown in Table I, which omits the washes. The auto-sampler automatically starts the exposure sequence, and after the exposure provides a water wash for the plasma while the results are being digitized and punched. It then moves to the next solution and repeats the operation. Thirty elements can be analysed on six samples, with duplicate readings, in 40 min. Once the plasma has been struck and the auto-sampler started, the apparatus can be left entirely unattended.

TABLE I

LOADING PATTERN FOR THE TURNTABLE

Number of samples	*Position in turntable*[a]																			
	1	*2*	*3*	*4*	*5*	*6*	*7*	*8*	*9*	*10*	*11*	*12*	*13*	*14*	*15*	*16*	*17*	*18*	*19*	*20*
1	A	B	T_1	C	D															
2	A	B	T_1	C	D	T_2	A	B												
3	A	B	T_1	C	D	T_2	A	B	T_3	C	D									
4	A	B	T_1	C	D	T_2	A	B	T_3	C	D	T_4	A	B						
5	A	B	T_1	C	D	T_2	A	B	T_3	C	D	T_4	A	B	T_5	C	D			
6	A	B	T_1	C	D	T_2	A	B	T_3	C	D	T_4	A	B	T_5	C	D	T_6	A	B

[a] A, B, C and D are the four standard solutions and T_1–T_6 are the sample solutions.

THE SPECTROMETER

The direct-reading spectrometer employed is the 30-channel Hilger and Watts FA19 Polychromator; this uses a concave grating of 3-m radius and gives a dispersion of 0.173 mm A^{-1} in the first order. Radiation from the source is focused on the entrance slit and then reflected by a plane mirror on to the grating. The different wavelengths in the resulting spectrum are focused at different points on a circle where a series of exit slits passes the wavelengths of interest. The radiation transmitted by an exit slit is focused by a concave mirror to fall, after reflection by a plane mirror, on the cathode of a photomultiplier. There are thirty slits and photomultipliers.

When radiation strikes a photomultiplier, a current flows, proportional to the intensity of the radiation. The current from each photomultiplier charges a condenser for the duration of each exposure so that the voltages on the condensers provide measures of the integrated intensities. The conventional measuring system (comparison with a linear ramp) has been replaced by a system of our own design in which a digital voltmeter (Solartron LM 1426) is interfaced to an ASR 33 Teletype to provide punched paper tape. It was found necessary to have an

input impedance greater than that of the voltmeter and an interface with an apparent input impedance of 10^{11} ohm was constructed from F.E.T. transistors.

During a 40-min run there is some drift in the calibration curves which can amount to about $\pm 3\%$. This is probably due to the electronics associated with the photomultipliers, or perhaps may be an effect of the changing light levels on the photomultipliers when different standard solutions are run. Consequently, it is necessary to run a large number of standards to follow the drift; for accurate work, twice as many standards as samples are used to achieve adequate bracketing in time.

DATA PROCESSING

The tape produced by the Teletype is supplemented by a manually punched tape which specifies the number of samples and elements, the element names, weights, volumes, and concentrations of the standard solutions. Then, for each element, an individual calibration curve is computed for each sample. The calculated curves are hyperbolic, of the form $y=(px+r)/(1+qx)$. The parameters p, q and r are derived by a least-squares procedure from the four standard readings closest in time to the sample reading.

Curves of this form (which were taken over from x-ray fluorescence, where they can be shown to be appropriate) fit the calibration points well in a wide range of techniques. They have advantages over polynomials in having no maxima: thus they have only one root, and have more resemblance to real calibration curves outside the range in which they are fitted, making the dangerous practice of extrapolation somewhat less hazardous.

The values of the standard concentrations are calculated from the curve and compared with their known values. A column on the print-out summarizes the goodness of fit. If all four deviations are less than 1% of the highest standard concentration, the column is left blank. If there are deviations greater than this a number is printed, of which the least significant digit is the number of points whose deviations lie between 1% and 3%, the next more significant digit is the number of points between 3% and 10%, and the third digit is the number of points with deviations greater than 10%. Thus the number 120 means that one point has a deviation of greater than 10%, two points have deviations between 3% and 10%, and no points have deviations between 1% and 3%, so that by implication the fourth point has a deviation of less than 1%. If the points are not monotonic, *i.e.* if there is a maximum or minimum in the calibration points, the message "bad" is printed and further calculations on this sample reading are suppressed. If the equations which determine the parameters p, q and r are not soluble, the message "none" is printed and the calculations are again suppressed. The most likely cause of these aberrations is a mistake in the input of the sample concentrations. The majority of the curves obtained have the "fit" column blank, and the signalling of a deviation greater than 10% would indicate a pathological case.

If the turntable is sent round a number of times, there are this number of readings for each element and sample, and these are collected together so that the concentrations are printed together with the mean. The relative standard deviation

is printed, to highlight discordant results. In addition, the value of concentration which corresponds to the square root of the reading is printed; this can be thought of as a predicted error (on perhaps dubious assumptions) and is used as an indication of where the results should be rounded-off.

If a reading exceeds that of the highest standard by a large amount, the message "too high" is printed and no further calculation takes place; if it is only just in excess, calculation takes place normally but the message "high" is printed.

These precautions, although they may appear cumbersome, are essential when the interpretation of the data is left entirely to the computer.

RESULTS

Limits of detection

Low detection limits have come to be regarded as an indication of excellence in any technique involving small quantities, whether trace quantities in bulk samples or the assay of micro samples. They are often used as a means of comparing sources but it should be remembered that while complete systems can be compared in this way, an individual part cannot unless it is the only one in the system to be changed.

TABLE II

DETECTION LIMITS FOR SINGLE ELEMENTS BASED ON OPTIMAL CONDITIONS FOR EACH ELEMENT

Element	*λ nm*	*Detection limit*	
		Ultrasonic nebulizer (with de-solvation) ng ml^{-1} (p.p.b.)	*pneumatic nebulizer (without de-solvation) ng ml^{-1} (p.p.b.)*
Calcium	396.85	0.002	0.2
Barium	455.40	0.02	0.8
Magnesium	280.27	0.01	0.6
Arsenic	234.98	90	300
Manganese	257.61	0.03	0.2

Table II gives some detection limits obtained with the system used, both with an ultrasonic nebulizer with desolvation, and with a conventional pneumatic nebulizer without desolvation. These detection limits were obtained from measurements made with photomultipliers specially selected for high sensitivity and low dark current; in addition, optimal values of gas flows, power and position in plasma tail-flame for each element were used. The limits were derived by plotting calibration graphs for a concentration range of approximately ten times the detection limit and using the graph to find the concentration corresponding to an intensity twice the standard deviation of the background, this being estimated from replicate readings of the blank.

Of more importance in simultaneous multi-element analysis are the detection limits, similarly derived, obtained on multi-element mixtures determined simultaneously, with compromise conditions. Some typical values are shown in Table III.

TABLE III

SIMULTANEOUS MULTI-ELEMENT DETECTION LIMIT BASED ON COMPROMISE CONDITIONS

Element	*λ nm*	*Detection limit*	
		Ultrasonic nebulizer (with de-solvation) ng ml^{-1} (p.p.b.)	*Pneumatic nebulizer (without de-solvation) ng ml^{-1} (p.p.b.)*
Tin	317.51		100
Nickel	361.94	7	10
Sodium	589.00		30
Aluminium	396.15	10	10
Cadmium	508.58		100
Iron	263.11	5	40
Cobalt	345.35	23	20
Boron	249.77	5	100
Zinc	481.05	18	100
Lead	283.31	10	70
Calcium	396.85	0.2	10
Barium	455.40	0.3	1
Magnesium	280.27	0.5	2
Strontium	460.13		20
Manganese	257.61	3	3
Copper	324.75	16	10
Vanadium	309.31		9
Molybdenum	281.62		20
Titanium	336.12		30
Silicon	288.16		30
Chromium	425.43		20
Arsenic	234.98	90	

TABLE IV

AUTOMATIC, SIMULTANEOUS MULTI-ELEMENT ANALYSIS PRECISION OBTAINED ON A 1 P.P.M. SOLUTION

	λ nm	*Mean conc. determined (p.p.m.)*	*s_r (%)*
Vanadium	309.31	1.00	2.4
Aluminium	396.15	0.98	2.9
Cobalt	345.35	0.95	5.2
Calcium	396.85	0.96	3.3
Barium	455.40	0.98	3.2
Magnesium	280.27	0.99	2.4
Manganese	257.61	0.99	3.4
Copper	324.75	0.99	2.1
Sodium	589.00	0.93	4.0
Nickel	361.94	1.00	8.0
Strontium	460.73	0.99	6.7

TABLE V

AUTOMATIC SIMULTANEOUS MULTI-ELEMENT ANALYSIS
LOW ALLOY STEEL B.C.S. 408
(Percentage composition)

	V	*Ni*	*Mo*	*Cr*	*Si*	*Mn*	*Cu*
This work: 6 analyses							
Mean of 6 duplicate readings	0.0615	4.53	0.13	0.097	0.24	0.64	0.73
s_r (%)	0.64	0.69	0.91	1.22	1.09	0.74	0.55
B.C.S. certificate value	0.063	4.58	0.14	0.09	0.24	0.64	0.73
s_r (%) (8 Laboratories)	4.26	0.45	5.36	3.32	1.95	1.17	1.54

TABLE VI

AUTOMATIC SIMULTANEOUS MULTI-ELEMENT ANALYSIS
CHROME ORE 2 C.A.S. 5
(Percentage composition)

	SiO_2	TiO_2	Al_2O_3	Fe_2O_3	Cr_2O_3	*CaO*	*MgO*	*MnO*
This work: 6 Samples of 1 solution								
Mean of 6 duplicate readings	5.22	0.38	23.37	17.15	36.20	0.44	17.43	0.14
s_r (%)	1.13	2.26	0.67	1.59	1.29	2.64	1.17	1.87
This work: 6 analysts								
Mean of 6 duplicate readings	5.84	0.32	22.62	16.35	36.84	0.41	16.95	0.117
s_r (%)	2.50	4.28	0.74	1.95	0.69	9.24	1.57	5.4
Interlaboratory survey[1,2]								
Mean of 14 determinations	5.37	0.29	23.04	17.31	36.07	0.48	16.84	0.11
s_r (%)	4.3	30.0	3.4	5.2	3.09	43.0	1.90	54.0

TABLE VII

AUTOMATIC SIMULTANEOUS MULTI-ELEMENT ANALYSIS MAGNESITE 2 C.A.S. 10
(Percentage composition)

	SiO_2	TiO_2	Al_2O_3	Fe_2O_3	*CaO*	*MgO*	*MnO*	Na_2O
This work: 6 samples of 1 solution								
Mean of 6 duplicate readings	0.51	0.02	0.44	1.43	0.82	96.9	0.097	0.02
s_r (%)	3.80	66.0	5.80	1.40	0.50	0.6	1.00	18.0
This work: 6 Analysts								
Mean of 6 duplicate readings	0.49	0.1	0.39	1.36	0.83	95.9	0.096	0.01
s_r (%)	5.30	42.0	4.10	2.70	3.30	1.5	2.1	41.0
Interlaboratory survey[1,2]								
Mean of 14 Determinations	0.49	0.02	0.64	1.47	0.81	96.1	0.10	0.05
s_r (%)	24.0	58.0	49.0	18.0	29.0	0.76	32.0	43.0

Trace analysis

Table IV shows typical values of accuracy and precision, expressed as relative standard deviation, obtained from 12 analyses of a solution containing 1 p.p.m. of eleven elements with the equipment operating automatically under a single set of compromise conditions. The lower precision for nickel is due to the operating conditions used being far from the optimal conditions for this element, and this precision could be improved by using a different set of conditions.

TABLE VIII

AUTOMATIC SIMULTANEOUS MULTI-ELEMENT ANALYSIS

(The elements in a row were determined simultaneously in the concentration ranges shown.)

Sample	*0–9.9 p.p.m.*	*10–99 p.p.m.*
Raw phosphoric acid[a]	Ca, Sr, Mo, Co, Ba	Zn, Ni, Cd, Cr, Pb, Cu, B
Effluent[a]	Zn, Ni, Al, Cd, Fe, Cr, Pb, Cu	Sn
Recirculating water[a]	Zn	
Tetraphosphoric acid[a]		Fe
Chromium chloride[a]		
Phosphate glass[a]		
Aluminium sheet[b]	Co, B, Cd, Cr, Ca, Mg, Na, Ba	Sn, Pb, Mn, Cu
Phosphorus mud[b]	Al, Cd, V, Na, Ba, Sr, Mn	Cr, Mg, Cu
Tin(II) oxide[b]	Cu	Ni, Fe, Pb
Aluminium alloy[b]		
Calcium phosphate[b]	Pb	
Niobium steel[b]		
Deposit from dishwasher[b]	Al, Fe	
Copper/beryllium alloy[b]		
Calcium phosphate[b]		Fe
Stainless steel[b]		
Protein[c]	Cd, Fe, V, Ba, Sr	Al, Mg, Si
Effluent[d]	Pb, Cu, Zn, Sn, Ni, Al, Cd, Fe	
Organic material[e]		
PVC[c]		
Organic phthalate[c]	Cd, Fe, Pb, Cu	
Dyestuff[c]	Mn	Fe
Chrome ore[f]		
Celestite[f]		
Tin residue[f]		Cd
Condenser deposit[f]		
Valve deposit[f]		
Boiler scale[f]		
Sulphide residue[f]	Cd, Pb	
Toothpaste[f]		
Deposit from dishwasher[f]		
Sulphamic acid/ china clay[f]		

[a] Aqueous solutions were used.
[b] Samples were analysed after acid dissolution.
[c] Wet oxidation was used.
[d] Solvent extraction and wet oxidation were used.
[e] Wet oxidation and fusion were used.
[f] Fusion served as the method of dissolution.

Analysis in the high p.p.m. to low percentage range

A low alloy steel is typical of this range. A sample (0.1 g) of B.C.S. 408 low alloy steel was dissolved in 25 ml of 20% (v/v) sulphuric acid. When reaction was complete, the solution was oxidized by 2–3 drops of nitric acid and made up to 50 ml. This process was carried out on six samples of the steel, the resulting solutions being analysed in duplicate. The results are shown in Table V. The B.C.S. certificate values are also shown, with the published relative standard deviations for the results obtained by different methods in eight different laboratories.

100–999 p.p.m.	*0.1%–0.99%*	*1%–9.99%*	*10%–100%*
Mg, V, Na, Mn, Ce, La	Al, Fe, Ti		
Ni, Fe			
Al, Fe, Zr	Si		
Zn, Ni,	Fe		
Zn, Ni, Fe	Ca, Si		
Na			
Cu	Mg, Mn	Si	
			Ca
		Mn, Nb	
Co		Be	
			Ca, P
	Mo	Ni	Cr
Zn, Ni, Cu, Ca	Na		
			Ba
Sn, Pb			
		Cu	
	Mn, V	Al, Fe, Mg	Cr
Cu, Ca	Al, Fe, Pb, Mg, Ba, Mo		Sr
	Pb, B		Fe
		Zn, Mg	Ca
	Ca		Zn
		Mg	Ca
		Zn	
		Al, Ca	
		Al, Mg	Ca
		Cr	

Analysis in the low to medium percentage range

The analysis of a chrome ore, 2 C.A.S. 5, supplied by the British Ceramic Research Association, is representative. The sample (0.1 g) was fused with 3.00 g of sodium peroxide. After extraction with 50 ml of water in a polythene beaker, 25 ml of 50% (v/v) hydrochloric acid was added. The resulting solution was diluted to 500 ml. One solution was analysed six times in duplicate. The sample was then independently analysed in duplicate by six of our analysts, each one following the entire procedure. The results are shown in Table VI, which also gives the results of a survey[1,2] of analyses of this material carried out in fourteen laboratories.

Analysis in the high p.p.m. to high percentage range

A magnesite ore sample, 2 C.A.S. 10, also supplied by the British Ceramic Research Association, is representative of this type of sample. The sample (0.1 g) was dissolved in 20 ml of 50% (v/v) hydrochloric acid and made up to 100 ml. The scheme of analysis described above for 2 C.A.S. 5 was repeated. The results are presented in Table VII.

Overall performance

The results presented in Tables II–VII show not only the excellent sensitivity, accuracy and precision obtainable with the equipment but also indicate the wide concentration range and the widely differing matrices which it can handle. This point is emphasised by Table VIII which lists some of the 594 samples (involving 1707 requested determinations and 3444 actual determinations in duplicate) which were analysed in the first quarter of 1974 by emission spectroscopy with the plasma source. Each row in the Table corresponds to the simultaneous determination of all the elements shown for that type of sample, in the concentration ranges indicated.

The authors wish to acknowledge the considerable contribution made by C. T. Berry in the early days of this project. We are grateful to C. L. Brierley, E. Hobbs and J. A. R. Hill for assistance in technical matters, and to the several operators of the equipment for their observations.

SUMMARY

The equipment described for automatic multi-sample simultaneous multi-element analysis has been in everyday use for practical analysis for four years. Some important points in its design are discussed and reasons are advanced for using a high-powered, free-running oscillator to excite a plasma with two gas streams in addition to the stream carrying the sample aerosol. The frequently-used simple formulae for inductance, appropriate for long coils, were found inadequate; modified formulae, applicable to short coils, which agreed with experimental data, were used. Trace analysis and assay work can alike be performed with good accuracy and precision, and in a convenient way. Some typical results are given, with an indication of the versatility of the equipment.

REFERENCES

1 S. Greenfield, I. Ll. Jones and C. T. Berry, *Analyst (London)*, 89 (1964) 713.
2 R. H. Wendt and V. A. Fassel, *Anal. Chem.*, 37 (1965) 920.
3 T. B. Reed, *J. Appl. Phys.*, 32 (1961) 821.
4 G. I. Babat, *J. Inst. Elec. Eng.*, 94 (1947) 27.
5 S. Greenfield, I. Ll. Jones, C. T. Berry and D. I. Spash, British Patent 1, 109, 602.
6 British Standard Specification, B.S. 1799: 1952.
7 A. G. Bogle, *J. Inst. Elec. Eng.*, 87 (1940) 299.
8 P. G. Simpson, *Induction Heating*, McGraw-Hill, New York, 1960, p. 17.
9 S. Greenfield, unpublished.
10 G. W. Dickinson and V. A. Fassel, *Anal. Chem.*, 41 (1969) 1021.
11 A. Mironer and F. Hushfar, *A.I.A.A.* Electric Propulsion Conference, Colorado Springs, (1963), Paper 63045.
12 H. Bennett and R. H. Reed, Special Publication No. 80, British Ceramic Research Association, (1973).

Analytica Chimica Acta, 74 (1975) 247–252

A TRIPLE-FLOW GAS-SHEATHED D.C. ARC FOR SPECTROCHEMICAL ANALYSIS

H. K. EL-KHOLY*, J. C. BURRIDGE and R. O. SCOTT
The Macaulay Institute for Soil Research, Craigiebuckler, Aberdeen AB9 2QJ (Scotland)
(Received 24th July 1974)

Although Stallwood[1] introduced his gas-sheathed arc mainly to reduce selective volatilization and matrix effects, stabilization of the arc and the exclusion of air from the arc plasma are the more usual advantages claimed for the commercially-available Stallwood Jets. Boumans[2] has recently summarized some applications of special excitation sources including jet devices. The reduction of cyanogen (CN) band emission is often of particular importance because these bands can prevent the analytical use of lines of several elements. Weber and Darr[3], among other workers, used chambers to surround the arc with inert gas in order to reduce CN radiation to an acceptable level. Such chambers are inconvenient for routine analytical use on account of the frequent cleaning required, particularly when arcs are operated at currents above about 10 A.

The gas-sheathed arc described in this paper was developed during the course of an investigation[4] into the effects of d.c. arc conditions on the determination of trace elements in soils and rocks, with a Hilger and Watts Large Quartz Spectrograph, and combines a twin-jet around the anode with an independent gas sheath around the cathode counter-electrode. It was found that when argon–oxygen mixtures are used to enclose the arc column, CN emission is virtually eliminated without the use of a surrounding chamber; the arc sheathed in this manner has good stability at currents up to 20 A; and the limits of detection for trace elements in soils and rocks are better than are obtained with a cathode-layer arc.

SOURCE DESCRIPTION

The triple-flow gas-sheath is maintained around the arc by means of a twin-jet device and a counter-flow silica tube, illustrated in Fig. 1 by a cross-sectional diagram. Two gas streams (B and C, Fig. 1) are directed in opposite directions around the anode through independent chambers (G and H) of an annular twin-jet device. Stream (B), an upward flowing mixture of argon and oxygen, provides the atmosphere for the arc plasma while the downward flowing stream of argon (C) reduces the consumption of the electrode material. The third gas stream (E), a downward current of argon in the silica tube (F), ensures that the arc strikes only to the tip of the cathode counter-electrode (A). The flow rates normally used are (B) 10 l min^{-1} of an argon–oxygen mixture obtained by

* Present address: Faculty of Science, University of Sanaa, Yemen.

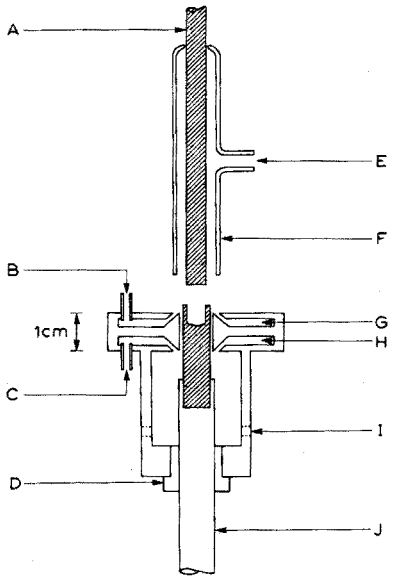

Fig. 1. Schematic cross-section of the arc system. The twin-jet was made from an aluminium alloy (BS1476, HE14-W). (A) Carbon counter-electrode (cathode); (B) argon–oxygen inlet to upper chamber of twin-jet; (C) argon inlet to lower chamber of twin-jet; (D) insulating anode-support guide; (E) argon inlet to sheath counter-electrode; (F) silica tube; (G) twin-jet upper annular chamber; (H) twin-jet lower annular chamber; (I) argon outlets; (J) aluminium alloy anode-support (sliding fit in D) for graphite anode.

combining flows of argon at 7 l min^{-1} and oxygen at 3 l min^{-1}, (C) 5 l min^{-1} argon and (E) 3 l min^{-1} argon.

An arc sheathed in the manner described above has been used chiefly for analyzing finely ground soil or rock samples. These are mixed 1:1 with carbon powder and packed into a cavity 4.7-mm diameter by 6-mm deep in a 6.15-mm diameter anode of graphite (National Carbon Company, grade AGKS). This cavity holds about 40 mg of sample mixture. A 5.5-mm diameter carbon rod (Morganite, grade SG905J) is used as the cathode and this projects some 2–3 mm beyond the silica tube (F in Fig. 1). Loss of sample when striking the arc is minimized by applying a few drops of a 5% solution of polymethyl methacrylate (Perspex) in chloroform to the filled electrode and allowing it to dry overnight. Throughout an exposure the tip of the sample electrode is kept 1 mm above the top surface of the twin-jet and a constant 5 mm arc gap is maintained by observation of a projected image of the arc. At 20 A the anode spot covers the sample completely and uniformly, gas flow (B) preventing the arc from wandering to the outer surface of the sample electrode. The rate of sample consumption is approximately proportional to the oxygen content of flow (B), and samples are consumed in about 3 min when a current of 20 A is used with flow (B) containing 30% oxygen. The prototype twin-jet used in this study was made from an aluminium-based alloy (Duralumin type BS1476, HE14-W) and despite the heat from the arc, water-cooling was not required.

For the present application to the trace element analysis of soils and rocks,

silica was selected as the most suitable material to sheathe the counter-electrode (A), as it does not create contamination problems. It would be possible to economize in the consumption of argon by using preset gas-control valves to reduce flow rates while electrodes are being changed.

ARC STABILITY

Although the choice of internal standard is probably the major single factor affecting analytical precision, the stabilities of both arc current and plasma position are also of considerable importance and a smoothly burning arc is generally essential. Good stabilization of both plasma position and arc current has been achieved in the present work by the use of the counter-flow (E). The effect of this counter-flow on arc current is shown in Fig. 2. Without the counter-flow (Fig. 2, curve a), there is a marked tendency for the arc to wander up the side of the counter-electrode, sometimes several centimetres from the tip, and a large reduction of arc current occurs when the arc plasma lengthens in this way. The strong upward flow of gas from the twin-jet hinders the return of the cathode spot to the tip of the counter-electrode. The improvement in current stability achieved by means of the counter-flow (Fig. 2, curve b), is very apparent. The

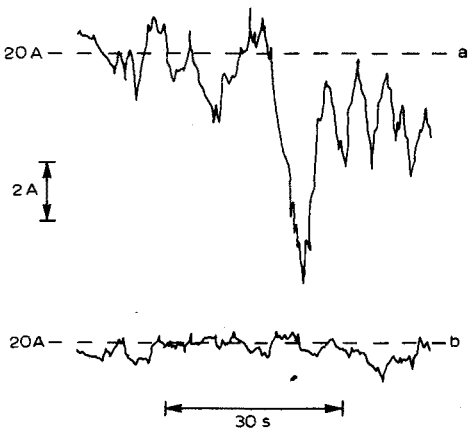

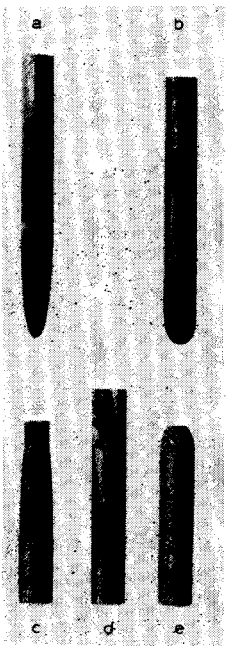

Fig. 2. Arc current fluctuation with time: (a) without and (b) with gas sheath around counter-electrode as shown in Fig. 1.

Fig. 3. Upper electrodes 5.5 mm diameter carbon: cathodes arced with twin-jet source, (a) without and (b) with the counter-flow gas sheath. Lower electrodes 6.15 mm diameter graphite: anodes, (c) arced with the simple cone-jet shown in Fig. 4, (d) un-arced sample electrode cut to show crater and (e) arced in twin-jet shown in Fig. 1.

recordings shown were made while the arc was being controlled by means of manually operated current regulators. Only 10 A was obtained from a d.c. supply with normal resistance ballasting, the other 10 A being supplied by an unballasted rectifier fed from a hand-adjusted variable auto-transformer. A solid-state stabilized-current supply capable of continuous operation at selected currents up to 30 A, at present under construction, should further improve the arc stability.

The efficiency with which the arc is confined to the counter-electrode tip is apparent in the photographs (Fig. 3) by comparing the shapes and surface textures of electrodes (a) and (b). Both had flat ends before arcing and it is obvious from the photographs that electrode (a), arced without counter-flow, has been heated and eroded over a greater area than has electrode (b), with counter-flow.

It can be seen from the photographs of arced anodes (Fig. 3) that the consumption of anode material is much lower with the triple-flow arc (electrode e) than with a Stallwood jet (electrode c) of the cone-shape illustrated in Fig. 4. The same argon–oxygen mixture and flow rate were used in both cases. Apart from the necessary consumption of the crater walls, shown in the cut-away unarced electrode (d) and weighing about 120 mg, there was an additional consumption of 280 mg of graphite for the Stallwood jet compared with one of 70 mg with the triple-flow arc.

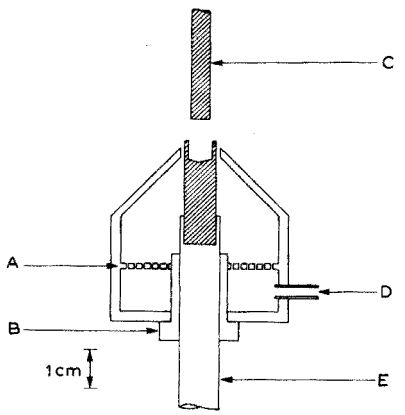

Fig. 4. Schematic cross-section of a simple cone-shaped jet. (A) Perforated plate; (B) insulating anode-support guide; (C) counter-electrode (cathode); (D) argon–oxygen inlet; (E) anode support (sliding fit in B).

This action of the lower half of the twin-jet, in reducing the consumption of sample electrode material, helps to improve the trace element determination limits in two different ways. First, the contribution of any contamination in the electrode material to the analysis is reduced, resulting in lower blank levels, and so the determination of low trace element contents in samples becomes possible without high-purity electrodes. Secondly, the smaller consumption of electrode carbon results in less background radiation with a consequent improvement in line-to-background ratios.

A further measure of source stability is the reproducibility of emitted line intensity. This was determined from twelve replicate arcings of a sample containing

100 p.p.m. of several trace elements in a synthetic soil matrix; a Hilger and Watts E492 Large Quartz Spectrograph was used with a seven-step rotating sector at the slit and a non-recording microphotometer. Line intensity coefficients of variation found were cobalt (3453.5 Å)±13.5, chromium (3578.7 Å)±14.7, molybdenum (3170.4 Å)±12.5 and tin (3175.0 Å)±21.9%. With palladium as internal standard for cobalt, and the line ratio Co 3453.5 Å/Pd 3460.8 Å, the coefficient of variation for the cobalt content of 100 p.p.m. was ±4.5%.

REDUCTION OF CYANOGEN BAND EMISSION

The United States Geological Survey standard diabase W-1 was arced in the triple-flow source; a tracing of part of the spectrum is shown in Fig. 5. The absence of the main CN band systems, whose positions in a carbon arc in air are indicated by the broken lines, demonstrates the efficient suppression of cyanogen emission. Neither the band heads nor the main lines of the (0,0), (1,1) and (2,2) CN systems could be identified when the spectra were examined with a Judd–Lewis comparator. Flanagan[5] has reported the scandium content of this material as about 35 p.p.m. and the distinct tracing of the line ScII 3911.8 Å in Fig. 5 illustrates that the triple-flow arc has reduced background emission in this wavelength region sufficiently for such lines to be readily measured.

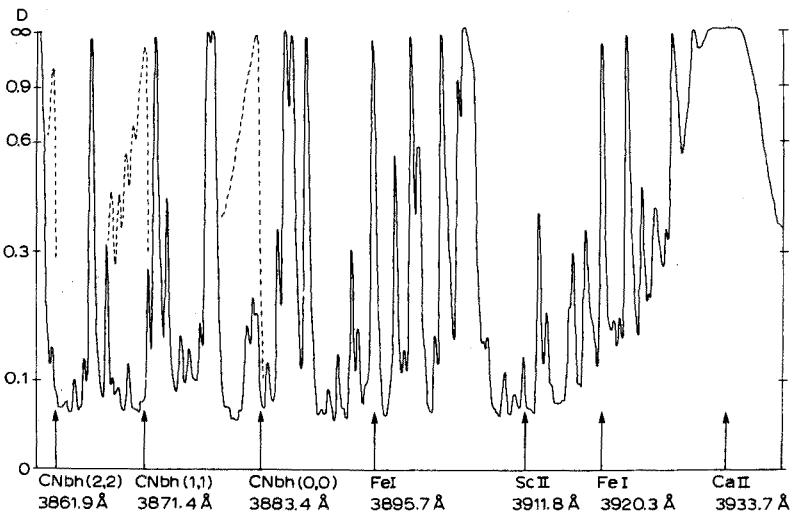

Fig. 5. Microphotometer trace of a spectrum from USGS rock W-1 arced with twin-jet and sheathed counter-electrode; argon at 7 l min^{-1} mixed with oxygen at 3 l min^{-1} was used to suppress cyanogen emission. The broken line indicates the positions of CN bands emitted by a carbon arc in air. Equipment: Hilger and Watts E492 Large Quartz Spectrograph; arc imaged on the collimator; Ilford G30 Chromatic plate developed in ID2 1:2; Leeds Northrup microphotometer with Speedomax recorder.

APPLICATION TO SOIL ANALYSIS

The practical application of the triple-flow arc has been tested by analyzing

some 60 soils and rocks for a wide range of trace elements; the detailed results have been presented elsewhere[4]. Limits of determination are lower than can be obtained with a cathode layer arc in air (Mitchell[6]). Some approximate values of these limits for the triple-flow arc, with a step sector at the spectrograph slit and with the arc imaged on the collimator, are arsenic (2349.8 Å), 300 p.p.m.; bismuth (3067.7 Å) and zinc (3345.0 Å), 30 p.p.m.; tin (3175.0 Å) and zirconium (3392.0 Å), 10 p.p.m.; germanium (3039.1 Å), indium (3039.4 Å), lead (2833.1 Å) and yttrium (3327.9 Å), 3 p.p.m.; cobalt (3453.5 Å), copper (3247.5 Å), lanthanum (4333.7 Å), nickel (3414.8 Å), scandium (3911.8 Å) and vanadium (4379.2 Å), 1 p.p.m.; beryllium (3130.4 Å), gallium (2943.6 Å), manganese (2801.1 Å) and silver (3280.7 Å), 0.3 p.p.m. The limits of detection for the same lines, when spectrograms taken with the arc imaged on the spectrograph slit are examined with a Judd–Lewis comparator, are about one third of these quantitative determination limits.

The improved detection limit for zinc is of particular value, as the zinc content of most soils and rocks is below the detection limit of about 300 p.p.m. in the cathode layer arc[6]. By improving the quantitative determination limit to around 30 p.p.m., the triple-flow arc has already provided useful new information about the zinc content of Scottish soils[4].

The stability of this triple-flow arc, confirmed by the coefficient of variation of less than 5% for cobalt, and the good limits of determination indicated above for a range of elements, demonstrate the considerable potential value of this arc arrangement for the analysis of non-conducting powders.

The twin-jet device was constructed in the Macaulay Institute instrument workshop and the authors wish to acknowledge the contribution of the workshop staff, in particular J. H. Normington and A. M. Fraser.

SUMMARY

A d.c. arc source sheathed by three independent gas streams is described. A mixed flow of argon at 7 l min^{-1} and oxygen at 3 l min^{-1} is used to support the arc plasma and isolate it from the surrounding air, while separate streams of argon are used to sheathe the base of the anode and lower part of the cathode counter-electrode. The anode holds about 40 mg of a sample mixture. The source is stable when operated with currents up to 20 A, cyanogen emission is eliminated, and the limits of detection of a wide range of trace elements in soils and rocks are better than with a cathode-layer arc in air.

REFERENCES

1 B. J. Stallwood, *J. Opt. Soc. Amer.*, 44 (1954) 171.
2 P. W. J. M. Boumans in E. L. Grove (Ed.), *Analytical Emission Spectroscopy, part II*, Dekker, New York, 1972, Ch. 1.
3 J. L. Weber and M. M. Darr, *Nat. Bur. Stand. (U.S.) Tech. Note 582*, 1972, p. 18.
4 H. K. El-Kholy, Ph. D. Thesis, University of Aberdeen, 1972.
5 F. J. Flanagan, *Geochim. Cosmochim. Acta*, 37 (1973) 1189.
6 R. L. Mitchell, *The Spectrochemical Analysis of Soils, Plants and Related Materials, Tech. Commun. Commonw. Bur. Soils, 44A*, 1964.

Analytica Chimica Acta, 74 (1975) 253–259

THE USE OF REFLECTANCE SPECTROMETRY FOR THE DETERMINATION OF MICROQUANTITIES OF MERCURY

R. REISFELD, E. GREENBERG and W. J. LEVENE*

Department of Inorganic and Analytical Chemistry, The Hebrew University, Jerusalem (Israel)

(Received 10th April 1974)

Reflectance spectroscopy as an analytical technique has been mostly limited to textile materials, paint, and the quality of paper and powders[1,2]; cation analysis by thin layer chromatography[3] has been used with reflectance measurements, but these were generally made on spots removed from the plates and packed into an appropriate cell. The advantages of reflectance over the techniques of transmission spectrophotometry lie in its high sensitivity and in the ease with which materials deposited on an absorbing surface, such as paper, can be measured. Precipitates as well as clear colored solutions can be deposited in this way. Reflectance spectrophotometry has largely been qualitative because of the disturbing effects of particle size and specimen surface on the reflectance. Ayers[4] used polychromatic light densitometry for the determination of inorganic materials. In this work, reflectance spectrometric techniques are proposed for the quantitative determination of colored complexes which are precipitated as spots on filter paper. The important factors which can affect accuracy are: (1) variations in the size of the spot on the filter paper; (2) inhomogeneous distribution of the colored material within the spot; (3) displacement of the spot relative to the incident light beam, which should fall wholly within the spot; (4) variations of precipitate particle size distribution, on which the light scattering is strongly dependent; and (5) interference from specularly reflected light in the measurement of diffuse reflectance.

For an ideal case of a uniform distribution and in the absence of reflectance from the background, the Kubelka–Munk[5] function, which connects the diffuse reflectance of the sample[6] with colorant concentration, can be used. The appropriate equation for such a case has the form

$$kC = \frac{K}{S} = \frac{(1-R_\infty)^2}{2R_\infty}$$

where k is a constant, C the concentration of the colored substance, K the absorption coefficient, S the scattering coefficient and R_∞ the monochromatic reflectance of a specimen of such thickness that a further increase in thickness does not change the reflectance. In order that this equation could be used in the actual analysis, the experimental difficulties mentioned above were overcome as follows.

*Present address: Electro-Optical Industry, Ltd., Rehovoth, Israel.

(1) A method was developed for reproducible transfer of solutions to obtain uniformity in spot size and concentration by use of a micro-syringe of constant flow rate.

(2) The optical measurement was performed on a small area (2 mm × 1 mm) so as to further reduce the effects of any remaining inhomogeneity.

(3) The light was projected centrally on the colored spot.

(4) A filter paper of the most suitable grade was selected.

(5) The measurements were made with an instrument having a high rejection of specularly reflected light.

Reflectance spectra of the given substance were first obtained as oscillograms, enabling rapid identification of characteristic reflection bands. Optimal wavelengths were thus chosen for quantitative reflectance measurements.

EXPERIMENTAL

Description of Spectrocolorimeter

Measurements of the diffuse spectral reflectance of specimens were made with a Fast Scanning Spectrocolorimeter Type SCF-1 (Israel Electro-Optical Industry, Ltd., Rehovoth, Israel). This is a filter spectrophotometer which allows instantaneous measurements over the whole of the visible spectrum (400–700 nm), at 25-nm resolution, which is scanned 30 times per second. It presents the spectral transmission or reflection curve of the specimen on a simple oscilloscope, the screen graticule of which is calibrated in percentage transmission (ordinate) and nanometers (abscissa). When a reflectance attachment is used, the oscilloscope displays percentage reflectance against wavelength. The scanning can be arrested for measurements at a fixed wavelength of interest. For this work, the instrument was used with the Diffuse Reflectance Attachment. This projects a beam of monochromatic light onto an area of the specimen 2.25 mm high, 0.75 mm wide, at normal incidence. Large-area photocells line a rectangular tube positioned immediately before the specimen to collect the light diffusely reflected from the specimen at angles between 5° and 85°, but respond to less than 2% of the light reflected specularly from the specimen.

A strip of black metal was used for setting the zero of the instrument, and a clean magnesium carbonate block was used for calibrating the 100% sensitivity.

Procedure

The diphenylcarbazone, mercury(II) chloride and other materials used in this work were all reagent grade. The filter paper was Whatman 120. The stock solutions were an alcoholic 1% (w/v) solution of diphenylcarbazone and a 200 p.p.m. solution of mercury in triple distilled water. This was diluted to the required concentrations. The filter paper was chosen after trials of several varieties such as Whatman Nos. 1, 42, 540 and 542, which were found unsuitable for our method of producing concentrated homogeneous spots. Macherey, Nagel and Co. Duren No. 6a was better and No. 640d excellent, giving strongly colored uniform spots. The results, however, were not repeatable with a new batch of paper. Whatman 120 proved to be the most suitable; it absorbs quickly so that the spot does not spread out too much, and it dries quickly. The drying time and

method were strictly controlled. In order to overcome any inhomogeneity in the paper, each set of spots of the same concentration was placed on different areas of the filter strip in a systematic fashion. The test spots were formed on the Whatman 120 filter paper as follows: the filter paper, which is a stiff white card, was cut into strips measuring 22×4.5 cm. Two semicircular notches were cut in one edge of the card 8 cm apart, to register with two pins on the spot dropper and afterwards with two pins on the diffuse reflectance attachment. In this way two lines of spots 1.5 cm apart, comprising 18 spots altogether, could be accommodated on each strip of paper (Fig. 1). The dropper was a simple motorized microsyringe which delivered a 7-μl drop of reagent onto a point on the center line of the strip midway between the two notches, at a constant and repeatable flowrate. The reagent dried to a uniform circular spot of 12 mm diameter, having well-defined edges. After the reagent had dried for 10 min on a warm (about 50°C) surface, a second microsyringe was used to supply an 8-μl drop of the solution under test; the syringe holder ensured that the drop fell exactly in the center of the reagent spot, to form, on drying, a spot of 4-mm diameter. The specimen strip was transferred to the reflectance attachment, the two pins of which registered with its notches to ensure that the center of the test spot lay exactly in the center of the rectangle illuminated by the light beam. An opaque black metal strip was placed immediately behind the specimen to exclude ambient light, because the specimens were slightly translucent.

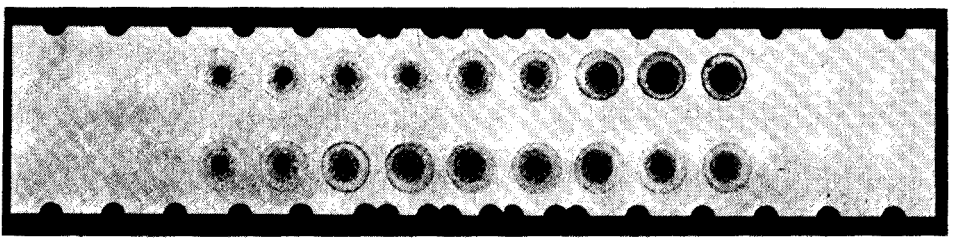

Fig. 1. Filter paper strip with specimen spots.

In the particular case of the mercury reaction, 2 drops of reagent were placed on the paper, one on top of the other, and after drying, a drop of water was delivered by the microsyringe. A reflectance measurement was made after further drying. Then one drop of test solution was added to the same spot and a second reflectance reading was made. From the Kubelka–Munk tables, the K/S values were obtained and $\Delta(K/S)$ (the difference in the values for water and solution) was plotted against concentration of mercury (Fig. 2).

From the reflectance spectrum obtained on the oscilloscope (Fig. 3a) it is seen that 560 nm, the minimum point on the curve, is the best wavelength for reflectance measurements.

RESULTS

The reaction used for the determination of mercury with diphenylcarbazone is the normal 1:2 complexation reaction[7], which takes place at pH 7.

Figure 3(a) shows 5 reflectance spectra. The upper curve is the spectrum of the diphenylcarbazone reagent, to which a drop of water has been added. The second curve is for the reagent to which had been added a drop of water and a drop of solution containing 20 p.p.m. Hg^{2+}. The third, fourth and fifth curves are for 40, 80 and 100 p.p.m. Hg^{2+}, respectively. The minimum point on the curve occurs at 560 nm. The $\Delta(K/S)$ values obtained at this wavelength are plotted versus concentration of mercury in Fig. 2. The curve increases monotonically for all concentrations of mercury(II), with a linear dependence of $\Delta(K/S)$ on mercury-(II) concentration up to about 40 p.p.m. Each point on the curve is the mean of measurements taken at three different places on the paper (as previously described). Six different concentrations can be measured on each filter paper strip, thus allowing an internal calibration for each set of measurements. Tests showed a standard deviation of less than 3% of the $\Delta(K/S)$ readings, so that the average reflectance of 3 spots is sufficiently accurate for our purposes.

Interfering ions

The ions Na^+, K^+, Mg^{2+}, Ca^{2+}, Sr^{2+}, Ba^{2+} do not interfere with the diphenylcarbazone tests for mercury(II), as demonstrated in the spectral reflectance curves of Fig. 3(b). The upper curve in the figure shows the spectral reflectance of the reagent alone; the lower curve is a multiple exposure from 5 spots of

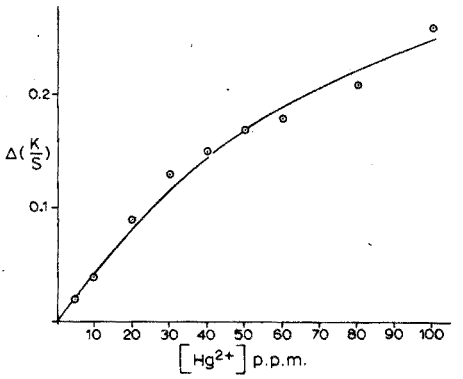

Fig. 2. $\Delta(K/S)$ *vs.* concentration of mercury.

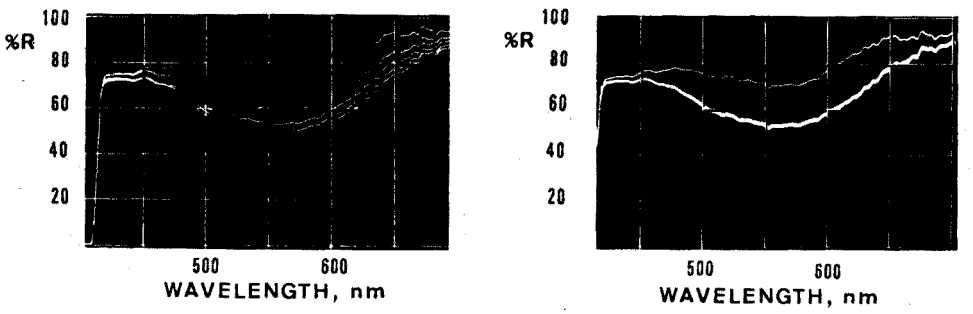

Fig. 3. Reflectance spectra of mercury-diphenylcarbazone: (a) at different concentrations; (b) in the presence of non-interfering ions.

mercury(II) solutions (50 p.p.m.) containing respectively 10 p.p.m. of Na^+, K^+, Mg^{2+} and Ba^{2+}, and the mercury(II) alone. Bismuth(III) does not interfere with the test, since it is not soluble at pH 7.

Figure 4(a) shows spectral reflectance curves for spots made with solutions containing cadmium(II). The upper curve is from a reagent spot to which a drop of water (representing 0 p.p.m. Cd^{2+} and 0 p.p.m. Hg^{2+}) had been added. Note that the reflectance at the test wavelength of 560 nm is slightly reduced, but that there is no confusion with the effect of mercury(II). The lower trace in the figure is the superimposed reflectance curves for spot tests with 40 p.p.m. Hg^{2+} solutions, respectively with and without 10 p.p.m. of Cd^{2+}. The two curves do not coincide exactly, but at the test wavelength of 560 nm, the interference of 10 p.p.m. of Cd^{2+} is seen to be negligible. This is demonstrated throughout the mercury(II) series quantitatively in Table I.

Figure 4(b) shows spectral reflectance curves for drops made from solutions containing lead(II). For reference, the second curve shows the reagent alone. The upper curve is for a spot test carried out with a 10 p.p.m. Pb^{2+} solution without any mercury(II). Note that this curve differs in shape from that obtained with mercury(II) in that there is a smaller reduction in reflectance at 420 nm and, as for cadmium(II), no reduction above 650 nm. The two lower curves are for spot tests with 40 p.p.m. Hg^{2+} solutions with (lowest curve) and without 10 p.p.m. of lead(II). The curves have similar shapes. The presence of lead(II) leads to an overestimate (in the order of 15% at the 10 p.p.m. level) in the determination of mercury(II) (see Table I) and lead(II) must be eliminated first.

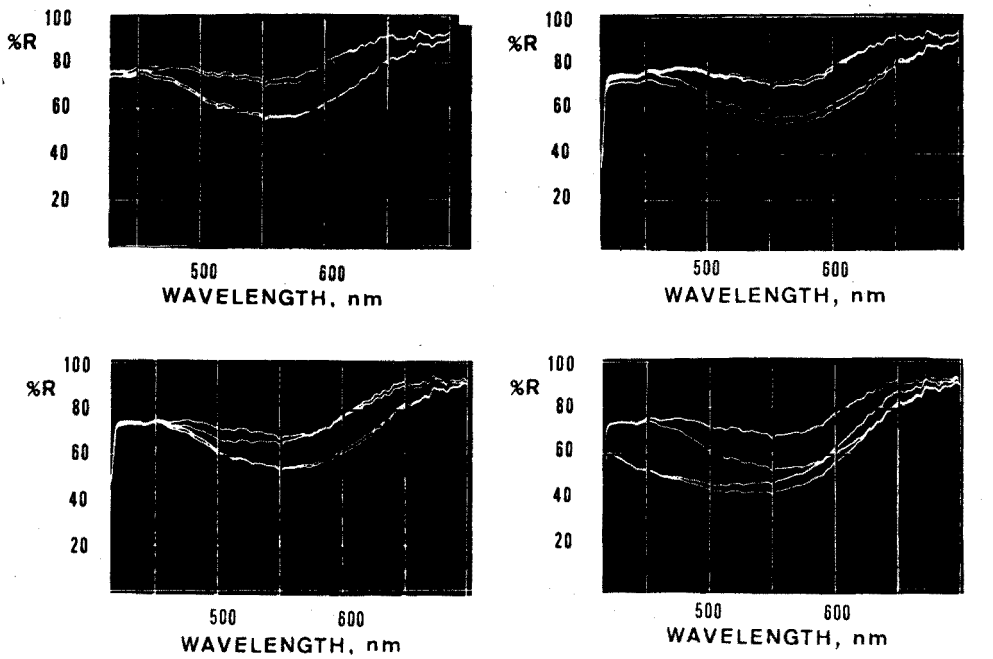

Fig. 4. Reflectance spectra of diphenylcarbazone with: (a) Cd^{2+}, Hg^{2+} and $Cd^{2+}+Hg^{2+}$; (b) Pb^{2+}, Hg^{2+} and $Pb^{2+}+Hg^{2+}$; (c) Fe^{2+}, Hg^{2+} and $Fe^{2+}+Hg^{2+}$; (d) Cu^{2+}, Hg^{2+} and $Cu^{2+}+Hg^{2+}$.

TABLE I

$\Delta(K/S)$ VALUES FOR MERCURY ALONE AND IN THE PRESENCE OF CADMIUM AND LEAD

Conc. Hg^{2+} (p.p.m.)	*Hg^{2+}*		
	Alone	*10 p.p.m. Cd^{2+}*	*10 p.p.m. Pb^{2+}*
5	0.02	0.02	0.02
10	0.04	0.04	0.06
20	0.09	0.08	0.12
30	0.14	0.14	0.17
40	0.18	0.17	0.21

Iron(III) interferes seriously with the test, producing a non-uniform spot with a bright purple ring surrounding a pale pink center. The spectral reflectance of the center is quite different from the mercury(II) spectrum. However, if the iron is reduced to iron(II), the interference is much less (see Fig. 4c). In this figure, the two upper curves are for the reagent with 0 and 10 p.p.m. iron(II); the two lower curves are for 40 p.p.m. mercury(II) with 0 and 10 p.p.m. Fe^{2+}. Copper(II) also gives an entirely different reflectance spectrum, unmistakeable from the mercury(II) curve. (The four spectra in Fig. 4(d) show respectively, reagent with water, reagent with 40 p.p.m. Hg^{2+}, reagent with 10 p.p.m. Cu^{2+} and reagent with 40 p.p.m. Hg^{2+} and 10 p.p.m. Cu^{2+}.)

A summary of these results is given in Table II.

CONCLUSIONS

Mercury can be characterized and determined in the range 5–100 p.p.m. by

TABLE II

INTERFERENCE OF OTHER IONS ON QUANTITATIVE SPOT TESTS FOR MERCURY(II)

Ion	*Tested alone*	*Present in [Hg^{2+}] test*
Na^+, K^+, Mg^{2+}, Ca^{2+}, Sr^{2+}, Ba^{2+}, Bi^{3+}	Reagent unaffected	Test unaffected
Sn^{2+}	Reflectance increased	[Hg^{2+}] underestimated
Cd^{2+}	Reflectance reduced, except for $\lambda > 650$ nm	Test unaffected
Pb^{2+}	Spectrum changed, especially for $\lambda < 560$ nm	[Hg^{2+}] overestimated
Cu^{2+}	Spectrum changed drastically and characteristically	Characteristic change in spectrum; [Hg^{2+}] determination impossible
Fe^{3+}	Drastic change in spectrum	Changes spectrum drastically; [Hg^{2+}] determination impossible
Fe^{2+}	Some change in spectrum, but none at 560 nm	At 10 p.p.m. Fe^{2+}, no interference

measurements of the compound formed with diphenylcarbazone as spot tests on filter paper. The following substances do not interfere with the determination: Na^+, K^+, Mg^{2+}, Ca^{2+}, Sr^{2+}, Ba^{2+} and Bi^{3+}. In the absence of mercury(II), cadmium(II) modifies the spot reflectance spectrum of the reagent, and can therefore be identified. The presence of cadmium(II) does not, however, affect the determination of mercury(II) in concentrations greater than 5 p.p.m. Pb^{2+}, Cu^{2+} and Fe^{3+} produce characteristically different reflectance spectra and must be masked before the determination of mercury(II). Iron(II) does not interfere.

A variety of ions can be determined by reflectance spectra of their colored compounds formed during the spot test. A collection of the reflectance spectra of a series of these ions is currently being prepared in this laboratory.

This work was supported by the Israel National Council of Research and Development.

SUMMARY

Reflectance spectra of mercury with diphenylcarbazone as spots on filter paper were measured by a scanning spectroreflectometer. A functional dependence was found between K/S values of the Kubelka–Munk equation and the concentrations of mercury(II) in solution within the range 5–100 p.p.m. Reflectance spectra of Na^+, K^+, Ca^{2+}, Sr^{2+}, Ba^{2+}, Mg^{2+}, Fe^{2+} and Cd^{2+} ions with the reagent show that these ions do not interfere. Pb^{2+} and Fe^{3+} do interfere. Cd^{3+}, Fe^{3+} and Cu^{2+} and Pb^{2+} produce characteristic changes in the reflectance spectrum.

REFERENCES

1 W. W. Wendlandt and H. G. Hecht, *Reflectance Spectroscopy*, Wiley–Interscience, New York, 1966.
2 G. Kortum, *Reflectance Spectroscopy*, Springer-Verlag, Berlin, 1969.
3 M. M. Frodyma, D. F. Zaye and Van T. Lieu, *Anal. Chim. Acta*, 40 (1968) 451.
4 C. W. Ayers, *Mikrochim. Acta*, 85 (1956) 1333.
5 P. Kubelka and F. Munk, *Z. Tech. Phys.*, 12 (1931) 593.
6 W. Braun and G. Kortum, *Zeiss Mitteilg.*, 4 (1968) 379; *Zeiss Inform.*, 16 (1968) 27.
7 F. Feigl, *Spot Tests in Inorganic Analysis*, Elsevier, Amsterdam, 1958.

Analytica Chimica Acta, 74 (1975) 261–268

TWO MICROMETHODS FOR THE DETERMINATION OF LOW SULPHUR DIOXIDE CONTENTS IN GLASS

A. H. GERRARD, N. A. MURPHY and C. PARTON

Pilkington Brothers Limited, Research & Development Laboratories, Lathom, Ormskirk, Lancashire (England)

E. PELL and H. PUXBAUM

Institute for Analytical Chemistry and Microchemistry, Technical University, Vienna (Austria)

(Received 14th July 1974)

Knowledge of both the fundamental properties of gases in glass and the gas contents of commercial glasses is of great interest to glass technologists. Large numbers of experiments have been carried out by various workers to determine the quantity and nature of dissolved gases in glass.

In the present investigation, the authors have studied sulphur dioxide since this is considered to be the most soluble gas in many commercial glasses and hence one of the most important. The main sources of sulphur dioxide are the sulphates added as part of the glass batch and the sulphur impurities present in the fuel oils. Several experimental methods have been reported concerning analyses for the sulphur dioxide content of glasses[1–8]. However, some of these techniques have not been used on commercial glasses, whilst some have given inconsistent results. It was considered by the authors that the best way to obtain precise and accurate analytical values was by means of co-operation between two laboratories, each investigating a different technique on fully comparable samples.

THE VACUUM FUSION–MASS SPECTROMETRIC METHOD

A vacuum fusion–mass spectrometric technique was developed at Pilkington Brothers Limited. This method involves the degassing of the glass sample by vacuum fusion at 10^{-6} torr at 1300–1500°C. The evolved gases containing sulphur dioxide are collected in a 2-l reservoir and then leaked into a MS2 mass spectrometer. The peak height of mass 64 corresponding to sulphur dioxide is measured directly and the amount of sulphur dioxide in the glass is expressed as percentage sulphur trioxide in accordance with the usual practice adopted in the Glass Industry.

Method

A diagrammatic representation of the apparatus is shown in Fig. 1. The extraction vessel consists of a Purox recrystallized alumina crucible (10-mm o.d. and 90 mm long) situated near the closed end of an L-shaped quartz tube. The section of the tube containing the crucible can be introduced into a small horizontal

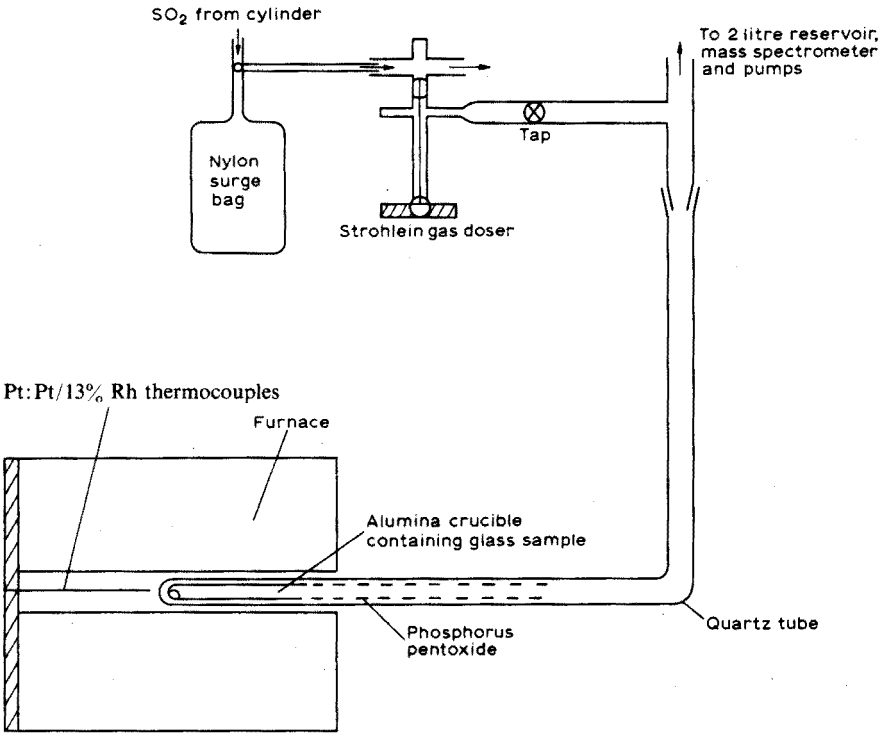

Fig. 1. Diagrammatic representation of the gas extraction apparatus.

tube furnace and is connected via a needle valve to the 2-l reservoir of the mass spectrometer.

The glass sample to be analysed is washed, dried, weighed and placed in the quartz tube at the elbow. Before the analysis, the quartz tube and crucible are fully degassed at 1300°C for 1 h at a pressure of 10^{-6} torr, and then taken slowly from the furnace and allowed to cool. The tube is disconnected from the vacuum system and the glass sample dropped into the crucible. A small quantity of phosphorus pentoxide is then added to the crucible and to the upper portions of the tube. The addition of A.R. phosphorus pentoxide is necessary to prevent alkali vapours, which are evolved from the glass on melting, from interfering with the sulphur dioxide determination. Without the presence of phosphorus pentoxide, very low and inconsistent results are obtained. The quartz tube is reconnected to the vacuum system and evacuated at room temperature. After the pumps have been isolated, it is installed in the furnace at 1300°C; the temperature in the central hot zone is continually recorded.

Sulphur dioxide is evolved and collected over the temperature range 1300–1500°C in the 2-l reservoir and then leaked into the MS2 mass spectrometer. The mass-64 peak height is continuously monitored until it reaches a maximum value. From this, the sulphur dioxide content of the glass can be calculated after suitable calibration of the instrument. The time taken for extraction and analysis is approximately 30 min.

Calibration

Glass standards of known sulphur dioxide contents are not available, and therefore the calibration of the system is achieved by introducing known volumes of anhydrous sulphur dioxide gas, corrected to NTP, into the hot extraction system. This is accomplished by the use of a gas-dosing device which is fed from a nylon surge bag to ensure that the gas is at atmospheric pressure. The maximum height of the mass-64 peak for each volume added is measured on a 7-channel recorder and plotted as a calibration curve (Fig. 2). The volume of sulphur dioxide from the sample is then determined and the percentage of sulphur trioxide calculated. A peak height of 10 mm on the recorder chart is equivalent to $7.4 \cdot 10^{-8}$ g of sulphur dioxide, which corresponds to $9.3 \cdot 10^{-8}$ g of sulphur trioxide.

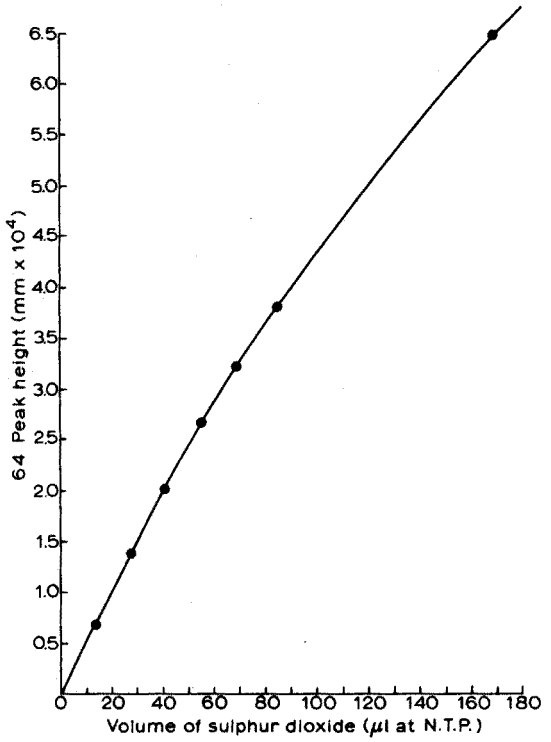

Fig. 2. Calibration curve for mass spectrometric method.

For direct comparison of values obtained by the two methods, an arbitrary standard glass was also used for calibration.

Results and discussion

Three glasses were selected for analysis; a commercial float glass (Glass 1), an experimental glass of similar basic composition but with a lower sulphur dioxide content (Glass 01) and an experimental highly viscous glass (Glass 3). These glasses were crushed into small pieces, washed and dried. For each

determination a sample (one or two pieces) weighing 100–150 mg was used. A total of 98 samples of Glass 1 was analysed; the results obtained are shown in Table I. The results of six individual series are shown. Each series relates to the use of a particular filament or ion source in the mass spectrometer. Table I also gives the results for eight samples of Glass 01 and eight samples of Glass 3.

In this technique the presence of phosphorus pentoxide in the extraction vessel appears to overcome the problems of reaction with alkali vapours. The method is specific for sulphur dioxide and errors can arise only from incomplete degassing of the glass or by reaction of the sulphur dioxide with other evolved species.

TABLE I

SULPHUR TRIOXIDE CONTENTS OF DIFFERENT GLASSES

Glass	n_x[a]	$\bar{x}$[b] (%SO_3) (SO_2 *gas standard*)	s[c] (%SO_3)	s_r[d] (%)	$\bar{x}$[b] (%SO_3) *(glass standard)*
1	20	0.220	0.014	6.5	0.248
1	10	0.228	0.011	4.8	0.257
1	10	0.224	0.0087	3.9	0.252
1	20	0.223	0.0118	5.3	0.251
1	30	0.216	0.0122	5.7	0.243
1	8	0.220	0.0113	5.1	0.248
01	8	0.018	0.0008	4.4	0.020
3	8	0.006	0.0007	11.7	0.006

[a] Number of samples analysed in each series.
[b] Mean SO_3 content.
[c] Standard deviation.
[d] Relative standard deviation.

THE CARRIER GAS FUSION–RELATIVE CONDUCTIMETRIC METHOD

The carrier gas fusion–relative conductimetric method is based on principles used in the determination of the sulphur content of ferrous and non-ferrous metals and in the determination of the sulphur content of organic substances[9–13]. The method consists of a gas extraction system based on the carrier gas fusion principle and a sulphur dioxide detection system involving relative conductimetry.

Preliminary experiments showed that under normal atmospheric pressure and a furnace temperature of 1250°C, a 50-mg sample of float glass required more than 2 h to be fully degassed. Efforts were therefore directed towards considerably reducing this time.

Glass technologists are aware that additions of oxides to melts rich in silica result in less viscous melts. Table II gives the reduction in the melting temperature of silica by the addition of various oxides. This table was compiled from data given in the literature[14].

The rate of degassing of 50-mg glass samples was studied with metal oxides and metals as a flux. The ratio of glass:flux was 1:10 with a furnace temperature

TABLE II

THE REDUCTION OF MELTING TEMPERATURE OF SILICA BY OXIDES ACCORDING TO PHASE DIAGRAM FOR CERAMISTS

System	t^0Eu[a]
SiO_2	1723
SiO_2–Al_2O_3	1595
SiO_2–FeO	1180
SiO_2–MnO	1251
SiO_2–CuO	1060 (91% CuO)
SiO_2–PbO	710

[a] t^0Eu = eutectic temperature for the phase SiO_2–MeO.

TABLE III

DEGASIFICATION OF GLASS WITH ADDITIONS IN THE WEIGHT RATIO OF 1:10 AT 1260 °C

Addition	*E(%)*[a]	*Addition*	*E(%)*
SiO_2	67		
Al_2O_3	70		
Fe_2O_3	57	Fe	43
CuO	98	Cu	98
MnO_2	98	Bi	98
PbO_2	93	Sn	57

[a] *E(%)* = Amount extracted expressed as a percentage of the expected value.

of 1250°C. The amount of sulphur dioxide extracted from the glass, expressed as a percentage of the expected content, is given in Table III. Further investigation showed that the most successful flux was a mixture containing 84% of elemental copper and 16% of elemental iron.

Commercial alkali glasses usually contain trace amounts of halides, particularly chloride, and in some special glasses fluoride. On combustion, the halides are evolved from the glass mainly as hydrogen chloride and hydrogen fluoride, respectively. These acidic gases interfere with the determination of the sulphur dioxide and are removed by a scrubbing agent consisting of granules made by melting equal parts of silver sulphate and potassium pyrosulphate in a nickel crucible and coarsely pulverizing the cooled melt. The absorption tube was packed with granules of 0.5–2 mm^3, and interposed in the gas stream between the combustion tube and the measuring cell.

Method

The arrangement of the apparatus is shown in Fig. 3. About 50 mg of powdered glass is weighed into a pre-degassed porcelain boat and is overlaid with 500 mg of a flux mixture; the whole is gently mixed with a nickel spatula. The flux consists of 84% elemental copper (electrolytic copper wire) and 16% elemental iron (carbonyl iron powder). The boat is pushed into the furnace and

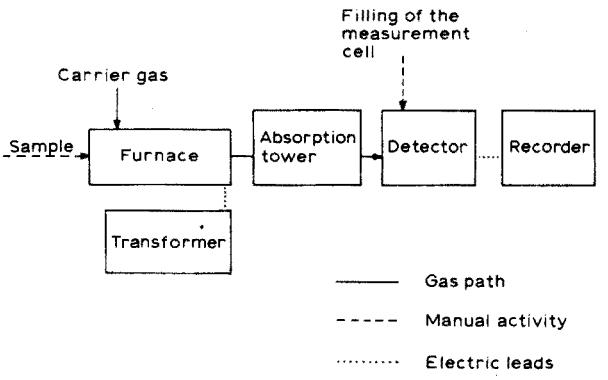

Fig. 3. Relative conductimetric apparatus for determining gases in glass.

heated in a stream of purified oxygen at 1250°C. The furnace is an impervious twin-tube silicon carbide rod unit with a 200 mm long hot zone. Combustion of the sample takes place in one of the impervious porcelain tubes while the other is used to outgas the boat for the next sample. The sulphur dioxide evolved from the glass is pulled through the halogen absorption tube and into the relative conductivity cell by a gas pump. This cell contains an absorption solution (0.001 *M* sulphuric acid and 0.015% hydrogen peroxide). The output from the conductivity cell is amplified and fed to a single-channel potentiometric recorder, and the peak height is measured. All the glasses investigated were fully degassed after 10 min under the specified conditions.

Calibration

The instrument was calibrated by the combustion of weighed samples (100–500 μg) of sulphanilic acid in a platinum crucible under the same conditions as the samples under test. The rate of evolution of sulphur dioxide from the sulphanilic acid was similar to that from the glass-flux melt and thus the standardization procedure suggested for this type of instrument[1,2] was accomplished.

A peak height of 10 mm on the recorder chart, for the above absorption

TABLE IV

THE SULPHUR TRIOXIDE CONTENTS OF DIFFERENT GLASSES

Glass	n_x	$\bar{x}$ (% SO_3) *(sulphanilic acid standard)*	s (% SO_3)	s_r (%)	$\bar{x}$ (% SO_3) *(glass standard)*
1	9	0.275	0.0038	1.5	0.256
1	10	0.271	0.0019	0.7	0.252
1	10	0.270	0.0019	0.7	0.251
1	6	0.273	0.00245	0.9	0.254
7	6	0.233	0.00403	1.7	0.217
8	6	0.265	0.00447	1.8	0.246
9	4	0.030	0.00060	2.0	0.028
3	7	0.007	0.00024	3.4	0.007

solution, was equivalent to $1.2 \cdot 10^{-5}$ g of sulphur dioxide, which corresponds to $1.5 \cdot 10^{-5}$ g of sulphur trioxide.

The same arbitrary standard glass as used in the mass-spectrometric method was also used for calibration, so that the two methods could be directly compared.

Results and discussion

For statistical reasons, a large piece (300 mm × 50 mm) of commercial float glass was pulverized under acetone in an agate mortar and the powder was homogenized by cone teeming. Four series of analysis were carried out with Glass 1. Similar experiments were made with other glasses. The results obtained (Table IV) demonstrate clearly that this method can be used with confidence for the glasses studied.

COMPARISON BETWEEN THE TWO METHODS

Table V compares the results obtained for two dissimilar glasses by the two analytical methods described. For convenience the results for each glass are grouped together.

TABLE V

COMPARISON BETWEEN THE RESULTS OF MASS SPECTROMETRIC METHOD AND THE RELATIVE CONDUCTIMETRIC METHOD

(A standard glass was used for calibration)

Method	*Glass*	n_x	$\bar{x}$ (% SO_3)	s (% SO_3)	s_r (%)
MS	1	98	0.248	0.013	5.2
MS	3	8	0.007	0.0008	11.4
RC	1	35	0.253	0.002	0.8
RC	3	7	0.007	0.0002	2.9

Both methods are suitable for the determination of the sulphur content of small glass samples in the range of 10–200 mg weight and for sulphur trioxide contents of 0.007 wt.% and above. For higher contents, only the size of the sample has to be changed or, in the conductivity method, the concentration of the absorption solution. The relative conductivity method is more precise than the mass spectrometric method but it is not suitable for the simultaneous determination of other gases. As far as the time factor is concerned, the relative-conductimetric method is faster.

The authors wish to thank Professor H. Malissa for his helpful advice, encouragement and hospitality throughout this investigation. The Pilkington authors wish to thank Miss M. Jones for her assistance with their experimental work. This paper is published with the permission of the Directors of Pilkington Brothers Limited, and Dr. D. S. Oliver, Group Director of Research and Development.

SUMMARY

Two experimental methods for the determination of the sulphur dioxide contents (70–5000 p.p.m.) of small glass samples are presented. The first method involves vacuum fusion–mass spectrometric techniques whilst the second method is based on fusion-carrier gas–relative conductimetric techniques. Incorporated into both methods are techniques for the removal of interfering species, such as alkali and hydrogen chloride. The first method allows simultaneous determinations of other gases, but the second method is faster and more precise.

REFERENCES

1 R. Boulin, R. Desguin and E. Jaudon, *Chin. Anal.*, 36 (1954) 123.
2 C. J. B. Fincham and F. D. Richardson, *Proc. Roy. Soc., Ser. A*, 223 (1954) 40.
3 T. Okamura, *Reports of Res Laboratory, Asahi Glass Co.*, V (2) (1955) 1.
4 V. T. Slavyanskii, *Steklo Keram.*, 14 (2) (1957) 11.
5 F. Gebhardt and A. Sistermanns, *Glastech. Ber.*, 39 (10) (1966) 458.
6 W. D. Johnston and F. D. Kessler, *Ceram. Bull.*, 46 (6) (1967) 570.
7 S. Holmquist, *J. Amer. Ceram. Soc.*, 49 (9) (1966) 467.
8 J. Zluticky, J. Stverak and L. Nemec, *Glastech. Ber.*, 45 (9) (1972) 506.
9 W. Koch and H. Malissa, *Arch. Eisenhuetten.*, 27 (1956) 695.
10 L. Machherndl, Dipl. Arbiet am Institut f. Analytische Chemie und Mikrochemie TH, Wien, 1961.
11 E. Pell, L. Machherndl and H. Malissa, *Mikrochim. Acta (Wien)*, 3 (1962) 835.
12 B. R. Chamberlain, *Anal. Chim. Acta*, 57 (1971) 81.
13 E. Pell, H. Malissa, N. A. Murphy and B. R. Chamberlain, *Anal. Chim. Acta*, 43 (1968) 423.
14 E. M. Levin, C. R. Robbins and H. F. McMurdie, *Phase Diagrams for Ceramists*, The American Ceramic Society, 1964.

Analytica Chimica Acta, 74 (1975) 269–274

NON-DESTRUCTIVE DETERMINATION OF TUNGSTEN IN MOLYBDENUM BY NEUTRON ACTIVATION ANALYSIS, FROM MULTIPLE γ- AND X-RAY PEAK RATIOS

N. LAVI

Isotope Applications Department, Soreq Nuclear Research Centre, Yavne (Israel)

(Received 24th June 1974)

In this laboratory generators which produce ^{99}Mo–^{99m}Tc from irradiated molybdenum trioxide have been constructed. The feasibility of using irradiated molybdenum metal instead of molybdenum trioxide has been investigated experimentally. The molybdenum metal used to prepare generators of ^{99}Mo–^{99m}Tc must be as free of impurities as possible. Molybdenum metal must be analyzed for tungsten because molybdenum and tungsten are members of the same group of elements in the Periodic Table, and may occur together in natural materials such as metals, rocks and ores.

Various workers have recommended the use of thiocyanate[1,2] as a reagent for the spectrophotometric determination of tungsten and molybdenum. The disadvantage of this method is its poor color stability. Dithiol[3] may also be used to

BLE I

CLEAR DATA FOR THERMAL NEUTRON ACTIVATION OF TUNGSTEN

get lide	*Abundance (%)*	*Neutron capture cross section (barn)*	*Product of thermal neutron activation*	*Half-life*	*Radiation and γ-energy (keV)*[12]	*K x-Ray energy(keV)*
W	0.135	20	^{181}W	130 d	E.C., 136.3, 152.5	$K\alpha_1$ Ta, 57.5 $K\alpha_1$ Ta, 56.3 $K\beta_1$ Ta, 65.2 $K\beta_2$ Ta, 67.0
W	26.41	0.5	^{183m}W	5.3 s	I.T., 46.5, 52.6, 99.1, 107.9, 160.5	$K\alpha_1$ W, 59.3 $K\alpha_2$ W, 58.0 $K\beta_1$ W, 67.2 $K\beta_2$ W, 69.1
W	14.40	10.2	^{184}W(stable)			
W	30.64	0.01	^{185m}W	1.6 min	I.T.,66.1, 122.1, 131.7, 173.8	$K\alpha$ W, $K\beta$ W
		1.8	^{185}W	74 d	β, 125.4	
W	28.41	38	^{187}W	23.8 h	β, 72, 134.2, 479.5, 551.5, 618.2, 625.4, 685.7, 735.6, 772.8	$K\alpha_1$ Re, 61.1 $K\alpha_2$ Re, 59.7 $K\beta_1$ Re, 69.3 $K\beta_2$ Re, 71.2

determine tungsten and molybdenum, but this determination of tungsten is inaccurate when more than trace amounts of molybdenum are present. A method based on counter-current extraction of 5 p.p.m. or more of tungsten in a molybdenum matrix has been described by Kallmann *et al.*[4]. Adsorption of molybdenum and elution of tungsten[5] on an anion-exchange column is also feasible, but a sample of at least 1 g is required and its preparation is time-consuming. Neutron activation analysis for tungsten has also been carried out[6], based on the short-lived nuclide ^{183m}W and the long-lived nuclide ^{187}W. The ^{187}W nucleus decays by β-ray emission with a half-life[7] of 23.8 h to excited levels of ^{187}Re. The depopulation of the ^{187}W levels to the ground state occurs via many γ-transitions, 44 in all[8], but some are very weak.

In the present work, tungsten was determined in a molybdenum matrix by thermal neutron activation analysis followed by high-resolution γ- and x-ray spectrometry. The nuclear reactions resulting from thermal neutron (n, γ) irradiation of tungsten are summarized in Table I. It can be seen that ^{187}W is formed with a comparatively large cross-section[7].

The γ-ray activities of ^{99}Mo and ^{187}W were measured with a calibrated Ge(Li) detector. The $K\alpha$ and $K\beta$ x-rays of Re, Mo and Tc derived from ^{187}W, ^{99}Mo and ^{99m}Tc, respectively, were measured with a calibrated Si(Li) detector. The peak ratios of γ- and x-ray activities derived from the ^{187}W were then calculated.

EXPERIMENTAL

Standards and irradiation

Twenty tungsten standards were made as follows: six were 200–400 μg of tungsten foil, eight were 60–200 μg of tungsten trioxide (Johnson Matthey Specpure reagent) and six were 10–30 μg of sodium tungstate, obtained by evaporating dilute solutions of sodium tungstate on aluminum foil. They were introduced into a quartz ampoule together with nine samples of molybdenum metal in the 6–10 mg range, and irradiated for 1 h in the IRR-1 reactor in a thermal flux of $1 \cdot 10^{13}$ n cm^{-2} s^{-1}. The γ- and x-ray activities derived from ^{187}W and ^{99}Mo were measured 2 days after the end of irradiation. Each sample was measured for 10 min.

Counting

The γ-rays were measured with a true coaxial 29 cm^3 Ge(Li) detector (Elscint, Israel) connected to a preamplifier (CA-N-1/C), an Ortec 410 amplifier and an Ortec 408 biased amplifier. The resulting pulses were analyzed by a 400-channel analyzer (T.M.C.). The energy resolution (F.W.H.M.) of the system was 2.6 keV for 122-keV ^{57}Co γ-rays and 3.5 keV for 1332-keV ^{60}Co γ-rays. The absolute photopeak efficiency of the detector was obtained by counting calibrated sources of ^{75}Se (ref. 9) and ^{166m}Ho (ref. 10). The x-rays were measured by means of a 100-mm^2, 4-mm depth Si(Li) detector (Seforad, Israel). The output signals from the detector were passed through an Ortec 118 preamplifier, an Ortec 410 amplifier and an Ortec 408 biased amplifier. The energy resolutions (F.W.H.M.) of the system for 6.4-keV Fe $K\alpha$ x-rays (obtained from ^{57}Co) and 31.7-keV Ba $K\alpha$ x-rays (obtained from ^{137}Cs) were 450 eV and 550 eV, respectively. A 1.6-mm

plastic absorber was used to avoid interference in x-ray spectrometry caused by β-decay.

RESULTS AND DISCUSSION

The activity of ^{187}W relative to that of ^{99}Mo, produced by irradiation in the reactor, increases with an increase in the cadmium ratio, which involves an increase of the thermal neutron flux, compared with the epithermal component. Because of the large ratio of the resonance integral to the thermal neutron activation cross-section for ^{98}Mo ($I_0/\sigma_0 = 49.56$)[11], it is necessary to irradiate the molybdenum in a high thermal neutron flux relative to the epithermal flux, in order to decrease the interference of ^{99}Mo produced by the epithermal flux. The interference of molybdenum is then very small, because the thermal neutron cross-section ^{98}Mo is low[11] (0.137 b) compared to that of ^{186}W (38 b) (ref. 7).

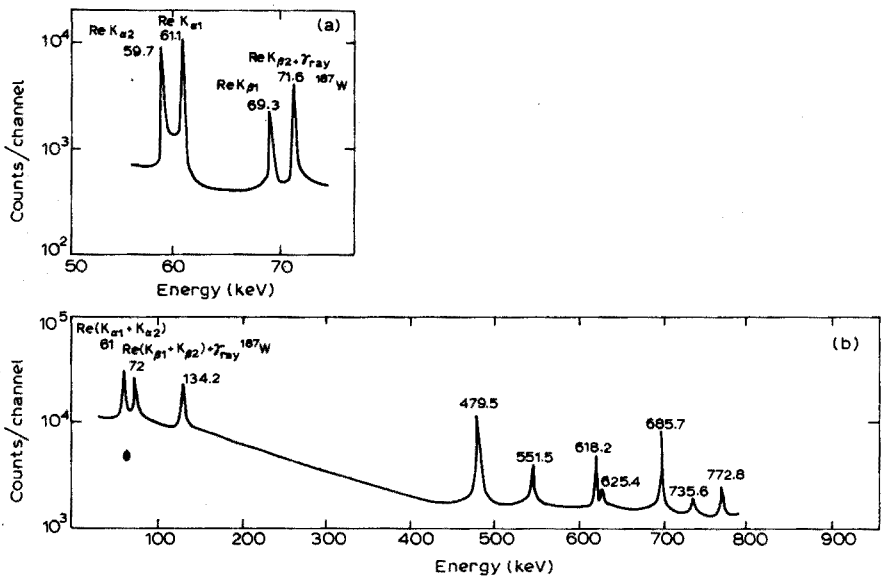

Fig. 1. Comparison of x-ray (a) and γ-ray (b) spectra obtained from a 380-μg sample of tungsten foil irradiated for 1 h and counted for 10 min after a cooling time of 2 days.

Typical γ- and x-ray spectra of ^{187}W are shown in Fig. 1. For evaluation, the 479.5, 551.5, 618.2+625.4, and 685.7-keV photopeak areas of ^{187}W were integrated and their ratios calculated. The (Re $K\alpha_1$+Re $K\alpha_2$), Re $K\beta_1$ and (Re $K\beta_2$+γ-ray) photopeak areas, (61.1+59.7), 69.3 and (71.6+72) keV, respectively, were also integrated and their ratios calculated.

The values of 8 γ- and x-ray ratios are summarized in Table II. The values of photopeak area ratios of ^{187}W derived from the tungsten standards are in agreement with those obtained from the tungsten in molybdenum metal. The method described above gives an accurate calculated result matching the measured ones within experimental error. It can be seen from Table II that values of

TABLE II

COMPARISON BETWEEN PHOTOPEAK AREA RATIOS OF ^{187}W γ-RAYS AND Re K X-RAYS DERIVED FROM TUNGSTEN[a] AND TUNGSTEN IN MOLYBDENUM[b] METAL

	479.5/551.5 keV	*479.5/618.2[c] keV*	*479.5/685.7 keV*	*685.7/618.2[c] keV*	*685.7/551.5 keV*
Tungsten standards	5.275±0.08 (1.5%)	4.26±0.07 (1.7%)	1.29±0.01 (0.7%)	3.29±0.06 (1.95%)	4.08±0.07 (1.67%)
Tungsten in Mo metal	5.265±0.13 (2.5%)	4.15±0.09 (2.2%)	1.27±0.02 (1.8%)	3.25±0.07 (2.2%)	4.03±0.09 (2.2%)

	Re $K\alpha_1+K\alpha_2/Re\ K\beta_1$	*Re* $K\alpha_1+K\alpha_2/Re\ K\beta_2+\gamma_1$[d]	*Re* $K\beta_2+\gamma_1$[d]$/Re\ K\beta_1$
	8.045±0.15 (1.9%)	3.16±0.05 (1.6%)	2.67±0.06 (2.4%)
	8.04±0.17 (2.1%)	3.12±0.07 (2.3%)	2.63±0.08 (2.9%)

[a] Mean of results of analyses of 20 tungsten standards: 6 W-foil, 8 WO_3 and 6 Na_2WO_4. The errors are standard deviations.
[b] Mean of results of analyses of 9 samples of tungsten in molybdenum metal.
[c] The figure, 618.2, relates to the composite peaks of 618.2 and 625.4-keV γ-rays.
[d] The term relates to the composite peaks of the 71.2-keV Re $K\beta_2$ x-ray and the 72-keV γ-ray (branching ratio 11%) of ^{187}W.

(3.16+0.05) and (3.12+0.07) for the tungsten standards and tungsten in molybdenum metal, respectively, were obtained from the ratio (Re $K\alpha_1 + K\alpha_2$)/(Re $K\beta_2 + \gamma$). This ratio is explained by the fact that the Re $K\beta_2$ peak is composed of Re $K\beta_2$ (71.2 keV) and a 72-keV γ-ray (branching ratio[12] 11%) of ^{187}W, unresolved by the spectrometer used. The precision of the results is greatly increased because more than one photopeak is used in the calculation. The peak area ratios given in Table II allow the absence of interferences to be ascertained. (A substance in the matrix interfering with one or several peaks will modify the corresponding ratios.)

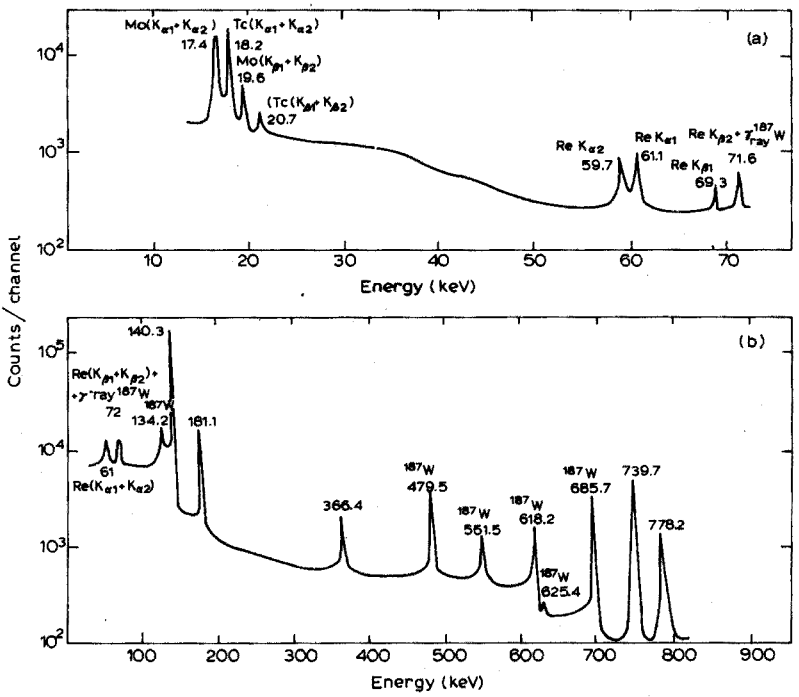

Fig. 2. Comparison of x-ray (a) and γ-ray (b) spectra obtained from a 9.21-mg sample of molybdenum foil, irradiated for 1 h and counted for 10 min after a cooling time of 2 days. Unlabeled peaks are derived from ^{99}Mo and ^{99m}Tc.

Typical x-ray and γ-ray spectra of ^{187}W in molybdenum metal are shown in Fig. 2.

The results obtained for the concentration of tungsten in varying amounts of molybdenum metal are compiled in Table III. A value of 0.199±0.038% of tungsten in molybdenum was found from the photopeak areas of γ-rays of ^{187}W. A precision of ±1.89% was obtained. The results are in good agreement with those obtained from the Re K x-rays, 0.195±0.004% (2.1%).

x-Ray spectrometry has the following advantages over γ-spectrometry: it is possible to determine several elements in a mixture, since each element gives rise to x-rays of characteristic and specific energies. Because of the low sensitivity of the Si(Li) detector to electromagnetic radiation above 60 keV, the higher-energy γ-rays do not interfere with the measurement of x-rays. Neutron activation analysis

TABLE III

TUNGSTEN CONTENT OF MOLYBDENUM METAL

Mo in sample (mg)	*Tungsten found*[a] *(μg)*	*Concentration of tungsten in molybdenum metal (%)*
7.980	15.84±0.37 (2.36%)	0.198
9.130	18.44±0.12 (0.65%)	0.202
8.480	16.42±0.24 (1.46%)	0.194
9.120	18.20±0.22 (1.21%)	0.200
7.720	14.88±0.26 (1.75%)	0.193
8.800	17.49±0.34 (1.94%)	0.199
9.210	18.55±0.17 (0.91%)	0.201
6.150	12.51±0.27 (2.15%)	0.203
8.380	17.01±0.28 (1.64%)	0.203
		Average 0.199±0.0038% (1.9%)

[a] Mean of 4 results obtained from 4 photopeaks (479.5, 551.5, 618.2+625.4, and 685.7 keV).

followed by high-resolution γ- and x-ray spectrometry, increases the accuracy of the determination of tungsten in the molybdenum matrix, and makes chemical separation unnecessary.

Irradiation of 1 μg of tungsten for 1 h in a thermal neutron flux of $1 \cdot 10^{13}$ n cm^{-2} s^{-1} produced 0.27 μCi ^{187}W. In order to obtain a higher sensitivity in the tungsten determination, samples may be irradiated for a longer period. The accuracy of these methods, based on γ- and x-rays photopeak area ratios, is generally better than $\pm 5\%$.

SUMMARY

Neutron activation analysis followed by high-resolution γ- and x-ray spectrometry has been applied to the determination of trace amounts of tungsten in molybdenum metal. The method is based on measurements of multiple γ-ray and x-ray peak ratios of ^{187}W activity. These peaks are used to calculate the amounts of tungsten in the sample, by the standard comparison technique. The tungsten concentration in molybdenum metal was found to be $0.199 \pm 0.004\%$.

REFERENCES

1 C. E. Crouthamel and C. E. Johnson, *Anal. Chem.*, 26 (1954) 1284.
2 A. T. Dick and J. B. Bingley, *Nature (London)*, 158 (1946) 516.
3 E. W. Hobart and E. P. Hurley, *Anal. Chim. Acta*, 27 (1962) 144.
4 S. Kallman, E. W. Hobart and H. K. Oberthin, *Anal. Chim. Acta*, 41 (1968) 29.
5 J. L. Hague, E. D. Brown and H. A. Bright, *J. Nat. Bur. Std.*, 53 (1954) 261; 62 (1959) 53.
6 H. Zinner, R. Henkelmann and H. Stark, *Radiochem. Radioanal. Lett.*, 10 (1972) 191.
7 *Chart of the Nuclides*, Bundensminister für Wissenschaftlich Forschung, Bonn, 3rd edn., 1968.
8 *Nucl. Data B1, No. 2*, June 1966.
9 N. Lavi, *Radiochem. Radioanal. Lett.*, 14 (1973) 385.
10 N. Lavi, *Nucl. Instru. Methods*, 109 (1973) 265.
11 G. H. E. Sims and D. G. Juhnke, *J. Inorg. Nucl. Chem.*, 29 (1967) 2853.
12 M. A. Wakat, *Nuclear Data Tables*, (1971) 8.

Analytica Chimica Acta, 74 (1975) 275–280

CATALYTIC–KINETIC DETERMINATION OF COPPER AND L-HISTIDINE WITH THE USE OF A LUMINOSTAT

SIEGBERT PANTEL and HERBERT WEISZ

Lehrstuhl für Analytische Chemie, Chemisches Laboratorium der Universität, Freiburg i.Br. (BRD)

(Received 14th August 1974)

In the "stat"-methods, a preset state of the catalyzed system,

$$A + B \xrightarrow{K} X + Y$$

is kept constant by adding a suitable reagent to such an extent as is necessary just to compensate the change of the concentration of a reactant, of a reaction product or of the ratio of both. Any suitable physical property of the system (after transformation of the measured effect into an equivalent voltage) which is proportional to the concentration of the substance which must be kept constant, may be used to regulate the rate of addition of a reagent.

This principle has been described for a pH-stat[1,2], potentiostat[3–5], absorptiostat[6] and biamperostat[7]. In this paper it will be shown that it is likewise possible by the regulated addition of an oxidizing reagent to keep a preset light level constant in catalyzed chemiluminescent reactions. To achieve this, the light level to be kept constant is transformed in a photomultiplier to an equivalent current and this current must be transformed to an equivalent voltage (mV range) by use of a current–voltage transducer; this potential is used to regulate the automatic titrator which adds the necessary oxidant to the catalyzed system. In analogy to the above-mentioned methods such an experimental set-up may be called a luminostat. It can be used for the determination of luminescence catalysts and their inhibitors.

In 1940 a mechanically working device was described[8] which was used to keep constant a definite luminescence for photographic purposes. It was in fact a flow-through-apparatus named "lumistat" by the author.

In the "stat"-method described here, use is made of the fact that various metal ions (*e.g.* Co, Mn, Cu, Pb) catalyze the chemiluminescent reaction between luminol (5-amino-2,3-dihydro-1,4-phthalazinedione) and hydrogen peroxide[9]. Simultaneously, these metal ions also catalyze the decomposition of hydrogen peroxide itself. The various metal ions catalyze these two reactions—luminescence and decomposition of hydrogen peroxide—to different extents. This means that—dependent on the catalyst used—sometimes the luminescence reaction predominates and sometimes the decomposition of hydrogen peroxide. In ammoniacal medium, for example, cobalt (II) has a much lower catalytic activity with regard to the decomposition of hydrogen peroxide than copper (II)[10]. Therefore, the higher the copper (II) concentration in the system, the more hydrogen peroxide per unit of time must be added to obtain an equal intensity of luminescence, because most of the hydrogen peroxide is decomposed.

In contrast, the higher the cobalt (II) concentration, the lower need be the rate of addition of hydrogen peroxide to maintain a steady luminescence. In both cases, the graphs of ml *vs.* time are almost linear.

When a luminostat is used, copper (II) and its inhibitors can easily be determined. The determination of cobalt (II) is more difficult because it is partially precipitated during the reaction, thus causing a heterogenous catalysis which is not always easily reproducible. To avoid these difficulties, it is necessary to work under well defined conditions. The determination range for cobalt is much smaller than in the case of copper.

The applicability of the luminostat will therefore rather be illustrated by the example of the copper(II)-catalyzed luminescent reaction of luminol with hydrogen peroxide; L-histidine is one of the possible inhibitors for copper in this reaction.

EXPERIMENTAL

Apparatus

As in all the "stat"-methods, it is necessary to keep constant a certain preset working potential. Again the "Combi-Titrator 3 D" (Metrohm, Herisau, Switzerland) consisting of a mV/pH meter, a controller (Impulsomat) and an automatic burette (1 ml) connected to a recorder (Mikrodosigraph) were used. The electrode input of the Impulsomat is connected to a current–voltage transducer (see Fig. 1a). This transducer converts the small current of the photomultiplier (Fig. 1a, PhM) to a proportional voltage (actual potential) in the mV-range. The potential difference between this actual potential and the preset working potential causes a signal to the automatic burette; the volume of the reagent consumed is recorded in relation to the time. The whole regulating circuit is arranged so that the motor-driven burette stops when the actual potential exceeds the preset working potential (compare instruction manual!) of 100 mV.

A 50-ml test tube (30-mm O.D.) is used as a reaction vessel. This test tube is

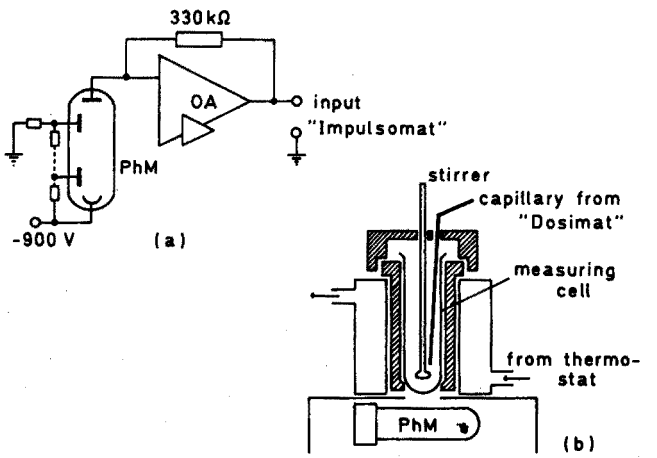

Fig. 1. (a) Schematic representation of the current–voltage transducer. PhM, photomultiplier MP-1021 (McKee-Pedersen Instruments, Danville, California). OA, operational amplifier MP-1031 (chopper-stabilized). (b) Schematic representation of the measuring cell.

kept in a hollow aluminium block connected to a thermostat. The aluminium block, with a suitable opening, is mounted on the photomultiplier (Fig. 1b). Stirrer and the capillary end of the burette are light-tight mounted on the aluminium block. All transparent parts of the apparatus outside the measuring cell are painted black.

The working temperature is 22.5 ± 0.2°C, and the recorder speed 15 mm min^{-1}.

Determination of copper by use of the copper (II)-catalyzed luminescent reaction of luminol with hydrogen peroxide

The chemiluminescent reaction of luminol with hydrogen peroxide is catalyzed by copper (II) in potassium hydroxide solution (heterogeneous catalysis) as well as in ammoniacal solution (homogeneous catalysis)[11-14]. During this reaction, hydrogen peroxide is consumed (by luminescence and self-decomposition, see above), the luminescence thus being reduced; after a new addition of hydrogen peroxide the luminescence increases again. The rate of addition of hydrogen peroxide necessary to maintain a preset potential (*i.e.* a defined intensity of luminescence) varies with the concentration of copper in the reaction system. For evaluation, the tangent of the inclination angle α of the recorder graphs (Fig. 2) is used.

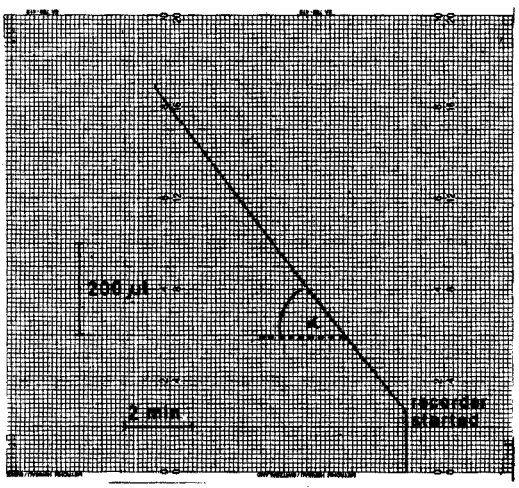

Fig. 2. Recorder graph for 45 µg of copper (II).

Procedure. Into the measuring vessel the following solutions are added: 1–10 ml of a copper solution (10 µg Cu ml^{-1} as copper (II) acetate) for preparing a calibration graph or an equivalent amount of a neutralized sample solution, 2 ml of aqueous 2 *M* ammonia, 0.5 ml of 0.1 % (w/v) luminol in 0.02 *M* sodium hydroxide, and twice-distilled water to 20 ml. After thermostating for 10 min, the automatic addition of hydrogen peroxide (2 mg H_2O_2 ml^{-1}) with the automatic burette is started. The recorder is started 2 min later, to obtain a linear graph after the adjustment of the system.

Figure 3 shows a calibration graph; some results are given in Table I.

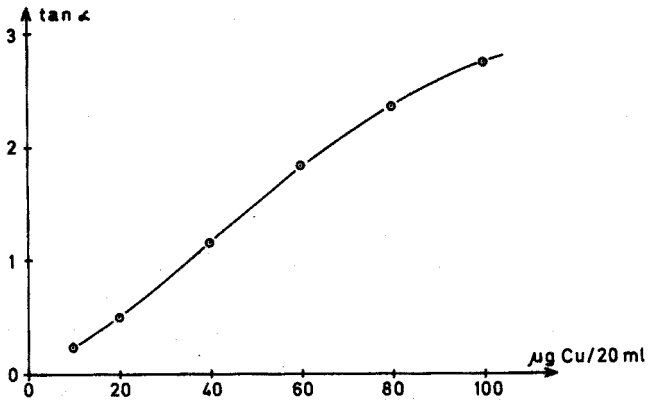

Fig. 3. Calibration graph for the determination of copper.

TABLE I

DETERMINATION OF COPPER

µg Cu/20 ml		Error (µg)
Given	*Found*	
11.2	10.0	−1.2
25.7	27.0	+1.3
35.0	34.0	−1.0
42.5	43.0	+0.5
50.0	50.6	+0.6
61.0	60.0	−1.0
67.0	68.5	+1.5
80.0	79.5	−0.5
90.0	91.0	+1.0
100.0	97.5	−2.5

Determination of L-histidine by its inhibiting effect on the copper(II)-catalyzed luminescent reaction of luminol with hydrogen peroxide

Because histidine shows a strongly inhibiting effect towards the system copper–luminol–H_2O_2[15,16] it is possible indirectly to determine histidine by measuring the remaining activity of the catalyst, copper (II).

Procedure. Into the measuring vessel the following solutions are added: 1–10 ml of a histidine solution (40 µg of L-histidine as hydrochloride per ml) for preparing a calibration graph, or an equivalent amount of a sample solution, 63.5 µg of copper (as copper(II) acetate), 2 ml of aqueous 2 *M* ammonia, 0.5 ml of 0.1% luminol in 0.02 *M* sodium hydroxide, and twice-distilled water to 20 ml. The procedure is completed as described for copper.

Figure 4 shows a calibration graph; some results are given in Table II.

Cobalt (II) (in aqueous 0.2 *M* ammonia), manganese (II) (in 0.1 *M* ammonium carbamate) and lead (II) (in 0.05 *M* sodium hydroxide) can likewise be determined with this method, although only with a lower degree of reproducibility, and for cobalt

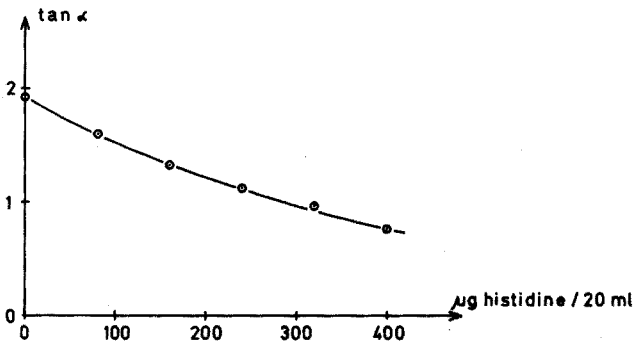

Fig. 4. Calibration graph for the determination of L-histidine.

TABLE II

DETERMINATION OF L-HISTIDINE

μg L-Histidine/20 ml		*Error (μg)*
Given	*Found*	
50.2	45.0	− 5.2
70.5	75.0	+ 4.5
102.3	100.0	− 2.3
137.0	125.0	−12.0
150.8	162.0	+11.2
180.8	190.0	+ 9.2
211.6	223.0	+11.4
250.1	270.0	+19.9
286.0	275.0	−11.0
377.3	370.0	− 7.3

and lead, in narrower ranges of concentration (10–50 μg Co/20 ml, 10–100 μg Mn/20 ml and 25–125 μg Pb/20 ml).

SUMMARY

A luminostat, a new type of "stat"-method is described. Copper (II) catalyzes the chemiluminescent reaction between luminol and hydrogen peroxide. The intensity of the luminescence is used via a photomultiplier and a current–voltage transducer to regulate the addition of hydrogen peroxide from an automatic burette. The rate of this addition necessary to keep constant a preset luminescence is a measure of the copper (II) concentration. As L-histidine acts as an inhibitor for copper (II) in this reaction, it can be determined indirectly. Copper (II) can be determined in the range 10–100 μg/20 ml, and L-histidine in the range 50–400 μg/20 ml.

REFERENCES

1 K. M. Møller, *Biophys. Acta*, 16 (1955) 162.

2 H. V. Malmstadt and E. H. Piepmeier, *Anal. Chem.*, 37 (1965) 34.
3 H. Weisz, D. Klockow and H. Ludwig, *Talanta*, 16 (1969) 921.
4 D. Klockow, H. Ludwig and M. A. Giraudo, *Anal. Chem.*, 42 (1970) 1682.
5 H. Weisz, K. Rothmaier and H. Ludwig, *Anal. Chim. Acta*, in press.
6 H. Weisz and K. Rothmaier, *Anal. Chim. Acta*, 75 (1975) 119.
7 S. Pantel and H. Weisz, *Anal. Chim. Acta*, 70 (1974) 391.
8 E. W. Cottman, *Proc. Indiana Acad. Sci.*, 50 (1940) 84.
9 U. Isacsson and G. Wettermark, *Anal. Chim. Acta*, 68 (1974) 339 (and refs. therein).
10 W. Meiners, Diploma Thesis, Freiburg, 1974.
11 H. O. Albrecht, *Z. Phys. Chem. Leipzig*, 136 (1928) 321.
12 K. Weber and M. Krajcinovic, *Ber. Deut. Chem. Ges.*, 75 B (1942) 2051.
13 A. K. Babko and L. I. Dubovenko, *Zh. Neorg. Khim.*, 12 (1967) 174; *Chem. Abstr.*, 66 (1967) 108712.
14 A. K. Babko and N. M. Lukovskaya, *Zh. Anal. Khim.*, 17 (1962) 50; *Z. Anal. Chem.*, 194 (1963) 282.
15 J. E. Vorhaben and R. H. Steele, *Biochem. Biophys. Res. Commun.*, 19 (1965) 187; *Chem. Abstr.*, 63 (1965) 5130 c.
16 A. A. Ponomarenko and L. M. Amelina, *Zhur. Obshch. Khim.*, 35 (1965) 750, 2252; *Chem. Abstr.*, 63 (1965) 10688 d; *Chem. Abstr.*, 64 (1966) 14966 b.

Analytica Chimica Acta, 74 (1975) 281–288

STUDIES IN ATOMIC FLUORESCENCE SPECTROMETRY

PART III. THE DETERMINATION OF TIN IN STEELS

L. EBDON, D. P. HUBBARD* and R. G. MICHEL

Department of Chemistry and Biology, Sheffield Polytechnic, Sheffield S1 1WB (England)

(Received 11th March 1974)

In Part II of this series[1], the interference effects were reported of twenty-seven elements, six acids and four organic liquids on the atomic fluorescence determination of tin with argon–hydrogen, argon–oxygen–hydrogen and argon-separated air–acetylene flames. The addition of 1000 p.p.m. of iron(III) chloride eliminated most element interferences but not acid interferences. A comparison of the interference effects in the argon–hydrogen flame with those reported by Nakahara *et al.*[2] for the atomic absorption determination of tin in the same flame showed that the basic trends in both techniques were similar. However, superior detection limits were possible with the atomic fluorescence method.

Elements which have been determined in steels by atomic fluorescence spectrometry are lead[3], silicon[4], bismuth[5], chromium[6], manganese[6], cobalt[7] and nickel[7]. Atomic absorption has been used widely for the analysis of steels; such analyses have been reviewed by Scholes[8] and comprehensive schemes for the analysis of a wide range of steels have been proposed[9,10]. Scholes concluded that most metals which occur in minor amounts above 0.1% can, in general, readily be determined. However, the difficulty in achieving adequate sensitivity has rendered the technique unsatisfactory for trace analysis below 0.1% without a concentration stage.

This paper describes a method for the determination of trace amounts of tin in steel by atomic fluorescence, which does not involve the preconcentration step usually necessary in the atomic absorption method[11,12]. Tin is usually present in steels within the range 0.005–0.1%.

EXPERIMENTAL

Apparatus

The atomic fluorescence instrument used has been fully described in Part I of this series[13]. However, in the work described here further improvements in signal-to-noise ratio were obtained by replacing two of the mirrors (M1 and M2, Fig. 1), which were part of the original optical arrangement, by mirrors of better quality and larger diameter. Also the electrodeless discharge lamp was temperature-controlled to allow control of its radiant output.

* Present address: Department of Chemistry, University of Otago, Box 56, Dunedin, New Zealand.

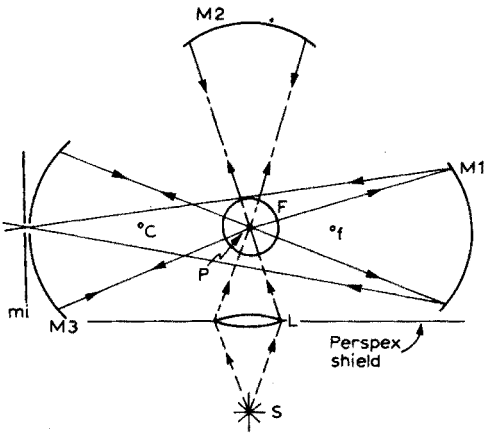

Fig. 1. Optical arrangement. (F) Flame; (S) source; (mi) monochromator entrance slit; (C and f) centre of curvature and focal point of mirror M1; (P) centre of curvature of mirror M3 at flame position. All mirrors are front-silvered, spherical, concave and are 90 mm in diameter (Optiglass Ltd., Walthamstow, London). M1 and M2 each have a focal length of 50 mm. M3 has a rectangular slit in the vertex (5 × 20 mm) and a focal length of 57.5 mm. Mirror to flame distances are: (M1–F) 85 mm; (M2–F) 100 mm; (M3–F) 115 mm. The silica lens (L) has a focal length of 50 mm and the source and lens are positioned to give the best fluorescence signal.

A factor of 4.4 improvement in the signal-to-noise ratio was reported in Part I of this series for the atomic fluorescence of tin in an argon-separated air–acetylene flame with the original mirrors. With the new larger mirrors the signal-to-noise ratio was improved by a factor of 6. This includes not only a total increase in the fluorescence signal of 12 times but also a two-fold increase in the noise associated with the signal (Table I). No increase in noise was observed with

TABLE I

IMPROVEMENT IN SIGNAL-TO-NOISE RATIO CAUSED BY MODIFIED OPTICAL ARRANGEMENT

(A 10-p.p.m. tin solution 0.4 *M* in hydrochloric acid was nebulized into three flames. Fluorescence was measured at 303.4 nm in all but the argon–hydrogen flame, when the wavelength used was 317.5 nm[13])

Mirrors in use	*Signal (arbitrary units)*	*Noise*	*Signal-to-noise ratio*	*Improvement factor with mirrors*
Argon-separated air–acetylene flame				
None	6	2	3	
M1	14	—		
M1 and M3	20	—		
M1, M2 and M3	72	4	18	6
Argon–hydrogen or argon–oxygen–hydrogen flame				
None	10	2	5	
M1	37	—		
M1 and M3	73	—		
M1, M2 and M3	292	3	73	14.5

the original mirrors. This indicates the advantage of using good large mirrors for fluorescence measurements.

In the argon–oxygen–hydrogen and argon–hydrogen flames the improvement in the fluorescence signal for the improved optical arrangement is more marked (Table I), a 29-fold signal enhancement being obtained. Again, a twofold increase in noise was observed, giving a net 14.5-fold increase in signal-to-noise ratio. Compared to the air–acetylene flame, the effect of the mirrors with the argon flames is larger probably because there is less quenching of the fluorescence radiation and less absorption of the source radiation by the flame gases.

It has recently been suggested that the temperature of microwave-excited electrodeless discharge lamps is the most important variable in controlling radiant output[14–17]. Browner and Winefordner[17] have described in detail the optimization of thermostatted electrodeless discharge lamps as sources for analytical atomic spectrometry. In their work, air from a small fan was heated with a nichrome heater coil and then passed over the electrodeless discharge lamp.

The tin lamp used for the work described here was temperature-controlled in a similar way, except that the air was supplied by an air-compressor (PR303E portable rotary air-compressor, Mk. V, Binks–Bullows), and the current to the heater coil was not precisely regulated. The procedure used to measure lamp temperatures was the same as that used by Browner and Winefordner[17], *i.e.* the temperature of the lamp was measured with a chromel–alumel thermocouple placed against the cooler, lower, front portion of the lamp. Spectroscopic measurements were not made while the thermocouple was in position because the thermocouple disturbed the microwave field.

The radiance of the tin electrodeless discharge lamp was measured as a function of the temperature of the lamp with the normal instrumental settings[1] and an optimal 40-W incident microwave power. The measurements were made while operating the lamp in a $\frac{1}{4}$-wave cavity (Type 214L, Electromedical Supplies Ltd., Wantage). The radiant output showed a marked dependence on temperature and a maximum was obtained at 385 °K. The lamp extinguished itself at 410 °K and could not be relit until the temperature was again stable at 385 °K. Observation of the atomic fluorescence of tin in the air–acetylene flame indicated that maximum fluorescence radiance was also obtained while running the lamp at 385 °K. When the lamp was operated without temperature control, the temperature equilibrated at *ca.* 380 °K and the optimal incident microwave power was still 40 W. The lamp would not remain alight in the unthermostatted Broida $\frac{3}{4}$-wave cavity unless it was cooled with a strong flow of compressed air, because the unthermostatted $\frac{3}{4}$-wave cavity reaches a higher equilibrium temperature than the unthermostatted $\frac{1}{4}$-wave cavity.

No significant net increase in radiant output was achieved by temperature control of the tin lamp, because the equilibrium temperature of the lamp in the unthermostatted $\frac{1}{4}$-wave cavity (380 °K) was close to the operating temperature of the lamp which gave maximum output (385 °K). However, the reproducibility of the spectral radiance and the stability of the tin lamp were considerably improved by temperature control.

Throughout this work, the tin lamp was modulated at 10 KHz, as in the previous studies[1,13] and the percentage modulation was maintained at maximum.

It is interesting that Winefordner *et al.*[14,17], in their work on thermostatted electrodeless discharge lamps, mechanically chopped the source radiation. This study shows that thermostatted lamps can also be used with advantage in the more convenient electronically modulated mode.

Reagents

All reagents were analytical-reagent grade or spectrographically standardized metals. Unless otherwise stated, all solutions were made up in 0.4 *M* hydrochloric acid for reasons discussed previously[1].

Fixed instrumental conditions

Apart from the above modifications, the instrumental conditions used were identical to those used previously[1]. All measurements of solutions containing greater than 0.1 p.p.m. tin were made with a 4.7-s time constant at the output of the lock-in amplifier. An 18.2-s time constant was used for solutions of lower concentration, and detection limits were measured for the 18.2-s time constant. At all times, the fuel flows in all three flames were the optimal flows reported previously[1].

RESULTS AND DISCUSSION

Effect of iron(III)

Nakahara *et al.*[2] pointed out that the effect of iron(III) chloride in eliminating interferences facilitates the determination of tin in steels by atomic absorption. These workers reported the determination of tin in steel by dissolving 1 g of a steel in aqua regia, evaporating to dryness, taking up in 10 ml of 6 *M* hydrochloric acid, diluting to 100 ml in a volumetric flask, and measuring the absorption of the resulting solution in the argon–hydrogen flame. In the work reported here, the above atomic absorption method was repeated, *i.e.* calibration curves were obtained for standards containing 1000 p.p.m. iron, and aqua regia was used to dissolve 1-g samples of five B.C.S. standard steels. The resulting solutions were nebulized and the atomic fluorescence was measured at the 303.4-nm line. However, all the fluorescence signals from the steel solutions were severely depressed by 50–90% in both the argon–hydrogen and argon–oxygen–hydrogen flames, and enhanced by up to 40% in the air–acetylene flame.

Norris and West[6], investigating the determination of chromium and manganese in steels by atomic fluorescence spectrometry, found that iron above a 250-fold amount caused a depressing effect on chromium signals; it was necessary to remove most of the iron by extracting it from strong hydrochloric acid–nitric acid solution, immediately after dissolution, with an equal volume of amyl acetate.

The effect of iron(III) chloride, present in the range 0–10000 p.p.m., on the fluorescence of a 50-p.p.m. tin solution was determined in this work for the two argon flames and the separated air–acetylene flame. The results are plotted in Fig. 2. The severe depression caused by iron in the argon–hydrogen flame presents difficulties in the use of this flame for sensitive atomic fluorescence measurements of steel solutions.

Figure 2 shows that iron(III) chloride in concentrations as high as 10000

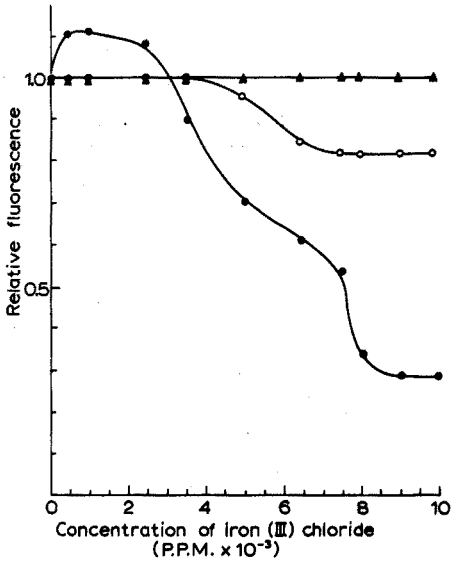

Fig. 2. The effect of iron(III) chloride on the atomic fluorescence determination of tin. Solutions 0.4 *M* in hydrochloric acid. 50 p.p.m. tin. (●) Argon–hydrogen flame. (⊙) Argon–oxygen–hydrogen flame. (▲) Argon-separated air–acetylene flame. Relative fluorescence is the ratio of the fluorescence of tin in the presence of iron(III) chloride to the fluorescence of tin alone.

p.p.m. has no effect on tin atomic fluorescence in the separated air–acetylene flame. Thus the enhancements obtained in this flame cannot be explained by the effect of iron(III) chloride. Results of further analyses of standards containing 8000 p.p.m. iron(III) chloride demonstrated that even in the argon flames the large depressions obtained could not be wholly attributed to the effect of iron; a *ca.* 40% depression was still observed in the argon–oxygen–hydrogen flame.

Effect of silicates

Silicates in solution are well known to cause marked depressions on the atomic absorption determination of a variety of elements; magnesium, calcium and strontium are notable in this respect[18]. Silicon in steel ranges from 0.001 to 5%. The traditional method of minimizing the depressive effect of silicates is to filter the steel solution after dissolution. This is effective because gelatinous silica partly precipitates during dissolution techniques which do not include a dehydration step. A method of complete removal of silica is volatilization as silicon tetrafluoride with hydrofluoric acid during the dissolution process. Tin tetrafluoride is an involatile solid which sublimes at 978 °K and is unlikely to be volatilized from solution.

The above two methods of removing silicon were applied to the determination of tin in three standard steels from the B.C.S. range (Bureau of Analysed Samples Ltd., Middlesbrough). The calibration curves for these determinations were obtained by means of standards containing 8000 p.p.m. iron(III) chloride which were 0.4 *M* in hydrochloric acid. The curves were linear from the detection limit to 250 p.p.m. with both the argon–oxygen–hydrogen and the argon-separated air–acetylene flames. The results of the determinations are given in Table II. The depression in the

TABLE II

THE DETERMINATION OF TIN IN STEEL

(The following trace elements[a] are present in all or most of the steels: C, Si, S, P, Mn, Ni, Cr, Mo, Cu, V, W, Ti Al, Sb. Arsenic, niobium, antimony, vanadium, titanium and aluminium are present at levels not likely to inte with the determination (less than 0.2%)

British Chemical standard Steel No.	*Description of steel*	*Tin content*				
		Certificate value (%)	*Atomic fluorescence (duplicate analyses)*			
			Method A[b]		*Method B*[b]	
			Air–C_2H_2	*Ar–O_2–H_2*	*Air–C_2H_2*	*Ar–O_2–*
322	Mild	0.24	0.24	0.23	0.23	0.23
			0.24	0.24	0.24	0.24
323	Mild	0.024	0.024	0.023	0.024	0.024
			0.024	0.024	0.023	0.024
431	Plain carbon	0.006	0.006	0.005	0.006	0.006
			0.005	0.005	0.006	0.005

[a] The standardised analyses of the steels can be obtained by referring to the list of analysed samples published the Bureau of Analysed Samples Ltd.
[b] See text.

argon–oxygen–hydrogen flame and the enhancement in the air–acetylene flame are no longer evident. The enhancement in the air–acetylene flame was probably due to scatter of source radiation by silica particles in the flame. Enhancement by scattering is often a possibility in atomic fluoresence. Significant scattering of source radiation when nebulizing the unfiltered sample solution was confirmed by measurements made at non-resonance lines, whereas under the same conditions no significant scattering was observed when calibration solutions were nebulized.

The two methods of dissolution of the steel samples (A and B), were both based on the use of hydrochloric acid–nitric acid mixtures.

Method A. The steel sample (1 g) was dissolved in 7 ml of concentrated hydrochloric acid and 3 ml of concentrated nitric acid, and the resulting solution was heated gently until oxides of nitrogen ceased to be evolved. The solution was then evaporated almost to dryness, and the residue was taken up with 10 ml of concentrated hydrochloric acid, and filtered through a No. 4 sinter crucible. The solution was then transferred to a 100-ml volumetric flask and diluted to the mark.

Method B. The steel sample (1 g) was dissolved in a 100-ml PTFE beaker with 7 ml of concentrated hydrochloric acid and 3 ml of concentrated nitric acid. The resulting solution was heated gently until the evolution of brown fumes ceased and then 2 ml of hydrofluoric acid was added. The solution was then boiled gently for 10 min, to volatilize the silicon tetrafluoride, evaporated almost to dryness, taken up with 10 ml of hydrochloric acid and diluted to 100 ml in a volumetric flask.

The detection limit, defined as the solution that gives a signal-to-noise ratio of two, in the argon-separated air–acetylene flame was 0.05 p.p.m., which is the same as reported previously[1] for standard tin solutions containing only 1000 p.p.m.

of iron(III) as chloride. In the case of the argon–oxygen–hydrogen flame, the presence of 8000 p.p.m. iron in the standard solutions increased the flame noise as well as depressing the fluorescence signal. This degraded the detection limit from 0.006 p.p.m. to 0.01 p.p.m. The detection limits in the argon–oxygen–hydrogen and argon-separated air–acetylene flames were measured respectively using 0.025 and 0.05 p.p.m. standard tin solutions each containing 8000 p.p.m. iron(III) chloride.

The precision of the method was investigated for one of the standard steels (B.C.S. No. 323, a mild steel). Six samples of this steel were treated by Method B, and the average of three atomic fluoroescence readings was taken for each sample. The relative standard deviation was 3.1% for the air–acetylene flame and 2.3% for the argon–oxygen–hydrogen flame.

A third dissolution method based on aqua regia but followed by oxidation with perchloric acid and a filtration step, gave results similar to those obtained for Methods A and B above. No evaporation to dryness was attempted in this perchloric acid method. However, some large enhancements were observed in both the argon–oxygen–hydrogen and the air–acetylene flame when more than 10% perchloric acid was present in the final steel solution. Also the effect of perchloric acid on the fluorescence of tin in the argon–oxygen–hydrogen flame is not constant below 10%[1]. This method could only be considered reliable if accurately controlled concentrations of perchloric acid were used.

CONCLUSION

A method has been developed for the determination of tin in steel based on the atomic fluorescence of tin at the 303.4-nm line in the argon-separated air–acetylene flame and the argon–oxygen–hydrogen flame. The effects of interferences have been eliminated by the addition of iron(III) chloride to the calibration standards in about the same amount as found in the sample, and by removal of silicon from the sample. The preferred procedure involves the dissolution of the sample in aqua regia followed by volatilization of silicon with hydrofluoric acid. Alternatively, silica could be removed by filtration.

Although it has been known for some time that improvements in sensitivity can be obtained, if atomic fluorescence is used instead of atomic absorption, there are relatively few publications on the applications of atomic fluorescence. In this work, the superior sensitivity of the fluorescence technique has allowed tin to be determined in steels without preconcentration, and the popular air–acetylene flame is used rather than a cooler flame. If necessary, further improvements in sensitivity can be obtained with the argon–oxygen–hydrogen flame. Further, it has been shown that atomic fluorescence shares the remarkable freedom from interference that atomic absorption enjoys.

The authors acknowledge with thanks the Science Research Council for the provision of an S.R.C. (CAPS) studentship for one of us (R.G.M.). Our thanks are also due to BISRA, the Corporate Laboratories of the British Steel Corporation, for the loan of equipment.

SUMMARY

A method has been developed for the determination of tin in steel based on

the atomic fluorescence of tin at the 303.4-nm line in an argon-separated air–acetylene flame (detection limit 0.05 p.p.m.) or argon–oxygen–hydrogen flame (detection limit 0.01 p.p.m.). A temperature-controlled, electronically modulated electrodeless discharge tube was used as the source. The effects of interferences were eliminated by addition of iron(III) chloride to the calibration standards in about the same amount as found in the sample and by removal of silicon from the sample. The preferred procedure involves dissolution of the sample in aqua-regia followed by either the volatilization of silicon tetrafluoride or filtration of silicic acid. Tin can be determined in steels without any preconcentration step.

REFERENCES

1 D. P. Hubbard and R. G. Michel, *Anal. Chim. Acta*, 72 (1974) 285.
2 Taketoshi Nakahara, Makoto Munemori and Soichiro Musha, *Anal. Chim. Acta*, 62 (1972) 267.
3 M. R. G. Taylor, R. M. Dagnall and T. S. West, *Lab. Pract.*, 20 (1971) 209.
4 G. F. Kirkbright, A. P. Rao and T. S. West, *Anal. Lett.*, 2 (1969) 465.
5 M. E. Hofton and D. P. Hubbard, *Anal. Chim. Acta*, 62 (1972) 311.
6 J. D. Norris and T. S. West, *Anal. Chim. Acta*, 59 (1972) 474.
7 J. D. Norris and T. S. West, *Anal. Chim. Acta*, 55 (1971) 359.
8 P. H. Scholes, *Analyst (London)*, 93 (1968) 197.
9 D. R. Thomerson and W. J. Price, *Analyst (London)*, 96 (1971) 825.
10 W. J. Price, *Analytical Atomic Absorption Spectrometry*, Heyden, London, 1972, p. 126.
11 K. E. Burke, *Analyst (London)*, 97 (1972) 19.
12 J. B. Headridge and A. Sowerbutts, *Analyst (London)*, 97 (1972) 442.
13 D. P. Hubbard and R. G. Michel, *Anal. Chim. Acta*, 67 (1973) 55.
14 R. F. Browner, M. E. Rietta, T. H. Glenn and J. D. Winefordner, *Pittsburgh Conference on Analytical Chemistry and Applied Spectroscopy*, Cleveland, Ohio, 1972, Abstract no. 136.
15 R. F. Browner, B. M. Patel, T. H. Glenn, M. E. Rietta and J. D. Winefordner, *Spectrosc. Lett.*, 5 (1972) 311.
16 B. M. Patel, R. F. Browner and J. D. Winefordner, *Anal. Chem.*, 44 (1972) 2272.
17 R. F. Browner and J. D. Winefordner, *Spectrochim. Acta, Part B*, 25 (1973) 263.
18 J. Ramirez-Munoz, *Atomic Absorption Spectroscopy*, Elsevier, New York, 1968, p. 271.

Analytica Chimica Acta, 74 (1975) 289–297

A METHOD FOR THE FORMATION OF PYROLYTIC GRAPHITE COATINGS AND ENHANCEMENT BY CALCIUM ADDITION TECHNIQUES FOR GRAPHITE ROD FLAMELESS ATOMIC ABSORPTION SPECTROMETRY

K. C. THOMPSON, R. G. GODDEN and D. R. THOMERSON

Shandon Southern Instruments Ltd., Frimley Road, Camberley, Surrey GU16 5ET (England)

(Received 10th June 1974)

Pyrolytically coated graphite rods and tubes have been advocated for use in flameless atomization techniques for some time now[1–3]. Pyrolytic graphite coatings have been found to improve the sensitivities for certain elements, to increase the lifetime of operation, and to improve the reproducibility by decreasing the porosity of the graphite. The main disadvantage of these pre-coated rods is that the pyrolytic graphite coating is progressively removed from the rod surface during use. This is especially true when high temperatures are required to atomize elements such as Al, Ba, Be, Mo, Si, Sn, Ti and V, and results in a gradual reduction in performance during the rod lifetime.

Other methods that have been used to increase the lifetime of the graphite rod and minimize carbide formation are: decomposition of an organic tantalum or niobium compound at 400–450°C onto the graphite surface[4], and the insertion of a thin tantalum liner inside a graphite tube[5,6]. The addition of methane[7] or propane[8] to the nitrogen or argon purge gas has been reported to create a pyrolytic graphite coating by decomposition of the hydrocarbon on the hot graphite surface during the atomization heating cycle.

The present study has shown that the addition of propane, ethylene, acetylene or methane to the purge gas results in deposition of pyrolytic graphite on the rod. A significant improvement in performance was observed in determinations of elements such as Al, Ba, Be, Si, Sn, Ti and V. A substantial increase in the rod lifetime was also found. The optimal coating conditions for a graphite rod atomization system are described below.

The addition of a large excess of calcium (as the nitrate) was also found to enhance markedly the responses for aluminium, barium, beryllium, silicon and tin.

EXPERIMENTAL

Apparatus

A Shandon Southern A3470 Flameless Atomizer and an A3400 Atomic Absorption Spectrophotometer were used. The output from the spectrophotometer was measured on a Kipp and Zonen BD8 recorder (response time 0.8 s f.s.d.). The time constant of the spectrophotometer output was 40 ms. The graphite rod mounting head of the flameless atomizer is shown in Fig. 1. The temperature of one

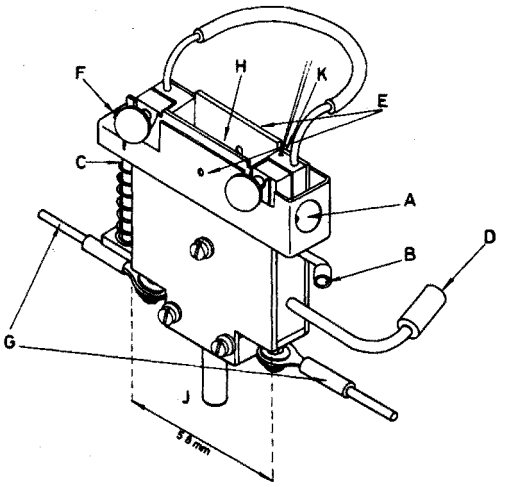

Fig. 1. Graphite rod head: (A) access to graphite rod; (B) air cooling in; (C) air cooling out; (D) purge gas in; (E) aperture; (F) aperture height adjusting screw; (G) transformer connections; (H) graphite rod; (J) mounting pillar; (K) thermistor.

of the air-cooled graphite rod head pillars was monitored with a thermistor and the A3478 temperature indicator unit.

Samples were added to the graphite rod when the pillar temperature was 50°C. This temperature increased to 75–80°C immediately after the atomization stage of the heating cycle. Subsequent samples were always added when the pillar temperature had fallen to 50°C, which took about 20 s. As rod degradation for most elements was not apparent until at least 200 firings had occurred, it was assumed that the temperature of the rod sample cavity would be constant for each sample addition. If the samples were added to the rod at varying pillar temperatures poor precision was observed, because the response for most elements increased with increasing pillar temperature.

Two types of rod were used in this study, a type 1 rod (Fig. 2a) which has a hemispherical sample cavity that can accept sample volumes up to 5 μl, and a type 2 (Fig. 2b) which has a larger cylindrical sample cavity that can accept sample volumes up to 10 μl. The diameter of both rods was 3.05 mm. The type 2 rod gave slightly better sensitivity figures (*ca.* 20%) for most elements, but slight memory effects were observed with molybdenum, titanium and vanadium even at the

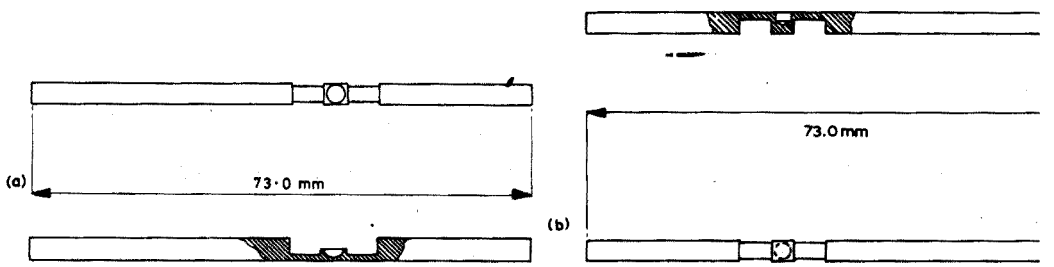

Fig. 2. Graphite rods: (a) type 1; (b) type 2.

maximum useable rod voltage (8.5 V). At higher rod voltages appreciable graphite volatilization occurred, leading to very short rod lifetimes. No memory effects were observed with the type 1 rod, when the atomization voltage was set up as described later. The maximal operating temperature of the coolest part of the sample cavity of the type 1 rod must be slightly higher than that of the type 2 rod. A type 1 rod was used for the determination of molybdenum, titanium and vanadium, and a type 2 rod was used for the other elements reported here. An Oxford 5-μl pipette with disposable PTFE tips (Boehringer Corp. Ltd.) was used to apply the sample to the rod.

The argon and the gas used for pyrolytic coating were passed through separate flow-meters and fed into a T-piece connected to the graphite rod head via a 2-m length of PVC tubing.

Two circular apertures, 1.8 mm in diameter and 15 mm apart (see Fig. 1.), were used to collimate the light beam above the sample cavity. The aperture height for all elements except barium was set by passing a No. 51 drill blank (1.7 mm diameter) through the two apertures and lowering the aperture height until slight pressure was felt between the top of the rod sample cavity and the drill blank. The drill blank was then removed. Other workers[9] have stressed the importance of working with a well defined collimated light beam just above the sample cavity of the graphite rod. In order to minimize the effect of the intense thermal emission from the graphite rod above 350 nm, narrow-bore barium and titanium hollow-cathode lamps (Southern Spectral Sources Ltd.), run at 90% of their maximal current rating, were used. For barium the thermal emission from the rod at 553.6 nm was so intense that it was also necessary to raise the aperture by 0.3 mm to avoid overloading of the demodulator.

Gases

High-purity nitrogen, argon and 10% methane–90% argon (v/v) were used. This gas mixture is used for radio-counting techniques and is readily available commercially. Technical-grade acetylene, ethylene and propane were passed through an activated charcoal filter before being mixed with the high-purity argon. The filter removed impurities which sometimes caused erratic results when cylinders were nearly empty. All gas flows were checked by the soap bubble method.

Argon resulted in better sensitivity than nitrogen for barium (3.1 times), molybdenum (1.3 times) and titanium (2.8 times). Unfortunately, the use of argon in titanium determinations resulted in memory effects that could not be eliminated without drastically shortening the graphite rod lifetime. The reduced sensitivity and lack of memory effects with nitrogen were thought to be due to reaction between titanium species and nitrogen, resulting in nitride formation. All results, except those for titanium, were obtained with argon rather than nitrogen.

In general, the response did not depend on the inert gas flow rate. This was checked at flow rates varying between 2.5 and 4.0 l min^{-1}. A flow rate of 3.2 l min^{-1} was used for all determinations, except those involving a hydrocarbon gas, when the flow rate of the inert gas was reduced to an optimum of 2.5 l min^{-1}.

Setting the atomization voltage and time

An atomization time of 1.5 s was used for all elements except titanium,

where a time of 2.0 s was used to avoid memory effects. The atomization voltage for both Type 1 and Type 2 rods was then set to give a small signal (0.02–0.03 absolute absorbance units) which arose from volatilized graphite. The atomic absorption signal always preceded this background absorption signal. This procedure ensured that no memory effects were observed for any of the elements studied when a Type 1 rod was used. In the presence of the hydrocarbon gas this technique did not appreciably shorten the graphite rod life-time. When a Type 2 rod was used, slight memory effects were observed for molybdenum, titanium and vanadium. For aluminium, beryllium, silicon and tin the graphite peak was completely resolved from the atomic peak that preceded it. With barium, molybdenum, titanium and vanadium there was slight overlap (Fig. 3).

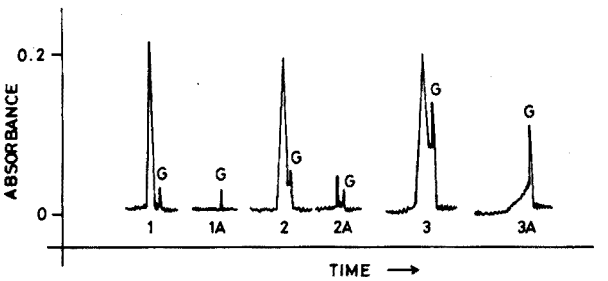

Fig. 3. Typical traces showing the graphite absorption peak. Wavelengths as given in Table II. Argon 2.5 l min^{-1}, 90% argon–10% methane 0.150 l min^{-1}. (1) 5 μl of 0.5 μg Sn ml^{-1} + 1000 μg Ca ml^{-1}; (1A) 5 μl of 1000 μg Ca ml^{-1}; (2) 5 μl of 0.15 μg Ba ml^{-1} + 10,000 μg Ca ml^{-1}; (2A) 5 μl of 10,000 μg Ca ml^{-1} (shows slight barium contamination of the calcium carbonate); (3) 5 μl of 0.1 μg V ml^{-1} (divide ordinate by 5); (3A) 5 μl of distilled water (divide ordinate by 5). (G) Graphite peak.

RESULTS

Nature of the hydrocarbon gas

The effect of bleeding small amounts of methane, ethylene, propane, and acetylene into the argon purge gas supply was investigated. Each new graphite rod was initially coated with pyrolytic graphite by increasing the hydrocarbon gas flow rate to about ten times above the optimal flow rate (see Table I) and firing the rod three times with the argon flow rate set to 2.5 l min^{-1}. When the 10% methane–90% argon gas was used, the rod was coated by turning off the auxiliary argon supply and increasing the methane–argon flow rate to 1 l min^{-1}. The centrally heated region of the graphite rods (Fig. 2) could then be seen to be coated with a shiny layer of pyrolytic graphite. Unless strongly acidic solutions were used, the rod could then simply be operated with an argon flow of 2.5 l min^{-1} and the optimal hydrocarbon gas flow rate (see Table I). With highly acidic solutions, the rod surface could be recoated as just described whenever the surface appeared to have degraded.

Table I gives the range of optimal hydrocarbon gas flow rates and also gives the approximate flow rate for onset of background (non-specific) absorption from the pyrolysis of the hydrocarbon gas. The response for a given element was found to be almost constant over the gas flow ranges given.

TABLE I

OPTIMAL HYDROCARBON GAS FLOW RATES

Gas	*Optimal flow rate (ml min^{-1})*[a]	*Flow rate for onset of background absorption*[a,b] *(ml min^{-1})*
90% Argon–10% methane	120–180	500[c]
Propane	8–12	28
Ethylene	12–18	40
Acetylene	5–8	16

[a] Argon flow rate, 2.5 l min^{-1}.
[b] Measured at 283.3 nm, 0.01 absorbance units.
[c] Argon flow rate 2.0 l min^{-1}.

Although similar results for aluminium and vanadium were obtained with all the hydrocarbon gases tried, the use of 10% methane–90% argon was preferred. It was easier to monitor and control a flow rate of 100–200 ml min^{-1} than the 5–18 ml min^{-1} flow rate required for the other gases. There was no apparent advantage in using acetylene instead of methane, ethylene, or propane. It was initially thought that the energy released from the pyrolysis of acetylene might increase the free atom population above the rod.

Table II shows the improvement in sensitivity for a number of elements when methane was used (columns 5 and 7 should be compared). These improvements

E II

CT OF ADDITION OF METHANE TO THE ARGON PURGE GAS AND THE EFFECT OF TION OF CALCIUM

it	*Wavelength (nm)*	*Rod type*	*Spectral bandpass (nm)*	*Sensitivity for 1% absorption for 5 µl sample addition (µg ml^{-1})*			
				Argon 3.2 l min^{-1}		*Argon 2.5 l min^{-1} 90% Argon–10% Methane 0.150 l min^{-1}*	
				No Ca	*1000 µg Ca ml^{-1} present*	*No Ca*	*1000 µg Ca ml^{-1} present*
	309.3	2	0.3	0.06	0.0085	0.023	0.01
	553.6	2	0.18	0.035	0.003[a]	0.028	0.0035[a]
	234.9	2	0.3	0.0007	0.00035	0.0004	0.0003
	313.3	1	0.18	0.005	0.007	0.005	0.007
	251.6	2	0.3	0.10	0.037	0.06[b]	0.025[b]
	286.3	2	0.6	0.13	0.013	0.05	0.01
	364.3	1	0.18	0.075	0.08	0.03	0.05
	318.4	1	0.18	0.02	0.019	0.01	0.02

0 µg Ca ml^{-1} present.
upted hydrocarbon gas flow (see text).
gen purge gas used (see text).

were thought to result from reduced carbide formation on the graphite rod surface because of the pyrolytic graphite coating. They may also be partly due to a reduction in the free oxygen concentration in the atmosphere just above the sample cavity by combustion of the methane. Significant improvements in sensitivity were not observed for elements such as lead and cadmium which do not form stable carbides or oxides. There was no improvement for silicon with the standard method of continually bleeding in the hydrocarbon gas, but an improvement was observed if the hydrocarbon gas was turned off during the atomization sequence. The rod was then fired with twice the optimal hydrocarbon gas flow rate before the next silicon sample was added. This procedure of rod coating with no sample and subsequent measurement without the hydrocarbon gas flow was adopted for silicon. The effect was attributed to silicon carbide formation above the rod caused by reaction of silicon and the hydrocarbon gas.

The addition of the hydrocarbon gas increased the rod lifetime often by up to five times that obtained without this addition. For instance, in the determination of titanium the rod lifetime was increased from 50 to over 200 firings.

The other advantage of continually bleeding in a hydrocarbon gas to the argon purge gas was improved precision, resulting from decreased porosity of the graphite. The relative standard deviation (10 measurements) for the signal from 5 μl of 0.1 μg Pb ml^{-1} solution improved from 3.8 to 2.7%.

Enhancing effect of calcium

When a large excess of calcium (as the nitrate) was added to Al, Ba, Be, Si and Sn solutions, a substantial enhancement in signal was observed.

It was essential to set the intermediate dry ashing voltage so that the calcium nitrate added to the rod was decomposed to calcium oxide before the atomization step, otherwise severe background absorption was observed. A rod temperature corresponding to bright red heat was adequate for dry ashing. The enhancement for Al, Ba, Be, Si, and Sn, with increasing calcium concentration is shown in Fig. 4. Table II shows the effect of 1000 μg Ca ml^{-1} on these elements. The large increase in the barium sensitivity is of special note. In this case, a higher concentration of calcium was required to give the maximum response. Renshaw *et al.*[5,6] found a similar increase in sensitivity for barium by lining a graphite tube with a tantalum liner. The addition of the hydrocarbon gas gave a slight decrease in the barium sensitivity in the presence of 10,000 μg Ca ml^{-1} (Table II) but reduced the background absorption from 0.04 A to less than 0.010 A at the 10,000 μg Ca ml^{-1} level.

The enhancements observed on adding calcium were thought to be due to preferential formation of carbide by the calcium and also possibly to a reduction in the oxygen concentration just above the sample cavity by reaction with volatilized calcium atoms. With molybdenum and titanium a depression was observed on adding calcium. It was thought that most of the calcium would volatilize before these involatile elements.

Table II (columns 6 and 8) also shows the effect of 1000 μg Ca ml^{-1} with addition of methane to the argon. The addition of methane did not have much effect, *i.e.* the pyrolytic graphite coating and calcium addition enhancements were not additive. With aluminium a small shoulder was observed on the trailing edge of the aluminium peak when the pyrolytic coating and calcium

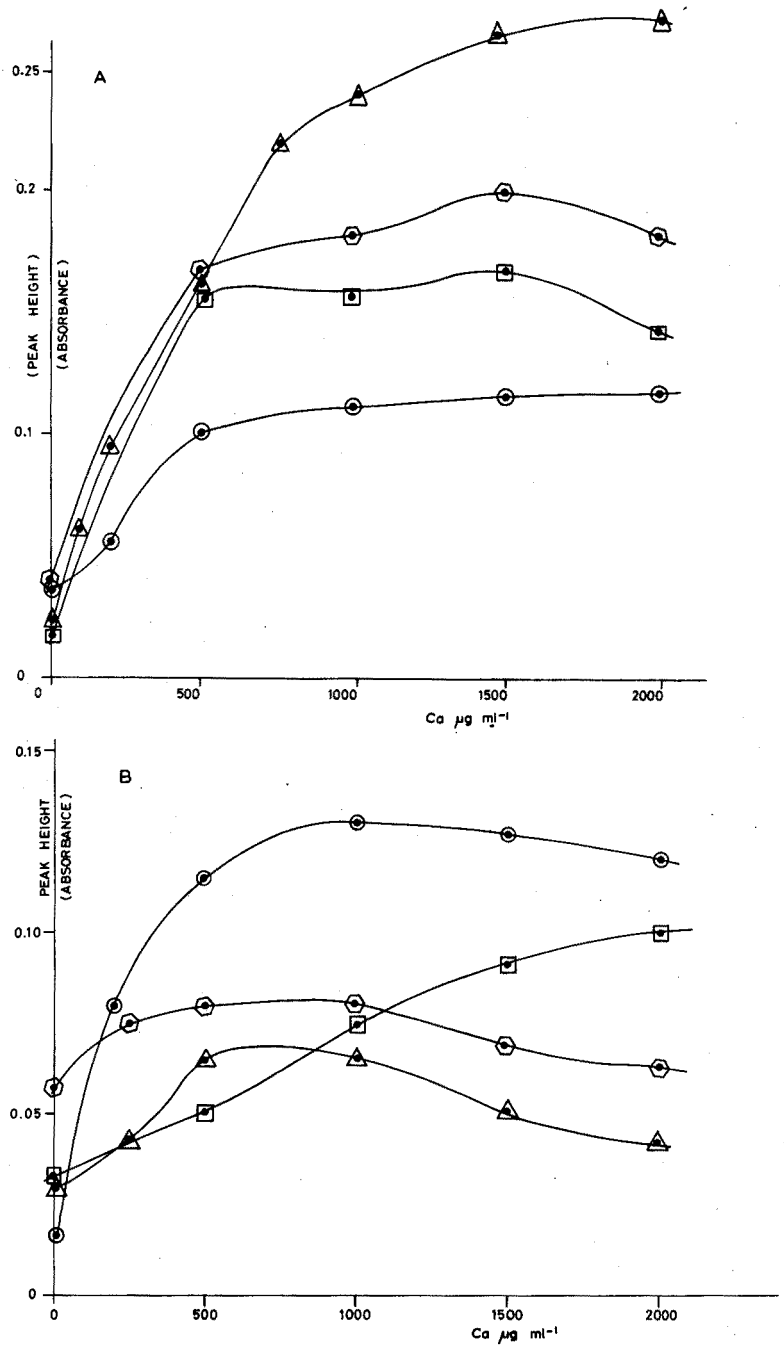

Fig. 4. Calcium enhancement effects. (A): (⊙) 1 μg Si ml^{-1} (3.2 l Ar min^{-1}); (⊡) 0.5 μg Sn ml^{-1} (3.2 l Ar min^{-1}); (⊙) 0.5 μg Sn ml^{-1} (2.5 l Ar min^{-1}, 90% Ar–10% Methane 0.150 l min^{-1}); (△) 0.2 μg Ba ml^{-1} (2.5 l Ar min^{-1}, 90% Ar–10% Methane, 0.150 l min^{-1}). (Abscissa multiplied by 10 for barium), (B): (⊙) 0.25 μg Al ml^{-1} (3.2 l Ar min^{-1}); (△) 0.005 μg Be ml^{-1} (3.2 l Ar min^{-1}); (⊡) 0.25 μg Al ml^{-1} (2.5 l Ar min^{-1}, 90% Ar–10% Methane 0.150 l min^{-1}); (⊙) 0.005 μg Be ml^{-1} (2.5 l Ar min^{-1}, 90% Ar–10% Methane 0.150 l min^{-1}).

addition were combined.

In all cases it was essential to ensure that the atomization voltage was set up so that a small graphite background absorption peak was observed after the element atomization peak. This ensured complete removal of the added calcium. The background (non-specific) absorption caused by the added calcium (1000 μg ml^{-1}) was determined by means of a deuterium hollow-cathode lamp; it was less than the 1% sensitivity figures quoted in Table II (column 6).

If the calcium was added as the chloride or the solution contained large amounts of chloride, background absorption peaks from volatilization of calcium chloride molecules were observed. In these cases, a suitable excess of sulphuric acid could be added to the solution to ensure removal of chloride during the dry ashing phase. Argon was the preferred purge gas. In the presence of high concentrations of calcium (>2000 μg ml^{-1}), a small background peak was observed if nitrogen was used, probably because of calcium nitride formation.

CONCLUSIONS

The addition of a hydrocarbon gas to the inert gas used in conjunction with a graphite rod atomizer has shown a number of improvements resulting from the pyrolytic graphite coating formed on the rod surface. The graphite rod lifetime is increased, the precision of results is improved, carbide formation is minimized, and the sensitivity for various elements that form refractory oxides or carbides is improved. In order to eliminate memory effects for molybdenum, titanium and vanadium, the atomization voltage must be set to give a small non-specific absorption signal from volatilized graphite.

The addition of a large amount of calcium (as the nitrate) to solutions of aluminium, barium, beryllium, silicon and tin, markedly increased the sensitivity for these elements when argon was used as purge gas. The calcium addition and pyrolytic graphite coating enhancement effects were not additive.

The authors thank the Directors of Shandon Southern Instruments Ltd. for permission to publish this work.

SUMMARY

The addition of a small amount of methane to the argon purge gas of a graphite rod atomizer results in the formation of a pyrolytic graphite coating on the rod surface. This coating increases the graphite rod lifetime, improves the precision of results and increases the sensitivity for many refractory oxide-forming elements. The addition of a large excess of calcium markedly increases the sensitivity for aluminium, barium, beryllium, silicon and tin. The effects of calcium and the pyrolytic graphite coating are not additive.

REFERENCES

1 B. V. L'vov, *Spectrochim. Acta B.*, 24 (1970) 53.
2 B. V. L'vov, *Atomic Absorption Spectrochemical Analysis*, (translated by J. H. Dixon), Adam Hilger,

London, 1970.
3 K. I. Aspila, C. L. Chakrabarti and M. P. Bratzel, *Anal. Chem.*, 44 (1972) 1718.
4 I. A. Kuzovlev, Yu. N. Kuznetsov and O. A. Sverdlina, *Zav. Lab.*, 39 (1973) 428.
5 G. D. Renshaw, C. A. Pounds and E. F. Pearson, *At. Absorption Newslett.*, 12 (1973) 55.
6 G. D. Renshaw, *At. Absorption Newslett.*, 12 (1973) 158.
7 R. W. Morrow and R. J. McElhaney, *At. Absorption Newslett.*, 13 (1974) 45.
8 D. R. Thomerson and K. C. Thompson, *Amer. Lab.*, 6 (1974) 53.
9 R. G. Anderson, H. N. Johnson and T. S. West, *Anal. Chim. Acta*, 57 (1971) 281.

Analytica Chimica Acta, 74 (1975) 299–307

BESTIMMUNG VON SCHWERMETALL-SPUREN IN ALKALI- UND ERDALKALISALZEN DURCH ATOMABSORPTIONS-SPEKTROMETRIE NACH ANREICHERUNG AN AKTIVKOHLE

E. JACKWERTH und H. BERNDT

Institut für Spektrochemie und angewandte Spektroskopie, D-4600 Dortmund, Bunsen-Kirchhoff-Strasse 11 (Bundesrepublik Deutschland)

(Eingegangen den 5 August 1974)

Der Gehalt an Schwermetall-Verunreinigungen in Reagentien wird von alters her durch einen einfachen, den Prüfvorschriften der Arzneibücher entnommenen Test charakterisiert: Die beim Einleiten von Schwefelwasserstoff in eine gepufferte Lösung des Präparats auftretende Dunkelfärbung darf nicht stärker sein als die, welche von einer durch das Reinheitsgebot vorgeschriebenen und in einer Vergleichsprobe eingesetzten Menge an Bleiionen hervorgerufen wird. Es handelt sich also um eine visuelle "halbquantitative" Pauschalprüfung auf die mit H_2S dunkelfarbige Sulfide bildende Elementgruppe (Ag, Bi, Co, Cu, Fe, Ni, Pb, Tl, ...). Eine differenzierte Aussage über das Vorhandensein oder die Konzentration der die Färbung verursachenden Einzelelemente ist nicht möglich. Dieser Test wird in der Regel zur Reinheitskontrolle sowohl der in Apotheken vorrätigen Arzneibuchpräparate als auch bei den durch die Qualitätsbezeichnungen "rein", "reinst", "zur Analyse" u.dgl. charakterisierten Laborchemikalien durchgeführt und liefert die Analysenaussage: Schwermetalle (als Pb) maximal...%.

Bei Arzneibuchpräparaten ist dieser Schwermetalltest gesetzlich vorgeschrieben; er erfüllt den Zweck, durch ein schnelles und einfaches Prüfverfahren sicherzustellen, dass keine gesundheitsschädlichen Mengen an Metallsalzen in Arzneizubereitungen gelangen. Ähnliche Vorschriften gelten im Bereich der Lebensmittelgesetze. Für die Beurteilung der Qualität von Laborchemikalien jedoch reicht dieser Test seit langem nicht mehr aus. Allein durch den zunehmenden Einsatz nachweisstarker Analysenverfahren sind Informationen über die durch die Eigenverunreinigungen der Reagentien zu erwartenden Blindwertanteile von grossem Interesse. Dabei ist gerade der Gehalt an Spuren von Übergangselementen ein wichtiges Kriterium für die Bewertung der Reinheit und Anwendbarkeit von Reagentien unterschiedlicher Provenienz. Eine Auswahl unter den in abgestuften Qualitäten im Handel angebotenen Chemikalien würde beträchtlich erleichtert, wenn sich die Hersteller dazu entschliessen könnten, Garantiescheine und Angaben über Typanalysen wenigstens bei den wichtigsten Laborchemikalien zu spezifizieren, wie es bei den "hochreinen" Qualitäten bereits seit längerer Zeit üblich ist.

Die im folgenden beschriebene Arbeit ist ein Versuch, ein schnelles sowie unkompliziertes und besonders für die serienmässige Reinheitskontrolle von Alkali- und Erdalkalisalzen geeignetes Verfahren zur Anreicherung von Schwermetallspuren zu entwickeln. Die Kenntnis des Spurengehaltes ist gerade hier von besonderer

Bedeutung, da zahlreiche Alkali- und Erdalkaliverbindungen als Grundchemikalien in analytischen und präparativen Prozessen in oft hoher Konzentration benötigt werden (Puffersubstanzen, Maskierungsmittel u.dgl.). Entsprechend der Reinheitsgarantie bei diesen Salzen in "analysenreiner" Qualität liegen die vom Hersteller zugelassenen Gehalte an "Schwermetallen", je nach Präparat und Herkunft, gewöhnlich zwischen 2 und 50 p.p.m. Um die deklarierte Reinheit garantieren zu können, ist ein Analysenverfahren erforderlich, dessen Nachweisvermögen für jedes unter den Sammelbegriff "Schwermetall" fallende Element etwa bei 0,1 p.p.m. liegt. Dabei wird angenommen, dass an der noch zugelassenen Gesamtkonzentration an Verunreinigungen etwa 10 Elemente gleichmässig beteiligt sein können.

Grundlage des hier vorgeschlagenen Verfahrens ist die auf viele Salze anwendbare gleichzeitige Anreicherung der Diäthyldithiocarbamidat–Chelate zahlreicher Elementspuren an Aktivkohle als Sorptionsmittel. Die angereicherten Elemente werden nach ihrem Ablösen vom Trägermaterial durch Atomabsorptions–Spektrometrie (A.A.S.) bestimmt. Wegen der erreichten praktisch vollständigen Abtrennung der Matrixbestandteile kann die Spurenbestimmung jedoch leicht auch auf Verfahren, die für die serienmässige Multi-Element-Bestimmung geeigneter sind als die A.A.S. (Spektrochemie mit Gleichstrombogen, Plasmabrenner u.a.) übertragen werden.

ZUR ANREICHERUNG DER DIÄTHYLDITHIOCARBAMIDAT-KOMPLEXE VON Ag, Bi, Cd, Co, Cu, Fe, In, Ni, Pb, Tl UND Zn

Zur Anreicherung gleichzeitig vieler Elementspuren sind Trennmethoden unter Verwenden chelatbildender Gruppenreagentien besonders geeignet. Alkali- und Erdalkaliionen als Matrix stören die Chelatbildung der Übergangselement-Spuren im allgemeinen nicht, da sie nur in Ausnahmefällen vergleichbar stabile Komplexe bilden. Unter den infrage kommenden Gruppenreagentien nehmen die disubstituierten Dithiocarbamidate einen besonderen Rang ein; je nach Wahl der Analysenbedingungen können bis zu 30 Elemente gleichzeitig komplexiert werden[1]. Es bilden sich in Wasser schwerlösliche, in zahlreichen organischen Lösungsmitteln aber lösliche, teils farblose, teils farbige 4-Ring-Chelate. Bei Verwenden geeigneter Hilfskomplexbildner und bei definierten pH-Werten können gezielt auch Einzelelemente oder ausgewählte Elementgruppen gefällt und durch Extraktion angereichert werden. Gebräuchliche Extraktionsmittel sind Chloroform bzw. Tetrachlorkohlenstoff sowie einige höhere Alkohole, Ester oder Äther[1]. Seit Einführung der A.A.S. wurden mehrere Verfahren beschrieben, bei denen solche Extrakte zur Spurenbestimmung zerstäubt und in der Flamme analysiert wurden[2]. Gegenüber wässrigen Probenlösungen ist die Empfindlichkeit der A.A.S. organischer Extrakte in der Regel grösser[2]. Das preiswerteste und am meisten verwendete Dithiocarbamidat ist das Natriumdiäthyldithiocarbamidat (NaDDTC). Analoge Verbindungen, die anstelle des Diäthylamins andere Amine enthalten, sind bei kleineren pH-Werten häufig beständiger als NaDDTC und unterscheiden sich von diesem durch den pH-Bereich, in dem die einzelnen Metall–Chelate gebildet werden. Bei Alkali- und Erdalkalisalzen als Probenmatrix haben sie gegenüber NaDDTC praktisch keinen Vorteil.

Versuche zur Sorption der DDTC–Chelate an Aktivkohle

Die Untersuchungen zur Elementspuren-Anreicherung wurden an insgesamt etwa 40 Salzen mit Li^+, Na^+, K^+, NH_4^+, Ca^{2+}, Sr^{2+} und Ba^{2+} als Kation sowie etwa 20 unterschiedlichen Anionen durchgeführt (Tab. I) Die meisten der ausgewählten Salze waren Natrium- und Kaliumsalze. Es kann aber angenommen werden, dass die an einem bestimmten Salz aus dieser Auswahl erzielten Ergebnisse der Spurenanreicherung im wesentlichen auch auf andere Alkali- und Erdalkalisalze mit gleichem Anion übertragen werden können. Wegen der geringen Neigung der in hoher Konzentration vorhandenen Alkali- und Erdalkaliionen zur Bildung stabiler DDTC–Chelate, treten von diesen Kationen herrührende Störungen nur in Ausnahmefällen auf. Für alle Verbindungen der Tab. I wurde deshalb eine einheitliche Arbeitsvorschrift für die Anreicherung und Bestimmung der Elementspuren verwendet. Lediglich in Wasser unlösliche Salze müssen vor Beginn der Analyse geeignet gelöst werden.

TABELLE I

LISTE DER ALS PROBENMATERIAL EINGESETZTEN SALZE

	Li^+	Na^+	K^+	NH_4^+	Ca^{2+}	Sr^{2+}	Ba^{2+}
F^-			×				
Cl^-			×	×	×	×	×
Br^-	×		×	×			
I^-		×	×				
SCN^-		×	×				
NO_3^-	×		×	×	×	×	×
SO_4^{2-}			×				
HCO_3^-		×					
CO_3^{2-}		×					×
SO_3^{2-}		×					
$S_2O_3^{2-}$		×					
$S_2O_4^{2-}$		×					
$S_2O_5^{2-}$			×				
ClO_4^-		×					
BrO_3^-			×				
$B_4O_7^{2-}$		×					
$H_2PO_4^-$			×	×			
HPO_4^{2-}		×		×			
Acetat		×					
Oxalat		×		×			
Tartrat		×					
Citrat		×					

Arbeitsbedingungen

Das Alkali- bzw. Erdalkalisalz (10 g) wird zu etwa 150 ml in Wasser gelöst. Nach Zusatz von 10 ml Pufferlösung (a) wird der pH-Wert kontrolliert und gegebenenfalls auf etwa pH 8 gebracht. Die Lösung wird mit 1 ml frisch bereiteter 2%iger NaDDTC-Lösung versetzt und sofort anschliessend durch ein mit 50 mg feinpulvriger Aktivkohle (Merck, Darmstadt, Art.-Nr. 2186) beschichtetes Weissbandfilter (∅ 25 mm) filtriert.

Dazu wird die Kohle als aliquoter Teil (10 ml) einer wässrigen Suspension (1 g Aktivkohle pro 200 ml bidest. Wasser), deren Absetzen durch intensives Rühren verhindert wird, abpipettiert. Durch Absaugen des Wassers wird das Filter mit einer etwa millimeterstarken, gleichmässigen Kohleschicht bedeckt. Einzelheiten über die Eigenschaften der verwendeten Aktivkohle siehe[3]. Als Filtriereinrichtung verwenden wir eine auch bei radiochemischem Arbeiten gebräuchliche zerlegbare Hahn'sche Nutsche mit aufgesetztem Trichter, welcher das gesamte Volumen einer Probenlösung fasst (Abb. 1). Nach Trocknen des mit den Spuren beladenen Aktivkohle-Filters bei 110°C im Trockenschrank wird die Kohleschicht mit einem Spatel abgeschabt und im 50 ml-Becherglas mit 1 ml 65%iger Salpetersäure abgeraucht. Der Rückstand wird mit 10,0 ml 20%iger Salpetersäure aufgenommen; nach kurzem Zentrifugieren wird die überstehende Lösung durch A.A.S. analysiert. Messgerät: Varian-Techtron Atomabsorptions-Spektrometer Modell A 1000 mit zugehörigen Hohlkathodenlampen; Acetylen–Luft-Flamme.

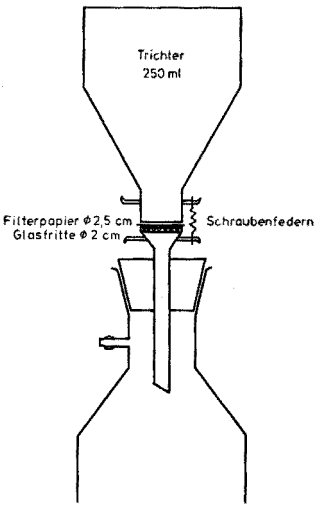

Abb. 1. Filtriergerät zur Spurenanreicherung an Aktivkohle.

Puffer pH 8,4 nach Clark und Lubs; Lösung A: je 0,5 *M* an H_3BO_3 und KCl; Lösung B: 0,5 *M* NaOH. 1000 ml der Lösung A und 150 ml der Lösung B werden gemischt und nach Zusatz von 10 ml 2%iger NaDDTC-Lösung mit 200 mg Aktivkohle 5 min geschüttelt und filtriert. Der gewünschte pH-Wert von etwa 8,4 wird erst beim Verdünnen dieser Lösung 1:10 mit Wasser erreicht.

Bei jedem der Salze wurde die Vollständigkeit der Anreicherung durch vergleichende Analysen der Spurenkonzentrate sowie von Eichmischungen mit entsprechenden Spurenmengen überprüft. Dazu wurden zu je 6 Lösungen des Salzes (10 g in 150 ml Wasser) ansteigende Mengen (1–20 μg) der Elemente Ag^+, Bi^{3+}, Cd^{2+}, Co^{2+}, Cu^{2+}, Fe^{3+}, In^{3+}, Ni^{2+}, Pb^{2+}, Tl^+ und Zn^{2+} gegeben. Entsprechend der Arbeitsvorschrift wurden die Spuren angereichert und bestimmt. Parallel dazu wurden die Analysensignale der als Spurenzusatz verwendeten aliquoten Teile der Eichlösung unter Umgehen des Anreicherungsprozesses gemessen.

Aus dem Quotienten der Steigungen zusammengehöriger Eichgeraden wurde für jedes der zugesetzten Elemente die Ausbeute der Anreicherung berechnet.

Die Standardabweichung des Verfahrens wurde an jeweils 14 vollständigen Analysen mit Natriumacetat, Ammoniumchlorid sowie Calciumnitrat als Probenmaterial durchgeführt (Tab. II). Dazu wurden die zuvor aufgereinigten Lösungen der Salze einheitlich auf bestimmte Spurenkonzentrationen eingestellt (Tab. II, Spalte 2). Die Nachweisgrenze (3 σ-Grenze) wurde aus den Blindwert-Streuungen bei Analyse der sorgfältig aufgereinigten Präparate ermittelt.

ELLE II

TISTISCHE DATEN FÜR ANREICHERUNG UND A.A.S.-BESTIMMUNG VON ELEMENTSPUREN USGEWÄHLTEN SALZEN

ntspur	Rel. Standardabweichung ($N=14$) $s/\bar{x}$			Nachweisgrenze (p.p.m.)	
(p.p.m.)	CH_3COONa	NH_4Cl	$Ca(NO_3)_2 \cdot 4H_2O$	CH_3COONa	NH_4Cl
0,4	0,023	0,021	0,025	0,06	0,03
2	0,019	0,024	0,024	0,2	0,2
0,1	0,020	0,019	0,019	0,01	0,03
0,5	0,029	0,026	0,016	0,08	0,05
0,5	0,032	0,015	0,019	0,02	0,02
0,8	0,056	0,028	0,031	0,03	0,04
3	0,026	0,023	0,020	0,3	0,2
1	0,042	0,014	0,020	0,05	0,07
0,4	0,018	0,027	0,025	0,1	0,1
0,3	0,047[a]	0,013	0,015	1,1[a]	0,3
0,2	0,064[b]	0,020	0,023	0,08[b]	0,03

ssung mit stark verrauschter Hohlkathoden-Lampe.
n Zeitpunkt der Messungen wurden im gleichen Labor Zinkpräparate untersucht.

Ergebnisse

Die zahlreichen Einzelergebnisse der Untersuchungen können zu folgenden Aussagen über die Anreicherung von Spurenverunreinigungen aus Alkali- und Erdalkalisalzen zusammengefasst werden:

Ag. Bei der Mehrzahl der Salze erhält man Ausbeuten >95%; das gilt trotz der Schwerlöslichkeit der Silberhalogenide auch für Chloride, Jodide und Thiocyanate. Werte <90% werden nur bei den Salzen mit Bromid und Bromat als Anion gefunden. Hier liegen die Werte durchweg unter 10% Ausbeute.

Um die Ursache für das abweichende Verhalten des Silbers bei der Anreicherung aus Lösungen der verschiedenen Alkali- und Erdalkalibromide und -bromate zu finden, wurden einige zusätzliche Versuche durchgeführt. (1) Analog zu den Bedingungen der Arbeitsvorschrift wurde die Anreicherung von Silber (1–5 μg) aus KCl, KBr, KI und KSCN ohne Zusatz des Chelatbildners NaDDTC versucht. Die Ergebnisse sollten zeigen, ob Ag^+ in diesen Mengen auch als schwerlösliches Silberhalogenid an der Kohleoberfläche sorbiert und angereichert wird. (2) Anstelle des einmaligen Abrauchens mit Salpetersäure, wie unser Arbeitsverfahren vorschreibt, wurde die mit Spuren beladene Aktivkohle mit HNO_3–H_2SO_4-Mischsäure vollständig aufgeschlossen und analysiert. Hierdurch sollte

TABELLE III

VERBLEIB VON SPUREN SILBER BEI DER ANREICHERUNG AUS ALKALIHALOGENIDEN

Analysenmaterial	*% des eingesetzten Silbers im Spurenkonzentrat wiedergefunden*			
	Anreicherung unter NaDDTC-Zusatz		*Anreicherung ohne NaDDTC*	
	Abrauchen mit HNO_3	*Aufschluss mit HNO_3–H_2SO_4*	*Abrauchen mit HNO_3*	*Aufschluss mit HNO_3–H_2SO_4*
KCl	>95	Nicht bestimmt	38	31
KBr	< 5	94	<5	Etwa 90
KI	>95	Nicht bestimmt	Etwa 90	Nicht bestimmt
KSCN	>95	Nicht bestimmt	Etwa 90	Nicht bestimmt

festgestellt werden, ob der bei Bromiden und Bromaten beobachtete Ausbeuteverlust tatsächlich durch unvollständige Anreicherung des Silbers verursacht wird, oder ob die geringe Sorption nur vorgetäuscht wird, weil das angereicherte Silber bei der Behandlung mit Salpetersäure unter den Bedingungen der Arbeitsvorschrift am Trägermaterial Kohle haften bleibt. Tabelle III enthält die Ergebnisse dieser Untersuchungen.

Aus KCl wird danach ohne NaDDTC nur ein Teil des Silbers, vermutlich als AgCl, von der Kohle sorbiert; erst in Gegenwart des Chelatbildners ist die Anreicherung quantitativ. Beim anschliessenden Behandeln der Kohle mit Salpetersäure wird sorbiertes AgDDTC zersetzt; als AgCl gebundene geringe Anteile des Silbers werden mit aufgelöst. Silber wird folglich bei allen Chloriden ohne Verlust im Spurenkonzentrat wiedergefunden. Aus KI und KSCN werden Silberspuren, unabhängig davon, ob den Probenlösungen NaDDTC zugesetzt wird oder nicht, angereichert; aus KBr dagegen werden weder mit noch ohne Chelatbildner merkliche Silbermengen im Spurenkonzentrat wiedergefunden. Die nach dem Mischsäure-Aufschluss der Kohle gewonnenen Werte zeigen jedoch, dass das Silber auch in diesem Fall von Aktivkohle sorbiert wurde. Offensichtlich wird der bei der Analyse des Spurenkonzentrats beobachtete Verlust allein durch die geringe Säurelöslichkeit des nach HNO_3-Zusatz aus AgDDTC gebildeten oder von vornherein sorbierten AgBr verursacht. AgBr entsteht vermutlich auch bei der Anreicherung von Spuren Silber aus Bromaten, so dass hier dieselben Überlegungen gelten. AgI und AgSCN werden, anders als AgBr, bei Einwirken von Salpetersäure wahrscheinlich oxidativ zersetzt, wodurch Anreicherung und Bestimmung des Silbers bei Jodiden und Thiocyanaten mit und ohne Chelatbildner-Zusatz problemlos gelingen. AgBr nimmt anscheinend eine Zwischenstellung ein: es ist in Salpetersäure zu wenig löslich, gleichzeitig aber zu stabil, um von HNO_3 zersetzt zu werden. Zur Bestimmung der aus Bromiden und Bromaten angereicherten Silberspuren muss das Trägermaterial Kohle deshalb vollständig aufgeschlossen werden.

Bi. Die Ausbeuten erreichen bei etwa der Hälfte aller untersuchten Salze Werte $\geqslant 95\%$; aus den übrigen Verbindungen wird Bi^{3+} mit Ausbeuten zwischen 88 und 95% angereichert. Ein Einfluss bestimmter Anionen auf die Bi^{3+}-Anreicherung ist nicht erkennbar.

Cd. Ausbeuten überwiegend* $\geqslant 95\%$; bei KF $\sim 90\%$.

Co. Ausbeuten überwiegend $\geqslant 95\%$; bei KF, Na-Citrat sowie den Thiocyanaten $\sim 90\%$.

Cu. Ausbeuten überwiegend $\geqslant 95\%$; bei KF, Na-Tartrat und einzelnen Phosphaten 90–95%.

Fe. Bei KF, den Phosphaten, Na-Citrat und Na-Tartrat sind die Ausbeuten im allgemeinen $< 50\%$; bei den Oxalaten, Thiocyanaten, Na_2SO_3 und $Na_2S_2O_4$ $\sim 90\%$. Sonst $\geqslant 95\%$.

In. Ausbeuten überwiegend $\geqslant 95\%$; bei Na-Citrat und den Phosphaten $\sim 90\%$.

Pb. Ausbeuten überwiegend $\geqslant 95\%$; bei Na-Tartrat $\sim 70\%$. Bei allen Bariumsalzen sind die Ausbeuten der Pb^{2+}-Anreicherung $< 50\%$; nähere Untersuchungen wurden hierzu nicht durchgeführt.

Tl. Ausbeuten überwiegend $\geqslant 95\%$.

Zn. Die Ausbeuten erreichen bei etwa der Hälfte aller untersuchten Salze Werte $\geqslant 95\%$; bei den Phosphaten wurden unterschiedliche Werte $< 90\%$ erhalten. Sonst 90–95%.

Die statistischen Daten für die Analyse von Natriumacetat, Ammoniumchlorid und Calciumnitrat als ausgewähltem Probenmaterial sind in Tab. II zusammengestellt.

Der Eindampfrückstand der nach Filtration von Lösungen mit 10 g Alkali- bzw. Erdalkalisalz, Puffer und NaDDTC durch 50 mg Aktivkohle und Säurebehandlung der Kohle erhaltenen Spurenlösungen liegt durchweg unter 5 mg. Dieser Rückstand besteht zu einem wesentlichen Teil aus organischem Material, das von Kohle und Chelatbildner herrührt. Der hieraus und aus den Ausbeuten der Anreicherung errechnete Anreicherungsfaktor ist für die Mehrzahl aller untersuchten Elemente und Analysenmaterialien grösser als 10^3.

VERBESSERUNG DES NACHWEISVERMÖGENS DER A.A.S.-ANALYSE VON SPURENKONZENTRATEN DURCH ANWENDUNG DES "INJEKTIONSVERFAHRENS"

Wie hier beschrieben wurde, erhält man durch Sorption der DDTC–Chelate zahlreicher Elementspuren an Aktivkohle und Behandeln der Kohle mit Salpetersäure ein Spurenkonzentrat, das weitgehend frei von Bestandteilen der Probenmatrix ist und leicht auf ein sehr kleines Messvolumen gebracht werden kann. Um bei der Analyse möglichst wenig an Empfindlichkeit und Nachweisvermögen zu verschenken, wird das Volumen nur so gross gewählt, dass es zur Bestimmung der interessierenden Elemente gerade ausreicht. Mit den heute üblichen A.A.S.-Geräten werden die verschiedenen Elementspuren einer Probenlösung jeweils nach Wechseln der Hohlkathoden-Lampen nacheinander bestimmt, wobei bis zur Stabilisierung des Messsignals für jedes Element etwa 0,5–1 ml der Lösung verbraucht werden. Je mehr Elemente zu bestimmen sind, desto grösser ist das insgesamt benötigte Probenvolumen; Empfindlichkeit und Nachweisvermögen nehmen mit der Zahl der zu bestimmenden Elemente zwangsläufig ab. Tatsächlich ist die Atomabsorptions-Spektrometrie in ihrer heutigen Ausstattung für Multi-Element-Analysen nur ein Notbehelf.

---

* "Überwiegend" bedeutet, dass der angegebene Wert lediglich in Einzelfällen nicht ganz erreicht wird, in jedem Fall aber $> 90\%$ ist.

Änderungen am Bestimmungsverfahren, bei denen Probenlösung eingespart werden kann, ohne dass das Verhältnis der Grösse der Analysensignale zu ihrem Untergrund verkleinert wird, bedeuten deshalb eine Verbesserung jedes Verbundverfahrens aus chemischer Anreicherung und A.A.S.-Bestimmung von Elementspuren. Ein Beispiel hierfür ist das kürzlich von Sebastiani *et al.*[4] beschriebene "Injektionsverfahren". Bei dieser Variante der Flammen-A.A.S. wird die Probenlösung, anstelle des sonst üblichen Ansaugens, mit Hilfe einer Kolbenpipette als abgemessenes Volumen in einen auf den Ansaugschlauch des Zerstäubersystems gesetzten kleinen Trichter eingespritzt. Die Autoren zeigen, dass die nach Injektion von nur 50–100 µl in Form scharfer Extinktionsspitzen erhaltenen Analysensignale nur wenig kleiner sind als die bei konventioneller Bestimmung gemessenen stationären Signale. Von uns durchgeführte systematische Untersuchungen zur Analyse von Spurenkonzentraten zeigten, dass zur Bestimmung von etwa 10 Elementen mit diesem Verfahren ein Gesamtvolumen von 1 ml ausreicht[5]. Die Signalhöhe ist—bei allen Elementen in etwa gleicher Weise—vom Injektionsvolumen, von der Ansprechzeit des Messsystems, insbesondere von der Dämpfung, sowie von der Saugleistung des Zerstäubersystems abhängig. Für jedes Injektionsvolumen gibt es eine in Bezug auf die Messempfindlichkeit optimale Ansaugrate, die in Vorversuchen ermittelt und am Gerät eingestellt werden muss. Nähere Einzelheiten sind den zitierten Arbeiten[4,5] zu entnehmen.

TABELLE IV

VERBESSERUNG DES NACHWEISVERMÖGENS DER FLAMMEN-A.A.S. DURCH PROBENINJEKTION

Bestimmung durch Injektionsverfahren				*Konventionelle Bestimmung*
Elementspur		*Rel. Standardabweichung (N = 10)*	*Nachweisgrenze (3 σ-Grenze) (p.p.m.)*	*Nachweisgrenze (3 σ-Grenze) (p.p.m.)*
Me^{n+}	*(p.p.m.)*			
Ag^{+}			0,004	0,03
Bi^{3+}	0,3	0,036	0,06	0,2
Cd^{2+}	0,04	0,030	0,003	0,03
Co^{2+}	0,05	0,027	0,01	0,05
In^{3+}	0,3	0,033	0,04	0,2
Ni^{2+}	0,1	0,037	0,01	0,07
Pb^{2+}	0,1	0,041	0,02	0,1
Tl^{+}	0,3	0,032	0,03	0,3

Tabelle IV zeigt am Beispiel der Analyse von NH_4Cl den durch Anwenden des Injektionsverfahrens gegenüber der üblichen Arbeitsweise erzielten Gewinn an Nachweisvermögen durchschnittlich um den Faktor 7. Die Werte für die Nachweisgrenze (3 σ-Grenze) wurden aus den Streuungen der Blindsignale von besonders aufgereinigtem NH_4Cl ermittelt. Die Tabelle enthält ferner für die untersuchten Elemente die aus 10 Parallelanalysen von NH_4Cl mit den jeweils angegebenen Spurengehalten errechnete relative Standardabweichung. Bei diesen Messungen musste auf die Bestimmung von Cu, Fe und Zn verzichtet werden, da die zur

Verfügung stehende Aktivkohle wegen ihres relativ hohen Eigengehaltes in dem hier interessierenden Spurenbereich für diese Elemente nicht mehr zu verwenden ist.

Wir danken der Deutschen Forschungsgemeinschaft sowie dem Fonds der Chemischen Industrie für die finanzielle Unterstützung dieser Arbeit Frau I. Pesé danken wir für ihre sorgfältige experimentelle Mitarbeit.

ZUSAMMENFASSUNG

Es wird ein für die Reinheitskontrolle von Alkali- und Erdalkalisalzen geeignetes Analysenverfahren beschrieben. Die mit Natrium-diäthyldithiocarbamidat reagierenden Elementspuren (Ag, Bi, Cd, Co, Cu, Fe, In, Ni, Pb, Tl, Zn) werden durch Filtrieren der 10 g Salz enthaltenden Probenlösung durch ein mit 50 mg Aktivkohle beschichtetes Filter abgetrennt. Die Chelate werden dabei adsorbiert und an der Kohleoberfläche angereichert. Nach Behandeln der Kohle mit Salpetersäure werden die angereicherten Elemente durch Flammen-Atomabsorptions-Spektrometrie bestimmt. Durch Anwenden des "Injektionsverfahrens" werden Nachweisgrenzen, je nach Element, zwischen 0,06 und 0,003 p.p.m. erzielt. Die relative Standardabweichung $s/\bar{x}$ liegt im allgemeinen bei 0,04.

SUMMARY

A method is described for the purity control of alkali and alkaline earth salts. Trace elements reacting with sodium diethyldithiocarbamate (Ag, Bi, Cd, Co, Cu, Fe, In, Ni, Pb, Tl, Zn) are separated by filtration of the solution containing 10 g of the sample through a filter paper coated with 50 mg of activated carbon. The chelate compounds are adsorbed and collected at the surface of the carbon particles. After the carbon collector has been treated with nitric acid, the concentrated elements are determined by flame atomic absorption spectrometry. By application of the "injection method" the limit of detection for different elements was found to be between 0.06 and 0.003 p.p.m. The relative standard deviation $s/\bar{x}$ generally is about 0.04.

LITERATUR

1 O. G. Koch und G. H. Koch-Dedic, *Handbuch der Spurenanalyse*, Springer-Verlag, Berlin, 1974.
2 B. Welz, *Atom-Absorptions-Spektroskopie*, Verlag Chemie, Weinheim/Bergstr., 1972.
3 E. Jackwerth, J. Lohmar und G. Wittler, *Z. Anal. Chem.*, 266 (1973) 1.
4 E. Sebstiani, K. Ohls und G. Riemer, *Z. Anal. Chem.*, 264 (1973) 105.
5 H. Berndt und E. Jackwerth, *Spectrochim. Acta*, im Druck.

Analytica Chimica Acta, 74 (1975) 309–319

DETERMINATION OF CHLORIDE IN NATURAL AND POTABLE WATER SAMPLES BY TURBIDIMETRIC DISCRETE-SAMPLE AUTOMATIC ANALYSIS

J. RAMÍREZ-MUÑOZ

Beckman Instruments, Inc., Irvine, California 92664 (U.S.A.)

(Received 24th July 1974)

Chloride is a component of virtually all natural and potable water samples; several analytical methods have been proposed for its manual determination[1,2]. Recently, Westcott developed an automatic colorimetric method by means of discrete-sample automatic analysis[3]; an automated analyzer capable of performing 40 readings in each run was used. This automated analyzer has already been described[4,5]. The results obtained by Keller[6] in turbidimetric determination of sulfates in water by discrete-sample automatic analysis have been taken as a basis for the turbidimetric determination of chlorides by using the classical procedure of precipitation of chloride with silver ions[7].

The following points were considered before laboratory tests were begun.

(a) Turbidimetric tests usually do not show the reproducibility (different instruments and/or operators) normally found with the stoichiometric reactions of colorimetry, and are much more subject to operating conditions (temperature, acidity, time, order of addition of reagents, stirring or shaking, etc.).

(b) Chloride concentration in waters is low (with the exception of highly saline waters). Thus, it is often necessary to work close to the limiting conditions imposed by the solubility product of AgCl ($P_s = 2 \cdot 10^{-10}$ at 25°C). This situation produces lack of linearity in the low-concentration ranges of analytes, an effect already verified[8] in a study involving linearity tests in indirect methods for flame photometric determination of sulfates, after precipitation with barium or strontium ions.

(c) Even if all operating conditions are standardized by automatic techniques, repeatability still may not be high because of slight differences in media composition which result from random differences in the growing conditions of micro-particles of the precipitate.

However, it was decided to establish operating parameters and to study linearity, sensitivity, repeatability and accuracy with the aim of arriving at a tentative procedure. The main objective was to establish a procedure which would be rapid, low in cost per analysis, flexible for a wide range of concentrations, and precise and accurate enough for routine testing of chlorides in large numbers of water samples.

Instrumentation, procedure, working conditions and results are summarized below. These results are promising and form a basis for future efforts on the turbidimetric determination of chlorides by discrete-sample automatic analysis of different samples.

EXPERIMENTAL

Instrumentation

All automatic analytical tests were done with a Beckman Automated Materials Analyzer (AMA 40) equipped with a Beckman Model 25 Spectrophotometer and a Low-Profile Recorder as readout module. The unit was connected with a teletypewriter (as printer and tape puncher) via an intercoupler.

Spectral scanning tests were performed with a Beckman Model 25 Spectrophotometer and a Low-Profile Recorder.

Reagents

Deionized–distilled water was used in the preparation of all solutions.

Silver nitrate solution (0.05 M). Silver nitrate (8.4946 g) was dissolved in 800 ml of water, 10 ml of concentrated nitric acid were added, and the solution was diluted to 1 l with water. Addition of nitric acid prevents the precipitation of many anionic species which might otherwise interfere. Of those that might precipitate (*e.g.* iodides and bromides), concentrations are normally so small that interferences are negligible.

A 0.025 *M* silver nitrate solution was prepared similarly.

Standards

Sodium chloride stock solution (500 p.p.m.). Sodium chloride (0.8241 g), already dried at 140°C, was dissolved in 800 ml of water and the solution was diluted to 1 l with water.

Sodium chloride working standards. Solutions containing 250 p.p.m., 100 p.p.m. and 40 p.p.m. were prepared by suitable dilution with water.

Blanks

In preliminary tests, deionized–distilled water was used as blank. In further tests, concentrated ammonia solution was used as blank (see below).

Deionized–distilled water was used in the reference cell of the spectrophotometer for all tests.

Filtering

No filtering was used in the tests described. However, if samples are observed to contain suspended matter, they should be filtered.

Operating conditions

Operating conditions established after the preliminary research work are summarized in Table I. The recorder was set at full scale 0.5 absorbance unit. Turbidity was measured in terms of absorbance. Signals shown in the Figs. correspond to full scale 0.5 absorbance unit.

Experimental set-up

Figure 1 shows the experimental set-up for automated analysis. The pipetter–diluter (P–D) setting 1.00 ml + 4.00 ml was used for most of the experimental work covering the concentration range 5–250 p.p.m. chloride in the original solution.

TABLE I

OPERATING CONDITIONS

Disruption timer[a]	15 s
Filter probe[b]	Not used
Pipetter–diluter	Pedestal position No. 5 Diluting solution: water Volumes: 1 ml + 4 ml TC→TT1
Reagent pump	Pedestal position No. 6 Reagent: Silver nitrate solution (0.05 *M*) Volume: 2 ml TT1
Mixer	Pedestal position No. 7 TT1
Sampling probe	Pedestal position No. 8 TT1
Wavelength	600 nm
Reference cell	Water
Sampling timer	10 s (4.5 ml)
Slit program	Normal
Recorder chart speed	5 in./min
Recorder span setting	100 mV
Solvent pump	Not used
Sample vacuum	15 in.
Model 25 Spectrophotometer operation[c]	Double beam
Lamp	Tungsten
Setting	0.5 absorbance unit
Sequence	Two blanks, standards, two blanks, five samples, two blanks, five samples, two blanks, etc. Ammoniacal blanks and standards in special reference tubes

[a] Disruptor is not used. Disruption time is set at 15 s to perform each working cycle in 60 s (40 working positions in 48 min).

[b] Not used if samples are not to be filtered.

[c] Since readings are obtained at 600 nm, a Model 24 Spectrophotometer can also be used.

In the case of high chloride samples, a second P–D and the corresponding mixer can be used (Fig. 2).

Working range flexibility for work with high concentrations of chloride in the original solution can be achieved by changing the setting in the P–D or by using a second couple P–D/mixer.

However, for some diluted original solutions, it might be necessary to use a special P–D (5+5 P–D)*. Low concentration ranges can be used: (a) by pipetting 5 ml of original sample in the T-tubes (no P–D, 1–50 p.p.m.); or (b) by using a special P–D (5+5) (2–100 p.p.m.). Higher concentration ranges can be used: (a) by decreasing the aliquot pipetted from the original sample with one P–D (0.50+4.50

* The 5+5 P–D has two pistons of 5 ml maximum, instead of 1.25 ml and 5 ml for normal P–D's.

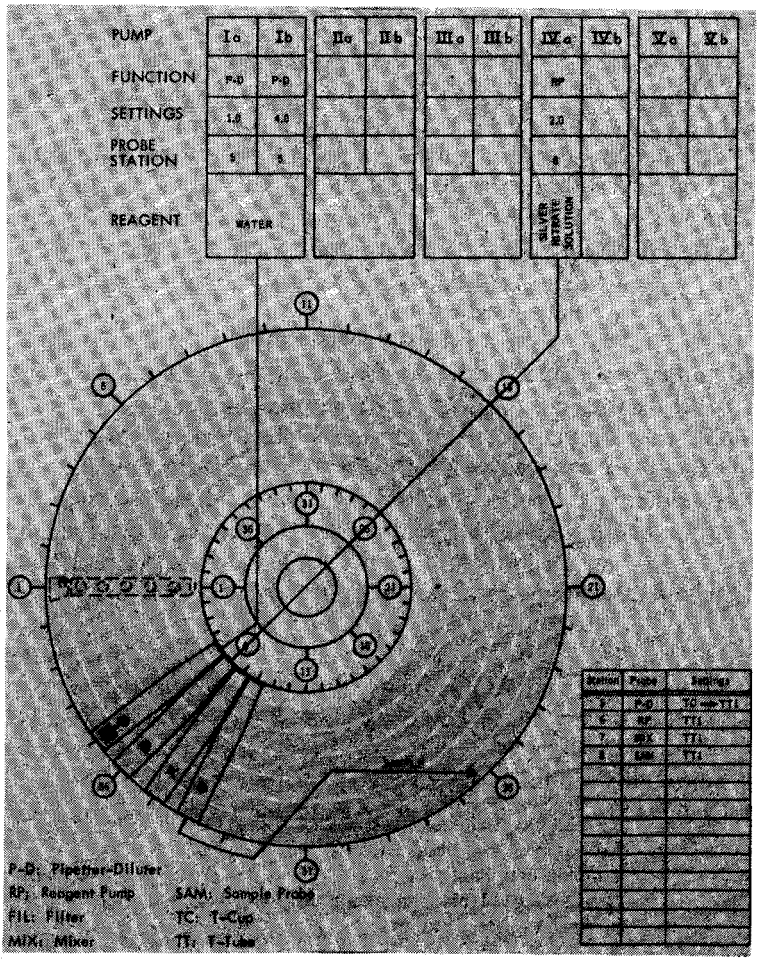

Fig. 1. Experimental set-up diagram for chloride determination for original samples containing up to 250 p.p.m. chloride (range: 5–250 p.p.m.).

ml, 10–500 p.p.m.); or (b) by using two P–D's (ranges 25–1250 p.p.m., 50–2500 p.p.m., or 100–5000 p.p.m., with different experimental settings).

Many other ranges can be chosen by variation of pump settings. Samples with more than 5000 p.p.m. can be examined by using aliquots smaller than 0.50 ml in one or both P–D's.

Data evaluation

Experimental data were evaluated by computer techniques by means of a time-shared terminal (IBM 370 System).

RESULTS AND DISCUSSION

Results of preliminary trials

Spectral scanning. Suspensions prepared with 250, 100 and 40 p.p.m. chloride

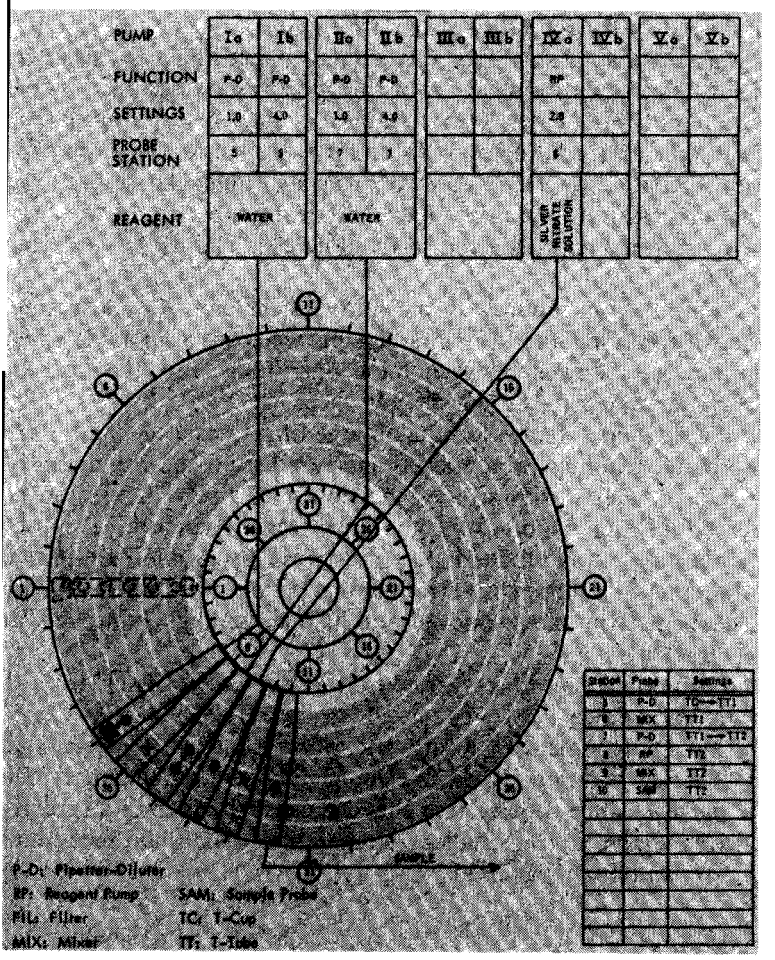

Fig. 2. Experimental set-up diagram for chloride determination for original samples containing up to 1250 p.p.m. chloride (range: 25–1250 p.p.m.).

were examined by scanning from 700 nm to 250 nm. Absorbance readings increased from the visible to the u.v. region.

Illumination of the flow-cell filled with freshly prepared silver chloride suspension produces photodecomposition of the silver halide. This causes a consequent darkening of the cell windows (silver deposit) and frequent cleaning of the cell is necessary. To eliminate this problem, it seemed desirable to utilize non-actinic regions of the spectrum and, therefore, subsequent readings were performed at 600 nm. Although this involves loss of sensitivity, the loss is not unduly severe.

Use of dilute silver nitrate solution (0.025 M). This solution was used in the first trials. Inconsistent results were obtained (low precision). Better repeatability was observed at various levels of chloride concentration with the 0.05 *M* silver nitrate solution, which was later used for all tests. In any case, excess of

precipitating agent decreases the solubility of the precipitate.

Use of glycerine solution as stabilizer. Glycerine was preliminarily tested as a means of stabilizing the suspension because of the good results obtained in the turbidimetric determination of sulfates. Other stabilizers may also be used. The author has used agar-agar and gelatine to keep uniform suspensions for analyses by atomic absorption spectroscopy. Here, however, agar-agar and gelatine were not used, in order to avoid significant changes of the physical properties of the final solutions which were aspirated and delivered to the flow cell. The use of glycerine was found undesirable.

Use of factor time. In connection with the study of single or double stirring, time was allowed between stirring and sampling. Results were not acceptable when more than one minute was allowed between these operations. For this reason, sampling should be done immediately after stirring.

Use of ammonia solution as blank. Results obtained with water as blank were not acceptable. The blank readings progressively increased from the beginning of the run up to the end of each working series. A deposit of finely divided silver chloride was observed in the windows of the flow cell. Therefore, 1 ml of concentrated ammonia liquor was pipetted and transferred by dilution by means of the P–D. The ammoniacal solution is active enough to dissolve films of silver chloride particles deposited on the windows, and blank readings improved in stability (no drastic drift).

Concentrated ammonia liquor was also used at the end of each run for cleaning the sampling line and cell.

Use of heat. No improvement of results was observed when the solutions were heated after silver(I) addition. In fact, even gentle heating enhances the formation of larger particles after cooling, and this decreases the turbidity (gravity separation of particles). Operation at ambient temperature makes the procedure simpler and faster. No incubation was used.

Linearity

Results attained in the present study indicated non-linear response. Concavity upwards was observed, which was accentuated in the low concentration range. This lack of linearity made it necessary: (a) to operate only at the medium or high level of concentration; (b) to use "sandwiching" interpolation between standards; or (c) to use curve plotting (graphically or by computer fitting) before interpolation.

Quadratic fitting gave satisfactory results. An example of curve fitting test is given in Fig. 3. In Table II, slopes for linear fitting and coefficients for quadratic fitting are given from a few linearity tests (only three experimental points plus blank).

Other points for curve fitting were obtained by varying the settings of the P–D, as shown in Table III.

Blank readings were subtracted from signals of standards in calculating linearity tests. Blanks were adjusted to read above the level of 0.00 absorbance unit in order to be accepted by the computer programs and also to give a rapid visual appreciation (on the recordings) of the stability (or drift) of the blank readings. Blank readings were later processed to help in the calculation of sensitivity.

```
LINEAR FIT.  SLOPE =       0.011174

PAIR    X VALUES    Y VALUES    Y CALCD.   DIFFERENCE      % ERROR

  1       5.7100      0.0440      0.0638      0.0198      45.0062
  2      14.3000      0.1400      0.1598      0.0198      14.1330
  3      35.7000      0.4100      0.3989     -0.0111      -2.7057


QUADRATIC FIT.  COEFFICIENTS:

T1 =       0.008254

T2 =       0.000091

PAIR    X VALUES    Y VALUES    Y CALCD.   DIFFERENCE      % ERROR

  1       5.7100      0.0440      0.0501      0.0061      13.8770
  2      14.3000      0.1400      0.1367     -0.0033      -2.3560
  3      35.7000      0.4100      0.4110      0.0010       0.2545
```

Fig. 3. Computer fitting calculation (linear and quadratic fittings). Original standards: 40, 100 and 250 p.p.m. chloride. Final concentrations, after dilution: 5.71, 14.3 and 35.7 p.p.m. chloride.

TABLE II

LINEARITY TESTS

Run	*Linear fitting slope*[a]	*Quadratic fitting coefficients*[b]	
		T1	*T2*
1	0.011174	0.008254	0.000091
2	0.013109	0.007470	0.000176
3	0.011131	0.008603	0.000079

[a] Slope of equation $A = mC$.
[b] Coefficients of equation $A = T1C + T2C^2$.

Repeatability

Repeatability was studied at various concentration levels with standard solutions. Results are summarized in Table IV; repeatability tests on standards of 40 and 100 p.p.m. are shown in Fig. 4(a) and (b).

Low levels of chloride (about 40 p.p.m. chloride in the initial solution) showed the highest variability; therefore, analyses should be performed on solutions containing more than 40 p.p.m. Although lower concentrations can be measured, readings will be less precise than those observed in solutions containing 40–250 p.p.m. chloride.

Slight variations observed at the top of each individual signal are caused by small changes of signal during the reading period. The use of active signals has the advantage of constantly showing the noise level of a particular signal and of recording, as a spike or depression, any abnormality occurring in the sampling line during signal recording.

Repeatability tests for standards were performed with a relatively small number of readings. This small number of readings produced relative standard deviations (s_r) comparable with values to be found in duplicate or triplicate readings of sample solutions.

TABLE III

CONCENTRATION OF WORKING STANDARDS PREPARED BY AUTOMATIC DILUTION

Pipetter–diluter setting (ml)	*Starting working standard (p.p.m. Cl^-)*	*Dilution ratio (after adding the reagent)*	*Calculated chloride concentration in the final solution (p.p.m. Cl^-)*
0.25+4.00	40	0.25:6.25	1.60
0.50+4.00	40	0.50:6.50	3.08
0.75+4.00	40	0.75:6.75	4.44
1.00+4.00	40	1.00:7.00	5.71[a]
1.25+4.00	40	1.25:7.25	6.90
0.25+4.00	100	0.25:6.25	4.00
0.50+4.00	100	0.50:6.50	7.69
0.75+4.00	100	0.75:6.75	11.11
1.00+4.00	100	1.00:7.00	14.28[a]
1.25+4.00	100	1.25:7.25	17.24
0.25+4.00	250	0.25:6.25	10.00
0.50+4.00	250	0.50:6.50	19.23
0.75+4.00	250	0.75:6.75	27.28
1.00+4.00	250	1.00:7.00	35.71[a]
1.75+4.00	250	1.25:7.25	43.10

[a] Values normally found in standard work with pipetter–diluter adjusted to 1.00 ml+4.00 ml, and starting from 40, 100, 250 p.p.m. Cl^- in the original solution.

TABLE IV

REPEATABILITY OF STANDARD READINGS

Standard (original concentration) (p.p.m.)	*Average[a] absorbance*	*s*	*s_r (%)*
40	0.052	0.0029	5.50
40	0.048	0.0053	11.12
100	0.179	0.0028	1.58
100	0.170	0.0084	4.96
100	0.172	0.0049	2.91
250	0.384	0.0172	4.48

[a] Average of 5 readings.

Ammoniacal blanks showed good repeatability. In this case, only standard deviation was calculated. In various runs in which the blank absorbance was set between 0.070 and 0.103, the standard deviations found for 9 readings at each setting varied from 0.0022 to 0.0032 absorbance unit.

Sensitivity

The sensitivity of the analytical methodology proposed is expressed in the more conventional sense, by the relationship between readings and concentration.

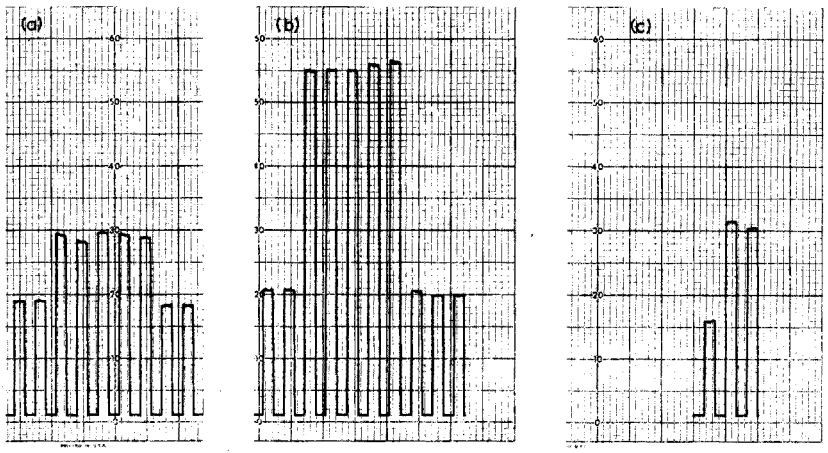

Fig. 4. Repeatability tests. (a) Signals of two blanks, five repeated readings of a 40 p.p.m. Cl^- working standard, and two blanks. (b) Signals of three blanks, five repeated readings of a 100 p.p.m. Cl^- working standard, and two blanks. (c) Signals of two repeated readings of a water sample and a blank. Recorder range was 0.0–0.5 absorbance unit in all cases.

Thus, the values of slopes and coefficient *T1* already given are a numerical representation of the sensitivity achieved (see Table II).

Detectability is a function of sensitivity, and should be expressed on the basis of sensitivity (signal size per given concentration) and on the basis of variability of the blank level. To calculate the smallest concentration detectable (concentration detection limit), only signals for low concentration should be considered. The curvature in the analytical curve at the low end makes it inadvisable to use high concentration signals as reference.

Standards of 40 p.p.m. gave average readings of 0.050 absorbance unit. The standard deviation average at the blank level was found to be 0.0028 unit. Then, if twice this value (calculated by averaging calculated s values) is close to the established reference level $2s$, the minimal concentration of chloride measured with confidence over the blank level would be 5 p.p.m. in the original solution. This value can be lowered down to 2.5 p.p.m. or 1 p.p.m. if a special P–D (5+5 type) is used, or samples are directly pipetted into the reaction T-tubes.

It is necessary to remember that 5 p.p.m. chloride, for instance, in the original sample yields a much lower concentration in the final measured solution. If the recommended set-up is used, 5 p.p.m. in the original sample becomes about 0.72 p.p.m. when measured; 5 ml of a 1 p.pm. solution directly pipetted in the T-tube becomes approximately 0.72 p.p.m. in the final solution after addition of 2 ml of reagent solution.

Working range

Lack of linearity can be observed at the lower end of the curves and coarse precipitates begin to form at the upper end. Whenever possible, measurements should be done on samples whose chloride concentrations are between 50 and 200 p.p.m. chloride.

TABLE V

REPEATABILITY OF WATER SAMPLE READINGS

Sample	*Cl^- concentration determined (p.p.m.)*	*Number of readings*	*Average absorbance*	*s*	*s_r (%)*
1	54.0	3	0.079	0.0044	5.52
2	51.0	2	0.074	0.0042	5.73

TABLE VI

WATER ANALYSIS, CHLORIDE DETERMINATION

Sample	*Chloride present[a] (p.p.m.)*	*Chloride added (p.p.m.) (b)*	*Total chloride found (p.p.m.) (c)*	*Increment found (p.p.m.) (a)*	*Difference (p.p.m.) (a−b)*	*Relative error (%)* $\left(100 \times \frac{a-b}{c}\right)$
A	53.0	31.2	85.0	32.0	0.8	0.94
B	58.0	31.2	86.0	28.0	−3.2	−3.7
A	52.5	12.5	73.0	20.5	7.0	9.6
B	54.0	12.5	73.0	19.0	6.5	8.9

[a] Determined by interpolation.

Water analysis

Water samples were analyzed by the procedures described. The repeatability of duplicate or triplicate readings of a given sample was comparable with the repeatability observed with standards (Table V). In Fig. 4(c), a duplicate reading of a water sample is represented.

Water samples were measured before and after addition of known amounts of chlorides. Results are collected in Table VI. The relative errors found when 31.2 p.p.m. chloride was added to samples containing 50–60 p.p.m. chloride were smaller than $\pm 5\%$. Relative errors found when only 12.5 p.p.m. chloride was added were higher than 5%, but still below 10%. This seems logical, since in addition tests, small ratios for the addition/original concentrations always produce large errors. Thus, the particularly low ratio here was tested purposely to place the analytical system in the worst circumstances.

CONCLUSIONS

The automated analyzer used is applicable to routine turbidimetric determination of chlorides in water samples. The method proposed is applicable between 5 and 250 p.p.m., but can be adapted for lower and higher ranges by easy variations of volume settings in the pumps of the instrument.

Repeatability proved to be very acceptable, considering that turbidity of suspensions was measured. The instrument standardizes all sample handling steps, thus eliminating any sources of variability from manual operations.

Interpolation of readings of samples can be done either graphically or by means of computer techniques after a curve-fitting process. Errors found by examining samples before and after standard additions were of the same order of magnitude as the variability observed in the repeatability tests. The curve-fitting tests were reproducible. Determinations should be done in duplicate or triplicate for better accuracy.

The use of ammonia liquor for blanks not only gives good reproducible blanks but also helps to keep the sampling line and flow cell clean.

The experimental set-up is simple to prepare and is programmed to provide one reading every minute. This reading speed is appropriate for the routine determination of chlorides in great numbers of water samples.

The procedure described can be used as an alternative to conventional colorimetric procedures with the following advantages: (a) flexibility for wide concentration range, (b) use of a single reagent, and (c) the absence of highly acidic reagents.

The author is grateful to Mr. R. Navone, California State Department of Health, for suggesting the trials of chloride determination by turbidimetry, and for advising on the preliminary manuscripts; to Dr. W. F. Ulrich for reading the original manuscript and for helpful suggestions; and to Miss Deborah Schroter for technical help.

SUMMARY

An automatic discrete-sample procedure is described for the turbidimetric determination of chlorides in water samples. Chlorides are precipitated with silver ions and the turbidity of the silver chloride suspension is measured at 600 nm. Up to 30 samples plus blanks and standards can be measured in 48 min. The procedure is applicable to the range of 5–250 p.p.m. chloride in the original samples, but can be easily modified to determine chloride at lower or higher concentrations.

REFERENCES

1 Environmental Protection Agency, *Methods for Chemical Analysis of Water and Wastes*, Cincinnati, Ohio, 1971, p. 29.
2 American Society for Testing and Materials, *1971 Annual Book of ASTM Standards*, Part 23, Philadelphia, Pa., p. 21.
3 C. C. Westcott, *Beckman Instruments, Inc. Automated Brief (Water Quality) No. WB-006*, 1974, Beckman Automated Procedure W-002, 1973.
4 D. G. Rohrbaugh and J. Ramírez-Muñoz, *Anal. Chim. Acta*, 71 (1974) 311.
5 J. Ramírez-Muñoz, *AMA-40 Chemical Operations Manual*, Beckman Instruments, Inc., Industrial Technical Report TR-581, 1973 (reprinted in 1974).
6 C. W. Keller, to be published.
7 F. D. Snell and C. T. Snell, *Colorimetric Methods of Analysis*, Vol. II, van Nostrand, New York, 1949, pp. 614, 714.
8 F. Burriel-Martí, J. Ramírez-Muñoz and M. L. Rexach M. de Lizarduy, *Actas do Congresso*, XV Congresso International de Química Pura e Aplicada (Quím. Anal.) Comm. No. IV-8, Lisbon, 1958; *Rev. Cienc. Apl. (Madrid)*, 12 (1958) 16; *Anal. Chim. Acta*, 17 (1957) 559.

Analytica Chimica Acta, 74 (1975) 321–331

THE EXTRACTION OF VARIOUS METALS AS THEIR ANIONIC COMPLEXES WITH EDTA BY SOLUTIONS OF ALIQUAT-336 CHLORIDE IN 1,2-DICHLOROETHANE

H. M. N. H. IRVING and R. H. AL-JARRAH*

Department of Inorganic and Structural Chemistry, University of Leeds, LS2 9JT (England)

(Received 6th August 1974)

Although there have been extensive studies of the use of long-chain tertiary amines and quaternary ammonium salts as liquid ion-exchange extractants for acids and for anionic complexes of metals with, for example, mineral acids, few publications deal with the liquid–liquid extraction of metal complexonates. Vickery was unable to extract EDTA complexes of lanthanons into chloroform[1] though Zolotov *et al.*[2] have reported the extraction of iron(III) and thorium(IV) from their aqueous solutions in EDTA (H_4Y) by solutions of tetraphenylarsonium chloride in various organic solvents.

Moore[3] has described the extraction of certain actinons and lanthanons at tracer level by a solution of Aliquat-336 chloride in xylene. Improved extraction resulted if the extractant solution was pre-conditioned by shaking with a large excess of EDTA (*cf.* Table I). Since we are dealing here with very stable complexes ($K_{MY} = 10^{17.0}$–$10^{18.2}$), this effect cannot be ascribed to any significant increase in the degree of formation of the metal complexonate as such but rather to replacing the reaction

$$MY^- + (Q^+Cl^-)_{org} \rightleftharpoons (Q^+MY^-)_{org} + Cl^-$$

(where M is the actinon or lanthanon and Q^+ is the methyltricaprylammonium ion) by the reaction

$$(4-n)MY^- + (Q^+_{4-n}H_nY^{4-n})_{org} \rightleftharpoons (4-n)(Q^+MY^-)_{org} + H_nY^{4-n}$$

which has a more favourable equilibrium constant. The extraction of americium was always greater than that of europium under similar conditions.

To extend these results, and those of our earlier study of the extraction of chromium(III)[4], we have investigated the extraction of a considerable number of metals in the form of their anionic complexes with EDTA. In some cases the metal complexonate was prepared as a solid salt by employing literature methods[5–7], while in other cases the effectively quantitative formation of complex at the pH used was ensured by using a 10% excess of EDTA. However, in order to be able to compare one result with another, the concentrations of the different metals, of EDTA, and of Aliquat-336 chloride in 1,2-dichloroethane were each kept constant at $4 \cdot 10^{-3}$ *M*, $4.4 \cdot 10^{-3}$ *M* and 0.2184 *M*, respectively. Extractions were carried

* Present address: The Atomic Energy Research Establishment, Baghdad, Iraq.

TABLE I

THE PERCENTAGE EXTRACTION OF TRACER EUROPIUM AND AMERICIUM FROM 0.002 *M* Na_2H_2Y BY A 20% SOLUTION OF ALIQUAT-336 IN XYLENE[3]

(Columns A and B refer, respectively, to extraction with Aliquat-336 chloride, and Aliquat-336 after pre-conditioning with excess EDTA.)

pH	*Europium*		*Americium*	
	A	*B*	*A*	*B*
2.5	3.3	—	3.6	—
3.1	—	68.6	—	82.6
4.4	14.8	—	27.6	—
4.7	—	95.0	—	98.4
7.1	—	93.6	—	97.5
9.1	—	97.6	—	99.1
9.3	—	95.4[a]	—	99.6[a]
9.3	—	89.8[b]	—	99.8[b]
9.4	—	62.6[c]	—	74.6[c]
9.4	—	37.3[d]	—	42.2[d]
10.3	95.8	93.7	99.9	99.1
10.5	94.0	93.1	94.8	96.8

[a–d] These refer to 0.002, 0.001, 0.0002 and 0.0001 *M* EDTA, respectively.

out from aqueous solutions of different pH values obtained by adding appropriate small quantities of dilute sodium hydroxide. Equal phase volumes were employed and the distribution ratios were determined from the concentration of metal in each phase after equilibration and are only reported if a satisfactory mass-balance was obtained.

Various analytical procedures were used for the determination of metal concentrations including absorption spectrophotometry for EDTA complexes of V(V), Cr(III), Mn(II), Fe(III), Co(II), Co(III), Ni and Cu(II); atomic absorption spectrometry was used for calcium and zinc. For the very stable and colourless complexes, a new procedure was devised in which excess of zirconium was used in an acidic medium to displace the desired metal from its EDTA complex before determination by other means[8]. Iron(III) was determined as a peroxy complex, and in some cases (*e.g.* with Bi, Pb and Mg) the ligand was completely destroyed by oxidation with hydrogen peroxide and the metals thus set free were determined by standard procedures. Experimental results are summarized in Table II and shown graphically in Figs. 1 and 2.

EXPERIMENTAL

Reagents

A suitable weight of Aliquat-336 chloride (commercial tricaprylmethylammonium chloride, kindly donated by General Mills Ltd.) was dissolved in redistilled 1,2-dichloroethane, b.p. 82–84°C, and to remove all traces of acid it was washed successively with dilute sodium hydroxide, with sodium chloride solution, and with distilled water. The concentration of the quaternary salt was then

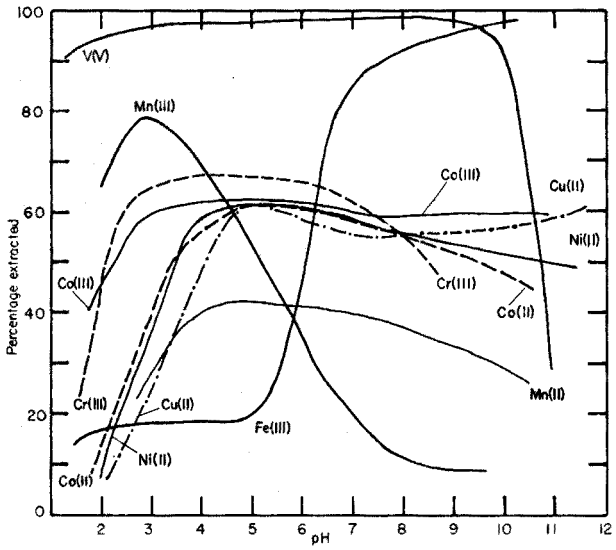

Fig. 1. The percentage of Co(II), Ni(II), Cu(II), Mn(II), Mn(III), Cr(III), Fe(III) and V(V) extracted as complexes with EDTA of concentration $4 \cdot 10^{-3}$ *M* containing a 10% excess of EDTA, by an equal volume of a 0.2184 *M* solution of Aliquat-336 chloride in 1,2-dichloroethane.

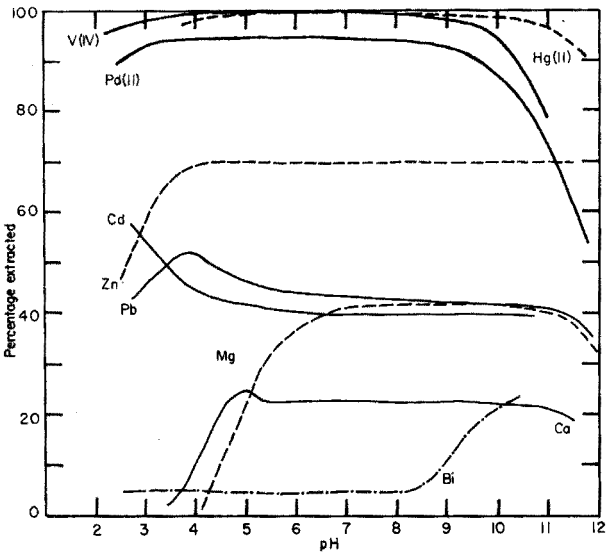

Fig. 2. The percentage of Bi(III), Ca(II), Mg(II), Pb(II), Zn(II), Cd(II), Pd(II), V(IV) and Hg(II) extracted as complexes with EDTA of concentration $4 \cdot 10^{-3}$ *M* containing a 10% excess of EDTA, by an equal volume of a 0.2184 *M* solution of Aliquat-336 chloride in 1,2-dichloroethane.

determined as described by Irving and Nabilsi[18] and adjusted to 0.2184 *M* with pure organic solvent.

Metal complexonates

The chromium–EDTA complex was prepared by boiling chrome alum and

TABLE II

PERCENTAGE EXTRACTION OF METAL IONS

($4.00 \cdot 10^{-3}$ *M* solution of metal ion containing a 10% excess of EDTA extracted by an equal volume of 0.2184 *M* Aliquat-336 chloride in 1,2-dichloroethane.)

Magnesium										
pH	4.18	4.75	5.48	7.48	10.37	11.14	11.65			
%*E*	2.5	16.1	31.5	41.0	40.1	39.8	35.4			
Calcium										
pH	3.71	4.02	4.57	4.84	5.01	5.31	7.60	8.40	10.40	11.24
%*E*	5.3	11.9	22.0	24.3	25.4	23.1	22.7	22.1	22.3	20.2
Vanadium(IV)										
pH	2.45	3.83	4.80	7.61	9.67	10.29	10.77			
%*E*	96.2	99.9	99.9	99.2	96.9	91.6	82.4			
Vanadium(V)										
pH	1.70	3.23	5.17	8.36	9.75	10.81				
%*E*	93.9	97.6	97.3	99.7	95.2	35.2				
Chromium(III)										
pH	1.57	2.56	4.86	6.86	7.97	8.19				
%*E*	26.2	62.3	66.8	63.0	55.4	53.5				
Manganese(II)										
pH	2.84	4.27	4.98	8.11	10.22					
%*E*	24.7	41.9	41.6	36.4	27.9					
Manganese(III)										
pH	2.05	2.79	2.82	3.99	5.20	6.24	8.84	9.47		
%*E*	67.0	78.8	77.1	69.7	50.4	29.8	9.1	8.7		
Iron(III)										
pH	1.54	2.21	3.34	4.90	5.96	6.45	9.73			
%*E*	15.1	17.5	18.4	19.0	44.2	73.0	97.7			
Cobalt(II)										
pH	1.61	3.22	4.65	7.24	8.94	10.52				
%*E*	2.6	46.5	59.8	56.5	52.6	44.9				
Cobalt(III)										
pH	1.66	2.91	5.66	7.29	10.46					
%*E*	39.8	59.7	62.8	59.5	59.4					
Nickel(II)										
pH	1.84	3.07	4.24	6.85	7.29	11.65				
%*E*	3.9	41.2	60.0	58.5	55.4	53.9				
Copper(II)										
pH	1.86	2.48	5.01	5.85	6.53	7.17	8.34	11.47		
%*E*	2.7	14.4	61.6	58.0	56.8	56.7	55.7	60.3		
Zinc(II)										
pH	2.52	4.10	4.90	6.56	7.56	9.14	9.50	10.95	11.55	
%*E*	46.3	69.9	70.0	69.6	68.6	69.4	69.9	68.9	68.9	
Cadmium(II)										
pH	2.90	3.62	4.38	5.90	8.30	9.54	10.38	10.69		
%*E*	55.4	47.2	43.3	40.1	39.9	40.1	39.8	39.9		

(Continued)

TABLE II *(Continued)*

Mercury(II)									
pH	4.10	5.49	6.06	6.37	6.62	9.53	11.02	11.66	
%*E*	99.1	99.5	99.4	99.4	99.4	98.6	97.1	91.6	
Palladium(II)									
pH	1.90	2.60	3.30	5.13	6.81	8.75	9.50	10.55	11.72
%*E*	79.8	90.7	94.2	94.7	94.2	93.1	91.3	80.7	56.2
Lead(II)									
pH	2.58	3.39	4.26	5.88	6.68	7.50	10.62	10.74	11.60
%*E*	43.8	49.7	50.0	44.4	43.5	42.7	41.2	41.0	37.3
Bismuth(III)									
pH	2.33	4.27	4.62	5.12	6.09	8.13	8.89	9.46	
%*E*	4.1	3.9	3.9	3.9	4.3	9.0	10.1	17.7	

$Na_2H_2Y \cdot 2H_2O$ in deionized water for 20 min. When cold, the solution was diluted to 100 cm^3 and aliquot portions (40 cm^3) were treated with dilute sodium hydroxide to give suitable pH values when the volume had been made up to 200 cm^3. The final concentration was $4.0 \cdot 10^{-3}$ *M* in $CrY(H_2O)^-$ and contained a $4 \cdot 10^{-4}$ *M* excess of EDTA.

A solution of the EDTA complex of cobalt(III) was prepared by shaking mechanically for 1 h, 20 cm^3 of 0.1 *M* cobalt(II) sulphate, 20 cm^3 of 0.11 *M* $Na_2H_2Y \cdot 2H_2O$ and 0.5 g of lead(IV) dioxide. The final red solution was made up to 100 cm^3 and separated from excess of lead salts, and its concentration[19] was determined from the absorbance of the solution at λ_{max} 538 nm (0.646 in a 0.5-cm cell), ε_{max} being 323 over the pH range 2–9.

The complex of manganese(III) was prepared as described by Pribil[20], by vigorously shaking 2.2-cm^3 portions of 0.1 *M* manganese(II) sulphate and 5.0 cm^3 of 0.11 *M* $Na_2H_2Y \cdot 2H_2O$ in a 50-cm^3 flask with glacial acetic acid (0.7 cm^3) and lead(IV) dioxide (0.07 g). After 2 min, the volume was made up to 50 cm^3 and excess of lead salts was removed. The concentration of the manganese(III) complex was determined absorptiometrically[11] at 500 nm ($\varepsilon = 468$ in the pH range 2.5–4). Aliquot portions (23 cm^3) were transferred to 25-cm^3 flasks and dilute ammonia solution was added to give suitable pH values after dilution to the mark. During these and all subsequent operations, vessels were covered with aluminium foil to minimize photodecomposition. All other metal–EDTA complexes were prepared from the appropriate cation so as to give solutions of concentration $4.0 \cdot 10^{-3}$ *M* containing a 10% excess of EDTA.

Extraction procedure

Aqueous solutions (5.0 cm^3) containing $4 \cdot 10^{-3}$ *M* metal complexonate with a $4 \cdot 10^{-4}$ excess of EDTA were adjusted to various pH values and shaken with an equal volume of 0.2184 *M* Aliquat-336 chloride in dichloroethane in stoppered centrifuge tubes for 5 min at room temperature. After equilibration, the phases were carefully separated and the pH of the separated aqueous phase was measured with a Radiometer pH-Meter Type pHM4C.

Although aqueous solutions of the manganese(III)–EDTA complex

decompose rapidly, organic extracts were found to be stable for several hours. However, to minimize decomposition in the aqueous phase, the extraction at each pH was carried out with a fresh portion of solution in a total time of 3 min, care being taken to avoid exposing any solutions to the light.

The general procedure for determining the concentration of metal in the organic phase was to "strip" this by equilibrating a 4.0-cm^3 aliquot portion with an equal volume of 0.5 *M* sodium perchlorate. This procedure was shown in every case to displace the complex quantitatively into the aqueous phase. From a knowledge of the original concentration of metal in the aqueous phase (*q.v.*) the percentage extraction, *E*, can readily be calculated.

Determination of the metal concentration in the aqueous phase

Absorptiometric methods. The concentration of the vanadium(V)–EDTA complex was determined with a Unicam SP 500 spectrophotometer from the absorbance at 360 nm in the pH range 6–8 by means of an appropriate calibration curve[7]. That of the chromium(III) complex was determined similarly[4] within the pH range 3–6, and that of the cobalt(III) complex[19] at 538 nm in the pH range 2.9–9.0 where $\varepsilon_{max} = 323.6$. The nickel complex was determined at 980 nm (pH 5–12), and the copper(II) complex at 730 nm (pH 4.9–10) as described by Bhat and Khrishnamurthy[21].

As described by Cheng and Lott[22], the best way of determining iron(III) in the presence of excess of EDTA was found to be by adjusting the pH to above 10 with ammonia, adding 30% hydrogen peroxide (1 cm^3) to a 2.0-cm^3 aliquot portion, and measuring the absorbance of the deep red-violet solution at 520 nm ($\varepsilon = 522$). The concentration of cobalt(II) was measured similarly[23] after oxidation with hydrogen peroxide to the blue complex $CoY(OH)^{2-}$ which has $\varepsilon_{max} = 241$ at 580 nm over the pH range 10–11.5.

Atomic absorption spectrometry. Calcium was determined[24] with a Perkin-Elmer atomic absorption spectrophotometer Type 303 at 422.7 nm. The effect of interference by sulphate was eliminated by using a large excess of EDTA (final concentration 0.4%) and strontium chloride (final concentration 0.2%). The presence of any Aliquat-336 and perchlorate ions in the sample solution was found to have a negligible effect on the determination. Zinc was determined similarly at 213.8 nm.

Zirconium displacement method. By adding an excess of zirconium to acidified solutions of mercury(II), palladium(II) and vanadium(IV)–EDTA complexes, these metals could be displaced and determined, respectively, by dithizone, by *p*-nitroso-dimethylaniline, or as a peroxy complex[8].

After destruction of EDTA by peroxide. Various authors have studied the oxidative destruction of EDTA as a means of recovering metals from their complexonates. Holzapfel and Dittrich[25] used cerium(IV) sulphate, and Cartwright[26] and Palei and Udal'tsova[27] employed hydrogen peroxide at concentrations where the liberated metals could be determined gravimetrically as phosphates or hydroxides. The applicability of this method to dilute solutions is illustrated here for the case of lead. To 10 cm^3 of aqueous 0.0002% lead nitrate in a 250-cm^3 beaker was added 2.0 cm^3 of 0.00532 *M* EDTA (excess) followed by 10 cm^3 of 0.0135 *M* hydrogen peroxide and 20 cm^3 of dilute nitric acid (1+99). The solution was boiled for 30 min and then taken to dryness, and the residue was taken up in

distilled water and made up to 100 cm^3 with dilute nitric acid (1+99). The lead content was determined by extraction with 0.001% dithizone from an ammonia–cyanide–sulphite buffer. The absorbance at 520 nm (1-cm cell) was 0.243 and that for an identical amount of lead that had not been complexed by EDTA but otherwise subjected to the whole procedure was 0.242. Similar procedures were checked and used for the determination of bismuth and cadmium. Magnesium was determined with eriochrome black T[28]. In all determinations of metal content, calibration curves were set up by taking known amounts of metal through the whole of the procedure that had been found most appropriate.

DISCUSSION

The extraction behaviour for different metals varies widely both as regards its extent and the effect of pH. The order of increasing extractability of the anionic complexes (with approximate percentage extractions in parentheses) is Ca, Mg < Bi (4) < Fe(III) (17) < Cu(II), Mn(II) (30) < Ni (41) < Co(II) (45) < Pb (48) < Zn, Cd (55) < Co(III) (60) < Cr(III) (65) < Mn(III) (80) < Pd (92) < V(V) (96) < Hg, V(IV) (99.9) at pH 3; Bi (6) < Mn(III) (10) < Ca (23) < Mg, Mn, Cd (40) < Pb (43) < Co(II), Ni, Cu(II) (55) < Co(III) (59) < Cr(III) (62) < Zn (69) < Fe(III) (83) < Pb (94) < V(IV), V(V), Hg (> 99.5) at pH 7; and Mn(III) (8) < Bi (20) < Ca (22) < Cr < Mn(II) (28) < Mg, Cd (40) < Pb < Co(II) (45) < Ni, Cu(II) (55) < Co(III) (60) < Zn (69) < V(V) (85) < Pd (88) < V(IV) (95) < Hg, Fe(III) (98) at pH 10. For several metals (*e.g.* V(V), Cr(III), Co(II), Co(III), Ni and Cu(II) in Fig. 1, and V(IV), Hg(II), Pd(II), Pb, Cd, Mg and Ca in Fig. 2), there is quite a wide range over which the percentage extraction is not much changed by variations in pH. In contrast, the behaviour of Mn(III) which is extracted up to 80% at pH 3 but only 10% at pH 10 is almost the opposite of that of iron(III) where the percentage extraction of 15–20% in acidic media increases abruptly above pH 5 to reach over 98% in the more strongly alkaline solutions.

Many of these variations in behaviour are readily interpreted when it is realised that individual metal complexonates can lose or add protons to give different species of varying charge and hydrophilicity[4]. Since, for example, vanadium(V) is extracted so well over a wide pH range (5.0–9.5), it can reasonably be assumed that the anionic vanadium–EDTA complex that is being extracted is also the dominant species in aqueous solution under these conditions of pH. This is substantiated by the report[7] that vanadium(V) forms a stable complex VO_2Y^{3-} ($K_{VO_2Y} = 10^{18.05}$) which exists over the range pH 5–9. The protonated species VO_2HY^{2-} ($pK = 3.6$) which predominates below pH 3 does not appear to be extracted so efficiently and the decrease in extractability above pH 10 is probably caused by the transformation of the vanadium–EDTA complex, VO_2Y^{3-}, into the less extractable pyrovanadate ion which exists[9] in aqueous solution of pH 10–12.

Schwarzenbach and Heller[10] have demonstrated the existence in solutions of iron(III) in EDTA of the species FeY^- (or $FeY(H_2O)^-$, $pK_1 = 7.6$), $FeY(OH)^{2-}$ ($pK_2 = 9.5$) and $FeY(OH)_2^{3-}$. Over the pH range 2–5 where the uninegative ion FeY^- predominates, the extractability is low though it increases rapidly above pH 5.6 as the species $FeY(OH)^{2-}$ appears. Since optimal extraction is above pH 9.5, it would

appear that $FeY(OH)_2^{3-}$ is even more readily extracted. Once more, it seems that complex ions which carry high negative charges and which would predictably be more hydrophilic than those of lower charge are in fact extracted better. The possibility that such species (or their salts with quaternary ammonium ions) are associated was not examined experimentally.

The behaviour of manganese(III) is particularly interesting for although Mn^{3+} is stabilized when coordinated by EDTA, the aqueous solutions of this complex anion are only stable for some 5 min[6,11], yet the organic extract could be kept for up to 5 h before decomposition became significant. Optimal extraction of the red complex, MnY^-, at pH 3 was reduced substantially by increase of pH as the unstable species $MnY(OH)^{2-}$ replaced it[11].

Other interesting cases are provided by palladium(II) and mercury(II), whose EDTA complexes are almost completely extracted from both acidic and alkaline media over the pH ranges 3.5–9.5 and 3.5–11.0, respectively (*cf.* Fig. 2). Stolyarov and Agrest[14] have shown that the complex HgY^{2-} exists over the pH range 3.4–11.35 which is consistent with the extraction behaviour of this very stable species, for which Schwarzenbach and Flaschka[15] report $K_{HgY} = 10^{21.8}$. Stolyarov and Agrest have also shown that the complexes MgY^{2-} and CaY^{2-} are stable over the pH ranges 3.5–10.8 and 3.05–11.45, respectively, ranges which should be compared with those for optimal extraction by Aliquat-336 at pH 6.5–11.0 for magnesium (*ca.* 40%) and 4.5–11.0 for calcium (*ca.* 22%). The case of bismuth which forms a very stable complex[15] ($K_{BiY} = 10^{27.9}$) is particularly interesting in that the extractability is very low (*ca.* 4%) over the range pH 2–8 and has only reached 17% at pH 9.5. Taken in conjunction with the above results and those yet to be reported on the extraction of iron(III) and chromium(III) from a wide range of different complexones, it emphasizes the many competing factors which would appear to govern the extraction of these anionic complexes. Certainly any simple working hypothesis based on the known behaviour of simple inorganic anions such as $Fe(CN)_6^{4-}$ and the halide ions, and on such orders[16] as $Cl^- < ClO_3^- < ClO_4^- < IO_4^-$, $BF_4^- < PF_6^-$, $BeF_4^{2-} < BF_4^-$, and $SiF_6^{2-} < PF_6^-$—which would suggest that, *ceteris paribus*, the extraction of anions would be favoured by increase in size and decrease in charge—cannot readily be applied to anionic metal–EDTA complexes. Provided that EDTA behaved as a hexadentate ligand in every case, it would not be unreasonable to picture the overall size of all the fully chelated complex anions MY^{n-4} derived from the hydrated cations M^{n+} to be much the same, irrespective of the nature of the metal enveloped by the bulky organic ligand. This would lead one to expect similar extractability for say Ca and Sr, or for divalent Mn, Co and Ni, or for tervalent Co, Cr and Fe; and taking the charges into account greater extractability for $Mn(III)Y^-$ than for $Mn(III)Y^{2-}$ and for $Co(III)Y^-$ than for $Co(II)Y^{2-}$. Although these simple predictions accord in broad terms with the experimental results, they cannot be expected to hold in general owing to our ignorance of the actual structures of these complex anions in solution. This is because potentiometric titrations can only confirm the stoichiometry of the components M^{n+} and Y^{4-} together with the number of readily detachable protons. The real structure must then be inferred from the ordinarily assumed coordination number: thus a formula such as MY^{n-4} does not disclose the presence of one or more molecules of coordinated water, nor can the species $MY(H_2O)^{n-4}$ and $M(HY)(OH)^{n-4}$—referring to the cases where a proton

is transferred from coordinated water to a carboxylate ion (which may then cease to be coordinated)—be differentiated by potentiometry alone. Yet the hydrophilicity of anions with such different configurations will certainly not be the same and, in consequence, their extractabilities will differ. Now x-ray crystallographic evidence shows that EDTA is in fact hexadentate in the 7-coordinate aquo complex $Fe(H_2O)Y^-$, whereas in the octahedral acido species $M(H_2O)(HY)$ (where M= Cr(III), Fe(III) or Ga(III)) or in $Ni(H_2O)(HY)^-$ the ligand is pentadentate and there must be a free $-CH_2COOH$ arm. However, protonation does not necessarily involve opening a chelate ring, for the structure of the acido species $Ni(H_2O)(H_2Y)$ shows that here one protonated arm remains chelated to the central metal atom[17]. Although these results underline the variations in behaviour from one metal complexonate to another, we should not naively apply evidence derived from studies of a species in a solid lattice, where it is surrounded by similar molecules, to the situation where the species is in an exclusively water environment.

The extraction of chromium(III) (*cf.* Fig. 1) reaches *ca* 50% at about pH 8, where the blue complex ion $CrY(OH)^{2-}$ predominates in the aqueous phase[4]. The spectrum of the blue-violet organic extract ($\lambda_{max} = 570$ nm) confirms the extraction of this species, a result that appeared to conflict with earlier work where the extracting agent was tetra-n-hexylammonium chloride[4] and where the extraction of the blue solution at pH 8 gave a violet extract of the species

TABLE III

VALUES OF SEPARATION FACTORS AT DIFFERENT pH VALUES

pH	*Mg*	*Ca*	*Cr(III)*	*Mn(II)*	*Fe(III)*	*Co(II)*	*Ni(II)*	*Cu(II)*	*Bi*
Separations of vanadium(V)									
1.5	*[a]	*	*	180	75	*	*	*	150
2.0	*	*	15	105	85	95	155	325	200
2.5	*	*	15	95	110	50	60	135	275
3.0	*	*	15	70	130	35	40	80	320
3.5	*	*	15	60	150	30	35	50	370
4.0	*	200	15	50	150	25	25	35	370
Separations of vanadium(IV)									
2.0	*	*	10	80	65	75	120	250	155
2.5	*	*	15	95	110	50	60	135	275
3.0	*	*	25	125	225	65	70	140	560
3.5	*	*	50	185	450	100	105	160	*
4.0	*	*	490	*	*	820	750	*	*
Separations of mercury(II)									
3.0	*	*	55	255	450	130	140	130	*
3.5	*	*	50	185	450	100	105	160	*
4.0	*	*	100	300	905	165	150	215	*
Separations of palladium(II)									
2.0	*	*	4	25	20	25	40	80	50
3.0	*	*	8	40	65	20	20	40	165
4.0	*	*	9	30	85	15	20	20	220

[a] Asterisks indicate that the separation factor exceeds 1000. All separation factors are rounded off values.

$CrY(OH)^-$ ($\lambda_{max} = 550$ nm). This experiment was repeated, confirming the earlier result, and it appears that the real differences arise from the comparatively small change in the nature of the extractants.

The behaviour of other metal–EDTA complexes calls for no special comment beyond noting again the facility with which complex anions of charge greater than unity can be extracted when compared with the simple inorganic ions such as SO_4^{2-}, PO_4^{3-} etc.; their considerably greater size is doubtless the significant factor here.

The wide variations between the behaviour of one metal system and another clearly present many possibilities for separations which can most easily be envisaged by calculating the separation factor $\alpha_{1,2} = q(M_1)/q(M_2)$ from individual values $q(M_1)$ and $q(M_2)$ of the distribution coefficients for the EDTA complexes of the metals M_1 and M_2 respectively. It is appreciated that this procedure is only approximate in that it implies that neither metal affects the distribution isotherm of the other. The values of the separation factors will, of course, depend on the pH and some typical calculations are summarized in Table III.

The separation of iron(III) in alkaline media from many other metals is one obvious possibility. Separation from manganese is improved by first oxidizing this to manganese(III). Advantage could be taken of the very high extractability of EDTA complexes of V(V), V(IV), Hg(II), and Pd(II) in acidic solutions to separate these metals from Ca, Mg, Cr(III), Fe(III), Co(II), Ni, Cu(II) and Bi.

SUMMARY

The extraction of anionic complexes of EDTA with Ca, Mg, V(IV), V(V), Cr(III), Mn(II), Mn(III), Fe(III), Co(II), Co(III), Ni, Cu(II), Zn, Cd, Hg(II), Pd(II), Pb and Bi by solutions of Aliquat-336 chloride in 1,2-dichloroethane has been studied as a function of the pH of the aqueous phase. The order and extent of the extractability varies greatly with the pH and provides a number of new possibilities for separation procedures. Thus iron(III) can be separated from many other metals in strongly alkaline solution while the extraction of V(V), V(IV), Hg(II) and Pd(II) exceeds 99% over wide pH ranges. The complex of Mn(III) with EDTA which is very unstable in aqueous solution can be preserved for up to 5 h when extracted by Aliquat-336.

One of us (R. H. Al-J.) wishes to thank the Ministry of Oil of the Republic of Iraq for financial support.

REFERENCES

1 R. C. Vickery, *J. Chem. Soc., London*, 103 (1951) 1817.
2 Yu. A. Zolotov, O. M. Petrukhin and I. P. Alimarin, *Zh. Anal. Khim.*, 20 (1965) 347.
3 F. L. Moore, *Anal. Chem.*, 37 (1965) 1235.
4 H. M. N. H. Irving and R. H. Al-Jarrah, *Anal. Chim. Acta*, 55 (1971) 135.
5 R. E. Hamm, *J. Amer. Chem. Soc.*, 75 (1953) 5670.
6 R. Pribil, *Collect. Czech. Chem. Commun.*, 14 (1949) 320.
7 A. Ringbom, S. Siitonen and B. Skrifvars, *Acta Chem. Scand.*, 11 (1957) 551.
8 H. M. N. H. Irving and R. H. Al-Jarrah, *Anal. Chim. Acta*, 68 (1974) 473.

9 J. F. Hazel, W. M. McNabb and R. Santini, *J. Phys. Chem.*, 57 (1953) 681.
10 G. Schwarzenbach and H. Heller, *Helv. Chim. Acta*, 34 (1951) 578.
11 Y. Yoshino, A. Ouchi, Y. Tsunoda and M. Kojima, *Can. J. Chem.*, 40 (1962) 775.
12 I. Sajó, *Acta Chim. (Budapest)*, 16 (1958) 115.
13 L. Przyborowski, G. Schwarzenbach and Th. Zimmermann, *Helv. Chim. Acta*, 48 (1965) 1556.
14 K. P. Stolyarov and F. B. Agrest, *Vop. Anal. Khim. Miner. Veshchestv, (1966)* Leningrad. Gos. Univ., p. 62.
15 G. Schwarzenbach and H. Flaschka (translated by H. M. N. H. Irving), *Complexometric Titrations*, Methuen, London, 1969.
16 H. M. N. H. Irving and A. D. Damodaran, *Anal. Chim. Acta*, 53 (1971) 267.
17 J. L. Hoard, C. H. L. Kennard and G. S. Smith, *Inorg. Chem.*, 2 (1963) 1316.
18 H. M. N. H. Irving and A. N. Nabilsi, *Anal. Chim. Acta*, 41 (1968) 505.
19 Y. Shimura and R. Tsuchida, *Bull. Chem. Soc. Jap.*, 29 (1956) 643.
20 R. Pribil and E. Hornychová, *Collect. Czech. Chem. Commun.*, 15 (1950) 456.
21 T. R. Bhat and M. Krishnamurthy, *J. Inorg. Nucl. Chem.*, 25 (1963) 1147.
22 K. L. Cheng and P. F. Lott, *Anal. Chem.*, 28 (1956) 462.
23 R. H. Al-Jarrah, M. Phil. Thesis, Leeds 1970.
24 T. V. Ramakrishna, J. W. Robinson and P. W. West, *Anal. Chim. Acta*, 36 (1966) 57.
25 H. Holzapfel and K. Dittrich, *Talanta*, 13 (1966) 309.
26 P. F. S. Cartwright, *Analyst (London)*, 86 (1961) 688.
27 P. N. Palei and N. I. Udal'tsova, *Zh. Anal. Khim.*, 16 (1961) 649.
28 F. H. Pollard and J. V. Martin, *Analyst (London)*, 81 (1956) 351.

Analytica Chimica Acta, 74 (1975) 333–338

A SOLVENT EXTRACTION METHOD FOR THE SEPARATION OF THIOCYANATE

A. S. LORICA and B. P. GONZALES
Department of Chemistry, University of the Philippines, Quezon City (The Philippines)
(Received 3rd June 1974)

In the course of studies on the solvent extraction of anions, which produced a method for the separation of iodide by solvent extraction, West and Lorica[1,2] reported high extraction efficiency for thiocyanate. A more detailed study of the solvent extraction of thiocyanate was therefore deemed desirable.

The thiocyanate ion forms stable complexes with Fe(III), Zn(II), Cd(II) and U(VI); with the hydrogen ion, it forms the slightly dissociated thiocyanic acid. Of these ions, cadmium(II) was chosen as coordinating cation. It had proved to be a good coordinating cation for iodide and there seemed a good possibility of having a cadmium group of anions all forming extractable ion-association complexes.

EXPERIMENTAL

Reagents

The following reagents were used: $AgNO_3$ (0.1000 *M*), KSCN (0.1000 *M*), $Cd(NO_3)_2$ (0.5000 *M*), EDTA (0.1000 *N*), HNO_3 (6 *M*), carbon tetrachloride, tri-n-butyl phosphate and methyl isobutyl ketone. A. R. grade chemicals were used.

Choice of solvent

Morgan *et al.*[3] have found thiocyanate to be extractable as thiocyanic acid with such organic solvents as carbon tetrachloride, n-hexane, chloroform, mesitylene, benzene and di-n-butyl ether. Of these solvents, n-hexane had the highest partition coefficient for thiocyanate (3.87). This value, however, was still smaller than that which had been obtained in earlier studies with 1:1 methyl isobutyl ketone–tri-n-butyl phosphate (MIBK–TBP) mixture. In choosing the 1:1 MIBK–TBP mixture as extracting solvent an important consideration was the possibility of extracting a cadmium group of anions.

Procedure

Potassium thiocyanate solution (10 ml) was pipetted into a 100-ml separatory funnel. Cadmium nitrate solution (1 ml) was added and the pH of the aqueous solution was carefully adjusted to the desired value with 6 *M* nitric acid. To this acidified solution, an equal volume of a 1:1 MIBK–TBP mixture was added. The funnel was shaken for about 30 s and then immersed in a thermostat to equilibrate at a predetermined temperature. In actual thiocyanate samples, the addition of cadmium nitrate may be omitted if the pH of the solution is first adjusted to 0.1.

The thiocyanate was recovered from the non-aqueous layer as described by West and Lorica[1] for iodide, and the Volhard method was used to determine the recovered thiocyanate. Cadmium in the aqueous layer was determined by EDTA titration with eriochrome black T as indicator.

The unextracted thiocyanate and the cadmium in the organic layer were obtained by difference.

RESULTS

Effects of variable conditions

The effects of various factors on the extraction of thiocyanate with 1:1 MIBK–TBP were studied; the factors were the hydrogen ion concentration, the thiocyanate–cadmium ratio, the initial concentration of cadmium thiocyanate, and the temperature.

The effect of pH. Table I shows the marked effect of changes in hydrogen ion concentration on the extraction of thiocyanate. There is a significant change in the pH of the aqueous phase after extraction, a change which is positive in acidic solution but becomes negative in slightly acidic and neutral solutions.

TABLE I

THE EFFECT OF pH

pH	*0.1*	*0.3*	*0.6*	*1.0*	*3.0*	*6.5*	*7.0*
SCN^- extracted (%)	90.7	84.8	76.5	71.5	58.2	58.9	59.2
Cd extracted (%)	4.79	17.6	36.9	50.6	67.6	68.6	68.6
[SCN]:[Cd] in extract	58.7	14.2	6.2	4.0	2.5	2.5	2.5
ΔpH in aqueous phase	0.20	0.25	0.20	0.35	0.60	−1.55	−1.65

The molar ratio of thiocyanate to cadmium. The [SCN]:[Cd] molar ratio clearly affects the extraction of thiocyanate (Table II). An excess of cadmium ions causes a decrease in the thiocyanate extracted; whereas an excess of thiocyanate at constant pH results in increased extraction. It would seem that other thiocyanate species, aside from the cadmium complexes, are being extracted.

TABLE II

THE EFFECT OF [SCN]:[Cd] MOLAR RATIO

[SCN]:[Cd] in aq. phase	*1:4*	*1:2*	*1:1*	*2:1*	*3:1*	*5:1*	*10:1*
SCN^- extracted (%)	76.8	84.1	87.9	87.8	90.7	91.0	91.8
Cd extracted (%)	4.55	5.02	5.80	3.05	4.79	5.04	13.0
[SCN]:[Cd] in extract	2.1	5.26	11.1	46.1	57.5	91.2	231.5

Initial concentration of cadmium thiocyanate. Cadmium thiocyanate solutions were prepared from cadmium nitrate and potassium thiocyanate. At a constant pH of 0.1 the initial concentration of cadmium thiocyanate did not appreciably affect

TABLE III

THE EFFECT OF THE INITIAL CONCENTRATION OF $Cd(SCN)_2$

$Cd(SCN)_2$, M	*0.05*	*0.015*	*0.005*	*0.0015*	*0.0005*
SCN^- extracted (%)	87.8	90.8	90.8	85.4	65.5
Cd extracted (%)	3.05	9.39	1.13	—	—
[SCN]:[Cd] in extract	57.6	214	72	—	—

the extraction of thiocyanate (Table III). A hundred-fold decrease in concentration only caused a 22% decrease in extraction.

Effect of temperature

As in a previous study[1], the temperature was not increased above 40.0°C. It is noteworthy that the decrease in the percentage extraction was accompanied by a slight increase in the percentage of cadmium extracted (Table IV). The molar ratio of thiocyanate to cadmium was initially 3:1, and the pH was held constant at 0.1.

TABLE IV

THE EFFECT OF TEMPERATURE

	27.5°C	*40.0°C*
SCN^- extracted (%)	90.0	89.2
Cd extracted (%)	1.60	1.96
[SCN]:[Cd] in extract	118	88

Extraction of thiocyanate without cadmium

The higher percentage extraction of thiocyanate below pH 1 in the absence of cadmium is significant. It is clear from the data of Tables I and V that the

TABLE V

EXTRACTION OF THIOCYANATE WITHOUT CADMIUM

(In all cases, 58.1 mg of thiocyanate was taken initially)

	pH				
	0.1	*0.3*	*0.6*	*1.0*	*3.0*
Aqueous phase					
SCN^- unextracted (mg)	3.6	4.9	8.50	22.1	53.6
SCN^- unextracted (%)	6.2	8.4	14.6	38.0	92.4
Non-aqueous phase					
SCN^- extracted (mg)	53.5	52.5	48.6	35.6	2.21
SCN^- extracted (%)	92.1	89.8	83.6	61.2	3.8
Distribution Ratio, *D*	14.9	10.7	5.72	1.61	0.0412

presence of cadmium below pH 1 serves to decrease rather than enhance the extraction of thiocyanate. It would seem that under certain conditions the hydrogen ion is more effective than cadmium(II) in the formation of extractable species with thiocyanate. This conclusion agrees with other studies involving the extraction of thiocyanate with other solvents[3].

DISCUSSION

Acidic solutions of cadmium thiocyanate contain the following ionic and molecular species: Cd^{2+}, SCN^-, HSCN, and the complexes of cadmium with thiocyanate, namely $CdSCN^+$, $Cd(SCN)_2$, $Cd(SCN)_3^-$, and $Cd(SCN)_4^{2-}$. The hydrogen ion competes with cadmium(II) for the thiocyanate ion forming the weak thiocyanic acid. This reaction predominates over the reactions between cadmium and thiocyanate which form the four above-mentioned thiocyanate complexes of cadmium. It is reasonable to assume that the species being extracted are the weakly ionized acid, HSCN and $Cd(SCN)_2$ and the ion-association complexes between the hydrogen ion and the cadmium thiocyanate complexes, *i.e.* $HCd(SCN)_3$ and $H_2Cd(SCN)_4$. In strongly acidic solution, below pH 1, when the cadmium(II) is about 0.04 *M* and thiocyanate is 0.12 *M*, the undissociated thiocyanic acid is probably the principal species being extracted. As the pH increases, the amount of thiocyanic acid formed decreases while more of the other species are formed, so that in the absence of cadmium(II) the percentage extraction of thiocyanate decreases. The data in Table V show that extraction can drop to as low as 3.8% at pH 3. This decrease is not unexpected because the low hydrogen ion concentration will limit the amount of thiocyanic acid formed. The distribution ratio *D* may involve the following equilibria:

$$(HSCN)_w \rightleftharpoons (HSCN)_o \quad K_D = [HSCN]_o/[HSCN]_w \tag{1}$$

In the aqueous layer, the following equilibria exist:

$$Cd^{2+} + SCN^- \rightleftharpoons Cd(SCN)^+ \quad k_1 \tag{2}$$

$$Cd(SCN)^+ + SCN^- \rightleftharpoons Cd(SCN)_2 \quad k_2 \tag{3}$$

$$Cd(SCN)_2 + SCN^- \rightleftharpoons Cd(SCN)_3^- \quad k_3 \tag{4}$$

$$Cd(SCN)_3^- + SCN^- \rightleftharpoons Cd(SCN)_4^{2-} \quad k_4 \tag{5}$$

$$H^+ + SCN^- \rightleftharpoons HSCN \quad K_{HSCN} \tag{6}$$

$$H^+ + Cd(SCN)_3^- \rightleftharpoons [HCd(SCN)_3] \tag{7}$$

$$2H^+ + Cd(SCN)_4^- \rightleftharpoons [H_2Cd(SCN)_4] \tag{8}$$

Near and above pH 7, the formation of an ion-pair, also takes place:

$$(CdSCN)^+ + HOH \rightleftharpoons [Cd(SCN)(OH)] + H^+ \tag{9}$$

causing a slight decrease in the pH of the aqueous layer.

The distribution ratio, *D*, defined as the ratio of the total concentration of thiocyanate in the non-aqueous phase to the total concentration of thiocyanate in the aqueous phase at equilibrium, is given by the following equation:

$$D = (C_{SCN^-})_o/(C_{SCN^-})_w \tag{10}$$

$$D = \frac{[HSCN]_o + [CdSCN(OH)] + 2[Cd(SCN)_2] + 3[HCd(SCN)_3^-] + 4[H_2Cd(SCN)_4^{2-}]}{[SCN^-) + [HSCN] + [Cd(SCN)^+] + 2[Cd(SCN)_2] + 3[Cd(SCN)_3^-] + 4[Cd(SCN)_4^{2-}]}$$

For convenience, the subscript w for the aqueous species has been dropped.

In acidic solutions, the formation of thiocyanic acid predominates over the complexation reactions between cadmium(II) and thiocyanate and the distribution ratio D may be simplified to the following equation:

$$D = [HSCN]_o/([HSCN] + SCN^-) \tag{12}$$

Dividing the numerator and denominator by [HSCN], the thiocyanic acid concentration in the aqueous layer, D becomes:

$$D = K_{D,HSCN}/\{1 + (K_{HSCN}/[H^+])\} = K_{D,HSCN}[H^+]/([H^+] + K_{HSCN}) \tag{13}$$

Thus, under the given conditions, the distribution ratio is significantly affected by the pH of the aqueous solution. However, in acidic solutions, as the ionic strength of the aqueous layer is increased, the rate of increase of D will be slower because of the accompanying increase in K_{HSCN}. The D *vs.* $[H^+]$ graphs with and without cadmium(II) are shown in Fig. 1. In the presence of cadmium, the ionic strength of the solution is greater and the slope of the line is smaller. As the hydrogen ion concentration decreases, D also decreases. At pH values near neutrality, K_{HSCN} will be much larger than $[H^+]$ based on literature values[3], and the denominator $([H^+] + K_{HSCN})$ becomes approximately equal to K_{HSCN}. The expression for D then reduces to:

$$D = (K_{D,HSCN}/K_{HSCN})[H^+] \tag{14}$$

According to this approximate equation at pH 3, the calculated value of $K_{D,HSCN}$, if K_{HSCN} is assumed[3] to be 2.0, is 82.4. With this value of $K_{D,HSCN}$, the value of K_{HSCN} at different pH values can be calculated from eqn. (13).

In acidic solutions, the predominant extractable species are probably HSCN and $[HCd(SCN)_3]$. On the basis of eqns. (2)–(8), it can be seen that while cadmium(II) can successfully compete with hydrogen ion for the thiocyanate ion (eqns. 2 and 6), the $Cd(SCN)^+$ complex ion cannot; therefore, the stepwise formation of the higher complexes will not proceed to a great extent. However, the $Cd(SCN)^+$ complex ion does not form a stable, extractable ion pair in acidic solutions. The net effect of the presence of cadmium(II) ions in acidic solution, therefore, is to decrease the extractability of thiocyanate. This conclusion is supported by the data of Tables I, II and V. Table I shows that the percentage extraction at pH 0.3 in the presence of cadmium(II) is slightly lower than the percentage extraction in its absence (Table V). However, as the pH increases, the thiocyanate complexes of cadmium, especially $Cd(SCN)_3^-$, contribute more significantly to the extractability of thiocyanate through ion pair formation.

In Table II, the harmful effect of reaction (2) on the extractability of thiocyanate from acidic solutions is evident from the large decrease in the percentage of thiocyanate extracted when the [SCN]:[Cd] ratio is decreased.

In the study of the effect of the initial concentration of cadmium thiocyanate, the [SCN]:[Cd] ratio was kept at 2:1 and the pH at 0.1. As the initial

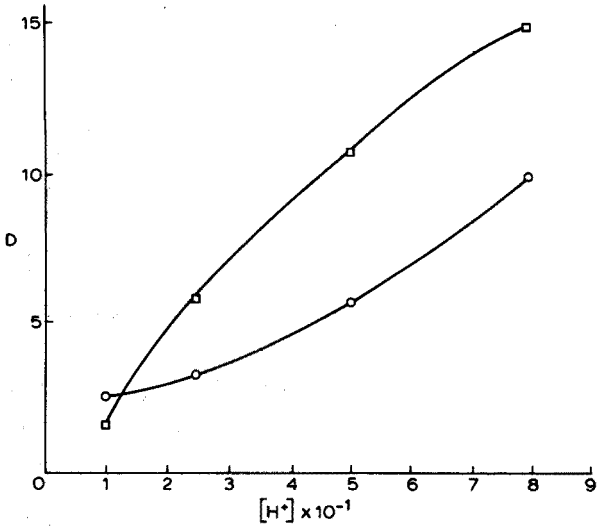

Fig. 1. Dependence of the distribution ratio on hydrogen ion concentration: (□), without cadmium; (○), with cadmium.

concentration was decreased, the percentage of thiocyanate extracted at first increased but on further decrease in initial concentration, it also decreased. The [SCN]:[Cd] ratio in the organic layer increased with decrease in initial concentration of cadmium thiocyanate, went through a maximum at about 0.01 *M* and then decreased again. This indicates that the principal species being extracted is thiocyanic acid. Below 0.001 *M* cadmium thiocyanate, only negligible amounts of cadmium ions could be detected in the organic layer. It would seem that because of the relatively high hydrogen ion concentration, and the very low supply of cadmium(II) ions, the formation of thiocyanic acid predominates over the formation of cadmium thiocyanate complexes. The decrease in the percentage extraction of thiocyanate with decrease in its initial concentration, at constant pH (0.3), can be attributed to the greater dissociation of thiocyanic acid with increasing dilution.

In the study of the effect of temperature, an increase in temperature caused a slight decrease in the percentage extraction of thiocyanate, but the percentage extraction of cadmium increased; thus the formation of the complexes of cadmium with thiocyanate becomes more important in the production of extractable species as the temperature is increased, because dissociation of thiocyanic acid increases at higher temperatures.

The financial support of the University of the Philippines' Natural Science Research Council is gratefully acknowledged.

REFERENCES

1 P. W. West and A. S. Lorica, *Anal. Chim. Acta*, 25 (1961) 28.
2 P. W. West and A. S. Lorica, *Chemists' Quarterly*, Philippines, 3, December 1962, 11.
3 T. D. B. Morgan, G. Stedman and P. A. E. Whincup, *J. Chem. Soc., London*, (1965) 4813.

Analytica Chimica Acta, 74 (1975) 339–345

ANION-EXCHANGE BEHAVIOR OF VARIOUS METALS IN HYDRAZOIC ACID MEDIA

KOICHI OGUMA, TSUTOMU MARUYAMA and ROKURO KURODA

Laboratory for Analytical Chemistry, Faculty of Engineering, University of Chiba, Yayoi-cho, Chiba (Japan)

(Received 28th May 1974)

Much information is now available about the anion-exchange behavior of metals in different acid media. Kraus and Nelson[1] summarized the behavior of metallic elements in hydrochloric acid over a broad range of concentrations. Since then systematic surveys of the behavior of elements on a strong base anion-exchange resin have been reported for nitric[2,3], hydrofluoric[4], phosphoric[5], sulfuric[6,7], thiocyanic[8], oxalic[9] and acetic[10] acids as well as for many other mixed acid media[11–15]. These comprehensive surveys of adsorption characteristics have resulted in a variety of analytical applications.

Since hydrazoic acid is a complexing agent similar to thiocyanic acid, belonging to a pseudohalogen acid, it was considered of interest to investigate the adsorption of metals from hydrazoic acid solutions, to extend the scope of anion-exchange separation methods. In the present study, the distribution coefficients for 43 metals on Bio-Rad AG1 were determined in a 0.5 *M* hydrazoic acid solution. Among the metals tested, the coefficients for V(IV), Fe(III), Cu(II), Zn(II), Se(IV), Mo(VI), Pd(II), Cd(II), In(III), Re(VII), Hg(II) and U(VI)—all of which except cadmium showed very strong adsorption on the resin—were measured as a function of hydrazoic acid concentration over the 0.5–0.05 *M* range. Differences in the coefficients allowed many useful separations to be conducted easily.

EXPERIMENTAL

Reagents

Analytical reagent-grade chemicals were used whenever possible. Standard solutions containing 1–10 mg of the element per ml were prepared. These solutions were mostly 0.5 *M* in hydrochloric acid, but 3 *M* in hydrochloric acid for Ti(IV), Zr(IV), In(III), Sn(IV), Sb(III), Bi(III), Hf(IV) and Ir(IV). Pure aqueous solutions were prepared for Se(IV), Mo(VI), W(VI) and Re(VII). The resin used was AG1–X8, a strongly basic anion-exchanger (Bio-Rad Laboratories, Richmond, Calif.). Resin of 100–200 mesh particle size in the azide form, dried over a saturated potassium bromide solution, was used throughout for determination of distribution coefficients and for column work.

Preparation of hydrazoic acid

A conventional glass column (I.D. 24 mm) containing 70 g of Dowex 50–X2,

in the hydrogen form, was used for the preparation of hydrazoic acid. Sodium azide solution (0.5 *M*) was placed on top of the column and allowed to flow through. An initial 150-ml portion of the effluent was discarded and the subsequent 140-ml portion was collected and stored. The hydrazoic acid thus obtained was standardized by both alkalimetry and Volhard's method. The results agreed well with each other. The 0.5 *M* hydrazoic acid solution stored at 25°C in a dark place kept its strength unchanged for at least eight days. Measured pH values of 0.5, 0.1 and 0.05 *M* hydrazoic acid were 2.5, 2.8 and 3.0, respectively. The corresponding calculated pH values were 2.54, 2.89 and 3.04 for 0.50, 0.10 and 0.050 *M* hydrazoic acid, respectively, assuming $pK_a = 4.77$ (ref. 16).

Determination of distribution coefficients

Column method. A conventional glass column of 7.0 mm I.D. containing 1.0 g of the resin in the azide form was used. The bed was 42 mm long, the void space being 0.8 ml. In advance, 10 ml of 0.5 *M* hydrazoic acid was passed through the column. Generally, a hydrochloric acid solution containing *ca.* 0.01 mmole of metal was placed into a small beaker and generally evaporated just to dryness. The residue was taken up in 1 ml of 0.5 *M* hydrazoic acid and transferred to the top of the column. The column was washed with two 1-ml portions of 0.5 *M* hydrazoic acid. The metal was then eluted with 0.5 *M* hydrazoic acid at a flow rate of about 0.5 ml min^{-1}. Stable 0.5 *M* hydrazoic acid solutions of Ti(IV), Sn(IV), Sb(III) and Bi(III) could not be prepared, because of the formation of hydrolytic precipitation. For Ge(IV), As(III), As(V), Pd(II), W(VI) and Hg(II) their 0.1 *M* hydrochloric acid solution (aqueous solution for W) containing 0.01 mmole of each ion was mixed with 4 ml of 0.5 *M* hydrazoic acid, loaded and then eluted. All the effluents were divided into 5-ml portions and whenever possible breakthrough, elution peak and total elution volumes were found by appropriate qualitative methods.

Batch method. The distribution coefficients of V(IV), Fe(III), Cu(II), Zn(II), Se(IV), Mo(VI), Pd(II), Cd(II), In(III), Re(VII), Hg(II) and U(VI) were measured as a function of hydrazoic acid concentration over the range 0.5–0.05 *M*. Because of the volatile nature of hydrogen azide, the stability of the hydrazoic acid concentration during the equilibrium study was first investigated. The resin in the azide form (0.5 g) was placed in ground glass-stoppered Erlenmeyer flasks containing 40 ml of 0.05 or 0.5 *M* hydrazoic acid solution. The mixtures were shaken in a mechanical device at 25°C, and the hydrazoic acid concentration was determined at timed intervals 15 min, 2 h and 5 h after the start of shaking. Filtration through a dry filter paper for phase separation was avoided, because it caused an appreciable decrease in hydrazoic acid concentration; 20% for 0.5 *M* and 13% for 0.05 *M* hydrazoic acid. Aliquots taken carefully from the supernatant solutions at the timed intervals were subjected to both alkalimetry and Volhard's method. The concentrations obtained are summarized in Table I.

As can be seen, the acid concentrations do not change appreciably during a 5-h equilibration, if well-stoppered Erlenmeyer flasks are chosen and used. Based on these observations, the following procedure was employed for the determination of the distribution coefficient by the batch method.

Portions of a hydrochloric acid solution (aqueous solution for Se(IV), Mo(VI)

TABLE I

STABILITY OF HYDRAZOIC ACID CONCENTRATION DURING THE EQUILIBRIUM STUDY

	Original concn., M	*Time elapsed*		
		15 min	*2 h*	*5 h*
Alkalimetry	0.0575	—	0.0546	0.0555
Volhard	0.0512	0.0536	0.0536	0.0559
Alkalimetry	0.508	0.487	0.481	0.478
Volhard	0.493	0.470	0.478	0.478

and Re(VII)) containing 0.01 mmole of metal were placed in Erlenmeyer flasks and evaporated just to dryness. The residues were taken up with 30.0 ml of hydrazoic acid of varying concentration (0.05, 0.1 and 0.5 *M*). The hydrazoic acid solutions were mixed with weighed portions of the resin (0.5 g) and shaken mechanically for 5 h at 25°C. Before and after the equilibration, the pH values of the mixtures were measured and recorded. For mercury(II), 20 ml of 0.025 *M* $Hg(NO_3)_2$ solution, which was 1 *M* in nitric acid, was adjusted to pH 2.4 with 1 *M* ammonia and diluted to 50.0 ml with distilled water. To 1.00-ml aliquots of this solution, 30.0 ml of hydrazoic acid of varying concentration and weighed portions of the resin (0.5 g) were added, and the mixtures were processed as described above. After a 5-h equilibration, the resin particles were allowed to settle, and an aliquot of the supernate was analyzed for the metal concerned colorimetrically or polarographically. The distribution coefficient was obtained from the formula:

$$K_d = \frac{\text{(amount of metal in the resin phase/g of resin)}}{\text{(amount of metal in solution phase/ml of solution)}}$$

The pH of the solution phases changed slightly during the equilibration; before and after the equilibration, pH was 2.90–2.99 and 2.90–3.10 for 0.05 *M* acid, 2.70–2.82 and 2.70–2.98 for 0.1 *M* acid, and 2.40–2.50 and 2.30–2.51 for 0.5 *M* acid, respectively, for eleven metals except for mercury(II). Mercury(II) showed somewhat higher changes in pH; initial pH values of 2.90 for 0.05 *M*, 2.70 for 0.1 *M* and 2.49 for 0.5 *M* hydrazoic acid changed to 3.90, 3.60 and 2.95, respectively, after the equilibration.

Column separation procedure

A column (I.D. 10.5 mm) containing 3 g of the resin was used, the bed being 6.2 cm long. The column was previously conditioned with 20 ml of hydrazoic acid, whose concentration was the same as used for the sample preparation. A metal mixture was evaporated to near dryness on a steam bath, the residue being taken up with 5 ml of hydrazoic acid of the desired concentration. This solution was loaded on the top of the column, allowed to percolate and then eluted with the same concentration of hydrazoic acid at a flow rate of about 0.7 ml min^{-1}. Individual procedures used are given in Table IV. Analytical methods used for the effluent analyses are summarized in Table II.

TABLE II

ANALYTICAL METHODS USED

Metal	*Method*
Al, Ga	Titration with EDTA, Cu–PAN
V(IV), U(VI)	Back-titration with Th in excess of EDTA, xylenol orange
Mn(II)	Colorimetrically with periodate
Fe(III)	Titration with EDTA, variamine blue B
Co(II), In(III), Th	Titration with EDTA, xylenol orange
Cu(II)	Titration with EDTA, PAN
Zn, Cd	Titration with EDTA, eriochrome black T
As(III)	Colorimetrically with hydrazine–molybdate
Se(IV)	Gravimetrically as metal
Mo(VI)	Colorimetrically with dithiol
Te(IV)	Colorimetrically with tin(II) chloride
Hg(II)	Titration with Cu(II) in excess of EDTA; Cu-selective indicator electrode
Re(VII)	Colorimetrically with thiocyanate

RESULTS AND DISCUSSION

Hydrazoic acid is a weak acid, being about as strong as acetic acid. The dissociation constant is $1.8 \cdot 10^{-5}$ ($pK_a = 4.77$) at 25°C[16]. Because of a high incidence of explosion with pure hydrogen azide, it is expedient to work with dilute solutions. Hydrazoic acid solution of about 0.5 to 1 *M* can be prepared very safely and easily by cation exchange as described above.

Because of lack of information about the adsorbability of metals on strong base resins from hydrazoic acid solutions, the general adsorption characteristics of 43 metals were first surveyed for a 0.5 *M* hydrazoic acid medium. The results obtained are summarized in Table III.

TABLE III

ANION-EXCHANGE ADSORPTION OF METALS FROM 0.5 *M* HN_3 SOLUTION

Metal	*BTV*[a], *ml*	*TEV*[b], *ml*	*Metal*	*BTV*[a], *ml*	*TEV*[b], *ml*
V(IV)	75	> 125	Pd(II)	> 100	> 100
V(V)	> 100	> 100	Cd(II)	0–5	20
Fe(III)	> 100	> 100	In(III)	> 100	> 100
Co(II)	0–5	15	W(VI)	> 100	> 100
Cu(II)	> 100	> 100	Re(VII)	> 100	> 100
Zn(II)	> 100	> 100	Ir(IV)	> 100	> 100
Ga(III)	25	> 100	Pt(IV)	> 100	> 100
Ge(IV)	0–5	10	Au(III)	> 100	> 100
As(V)	30	60	Hg(II)	> 100	> 100
Se(IV)	35	55	U(VI)	> 100	> 100
Mo(VI)	> 100	> 100	19 metals[c]	0–5	0–5

[a] Breakthrough volume.

[b] Total elution volume.

[c] Including Be, Mg, Al, Ca, Sc, Cr(III), Mn(II), Ni(II), As(III), Sr, Y, Zr, Te(IV), Ba, La, Sm, Yb(III), Hf and Th. Ti(IV), Sn(IV), Sb(III) and Bi(III) hydrolyzed.

V(V), Fe(III), Cu(II), Zn, Mo(VI), Pd(II), In(III), W(VI), Re(VII), Ir(IV), Pt(IV), Au(III), Hg(II) and U(VI) are adsorbed strongly from 0.5 *M* hydrazoic acid, their K_d values exceeding 100. V(IV), Ga, As(V) and Se(IV) are moderately adsorbed.

Be, Mg, Al, Ca, Sc, Cr(III), Mn(II), Co(II), Ni(II), Ge(IV), As(III), Sr, Y, Zr, Te(IV), Ba, La, Sm, Yb(III), Hf and Th are not retained to any great extent on the AG1 column from 0.5 *M* hydrazoic acid.

For zinc and cadmium, which form stable chlorocomplexes, the effect on their elution behavior of residual chloride resulting from stock solutions was examined. Accordingly, their chlorides and sulfates were taken up with 0.5 *M* hydrazoic acid, respectively, loaded, and eluted as described above. There was nothing to indicate any difference in elution behavior with the type of the acid used to prepare the metal solutions. Indeed, in hydrochloric acid media the adsorption is in the order Cd ≫ Zn over a wide range of hydrochloric acid concentration[1], while the order is reversed in hydrazoic acid medium (see also Fig. 1.)

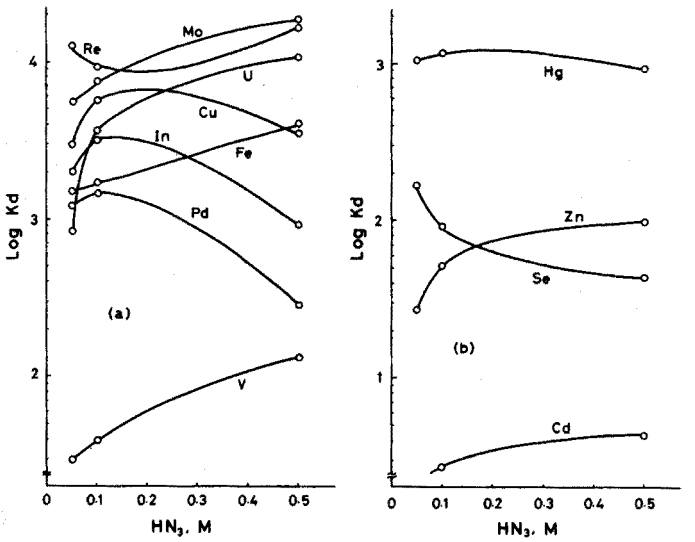

Fig. 1. Adsorption of metals from hydrazoic acid. (a) Mo(VI), Re(VII), U(VI), Fe(III), Cu(II), In(III), Pd(II), V(IV). (b) Hg(II), Zn, Se(IV), Cd.

In Fig. 1 the distribution coefficients are illustrated as a function of hydrazoic acid concentration for some selected metals which showed a distribution coefficient greater than 100 at 0.5 *M* hydrazoic acid, except for cadmium (see Table III). In general, azide ion behaves rather like a halide ion and is commonly considered as a pseudohalide, although the corresponding pseudohalogen $(N_3)_2$ is not known. It is noted that relative to the adsorption from as low as 0.5 *M* hydrochloric acid[1], there are strikingly strong adsorptions of Fe(III), Cu(II), Se(IV), Mo(VI), In(III) and U(VI) from *ca.* 0.5 *M* hydrazoic acid. It is also interesting to see that cadmium is not retained on the resin to any great extent from 0.1–0.5 *M* hydrazoic acid.

The thin-layer chromatographic characteristics of the transition metals on a weakly basic cellulose anion-exchanger, DEAE-cellulose, in 0.5 *M* hydrazoic acid solution have previously been reported[17]. The transition metals Fe(III), Cu(II), Mo(VI), Pd(II), Re(VII), Hg(II) and U(VI), which mostly showed K_d values greater than 10^3 on AG1 in 0.5 *M* hydrazoic acid, also gave the lowest R_F values on DEAE-cellulose layer at the same acid concentration. However, the sequence of adsorption on AG1 does not always coincide with that on DEAE-cellulose, *e.g.*, the R_F values of Pd(II) and U(VI) were 0–0.02 and 0.11–0.29, respectively, even though the K_d value of U(VI) on AG1 is about thirty times higher than that of Pd(II). In accord with their moderate to low distribution coefficients V(IV), Zn and Cd showed a chromatographic distribution on the DEAE-cellulose layer, their R_F values being 0–0.54, 0.61–0.72 and 0.67–0.77, respectively, in 0.5 *M* hydrazoic acid medium. Although the R_F values for Zn and Cd are close to each other, their selectivity toward AG1 differs considerably as indicated in Fig. 1.

The information contained in Table III and Fig. 1 indicates many possibilities for separations, even though the concentration range used in this study is very limited. The results of two- and three-component separations of analytical interest are listed in Table IV along with the separation conditions used.

TABLE IV

SEPARATIONS[a]

Run	*Metals separated*	*Added, mg*	*Found, mg*	*Eluent, eluent volume, ml*
1	Al(III)	13.1	13.0	0.5 *M* HN_3, 20
	Ga(III)	13.2	13.1	1 *M* H_2SO_4, 50
2	Co(II)	10.6	10.5	0.1 *M* HN_3, 75
	Cu(II)	11.5	11.8	1 *M* HNO_3, 40
3	Co(II)	10.8	10.6	0.1 *M* HN_3, 75
	Fe(III)	10.4	10.5	0.5 *M* H_2SO_4, 50
4	As(III)	0.245	0.234	0.5 *M* HN_3, 20
	V(IV)	9.01	9.00	3 *M* HCl, 50
5	Cd(II)	13.4	13.4	0.1 *M* HN_3, 75
	Zn(II)	10.2	10.2	1 *M* HNO_3, 45
6	Cd(II)	14.2	14.1	0.1 *M* HN_3, 75
	In(III)	12.1	12.0	1 *M* HNO_3, 60
7	Cd(II)	11.1	11.2	0.1 *M* HN_3, 75
	Hg(II)	16.9	16.6	3 *M* HNO_3–3 *M* $NaNO_3$, 120
8	Te(IV)	0.159	0.158	0.5 *M* HN_3, 20
	Se(IV)	19.3	19.6	1 *M* NaOH, 15
9	Th(IV)	12.9	12.7 ± 0.10^b	0.1 *M* HN_3, 30
	U(VI)	10.8	10.7 ± 0.70^b	0.5 *M* HCl, 45
10	Mn(II)	3.43	3.37	0.1 *M* HN_3, 20
	Mo(VI)	5.00	4.93	0.5 *M* NaOH–0.5 *M* NaCl, 15
	Re(VII)	4.65	4.40	4 *M* HNO_3, 65

[a] For each run the metals were eluted in the written order (from upper to lower). Run 4: 10 ml of sample solution loaded, which was 0.45 *M* in HN_3 and 0.005 *M* in HCl. Run 7: Nitrates of Cd and Hg(II) were dissolved in 10 ml of 0.1 *M* HN_3 and loaded. Run 8: 10 ml of 0.35 *M* HN_3 solution loaded, which contained sodium tellurite and selenite; pH 3.40. Run 10: 9 ml of 0.1 *M* HN_3 solution loaded, which contained the three metals indicated.

[b] Averages of three determinations given along with the standard deviation.

The separations can be conducted easily and quantitatively. In run 7, the adsorbed mercury(II) was removed completely from the column by elution with a mixture of nitric acid and sodium nitrate solution. This is in contrast to the difficulty of eluting mercury(II) adsorbed from a thiocyanic acid solution[8], which also belongs to the class of pseudohalogen acids.

SUMMARY

The adsorption characteristics for 43 metals on a strongly basic ion-exchange resin Bio-Rad AG1 were examined in 0.5 *M* hydrazoic acid solution. The distribution coefficients for V(IV), Fe(III), Cu(II), Zn, Se(IV), Mo(VI), Pd(II), Cd, In(III), Re(VII), Hg(II) and U(VI), which showed very strong adsorption except for Cd, were measured as a function of hydrazoic acid concentration over the range 0.05–0.5 *M*. Favorable differences in the distribution coefficients allow useful two- and three-component separations such as Co(II)–Fe(III), As(III)–V(IV), Cd–Zn, Cd–Hg(II), Te(IV)–Se(IV), Th–U(VI), Mn(II)–Mo(VI)–Re(VII), to be achieved on a small column.

REFERENCES

1 K. A. Kraus and F. Nelson, *Proc., Int. Conf. Peaceful Uses At. Energy*, United Nations, 7, 1956, p. 113.
2 F. Ichikawa, S. Uruno and H. Imai, *Bull. Chem. Soc. Jap.*, 34 (1961) 952.
3 J. P. Faris and R. F. Buchanan, *Anal. Chem.*, 36 (1964) 1157.
4 J. P. Faris, *Anal. Chem.*, 32 (1960) 520.
5 E. C. Freiling, J. Pascual and A. A. Delucchi, *Anal. Chem.*, 31 (1959) 330.
6 L. Danielsson, *Acta Chem. Scand.*, 19 (1965) 670.
7 F. W. E. Strelow and C. J. C. Bothma, *Anal. Chem.*, 39 (1967) 595.
8 K. Kawabuchi, H. Hamaguchi and R. Kuroda, *J. Chromatogr.*, 17 (1965) 567.
9 F. de Corte, P. van den Winkel, A. Speecke and J. Hoste, *Anal. Chim. Acta*, 42 (1968) 67.
10 P. van den Winkel, F. de Corte and J. Hoste, *Anal. Chim. Acta*, 56 (1971) 241.
11 F. Nelson, R. M. Rush and K. A. Kraus, *J. Amer. Chem. Soc.*, 82 (1960) 339.
12 E. A. Huff, *Anal. Chem.*, 36 (1964) 1921.
13 L. Danielsson, *Acta. Chem. Scand.*, 19 (1965) 1859.
14 F. W. E. Strelow, C. H. S. W. Weinert and C. Eloff, *Anal. Chem.*, 44 (1972) 2352.
15 F. de Corte, P. van Acker and J. Hoste, *Anal. Chim. Acta*, 64 (1973) 117.
16 J. C. Bailar, Jr., H. J. Emeléus, R. Nyholm and A. F. Trotman-Dickenson (Eds.), *Comprehensive Inorganic Chemistry*, Vol. 2, Pergamon, Oxford, 1973, p. 291.
17 R. Kuroda and N. Kojima, *Bull. Chem. Soc. Jap.*, 45 (1972) 3211.

Analytica Chimica Acta, 74 (1975) 347–356

REDOX TITRATIONS OF TIN(II) CHLORIDE IN NON-AQUEOUS SOLVENTS

WILLIAM J. MERGENS* and GALEN W. EWING
Seton Hall University, South Orange, N.J. 07079 (U.S.A.)
(Received 28th September 1973)

Many redox reactions in non-aqueous solvents have been described in the past two decades[1–18], but no systematic study of the field has appeared. This status contrasts with the study of acid–base reactions in similar solvents, where an extensive literature exists[19]. In the present paper, interactions between tin(II) and the redox couples Mn(VII)–Mn(II), Fe(III)–Fe(II), I_2–I_3^-, and Cu(II)–Cu(I) in acetone, acetylacetone (2,4-pentanedione), acetonitrile, pyridine, and acetic acid, in the virtual absence of water, are reported. The reactions were followed potentiometrically.

EXPERIMENTAL

Reagents and solvents

All solid reagents were ACS grade unless otherwise stated. The hydrated salts were dried over P_2O_5 in a desiccator until they assayed better than 97% on a dry basis, as determined by titration. After drying, the salts were stored over P_2O_5 until used.

Acetylacetone (Matheson, Coleman & Bell, pract.) was distilled through a Vigreux column. The fraction boiling between 139 and 141°C was collected.

Acetic acid (Baker Analyzed) was purified as described by Headridge and Pletcher[20]. The reagent was refluxed over chromium trioxide for 10 h, and thrice distilled through a Vigreux column. Each time the fraction boiling in the range 114–116°C was collected. The water content was determined by Karl Fischer titration and the requisite amount of acetic anhydride added to yield an anhydrous product.

Acetone (pract.) was purified as described by Coetzee and Siao[21]. The solvent was dried over anhydrous calcium sulfate (25–50 g l^{-1}) for two weeks, and then distilled from fresh calcium sulfate (10 g l^{-1}). The fraction boiling in the range 55.5–56.5°C was collected.

Pyridine (Mallinckrodt, ACS grade) was purified by standing over potassium hydroxide for one week, followed by fractional distillation at a high reflux ratio, as outlined by Audrieth and Kleinberg[22].

Acetonitrile (Matheson, Coleman & Bell) was purified by the method of Coetzee *et al.*[23]. The solvent was shaken intermittently with calcium hydride for

* Present address: Hoffmann-La Roche, Inc., Nutley, N.J. 07110, U.S.A.

at least two days, then decanted and fractionally distilled from P_2O_5 (5 g l^{-1}).

After purification, the solvents were stored over molecular sieve 4A until used. The water content of the various batches, as determined by Karl Fischer titration, was never larger than reported in Table I.

TABLE I

MAXIMUM WATER CONTENT OF DRIED SOLVENTS

Solvent	*Max. water (M)*
Acetonitrile	10^{-3}
Acetylacetone	10^{-2}
Acetone	10^{-3}
Pyridine	10^{-3}
Acetic acid	10^{-3}

Glove-bag procedure

All reactions and manipulations involving the dried solvents were carried out in a plastic glove bag (Model X-37-27, I^2R Company, Cheltenham, Pa.), inflated with tank nitrogen. An open dish containing fresh calcium hydride was present at all times.

Each solution was prepared by weighing a portion of the salt into a predried volumetric flask, in the amount needed to make an exactly 0.02 *N* solution ($\pm 0.5\%$) when diluted to volume. The flask was then placed in the glove bag, the bag was flushed with nitrogen, and only then was the stock bottle of solvent opened and the volumetric flask filled.

Of all the salts selected, tin(II) chloride was the only one that could not serve as its own primary standard for the order of precision required. Each solution of tin(II) chloride was standardized by titration with aqueous 0.02 *N* permanganate or iron(III) chloride. The concentrations of nonaqueous solutions of $KMnO_4$, $FeCl_3$, CuCl, and I_2 were checked against the previously standardized tin(II) chloride solution[24] or against the disodium salt of EDTA.

The titration cell

The cell consisted of a platinum electrode (Beckman 39273) and a saturated calomel reference electrode with a fiber junction (Beckman 39170). The latter, being filled with saturated aqueous KCl, was a potential source of both water and unwanted chloride ion. It was therefore placed inside a glass cylinder with a fine glass frit closing its lower end. This cylinder was filled with pure solvent to a level above that in the titration vessel, and the level of filling solution in the reference electrode was maintained still higher and open to the atmosphere. The entire cell in contact with the solution was of borosilicate glass. The cell was contained within the glove bag, as was the buret. The lead wires from the electrodes passed through the wall of the bag to a pH meter operated in its millivolt mode (Beckman Model H-2).

In most of the titrations, response of the electrodes was rapid and little drifting was observed. Titrations in pyridine presented the greatest difficulty. These

titrations gave a rather sharp immediate response upon addition of reagent, but then took a prolonged time to drift back to a stable potential reading. This effect is presumably due to adsorption at the electrode surface. In those titrations where a precipitate was generated, some drifting was also encountered, and addition of more reagent was withheld until a stable potential developed. Displacement of the electrodes in the solution during the titrations did not produce appreciable changes in the potentials observed, hence it was concluded that the *IR*-drop through the cell was negligible.

Before each series of redox titrations, a portion of the pure solvent was placed in the titration vessel and the potential between the electrodes was measured. The resulting data are plotted against the dielectric constant in Fig. 1. These observations on an unpoised system would be without significance were it not for the empirical fact that the points lie nearly on a straight line. Presumably the shift in potential is connected with variations in the liquid junction potential between the aqueous KCl solution and the solvent.

All titrations reported were run at least in duplicate. Those in which anomalous behavior was observed were performed at least five times with concordant results.

RESULTS AND DISCUSSION

Tin(II) titrated by iron(III)

In pyridine the titration curve (Fig. 2) exhibits a shape and magnitude of end-point break nearly identical to that in water, but with potentials about 400 mV more negative.

In acetonitrile and acetone, the curves show no break at equivalence, though iron(III) should be a strong oxidant in both solvents. A possible explanation for this behavior is complex formation. In water, the $FeCl_4^-$ complex is extremely weak[25] ($K_f = 10^{-2}$), and can only exist in significant amounts in the presence of a high concentration of chloride ion. To determine the likelihood of formation of similar complexes in acetonitrile, both the 0.02 *N* iron(III) chloride and tin(II) chloride solutions were titrated with 0.02 *N* tetramethylammonium chloride in the same solvent, with the results shown in Fig. 3. Both titrations were carried out with the platinum–calomel electrode system. The curves follow the redox potential as it changes with the addition of chloride ion. The logarithmic conditional formation constants calculated from the data of Fig. 3, through the relation $E^{0\prime} = (RT/nF) \log K_f$, are: $\log K_{FeCl_4^-} = 19.1$, and $\log K_{SnCl_3^-} = 11.5$.

The large formation constant for tetrachloroferrate(III) in acetonitrile suggests that when the equivalence point is approached in the redox titration, the unreacted iron(III) chloride is completely complexed with chloride ion from the $SnCl_2$. Hence one does not see the expected break, but rather a slow constant rise of the potential with added titrant.

It is interesting to speculate about the oxidizing power of iron(III) in the absence of complexing agents. Kratochvil and Long[16] have reported the use of iron(III) perchlorate in acetonitrile to oxidize various organic compounds. They report the formal potential of the Fe(III)/Fe(II) perchlorate couple to be +1.55 V *vs.* their Ag/0.01 *M* $AgNO_3$ reference electrode. This strongly indicates that

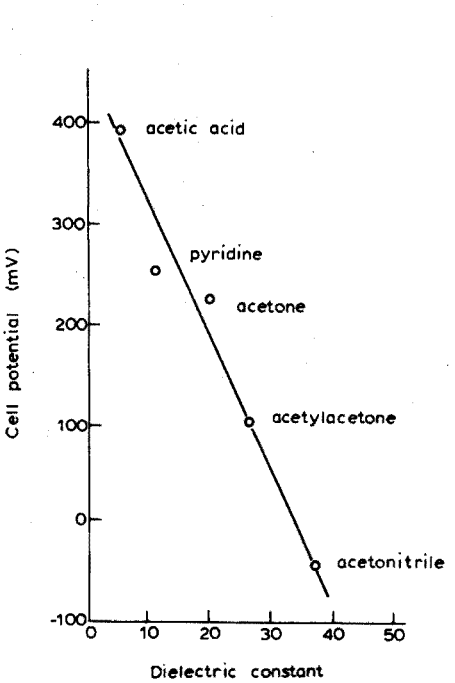

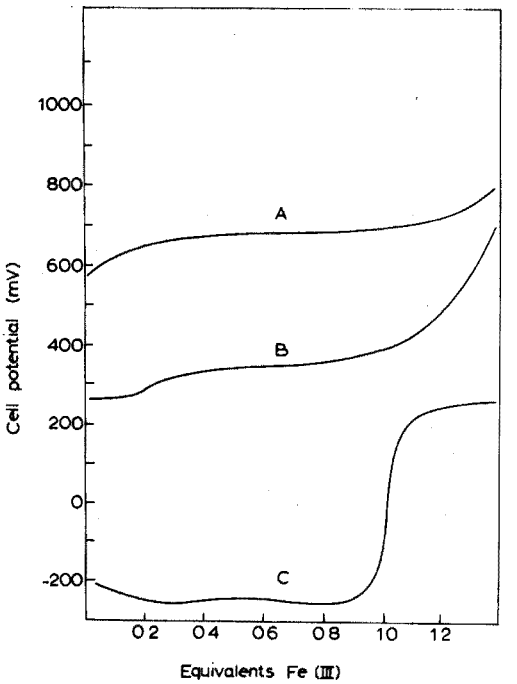

Fig. 1. Purified solvents: cell potential as a function of dielectric constant.
Fig. 2. Iron(III) chloride as oxidant for tin(II). A, Acetone; B, acetonitrile; C, pyridine.

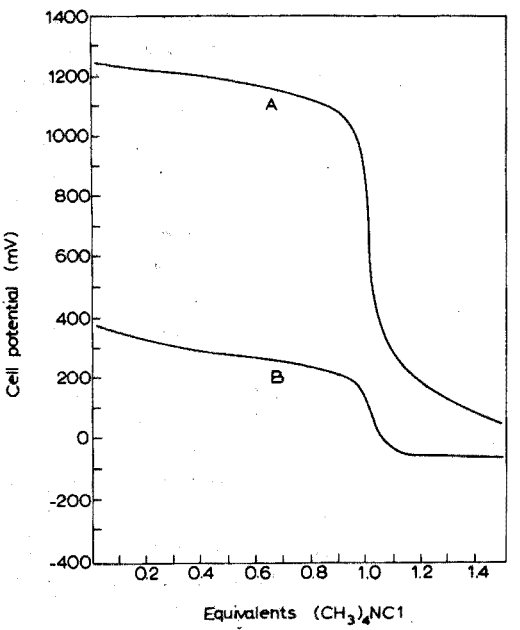

Fig. 3. Titrations with tetramethylammonium chloride. A, Iron(III) chloride; B, tin(II) chloride; solvent, acetonitrile.

iron is a more powerful oxidant in acetonitrile than in water. By use of the Rb^+/Rb couple as a reference for comparing potentials between water and acetonitrile, Coetzee and Champion[26] have estimated the reduction potential of the Fe(III)/Fe(II) couple to be 1.3 V greater in acetonitrile than in water. This increase may be partly attributed to an increase in the stabilization of iron(II), since the crystal field splitting energy for iron(II) in acetonitrile, measured spectrophotometrically by Hathaway and Holah[27], is 600 cm^{-1} greater in acetonitrile than in water. Acetonitrile is a solvent of lower dielectric constant than water, and this might also lead to a destabilization of iron(III).

The titration curve obtained in acetone was almost identical to that in acetonitrile. Both are aprotic solvents, so that it is safe to assume that the same complexation is taking place.

Titration of tin(II) by iron(III) in acetylacetone was unsuccessful, owing to the strong complexes formed with this solvent by both oxidation states of iron.

In acetic acid the titration was likewise unsuccessful. The yellow color of iron(III) was not discharged on addition to the tin(II) solution, and no potential break was found at the equivalence point. In an attempt to elucidate the system, iron(III) perchlorate was titrated in acetic acid with tetramethylammonium chloride. A potential break was observed corresponding to the addition of four moles of chloride ion per mole of iron(III). A precipitate was formed. A similar titration of tin(II) chloride showed a break corresponding to the formation of $SnCl_3^-$, and again a precipitate was formed. These precipitates were thought to be simple adducts of the general formula $M^{+n}Cl_{n+1}$ $(CH_3)_4N$. The infrared spectrum of the washed and dried precipitate from the tin titration matched well with the spectrum of a similar adduct isolated by Kuhn and Schretzmann[28] of tetramethylammonium bromide and silver bromide. The tin precipitate was subjected to elemental analysis, with the following results compared to calculation on the basis of $SnCl_3(CH_3)_4N \cdot HOAc$:

	Sn	Cl	N	H	C	O
% *Calc.*	33.1	29.6	3.89	4.45	20.00	8.90
% *Found*	31.5	32.0	3.60	4.15	19.58	9.1

(Oxygen "found" is by difference)

The formation of precipitates precluded determination of a true $E^{0\prime}$ and hence of formation constants of the chloro complexes in acetic acid. It is nevertheless clear that such complexes do form, and the explanation for non-observance of an end-point break in the redox titration is similar to that with acetonitrile solvent.

Tin(II) titrated by manganese(VII)

This titration in acetone, acetic acid, and pyridine (Fig. 4) proceeded in a manner analogous to the familiar aqueous titration. The first permanent pink color of excess of permanganate coincided with the potentiometric end-point in each case, and no evidence of oxidation of the chloride ion was observed.

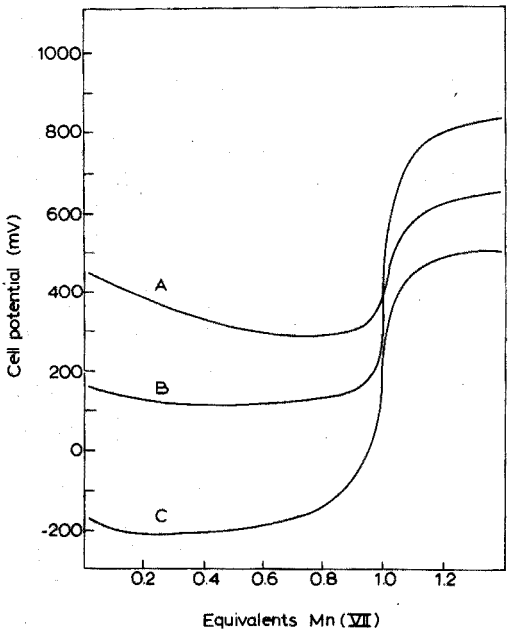

Fig. 4. Permanganate as oxidant for tin(II). A, acetone; B, acetic acid; C, pyridine.

Attempts to dissolve potassium permanganate in acetonitrile and acetylacetone resulted in decomposition of the solvent with the production of a brown precipitate, presumed to be manganese dioxide.

Acetone and pyridine solutions of permanganate were stable for approximately a day, after which a brown precipitate was formed. Acetic acid provided the only stable medium for this reagent; freshly prepared solutions showed the characteristic purple color, which on standing darkened almost to a brown-black with no apparent loss of titer.

Tin(II) titrated by copper(II)

In acetone and acetic acid solutions, the titration (Fig. 5) results in precipitation of copper(I) chloride. The electrode response is unsatisfactory, as the electrode is poorly poised after the equivalence point. A colorimetric end-point was clearly discernible. No color change was noted at the equivalence point in pyridine, and no precipitate formed.

The most interesting solvent for this titration is acetonitrile. During the titration a break is observed at one-half the equivalence point. This break, however, is in the negative direction, and so cannot be interpreted in terms of a tin(II) end-point. We have no satisfactory explanation of this anomaly. It should further be noted that copper(I) chloride does not precipitate from acetonitrile, as it does from acetone and acetic acid.

Like iron(III), copper(II) is a stronger oxidant in acetonitrile than in water, the result of complex formation between copper(I) and the solvent. In aqueous solution the uncomplexed copper(I) ion is unstable and disproportionates into

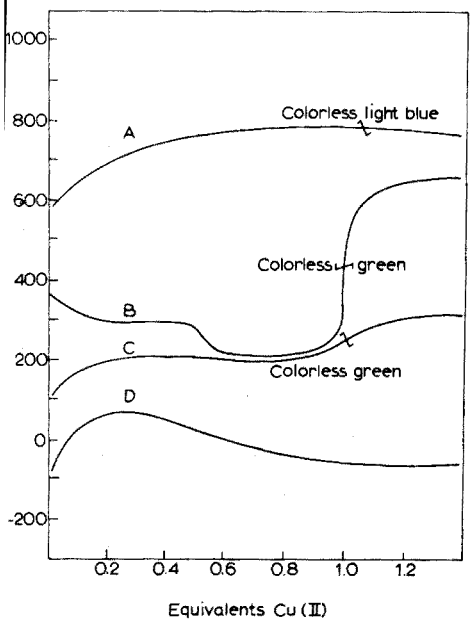

Fig. 5. Copper(II) as oxidant for tin(II). A, Acetone; B, acetonitrile; C, acetic acid; D, pyridine.

copper(II) ion and copper metal. However, in acetonitrile a solution of copper(I) perchlorate is not appreciably attacked by atmospheric oxygen[29]. Accordingly, the reduction of copper(I) at the dropping mercury electrode occurs at a relatively negative potential in acetonitrile (−0.36 V *vs.* SCE). This is unusual, because generally speaking the oxidized species forms stronger complexes than the reduced species. Here the copper complexation is analogous to the case of Fe(II)/Fe(III) with 1,10-phenanthroline, where the redox potential is considerably more positive than that of the iron aquo system. These exceptions are due to unusually stable electronic structures of the reduced species. Acetonitrile-coordinated copper(I) is sufficiently stable to disproportionation that it can be isolated readily as the perchlorate or fluoroborate salt[30].

Tin(II) titrated by iodine

This titration (Fig. 6) proceeds regularly in all solvents, as also in water[31]. At the start of each curve (except in pyridine) there is a drop in potential, presumably because of the formation of the SnI_3^- complex ion.

In acetonitrile, an orange-red precipitate was seen to form, starting at about one-third of the equivalent amount of iodine added. As the titration proceeded, the precipitate redissolved, disappearing completely just before equivalence. A portion of the precipitate was collected, washed with acetonitrile, and dried *in vacuo*. It did not melt below 230°C. The presence of iodine was established by neutron activation, and an 8-quinolinol extraction confirmed the presence of tin. The color and high melting point suggest SnI_2, m.p. 320°C; (SnI_4 is yellow, m.p. 144°C, sublimes at 180°C). Furthermore, its infrared spectrum showed no bands in the range 2–15 μm, whereas SnI_2 does show selective absorption in this region.

TABLE II

RELATIVE POSITIONS OF THE REDOX COUPLES STUDIED IN NON-AQUEOUS SOLVENTS COMPARED TO WATER[a]

H_2O[b]	*Acetone*	*Acetylacetone*	*Acetonitrile*	*Pyridine*	*Acetic acid*	*DMF*[31]
Mn(VII)–(II)	Fe(III)–(II)	I_3^-/I^-	Fe(III)–(II)	I_3^-/I^-	Mn(VII)–(II)	Cu(II)–(I)
Fe(III)–(II)	I_3^-/I^-	Sn(IV)–(II)	I_3^-/I^-	Mn(VII)–(II)	Fe(III)–(II)	Fe(III)–(II)
I_3^-/I^-	Mn(VII)–(II)	Fe(III)–(II)	Cu(II)–(I)	Fe(III)–(II)	I_3^-/I^-	
Cu(II)–(I)	Cu(II)–(I)	Cu(II)–(I)	Sn(IV)–(II)	Cu(II)–(I)	Cu(II)–(I)	
Sn(IV)–(II)	Sn(IV)–(II)			Sn(IV)–(II)	Sn(IV)–(II)	

[a] Abstracted from the titration curves at the respective half-equivalence points.
[b] Standard redox potentials in water.

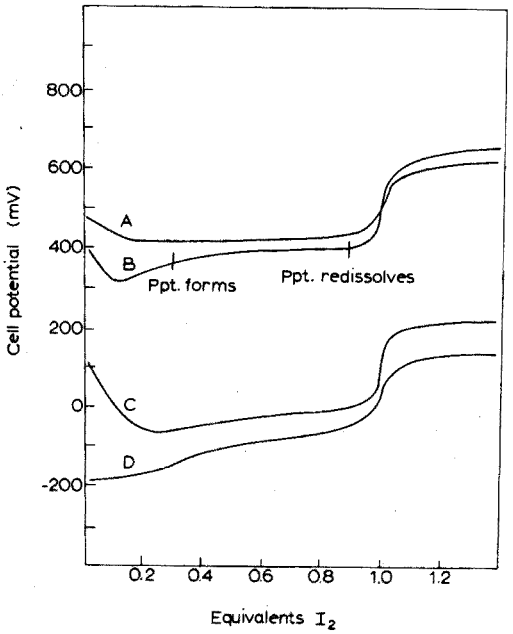

Fig. 6. Iodine as oxidant for tin(II). A, Acetone; B, acetonitrile; C, acetic acid; D, pyridine.

CONCLUSIONS

This work emphasizes the important role played by complexation in redox titrimetry. As one goes from solvents of high to low dielectric constant, there is less tendency for solvent molecules to occupy coordination sites, so that possible complexing ions such as chloride ions, if present in stoichiometric amounts, will be completely bound. Solvents of low dielectric constant act as leveling solvents for ligands, whereas solvents with high dielectric constants tend to differentiate between ligands.

Table II lists the couples studied in the order of their redox potentials in each solvent. It is readily apparent that non-aqueous solvents offer some special solvent effects which can change the redox behavior of a couple relative to water as a convenient reference solvent. The most striking examples are the strong oxidizing behavior of iron(III) and copper(II) in acetonitrile and the shift of the iron and copper couples in dimethylformamide[31]. The latter shift is so dramatic that the titration of iron(II) by copper(II) to give iron(III) and copper(I) is easily performed.

The elemental analyses were performed by Hoffmann-La Roche, Inc. This paper is abstracted from the M.S. Thesis of W. J. M. Seton Hall University, 1970.

SUMMARY

Tin(II) chloride is titrated by Fe(III), Mn(VII), Cu(II), and I(I), variously

in nonaqueous acetone, acetylacetone, acetonitrile, pyridine, and acetic acid. The reactions are followed potentiometrically. Titration by Cu(II) in acetonitrile shows an anomalous negative break at 1/2 equivalent. The significant role of complex formation is emphasized. Solvents of low dielectric constant exert a leveling effect toward ligands, whereas those with high dielectric constants tend to differentiate between ligands.

REFERENCES

1 E. F. Armstrong and T. P. Hilditch, *J. Soc. Chem. Ind., London*, 44 (1925) 437.
2 K. Fischer, *Angew. Chem.*, 48 (1935) 394.
3 J. Mitchell, Jr., D. M. Smith and W. M. D. Bryant, *J. Amer. Chem. Soc.*, 63 (1941) 2924.
4 O. Tomicek, *Chem. Listy*, 43 (1949) 193; 44 (1950) 245; 46 (1952) 263.
5 O. Tomicek and J. Heyrovský, *Chem. Listy*, 44 (1950) 169.
6 O. Tomicek and J. Valcha, *Chem. Listy*, 44 (1950) 283.
7 O. Tomicek, *Chem. Zvesti*, 4 (1950) 479; *Chem. Listy*, 47 (1953) 516; *Sb. Cel. Proc. Konf. Anal. Chem.*, 1 (1952) 246.
8 O. N. Hinsvark and K. G. Stone, *Anal. Chem.*, 28 (1956) 334.
9 J. F. Hinton and H. M. Tomlinson, *Anal. Chem.*, 33 (1961) 1502.
10 G. P. Rao and A. R. V. Murthy, *Indian J. Chem.*, 4 (1966) 49; *Z. Anal. Chem.*, 182 (1961) 358.
11 G. Piccardi, *Ann. Chim. (Rome)*, 52 (1962) 201; *Talanta*, 11 (1964) 1087.
12 N. Dahyabhal Shah, *Diss. Abstr.*, 17 (1957) 1316.
13 Z. Hladky, *Z. Chem.*, 5 (1956) 424a.
14 B. Kratochvil and D. A. Zatko, *Anal. Chem.*, 38 (1966) 770; 40 (1968) 422, 2120.
15 H. C. Mruthyunjaya and A. R. V. Murthy, *Anal. Chem.*, 41 (1969) 186.
16 B. Kratochvil and R. Long, *Anal. Chem.*, 42 (1970) 43.
17 K. S. Paul, *Anal. Chim. Acta*, 46 (1969) 131.
18 B. Kratochvil, *CRC Crit. Rev. Anal. Chem.*, 1 (1970) 415.
19 J. J. Lagowski, *CRC Crit. Rev. Anal. Chem.*, 2 (1971) 149.
20 J. Headridge and D. Pletcher, *J. Chem. Soc. A*, 6 (1966) 757.
21 J. F. Coetzee and W. S. Siao, *Inorg. Chem.*, 2 (1963) 14.
22 L. F. Audrieth and J. Kleinberg, *Chemistry in Non-aqueous Solvents*, Wiley, New York, 1953, p. 123.
23 J. F. Coetzee, G. P. Cunningham, D. K. McGuire and G. P. Padmanabhan, *Anal. Chem.*, 34 (1962) 1939.
24 A. A. Benedetti-Pichler in L. Meites (Ed.), *Handbook of Analytical Chemistry*, McGraw-Hill, New York, 1963, pp. 3–54.
25 P. A. McCusker and S. M. Scholastica Kennard, C.S.C., *J. Amer. Chem. Soc.*, 81 (1959) 2976.
26 J. F. Coetzee and J. F. Champion, *J. Amer. Chem. Soc.*, 89 (1967) 2513.
27 B. J. Hathaway and D. G. Holah, *J. Chem. Soc., London*, (1964) 2408.
28 R. Kuhn and H. Schretzmann, *Chem. Ber.*, 90 (1957) 559.
29 H. H. Morgan, *J. Chem. Soc., London*, 123 (1923) 2901.
30 F. Treadwell and W. Hall, *Analytical Chemistry*, Vol. 2, Wiley, New York, 8th edn., 1935.
31 Z. Hladky and J. Vrestal, *Collect. Czech. Chem. Commun.*, 34 (1969) 924.

Analytica Chimica Acta, 74 (1975) 357–365

SELECTIVE THERMOMETRIC TITRATION OF MANGANESE(II) WITH EDTA

KUNIO DOI

Department of Synthetic Chemistry, Nagoya Institute of Technology, Showa-ku, Nagoya 466 (Japan)

(Received 10th June 1974)

EDTA has occasionally been used in the thermometric titration of metals[1–5]. The differential thermometric titration of a mixture of calcium and magnesium is a successful example[1], in which calcium gives rise to an exothermic portion and magnesium an endothermic portion. The end-point of calcium is thus easily determined by extrapolating the exo- and endo-thermic portions of the thermometric titration curve.

In a previous communication[6], it was noted that the use of a ligand-substitution reaction:

$$MA_n + Y \rightleftharpoons (MY)' + nA \qquad (1)$$

would offer possibilities of improving the selectivity of EDTA thermometric end-points.

The enthalpies of formation of ethylenediamine complexes of divalent transition metal, $M(en)_n$, are generally much larger than those of the corresponding EDTA complex. Therefore it would be expected that reaction (1) in the titration of M with ethylenediamine as an auxiliary complexing agent would be endothermic because of the large enthalpy of dissociation of $M(en)_n$. Manganese(II)–ethylenediamine complex is less stable, and the enthalpy of formation of $Mn(en)_n$ is small. Thus, the heat of reaction (1) for manganese(II) being exothermic, the thermometric titration of manganese(II) in the presence of another divalent transition metal should be successful.

The present paper describes the selective thermometric determination of manganese(II) in the presence of nickel(II) or copper(II), and differential thermometric determinations of mixtures of manganese(II) and zinc(II), or manganese(II) and cadmium(II).

Calculation of the effective enthalpy

The reaction of a metal, M, with EDTA, Y, in the presence of ethylenediamine, en, is given by:

$$M(en)_n + Y' \rightleftharpoons (MY)' + n(en)' - \Delta H^{M}_{overall} \qquad (2)$$

where n is the number of en bound to M and (MY)'; all the 1:1 species involve M and Y. The heat of reaction (2), $-\Delta H^{M}_{overall}$, is termed the effective overall heat of reaction (2) and is expressed in kcal mole^{-1} of M.

In order to calculate the effective overall heat, the following two main reactions must be considered.

(a) $M+Y \rightleftarrows MY \qquad -\Delta H_{MY}$

where $-\Delta H_{MY}$ is the enthalpy of formation of MY. For simplicity we consider only the formation of MY.

(b) $M(en)_n \rightleftharpoons M+n(en) \qquad \Delta H_{M(en)_n}$

where $\Delta H_{M(en)_n}$ refers to the enthalpy of dissociation of $M(en)_n$ on titration. This value can be approximately calculated from the average pH during titration by using the effective enthalpy of formation of the metal complex MA_n in the previous communication[6]. Of course, in the calculation, the protolytic reactions of ethylenediamine, *i.e.*, $-Q_{en}$ (kcal mole^{-1} of M), and EDTA species, *i.e.*, $\Delta H_{Y'}$ (kcal mole^{-1} of M), during titration must also be taken into account. In the titration with the trisodium salt of EDTA, $\Delta H_{Y'}$ was assumed to be equal to the enthalpy of dissociation of HY, $\Delta H_{HY'}$, whereas with the tetrasodium salt of EDTA it was assumed to be equal to zero.

Therefore, for reaction (2) involving the above two main reactions and two additional reactions, the effective overall heat of the reaction (2) is obtained by a summation:

$$-\Delta H_{\text{overall}}^{M(m\text{Na})} = -\Delta H_{MY} + \Sigma \Delta H_{M(en)_n} - Q_{en} + \Delta H_{Y'}$$
$$= \Sigma \Delta H_{M(en)_n} + A(m\text{Na})$$

where $A(m\text{Na}) = -\Delta H_{MY} - Q_{en} + \Delta H_{Y'}$, and m is the ratio of sodium ion to EDTA in the titrant. The titration of M with the (m)-sodium salt of EDTA involves an exothermic process when $-\Sigma \Delta H_{M(en)_n}$ is smaller than $A(m\text{Na})$, whereas it involves an endothermic process when $-\Sigma \Delta H_{M(en)_n}$ is larger than $A(m\text{Na})$.

The enthalpies of formation of copper(II), nickel(II), cadmium(II), zinc(II) and manganese(II) ethylenediamine complexes as a function of pH are illustrated in Fig. 1. In this figure the values of $A(m\text{Na})$ in the titration of 10^{-2} M

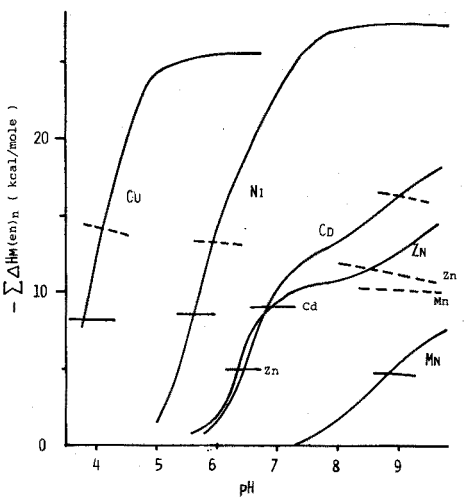

Fig. 1. Enthalpies of formation of metal ethylenediamine complexes as a function of pH; $c_M = 10^{-2}$ M, $c_{en} = 0.3$ M. (-----) A for titration with the trisodium salt of EDTA; (——) A for the titration with the tetrasodium salt of EDTA.

solutions of each metal are also given. As can be seen from Fig. 1, titration with the trisodium salt of EDTA is endothermic above pH 5–6 for Cu(II) or Ni(II), and slightly endothermic above pH 8.5 for Zn(II) or Cd(II), while it is exothermic for manganese(II) over an entire range of pH illustrated in Fig. 1. It can also be seen that the titration of Zn(II) or Cd(II) with the tetrasodium salt of EDTA is endothermic even at pH 7, and the titration of manganese(II) is slightly exothermic at pH 9.

EXPERIMENTAL

Reagents

About 0.1 *M* metal nitrate solutions were prepared from their G.R. salts (Katayama Chemical Co., Osaka) and standardized against a standard solution of EDTA with the following indicators: Mn(II), methylthymol blue; Ni(II), murexide; Cu(II), 4-(2-thiazolylazo)-resorcinol; and Zn(II) and Cd(II), eriochrome black T.

The trisodium salt solution of EDTA (0.4 *M*) was prepared by dissolution of 74.450 g of the disodium salt of EDTA (G.R., Dojindo Co., Kumamoto) in 300 ml of distilled water containing nearly one equivalent of sodium hydroxide, and dilution to 500 ml with distilled water. The solution was standardized against a standard solution of zinc(II) with eriochrome black T as indicator.

The tetrasodium salt solution of EDTA (0.4 *M*) was prepared from its G.R. salt (Dojindo Co., Kumamoto) and standardized.

Ethylenediamine solution (2 *M*) was prepared by dissolution of 6.01 g of anhydrous ethylenediamine (G.R., Tokyo Kasei Kogyo Co., Tokyo) in 100 ml of distilled water.

Hydroxyammonium chloride solution (1 *M*) was prepared by dissolution of 6.95 g of the salt (G.R., Katayama Kagaku Co., Osaka) in 100 ml of distilled water.

Apparatus

A thermistor bridge circuit (Hirama Rika Kenkyujo, Kawasaki), an automatic recording titrator Type-2P (Hiranuma Co., Mito) and a Radiometer pH Meter PHM22 (Copenhagen, Denmark) were used.

Recommended procedure

Place about 40 ml of a weakly acidic sample solution containing 10–60 mg of manganese in a 200-ml Dewar vessel covered with a block of polystyrene foam. Add 5 ml of 1 *M* hydroxyammonium chloride solution and 7.5 ml of 2 *M* ethylenediamine solution. Adjust the pH of the solution to 5.0–9.0 with 2 *M* nitric acid solution. Then titrate when the standard EDTA solution is delivered from an automatic titrator.

RESULTS AND DISCUSSION

The above considerations were confirmed experimentally in the thermometric titration of divalent transition metals with the trisodium and the tetrasodium salts of EDTA.

The thermometric titration of manganese(II) with EDTA

In the absence of a second metal. In the titration below pH 7.5, aquo manganese ion reacts with the EDTA anion as follows:

$$Mn + Y' \rightleftharpoons MnY \qquad -\Delta H^{Mn(mNa)}_{overall}$$

Above pH 7.5, manganese–ethylenediamine complexes react with the EDTA anion and the reaction is

$$Mn(en)_n + Y' \rightleftharpoons MnY + n(en)' \qquad -\Delta H^{Mn(mNa)}_{overall}$$

The titration of manganese(II) above pH 7.5 is less exothermic than that below pH 7.5, because of the dissociation of $Mn(en)_n$. Moreover, its enthalpy increases with increasing pH (*cf.* Fig. 1), hence the titration becomes less exothermic and the slope of the titration curve becomes smaller with increasing pH.

As is easily seen from Fig. 2, the titration with the trisodium salt of EDTA is more exothermic than that with the tetrasodium salt, because the hydrogen ion liberated from Y′ on formation of MY is neutralized by ethylenediamine.

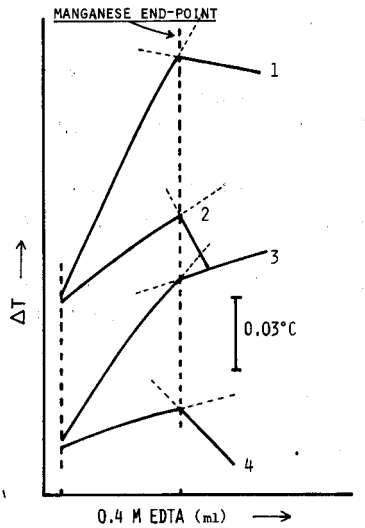

Fig. 2. Thermometric titrations of Mn(II) with EDTA. Conditions: $c_{Mn} = 1.12 \cdot 10^{-2}$ *M*, $c_{en} = 0.3$ *M*, $c_{NH_2OH} = 0.1$ *M*. Titration speed 1.2 ml min^{-1}. Temperature 24.8°C. (1) pH 7.0, with the trisodium salt; (2) pH 7.0, with the tetrasodium salt; (3) pH 9.0, with the trisodium salt; (4) pH 9.0, with the tetrasodium salt.

The observed values of $-\Delta H^{Mn(mNa)}_{overall}$, which were evaluated from the thermograms shown in Fig. 2, by titrating 0.01–0.05 *M* hydrochloric acid with 0.4 *M* sodium hydroxide and assuming the enthalpy for this neutralization reaction to be -13.4 kcal $mole^{-1}$, agreed, within 2 kcal with the calculated values discussed above.

In the presence of nickel(II). The titration of manganese(II) is exothermic at pH 5–9 as shown above, whereas that of nickel(II) should be endothermic above pH 6 (Fig. 1).

In the titration of a mixture of Mn(II) and Ni(II) around pH 6.8 with $c_{en} = 0.3$ *M* in excess where $K_{Mn'Y'} \approx K_{Ni'Y'}$, EDTA anion should react with both the aquo manganese ion and the nickel ethylenediamine complexes, but the end-point for manganese(II) appears first, as shown in Fig. 3. This end-point agrees with the equivalence point for manganese(II) above pH 7.8 with $c_{en} = 0.3$ *M* in excess, where $10^{-4} \cdot K_{Mn'Y'} \geqslant K_{Ni'Y'}$. Hence manganese(II) in the presence of larger amounts of nickel(II) can be titrated with the trisodium salt of EDTA above pH 7.8.

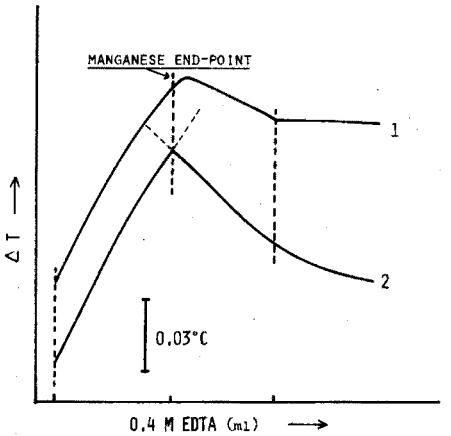

Fig. 3. Thermometric titrations of Mn(II) in the presence of Ni(II) with EDTA. Conditions: $c_{Mn} = 1.12 \cdot 10^{-2}$ *M*, $c_{Ni} = 1.03 \cdot 10^{-2}$ *M*, $c_{en} = 0.3$ *M*, $c_{NH_2OH} = 0.1$ *M*. Titration speed 1.2 ml min^{-1}. Temperature 24.8°C. (1) pH 6.8; (2) pH 7.8.

In the presence of copper(II). As copper(II) is reduced by hydroxylamine below pH 7 under the above experimental conditions, and above pH 7 the conditional formation constant $K_{Cu'Y'}$ with $c_{en} = 0.3$ *M* in excess is less than 4.0 in log units, manganese(II) can be titrated with EDTA in the presence of copper(II) above pH 7.

In the presence of zinc(II). The difference between log $K_{Mn'Y'}$ and log $K_{Zn'Y'}$ is as large as 3.6 at pH 9.0 with $c_{en} = 0.3$ *M* in excess, and the conditional formation constant $K_{Zn'Y'}$ with $c_{en} = 0.3$ *M* in excess is less than 6.5 in log units above pH 9.5.

As the enthalpy of dissociation of $Zn(en)_n$ is considerably larger than that of $Mn(en)_n$ (*cf.*, Fig. 1), the titration of zinc(II) with the trisodium salt of EDTA should be endothermic above pH 9 and that with the tetrasodium salt should be much more endothermic.

As shown in Fig. 4, at pH 9.0–9.5, manganese(II)–ethylenediamine complexes are titrated first with EDTA, giving rise to exothermic thermograms; the zinc(II)–ethylenediamine complexes react subsequently, constituting an endothermic portion.

In the titration at pH 9.3 with $c_{en} = 0.3$ *M* the observed values of $-\Delta H^{Zn}_{overall}$ obtained from Fig. 4 are equal to -1.5 kcal $mole^{-1}$ of zinc(II) with the trisodium salt of EDTA, and -7.2 kcal $mole^{-1}$ of zinc(II) with the tetrasodium salt of EDTA. These values agree, within *ca.* 2 kcal $mole^{-1}$, with the calculated values.

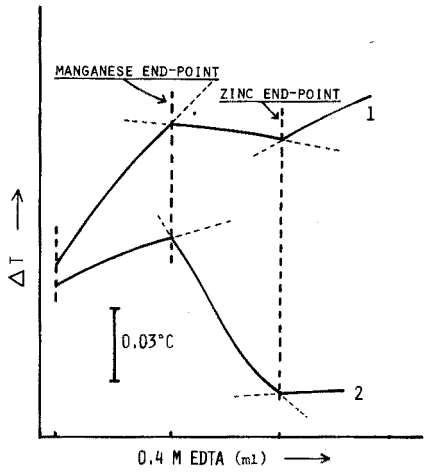

Fig. 4. Thermometric titrations of mixtures of Mn(II) and Zn(II) with EDTA. Conditions: $c_{Mn} = 1.12 \cdot 10^{-2}$ M, $c_{Zn} = 1.07 \cdot 10^{-2}$ M, $c_{en} = 0.3$ M, $c_{NH_2OH} = 0.1$ M, pH 9.3. Titration speed 1.2 ml min^{-1}. Temperature 24.8°C. (1) with the trisodium salt; (2) with the tetrasodium salt.

Titration with the tetrasodium salt of EDTA at pH 9.0–9.5 with $c_{en} = 0.3$ M is recommended.

In the presence of cadmium(II). Since the difference between log $K_{Mn'Y'}$ and log $K_{Cd'Y'}$ is equal to 3.3 at pH 9.5 with $c_{en} = 0.3$ M in excess, the shape of the end-point for the titration of a mixture of 10^{-2} M solutions of Mn(II) and Cd(II) becomes a slightly rounded hump below pH 9.5.

As can be seen from Fig. 5, the titration of cadmium(II) with the trisodium

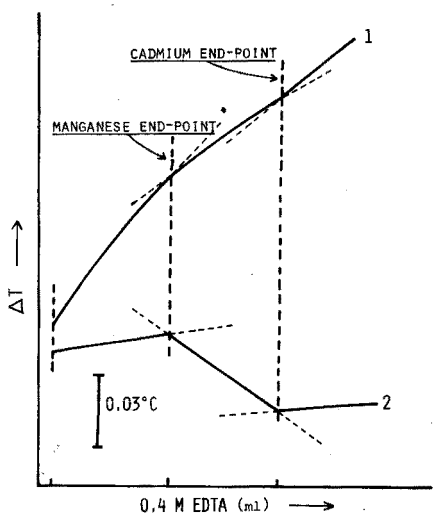

Fig. 5. Thermometric titrations of mixtures of Mn(II) and Cd(II) with EDTA. Conditions: $c_{Mn} = 1.12 \cdot 10^{-2}$ M, $c_{Cd} = 1.05 \cdot 10^{-2}$ M, $c_{en} = 0.3$ M, $c_{NH_2OH} = 0.1$ M. Titration speed 1.2 ml min^{-1}. Temperature 24.8°C. (1) pH 9.6, with the trisodium salt; (2) pH 9.8, with the tetrasodium salt.

salt of EDTA is slightly exothermic, hence it is not suitable for differential titrations. However, the reaction with the tetrasodium salt at pH 9.0–10.0 with $c_{en}=0.3$ *M* in excess, is endothermic, and the slope of the titration curve decreases with increasing pH. The slope of the titration curve expected from the calculated value of $-\Delta H_{overall}^{Cd(4Na)}$ increases with increasing pH. At pH 9.0–9.3 the observed values agree, within 2–3 kcal mole^{-1} of cadmium(II), with the calculated values. The discrepancy above pH 9.5 can probably be explained by the formation of (MY)′.

Titration with the tetrasodium salt of EDTA at pH 9.5–10.0 with $c_{en}=0.3$ *M* in excess is recommended.

In the presence of cobalt(II) or iron(II). Under the experimental conditions, cobalt(II) is oxidized gradually even in the presence of a reducing agent such as hydroxylamine or ascorbic acid, and the end-point in the titration of cobalt(II) appears before the equivalence point.

Iron(II) in the ethylenediamine buffer solution (pH 5–9) results in brownish precipitates even in the presence of the above reducing agents, and thus the titration of iron(II) under the experimental condition is impossible.

Analytical results

In Tables I and II are shown the results obtained by the thermometric titrations. These results indicate that the thermometric titrations discussed above can be used for determinations of the metals. The experimental conditions in the thermometric titrations are also summarized in these Tables.

TABLE I

DETERMINATION OF MANGANESE IN THE PRESENCE OF NICKEL OR COPPER

(Conditions: $c_{en}=0.5$ *M*, $c_{NH_2OH}=0.1$ *M*. pH 7.8–9.0 for nickel; pH 7.0–8.0 for copper. 10–60 mg of Mn/50 ml, less than 300 mg of Ni or Cu/50 ml.)

Sample no.	*Mn taken (mg/50 ml)*	*Other metal taken (mg/50 ml)*	*Ni or Cu/Mn*	*Mn found (mg/50 ml)*
In presence of nickel				
1	12.3	30.2	2.5	12.1
2	30.8	30.2	1.0	31.1
	30.8	100	3.2	31.2
	30.8	300	9.4	30.9
3	61.6	30.2	0.5	62.0
	61.6	300	4.8	61.8
In presence of copper				
1	12.3	32.1	2.6	12.2
	12.3	100	8.1	12.1
2	30.8	32.1	1.0	31.0
	30.8	160	5.2	30.8
	30.8	300	9.7	31.1
3	61.6	32.1	0.5	61.9
	61.6	160	2.6	61.9
	61.6	300	4.9	62.1

TABLE II

SIMULTANEOUS DETERMINATION OF MANGANESE AND ZINC OR CADMIUM IN THEIR MIXTI

(Conditions: $c_{en}=0.3$–0.5 *M*, $c_{NH_2OH}=0.1$ *M*. pH 9.0–9.5 for zinc; pH 9.5–10.0 for cadmium. 10–60 mg of Mn/. 15–70 mg of Zn/50 ml or 30–120 mg of Cd/50 ml.)

Sample no.	*Mn taken (mg/50 ml)*	*Mn found (mg/50 ml)*	*Zn or Cd taken (mg/50 ml)*	*Zn or Cd found (mg/50 ml)*
Manganese and zinc				
1	18.5	18.4	34.9	35.4
	18.5	18.3	69.8	70.5
2	30.8	31.1	20.9	21.1
	30.8	31.0	34.9	35.3
	30.8	31.3	69.8	70.9
3	49.3	49.5	20.9	21.3
	49.3	49.7	34.9	35.5
Manganese and cadmium				
1	18.5	18.3	35.4	35.9
	18.5	18.4	118.0	119.2
2	30.8	31.4	35.4	35.6
	30.8	31.8	94.4	94.9
3	49.3	49.7	35.4	35.2
	49.3	49.8	59.0	59.6

TABLE III

FORMATION CONSTANTS AND ENTHALPIES OF FORMATION OF SOME COMPLEXES[7,8]

Ion	*Complex*	*Ligand A*			
		EDTA		*Ethylenediamine*	
		log β_n[a]	ΔH[b] *(kcal mole*$^{-1}$*)*	*log* β_n[a]	ΔH[b] *(kcal mole*$^{-1}$*)*
H^+	HA	10.2	5.7	10.1	11.5
	H_2A	16.4	10.0	17.6	21.8
Cu^{2+}	MA	18.8	8.2	10.7	13.0
	MA_2	—	—	20.0	25.4
	MA_3	—	—	—	—
Ni^{2+}	MA	18.7	8.5	7.5	9.0
	MA_2	—	—	13.8	17.9
	MA_3	—	—	18.3	27.4
Zn^{2+}	MA	16.5	4.9	5.9	5.2
	MA_2	—	—	7.8	10.4
	MA_3	—	—	12.9	15.6
Cd^{2+}	MA	16.5	9.1	5.6	6.2
	MA_2	—	—	10.2	12.4
	MA_3	—	—	12.2	18.6
Mn^{2+}	MA	13.8	4.6	2.8	2.8
	MA_2	—	—	4.9	6.0
	MA_3	—	—	5.8	11.1

[a] Overall formation constant of H_nA; $\beta_n=[H_nA]/[H]^n[A]$. Overall formation constant of MA_n; $\beta_n=[MA_n]/[M][A]^n$.

[b] Enthalpy for protonation $nH+A \rightleftharpoons H_nA$. Enthalpy for complexation $M+nA \rightleftharpoons MA_n$.

Appendix

The thermodynamic quantities used for calculations in the present paper are shown in Table III.

The author wishes to thank Professor M. Tanaka of Nagoya University for his critical reading of the preliminary manuscript and valuable suggestions.

SUMMARY

The differential thermometric titrations of mixtures of Mn(II) and Zn(II), or Mn(II) and Cd(II), and the selective thermometric titrations of Mn(II) in the presence of larger amounts of Cu(II) or Ni(II) are described. The optimal conditions for these titrations are considered based on the effective enthalpy.

REFERENCES

1 J. Jordan and T. G. Alleman, *Anal. Chem.*, 29 (1957) 9.
2 P. T. Priestly, *Analyst (London)*, 88 (1963) 194.
3 J. C. Wasilewski, P. T. S. Pei and J. Jordan, *Anal. Chem.*, 36 (1964) 2131.
4 J. Jordan, R. A. Henry and J. C. Wasilewsky, *Microchem. J.*, 10 (1965) 260.
5 P. T. Priestly, W. S. Sebborn and R. F. W. Selman, *Analyst (London)*, 90 (1965) 589.
6 K. Doi and M. Tanaka, *Anal. Chim. Acta*, 71 (1974) 464.
7 J. J. Christensen and R. M. Izatt, *Handbook of Metal Ligand Heats and Related Thermodynamic Quantities*, Marcel Dekker, New York, 1970.
8 L. G. Sillen and A. E. Martell, *Stability Constants of Metal–Ion Complexes*, The Chemical Society, London, 1964.

Analytica Chimica Acta, 74 (1975) 367–385

A DIFFERENTIAL PULSE POLAROGRAPHIC EXAMINATION OF THE 1,4-BENZODIAZEPINES

M. A. BROOKS, J. J. BEL BRUNO, J. A. F. DE SILVA and M. R. HACKMAN
Hoffmann-La Roche Inc., Nutley, N.J. 07110 (U.S.A.)
(Received 18th April 1974)

The polarographic activity of the 1,4-benzodiazepines has been extensively reported. Oelschlager[1] has shown the analytical usefulness of d.c. polarography of chlordiazepoxide, reporting three reduction waves at pH 7.8; the sum of the heights of the first two waves was found to be proportional to concentration. Senkowski *et al.*[2] and Jacobsen and Jacobsen[3] have published comprehensive studies on the polarographic behavior of this class of compounds. Various assays have been developed for the determination of chlordiazepoxide[3–6]. diazepam[7–11], oxazepam[12,13], medazepam[14], nitrazepam[15–17], bromazepam[18], clonazepam and flunitrazepam[19] and lorazepam[20] in both biological samples and pharmaceutical dosage forms.

The mechanism of the reduction of the 1,4-benzodiazepines has been well documented. Oelschlager *et al.*[21] described the mechanism of the reduction of chlordiazepoxide at the dropping mercury electrode, utilizing d.c. and a.c. polarography. The three reported reduction peaks were attributed to a two-electron reduction of the N_4-oxide group, a two-electron reduction of the 4,5-azomethine and a two-electron reduction of the 1,2-azomethine. Jacobsen and Jacobsen[3] confirmed this mechanism for the first two polarographic reductions by constant potential coulometry.

Oelschlager *et al.*[22] have also discussed the mechanism of the polarographic reduction of diazepam, and reported that a single polarographic wave occurred corresponding to a two-electron reduction of the 4,5-azomethine bond. The polarographic reduction mechanism of medazepam which is identical to that of diazepam was reported by Oelschlager and Oehr[14]. Oelschlager *et al.*[12,23] have also reported on the reduction mechanism of oxazepam at the dropping mercury electrode in acid, neutral and alkaline supporting electrolytes. In acidic supporting electrolytes, the polarographic reduction yields the 1,3,4,5-tetrahydro derivative in a single four-electron step. A very complex mechanism is reported in alkaline solution. The mechanism of the reduction of nitrazepam has been discussed by Oelschlager *et al.*[15,24] and Havorsen and Jacobsen[16]. Two polarographic waves were noted in acidic solution. The first corresponded to the consumption of four electrons in the reduction of the 7-nitro substituent and the second was due to the consumption of four electrons in the simultaneous reduction of 4,5-azomethine and the hydroxylamine (formed as an intermediate of the nitro group reduction). However, under alkaline conditions the identical 4-electron 7-nitro reduction mechanism was followed by a mechanism corresponding only to the two-electron

4,5-azomethine reduction. It was noted that in alkaline solution the second wave is one-half the height of the first since the hydroxylamine is not reduced owing to insufficient protonation.

The Hammett equation[25] relates the reactivity of a compound to its structure, by means of equilibrium or rate constants. This relationship states that in a homologous series of aromatic compounds, for example, substituted benzoic acids, the rate or equilibrium constant of the reaction of any one of these compounds may be predicted from that of the parent compound (benzoic acid). The equation is written

$$\log(k/k_0) = \rho\sigma \tag{1}$$

where k and k_0 are the rate (or equilibrium) constants of the substituted and parent compound, respectively, σ is a constant depending only upon the substituent and is a measure of its inductance and resonance effects, and ρ is a constant for the series of compounds and denotes the sensitivity of the structure to ring substitution. Hammett substituent constants assume a negligible steric effect of the substituents on the reactive groups and for this reason exist only for *p*- and *m*-substituted compounds.

The standard reaction for the calculation of these constants is the ionization of benzoic acid in water at 25°C with ρ arbitrarily designated as one. The Hammett equation has been used to correlate the physical properties of various compounds with their structure in several spectrophotometric studies[26].

The correlation of polarographic half-wave potentials with Hammett substituent constants has been reported by Muller and Meyer[27] for 7- and 2'-substituted 1,3-dihydro-5-phenyl-2H-1,4-benzodiazepin-2-ones. Bogatskii *et al.*[28] confirmed the correlation for the same series of 7-substituted compounds and also report a relationship between the ease of polarographic reduction and psychopharmacological activities such as the inhibition of orientation reactions and protection from maximum electric shock.

A further expansion of this relationship of structure and polarographic activity was attempted in this study. Compounds were carefully chosen as to the substituent group and its position, and were divided into three classes. The three series were structurally related to medazepam [I-A], chlordiazepoxide [II-A], and N-desmethyldiazepam [III-A].

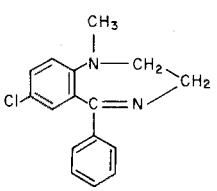

[I-A]
MEDAZEPAM

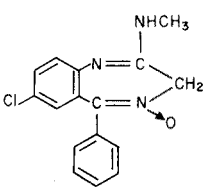

[II-A]
CHLORDIAZEPOXIDE

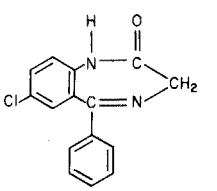

[III-A]
N-DESMETHYLDIAZEPAM

Since differential pulse polarography yields data with easily interpretable peaks and a high degree of resolution, compared to d.c. polarography, it is an excellent technique in the study of the correlation between polarographic activity

and the Hammett substituent constants. A typical differential pulse polarogram for the 7-acetyl-2′-fluoro analog of chlordiazepoxide in 3% methanolic pH 3.0 phosphate buffer is shown in Fig. 1. The polarogram shows four distinct peaks caused by the reduction of the N_4-oxide, 4,5-azomethine, carbonyl and 1,2-azomethine functional groups, respectively. The data shown in Fig. 1 were used to correlate peak potentials (E_p) and Hammett substituent constants for the three classes of compounds.

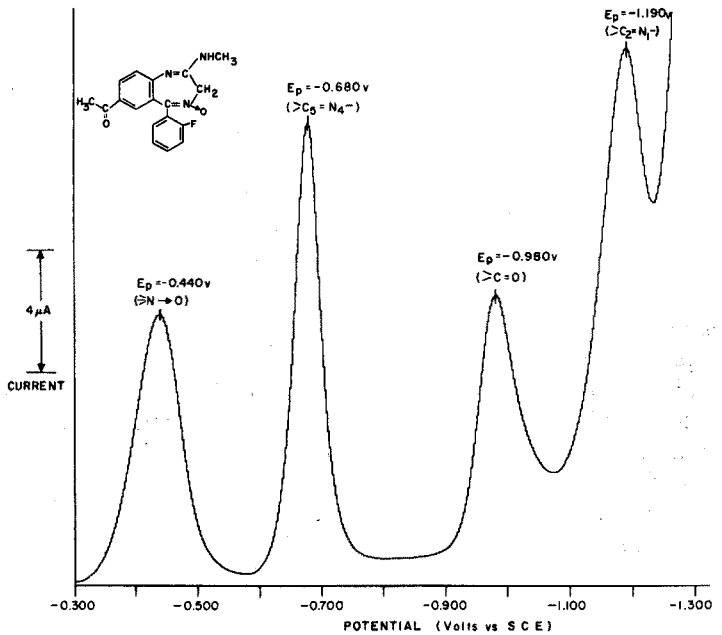

Fig. 1. Differential pulse polarogram of 100 μg of the 7-acetyl-2′-fluoro analog of chlordiazepoxide in 3 ml of 3% methanolic pH 3.0 phosphate buffer.

EXPERIMENTAL

Apparatus

The studies were made with a Princeton Applied Research Model 171 Polarographic Analyzer equipped with a P.A.R. Model 172A Drop Timer.

The instrumental parameters[29] were the derivative pulse mode of operation (*i.e.*, constant amplitude pulse superimposed on a linear d.c. ramp), differential current readout (signal is the difference in current sampled for a 16-ms interval before pulse application and a 16-ms interval before drop dislodgement) and a pulse amplitude of −50 mV peak-to-peak (applied for a 56-ms interval before drop dislodgement).

Other parameters included scanning from 0.000 V *vs.* SCE to the end of the analytical usable range for each of the supporting electrolytes employed, a scan rate of 5 mV s^{-1}, a scan range of 1.5 V and a current range of 20 μA.

The electrode assembly consisted of a three-electrode, 5-ml capacity,

polarographic cell containing a dropping mercury electrode (DME, E. H. Sargent No. S-29417, capillary tube of inside diameter 0.05–0.08 mm) as the working electrode, a saturated calomel electrode (SCE, Beckman No. 39178, fiber junction calomel) as the reference electrode and a platinum wire auxiliary electrode[30]. The drop mass was 2.75 mg s^{-1} $[m^{\frac{2}{3}} t^{\frac{1}{6}} = 2.2852]$ with a 0.5-s drop time.

Reagents

Supporting electrolytes (pH 3.0 and 7.0) were 1 *M* phosphate buffers made with reagent-grade chemicals and distilled water. Methanol (Fisher Certified) was also used.

Standard solutions

Solutions were made by dissolving 10.0 mg of each benzodiazepine in 10 ml of methanol to give a standard solution of 100 μg/0.1 ml.

Procedure

Samples were prepared in 15-ml centrifuge tubes by taking 0.1 ml of the standard solution and adding 2.9 ml of the appropriate buffer to give solutions of 100 μg/3 ml (approximate concentration of 10^{-4} *M*). The sample was deaerated for 5 min with nitrogen gas (prepurified, Matheson) by means of a coarse-porosity micro-filter stick (Scientific Glass Apparatus Inc., Bloomfield, N.J., Model JM-5385). The deaerated sample was then transferred to the polarographic cell[30] and was blanketed with a stream of nitrogen flowing over the surface. The polarograms were obtained for the previously mentioned parameters, scanning over the appropriate voltage range. The working ranges for the pH 3.0 and 7.0 phosphate buffers were −0.00– −1.100 V and −0.00– −1.750 V *vs.* SCE, respectively.

Calculations

The current resulting from the reduction of the various benzodiazepines was measured on the basis of peak height at the peak potential (E_p) for each reducible functional group. The current was calculated as follows[31].

$$d/D \cdot \text{current scale } (\mu A) = \text{sample } (\mu A) \tag{2}$$

where d is the sample peak height (cm) and D is full scale deflection (cm).

In order to have uniform values of current for comparison purposes, the slope value (μA/μg of sample) was calculated.

RESULTS AND DISCUSSION

Values of E_p for each series of compounds were plotted versus the Hammett substituent constants, as listed by Jaffe[26], to determine the effect of substitution of the various benzodiazepines upon the ease of polarographic reduction.

The relationship between E_p and the various substituents, for the 4,5-azomethine, was generally found to obey a modified Hammett equation[32], as is evident in Figs. 2–6. The modified equation is

$$E_p = \rho\sigma + E_p^0 \tag{3}$$

where E_p and E_p^0 are the peak reduction potential of the substituted and parent compound, respectively, and ρ and σ have the same definitions as in eqn. (1).

In several instances, disubstituted compounds were employed. In those cases, additive Hammett functions calculated by the method of Zuman *et al.*[33] for multi-substituted benzophenones were employed. When these additive functions are used, it is evident from Figs. 2–6, that the same correlation holds for mono- and di-substituted benzodiazepines.

Series I compounds

The parent compound of series I, medazepam [I-A] yields only one peak on polarographic analysis; this is due to the reduction of the 4,5-azomethine bond.

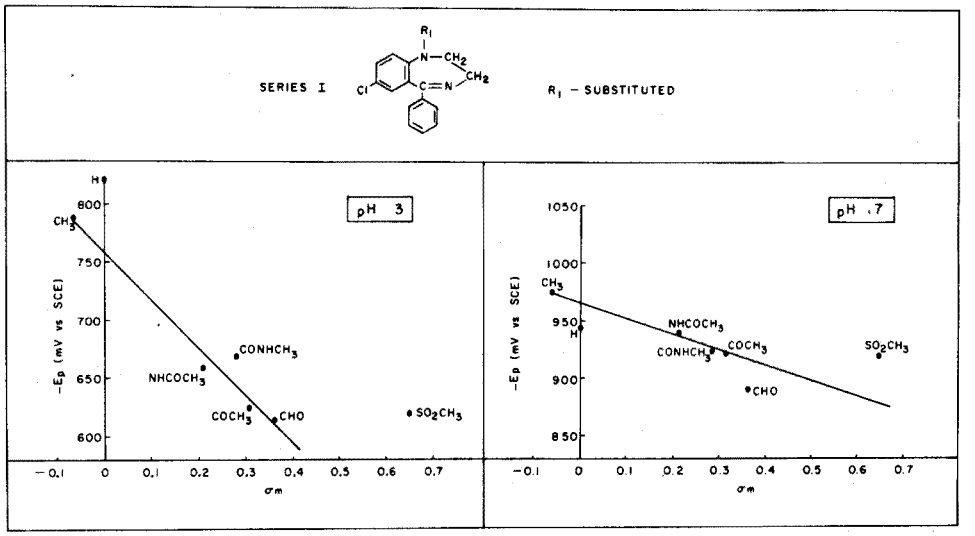

Fig. 2. Hammett plot for R_1 substitution in medazepam series [I] at pH 3.0 and 7.0.

Figure 2 and Table 1 indicate that for the R_1-substituted compounds studied, the effect of substitution is much more pronounced at pH 3 [$\rho = -0.417$ V] than at pH 7 [$\rho = -0.133$ V]. The amine-substituted compound [I-E] showed no polarographic activity. This inactivity may be due to resonance effects as suggested by Jaffe[26]. In addition to the peak arising from reduction of the 4,5-azomethine, secondary peaks were recorded for the acetyl [I-C] and methyl sulfonyl [I-B] substituted compounds in pH 3 supporting electrolyte. A second reduction, which took place in two steps, presumably of one electron each, was also observed for [I-D] in strongly acidic supporting electrolytes. This is in agreement with Perrin[34] who reported a similar mechanism for aromatic aldehydes in acid solution.

The R_2-substituted compounds (Table II) showed no linear relationship for the few compounds available. Two of the substitutions, the cyano [I-J] and acetamido [I-K], were found by Zuman *et al.*[33] to have conjugative interaction with the reaction center in the transition state for the benzophenones studies, and a similar phenomena may also occur for the 1,4-benzodiazepines.

TABLE I

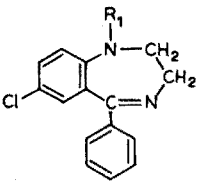

SERIES I: SUBSTITUENT R_1

Designation	*Substitution*	*pH 3*					*pH 7*	
		4,5-Azomethine		*Secondary*			*4,5-Azomethine*	
		E_p[a]	*Slope* ($\mu A/\mu g$)	*Group*	E_p	*Slope* ($\mu A/\mu g$)	E_p	*Slo* (μ
I-A	CH_3	−0.790	0.0750	S=O	−0.835	0.0806	−0.975	0.0
I-B	SO_2CH_3	−0.640	0.0118	C=O	−0.820	0.0686	−0.920	0.0
I-C	$COCH_3$	−0.625	0.0191	C=O	−0.800	0.0303	−0.915	0.0
I-D	CHO	−0.610	0.0248		−0.835	0.0093	−0.890	0.0
I-E	NH_2	No peak					No peak	
I-F	$NHCOCH_3$	−0.660	0.0014				−0.940	0.0
I-G	$CONHCH_3$	−0.670	0.0122				−0.925	0.0
I-H	H	−0.835	0.0963				−0.945	0.0

[a] In V *vs.* SCE.

TABLE II

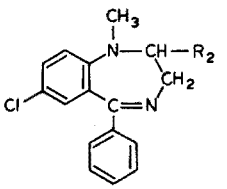

SERIES I: SUBSTITUENT R_2

Designation	*Substitution*	*pH 3*		*pH 7*	
		4,5-Azomethine		*4,5-Azomethine*	
		E_p[a]	*Slope* ($\mu A/\mu g$)	E_p	*Slope* ($\mu A/\mu g$)
I-A	H	−0.790	0.0750	−0.975	0.0466
I-I	OH	−0.795	0.0891	−0.995	0.0363
I-J	CN	−0.725	0.0902	−0.980	0.0047
I-K	$CONH_2$	−0.820	0.0784	−1.040	0.0707
I-L	COOH	−0.850	0.0660	−1.040	0.0676

[a] In V *vs* SCE.

Very few R_7-substituted compounds were available. The four that were obtained are shown in Fig. 3 and Table III. The ρ values of −0.056 at pH 3 indicated very little dependence of E_p on substitution in the 7-position. Compound [I-M] also showed an additional peak which appears to correspond to the nitro reduction to the hydroxylamine at both pH 3 and 7. Compound [I-O] was also substituted in the 2′-position with a chlorine atom; the resultant Hammett substituent constant used is the sum of the *m*-constants for both chlorine and iodine. At

TABLE III

SERIES I: SUBSTITUENT R_7

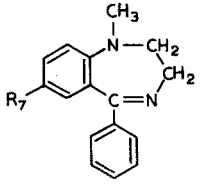

Designation	*Substitution*	*pH 3*				*pH 7*			
		4,5-Azomethine		*Secondary*[b]		*4,5-Azomethine*		*Secondary*[b]	
		E_p[a]	*Slope* ($\mu A/\mu g$)	E_p	*Slope* ($\mu A/\mu g$)	E_p	*Slope* ($\mu A/\mu g$)	E_p	*Slope* ($\mu A/\mu g$)
I-A	Cl	−0.790	0.0750			−0.975	0.0466		
I-M	NO_2	−0.770	0.0689	−0.240	0.1339	−1.010	0.0071	−0.525	0.0071
I-N	H	−0.810	0.0994			−1.010	0.0940		
I-O	I[c]	−0.765	0.0564			No peak			

[a] In V *vs.* SCE.

[b] The group involved is the nitro group.

[c] Also substituted 2′-Cl.

pH 7, compound [I-O] showed no polarographic behavior, and no correlation was attempted with only three data points.

The R'_2-substituted compounds (Fig. 4 and Table IV) show a much greater

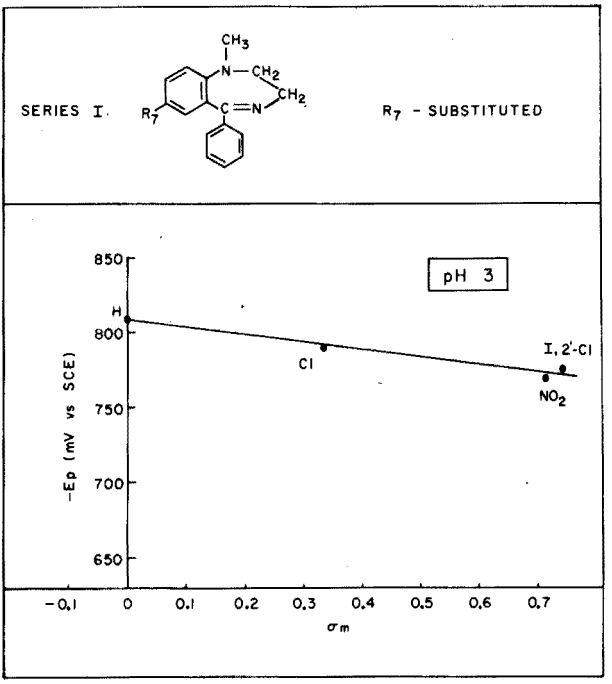

Fig. 3. Hammett plot for R_7 substitution in medazepam series [I] at pH 3.0.

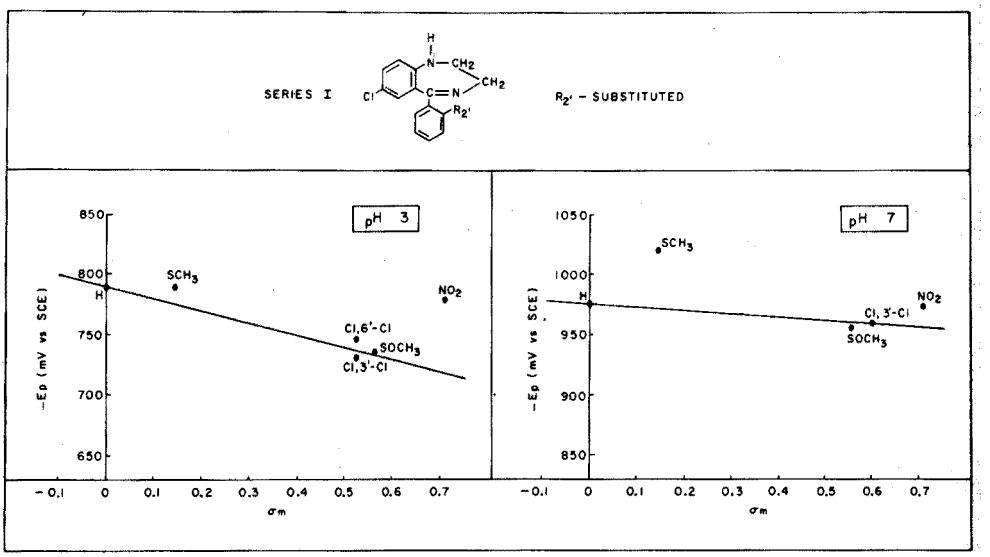

Fig. 4. Hammett plot for $R_{2'}$ substitution in medazepam series [I] at pH 3.0 and 7.0.

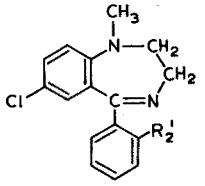

TABLE IV

SERIES I: SUBSTITUENT R'_2

Design-ation	*Substi-tution*	*pH 3*				*pH 7*			
		4,5-Azomethine		*Secondary*[b]		*4,5-Azomethine*		*Secondary*[b]	
		E_p[a]	*Slope* ($\mu A/\mu g$)	E_p	*Slope* ($\mu A/\mu g$)	E_p	*Slope* ($\mu A/\mu g$)	E_p	*Slope* ($\mu A/\mu g$)
I-A	H	−0.790	0.0750			−0.975	0.0466		
I-P	Cl[c]	−0.730	0.0763			−0.960	0.0023		
I-Q	Cl[d]	−0.750	0.0818			No peak			
I-R	NO_2	−0.780	N.M.[e]	−0.140	0.0114	−0.975	0.0087	−0.375	0.0236
I-S	NH_2	−0.770	0.0763			−0.965	0.0116		
I-T	SCH_3	−0.790	0.0838			−1.020	0.0047		
I-U	$S{\searrow}^{CH_3}_{O}$	−0.735	0.0699			−0.955	0.0540		

[a] In V *vs.* SCE.
[b] The group involved is the nitro group.
[c] Also substituted 3′-Cl.
[d] Also substituted 6′-Cl.
[e] Not measurable.

effect of substitution at pH 3 [$\rho = -0.132$ V] than at pH 7, [$\rho = -0.027$ V]. Compound [I-R] exhibited several secondary peaks, one of which overlapped the reduction peak of the 4,5-azomethine in both pH 3 and pH 7 supporting electrolyte. Because of the overlap the determination of the slope value for the reduction of the 4,5-azomethine was omitted. The additional overlapping peak may be attributed to the two-electron reduction of the hydroxylamine intermediate to the amine. For compounds [I-P] and [I-Q], which were 3′-Cl and 6′-Cl substituted, respectively, the 3,4-dichloro substituent constant reported by Jaffe[26] was employed (Fig. 5).

In general, the series I compounds showed a greater reduction current response (μA/μg) at pH 3 than at pH 7.

Series II compounds

The series II compounds exhibited three polarographic peaks in acid or neutral solution; these are attributed to the reduction of the N_4-oxide, 4,5-azomethine and 1,2-azomethine functional groups, respectively[21].

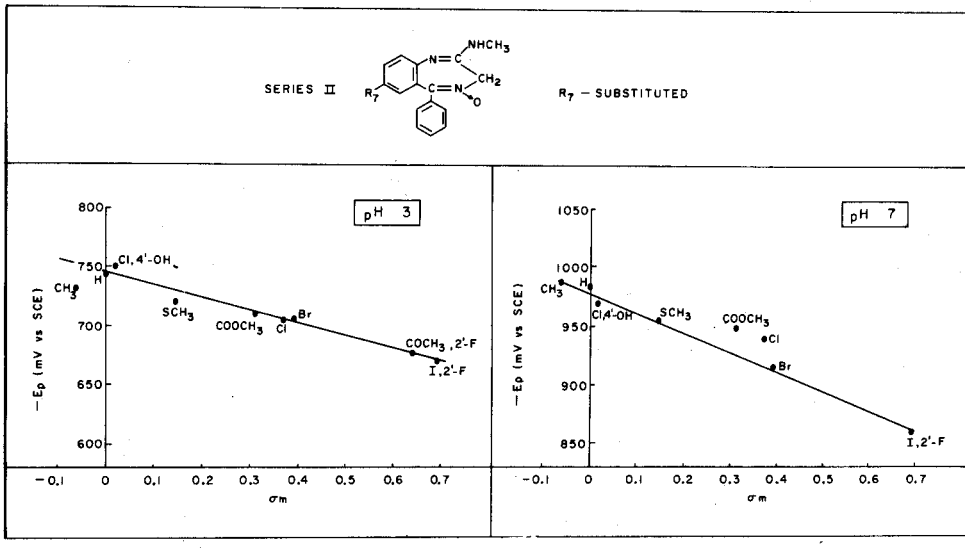

Fig. 5. Hammett plot for R_7 substitution in chlordiazepoxide series [II] at pH 3.0 and 7.0.

Compounds substituted in the R_2 position showed no correlation for the reduction of the 4,5-azomethine bond at pH 3 (Table V) or pH 7 (Table VI). However, it must be noted that most of the compounds employed in the study were substituted amines or nitrogen-containing compounds, and thus may not be truly representative of the effects caused by other types of groups substituted in the 2-position. The compounds with oxygen-containing functional groups [II-E, F, and G] did not yield the 1,2-azomethine reduction at pH 3. Neither the 1,2-azomethine nor the N_4-oxide showed a Hammett relationship, because of substitution. The sensitivity (μA/μg) of the 4,5-azomethine reduction was greater at pH 3 than at pH 7.

BLE V

RIES II: SUBSTITUENT R_2

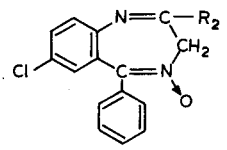

sign- on	Substi- tution	pH 3					
		4,5-Azomethine		1,2-Azomethine		N_4-Oxide	
		E_p[a]	Slope ($\mu A/\mu g$)	E_p	Slope ($\mu A/\mu g$)	E_p	Slope ($\mu A/\mu g$)
A	$NHCH_3$	−0.705	0.1040	−1.165	0.0882	−0.375	0.0654
B	$NH(CH_2)_3CH_3$	−0.705	0.0676	−1.075	0.100	−0.385	0.0550
C	NHC_2H_5	−0.700	0.0820	−1.160	0.0812	−0.380	0.0568
D	NH_2	−0.705	0.0862	−1.080	0.0551	−0.380	0.0599
E	$COCH_3$ | NCH_3	−0.720	0.0766	No peak	—	−0.410	0.0603
F	COC_2H_5 | NCH_3	−0.705	0.0395	No peak	—	−0.400	0.0284
G	OCH_3	−0.720	0.0831	No peak	—	−0.410	0.0602
H	$NHNH_2$	−0.690	0.0863	−1.075	0.100	−0.385	0.0550
I	$N(CH_3)_2$	−0.630	0.113	−1.030	0.0785	−0.300	0.0747
J	CH_3	−0.615	0.0232	−0.855	0.0127	−0.480	0.0554

1 V *vs.* SCE.

BLE VI

RIES II: SUBSTITUENT R_2

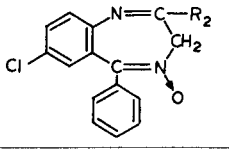

ign- m	Substi- tution	pH 7					
		4,5-Azomethine		1,2-Azomethine		N_4-Oxide	
		E_p[a]	Slope ($\mu A/\mu g$)	E_p	Slipe ($\mu A/\mu g$)	E_p	Slope ($\mu A/\mu g$)
A	$NHCH_3$	−0.940	0.0701	−1.370	0.0472	−0.760	0.0331
B	$NH(CH_2)_3CH_3$	−0.935	N.m.[b]	−1.300	0.145	−0.730	0.0802
C	NHC_2H_5	−0.930	0.0365	−1.360	0.0243	−0.750	0.0195
D	NH_2	−0.910	0.0168	−1.300	0.007	−0.725	0.0112
E	$COCH_3$ | NCH_3	−0.900	0.0322	−1.010	0.0193	−0.720	0.0241
F	COC_2H_5 | NCH_3	−0.920	0.0134	−1.350	0.007	−0.735	0.0055
G	OCH_3	−0.980	0.0373	−1.175	0.0191	−0.710	0.0221
H	$NHNH_2$	−0.925	0.119	−1.300	0.145	−0.730	0.0802
	$N(CH_3)_2$	−0.940	0.0907	−1.300	0.0694	−0.740	0.0434
I	CH_3	−0.870	0.0679	−1.000	0.0224	−0.750	0.0299

1 V *vs.* SCE.
ot measurable.

TABLE VII

SERIES II: SUBSTITUENT R_7

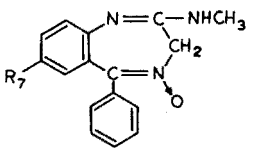

Designation	*Substitution*	*pH 3*					
		4,5-Azomethine		*1,2-Azomethine*		*N_4-Oxide*	
		E_p[a]	*Slope (μA/μg)*	E_p	*Slope (μA/μg)*	E_p	*Slope (μA/*
II-A	Cl	−0.705	0.1039	−1.165	0.0882	−0.375	0.065
II-K	Br	−0.705	0.0855	−1.155	0.0917	−0.390	0.059
II-L	H	−0.745	0.0998	−1.275	0.0747	−0.390	0.060
II-M	SCH_3	−0.720	0.0920	−1.175	0.1113	−0.380	0.064
II-N	$COOCH_3$	−0.710	0.1039	−1.100	0.0604	−0.400	0.062
II-O	Cl[b]	−0.750	0.0835	−1.165	0.0772	−0.375	0.057
II-P	I[c]	−0.670	0.0569	−1.170	0.1185	−0.400	0.046
II-Q	$COCH_3$[c]	−0.680	0.0588	−1.190	0.0385	−0.440	0.045
II-R	CH_3	−0.730	0.1174	−1.200	0.0740	−0.390	0.060

[a] In V *vs.* SCE.
[b] Also substituted 4′-OH.
[c] Also substituted 2′-F.

TABLE VIII

SERIES II: SUBSTITUENT R_7

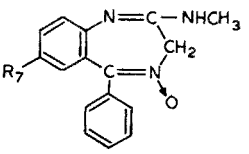

Designation	*Substitution*	*pH 7*					
		4,5-Azomethine		*1,2-Azomethine*		*N_4-Oxide*	
		E_p[a]	*Slope (μA/μg)*	E_p	*Slope (μA/μg)*	E_p	*Slope (μA/*
II-A	Cl	−0.940	0.0701	−1.370	0.0472	−0.760	0.033
II-K	Br	−0.915	0.0267	−1.350	0.0212	−0.715	0.014
II-L	H	−0.985	0.0960	−1.485	0.0442	−0.770	0.044
II-M	SCH_3	−0.995	0.0816	−1.375	0.0840	−0.755	0.040
II-N	$COCH_3$	−0.950	0.0894	−1.305	0.0805	−0.765	0.041
II-O	Cl[b]	−0.970	0.0843	−1.345	0.0640	−0.740	0.043
II-P	I[c]	−0.860	0.0265	−1.280	0.0078	−0.740	0.012
II-Q	$COCH_3$[c]	−0.805	0.0545	−1.300	0.0356	−0.790	0.019
II-R	CH_3	−0.990	0.1030	−1.390	0.0729	−0.775	0.046

[a] In V *vs.* SCE.
[b] Also substituted 4′-OH.
[c] Also substituted 2′-F.

The 7-substituted compounds (Fig. 5 and Tables VII, VIII) showed a greater effect of substituent on E_p for the reduction of the 4,5-azomethine bond at pH 7 [$\rho = -0.171$ V], than at pH 3 [$\rho = -0.118$ V]. In general, the sensitivity ($\mu A/\mu g$) was greater at pH 3 than pH 7. It was not possible to establish a Hammett relationship at either pH for the 1,2-azomethine reduction. The N-oxide reduction potentials showed little change with variation in the substituent and appeared to indicate no dependence of E_p on the 7-substitution. An additional peak was recorded for compound [II-Q]; this was attributed to the reduction of the carbonyl function. Compound [II-O] was also 4′-hydroxy-substituted and the σ value employed is the sum of the *m*-chloro and *p*-hydroxy constants. Compound [II-P] and [II-Q] are both 2′-fluoro-substituted and the Hammett constant plotted is the sum of the *m*-fluoro and the *m*-constant for iodine and the acetonyl, respectively.

Series III compounds

The series III compounds produced only a single peak for the polarographic reduction of the 4,5-azomethine bond.

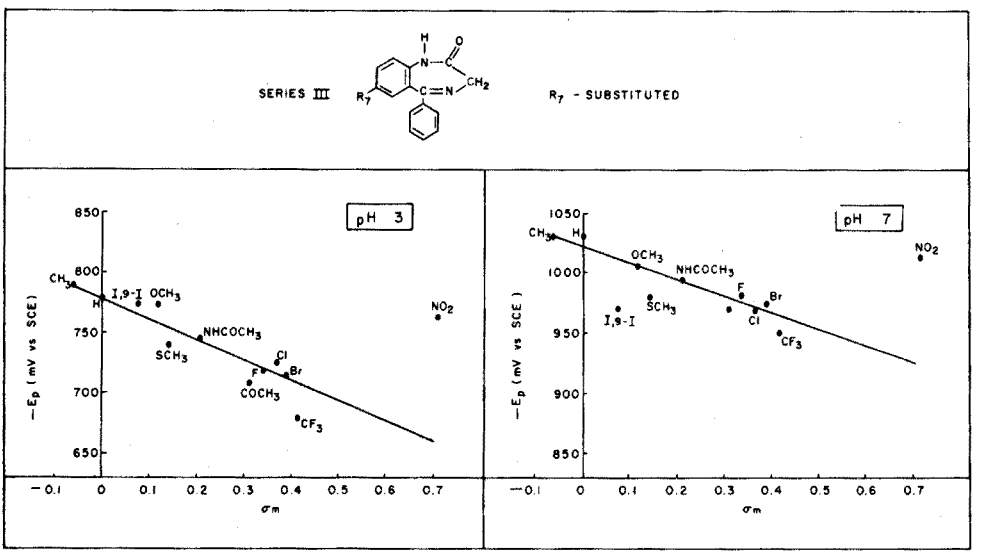

Fig. 6. Hammett plot for R_7 substitution in diazepam series [III] at pH 3.0 and 7.0.

The 7-substituted compounds (Fig. 6 and Table IX) showed a linear Hammett relation at pH values of 3 and 7, the effect of substitution being greater at pH 3 [$\rho = -0.172$ V] than at pH 7 [$\rho = -0.134$ V]. The values of ρ obtained are in good agreement with two similar studies which related substituents and ease of polarographic reduction for the benzodiazepines[27,28]. The sensitivity ($\mu A/\mu g$) is generally higher at pH 3 than at pH 7. Compound [III-L] exhibited a secondary peak corresponding to the carbonyl reduction. Compound [III-F] yielded a secondary peak which appears to correspond to the two-electron reduction of the iodine. This mechanism has been reported by Perrin[34]. Nitrazepam [III-D] also produced secondary peaks for the reduction of the nitro and hydroxylamine functional groups. The mechanism of this reduction has been reported[15,16,24].

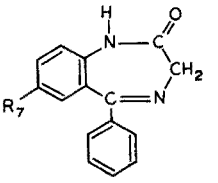

TABLE IX

SERIES III: SUBSTITUENT R_7

Designation	*Substitution*	*pH 3*		*pH 7*	
		4,5-Azomethine		*4,5-Azomethine*	
		E_p[a]	*Slope* ($\mu A/\mu g$)	E_p	*Slope* ($\mu A/\mu g$)
III-A	Cl	−0.725	0.0979	−0.970	0.0679
III-B	CH_3	−0.790	0.0854	−1.030	0.0956
III-C	Br	−0.715	0.0534	−0.975	0.0510
III-D	NO_2	−0.765	0.0039	−1.015	0.0252
III-E	$NHCOCH_3$	−0.745	0.0710	−0.995	0.0880
III-F	I[b]	−0.775	0.0339	−0.970	0.0039
III-G	OCH_3	−0.750	0.0880	−1.005	0.0618
III-H	SCH_3	−0.740	0.0766	−0.980	0.0038
III-I	CF_3	−0.680	0.0737	−0.950	0.0147
III-J	F	−0.720	0.0922	−0.985	0.1112
III-K	H	−0.780	0.1034	−1.030	0.1181
III-L	$COCH_3$	−0.710	0.0818	−0.970	0.0954

[a] In V *vs.* SCE.
[b] Also substituted 9-I

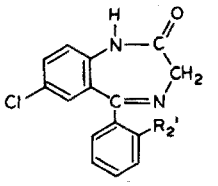

TABLE X

SERIES III: SUBSTITUENT R_2'

Designation	*Substitution*	*pH 3*		*pH 7*	
		4,5-Azomethine		*4,5-Azomethine*	
		E_p[a]	*Slope* ($\mu A/\mu g$)	E_p[a]	*Slope* ($\mu A/\mu g$)
III-A	H	−0.725	0.0879	−0.970	0.0679
III-M	F	−0.705	0.0414	−0.940	0.0712
III-N	Cl	−0.675	0.0831	−0.950	0.0373
III-O	OCH_3	−0.670	0.0779	−0.990	0.0685
III-P	CH_3	−0.790	0.0854	−1.030	0.0956

[a] In V *vs.* SCE.

The few available 2'-substituted compounds (Table X) showed no correlation for the reduction of the 4,5-azomethine at pH 3 or 7.

A comparison among the three series of compounds indicated that the E_p values of series II and III, compared to series I, have a relatively large dependence

on the 7-substitution at pH 3. Series II and III are nearly equally affected by substitution in the 7-position at both pH 3 and pH 7 (the ρ values are nearly identical). Of the 7-substituted compounds of the three series, series I compounds are the most difficult to reduce at pH 3, as noted by the most negative reduction peaks.

In general, the E_p values of the 4,5-azomethine group in the nitro-substituted compound have deviated from the experimentally drawn line. It has been postulated[26, 28] that this type of behavior can be due to strong resonance effects present in these molecules.

Methyl- and hydrogen-substituted compounds responded almost identically to polarographic reduction, yielding the most negative values of E_p. Substitution of a halogen or halogen-containing functional group causes a positive shift in E_p compared to hydrogen substitution. Carbonyl-containing functional groups also exert a positive shifting effect compared to hydrogen substitution, but to a lesser extent than the halogen-substituted compounds.

Heterocyclic substituted benzodiazepines

Two groups of heterocyclic substituted benzodiazepines related to series I and III compounds were also polarographically examined (Table XI). Compounds [IV-A,B,C,D] differ from N-desmethyldiazepam [III-A] by the heterocyclic substitution in the R_5 position. Compounds [IV-E] through [IV-K] differ from medazepam [I-C] in that the compounds are all substituted with a nitro function in the R_7 position in place of a chlorine and contain the heterocyclic substitution in the R_5 position.

The values of E_p for the reduction of the 4,5-azomethine and nitro groups and the sensitivity ($\mu A/\mu g$) for these compounds are presented in Table XI. Additional peaks were also obtained for these compounds, which were usually due to polarographic reduction of a functional group on the heterocyclic substitution. Each of the additional peaks obtained in the polarography of the heterocyclic compounds will be discussed individually.

Compound [IV-A] yielded an additional peak at -1.120 V, at pH 3, which is attributed to the reduction of the azomethine in pyridinyl substitution. At pH 3 the 4,5-azomethine reduction peak is slightly asymmetrical. Since this phenomenon does not occur in other compounds of similar structure, it is presumed that a more complicated reduction mechanism of the 4,5-azomethine than has been discussed previously, is probably occurring. Compound [IV-B] yielded only the 4,5-azomethine reduction peak at pH 3 and 7. At pH 3 the reduction occurs at an unusually high negative potential, owing to the indolyl group. Compounds [IV-C] and [IV-D], which are thiazolyl- and methylpyrozolyl-substituted, respectively, showed the same type of unsymmetrical reduction peak for the 4,5-azomethine reduction as [IV-A], with the effect rather dramatically noted for [IV-D]. In addition, at pH 3, compound [IV-C] has an additional peak at -1.040 V *vs.* SCE; this is attributed to the reduction of the azomethine in the heterocyclic ring. Both compounds [IV-C] and [IV-D] exhibited high sensitivity at pH 7.

Compound [IV-E] yielded peaks in pH 3 and 7 buffers at -1.030 V and -1.190 V, respectively, in addition to those listed in Table XI. This activity is attributed to a reduction in the pyridyl ring.

TABLE XI

HETEROCYCLES

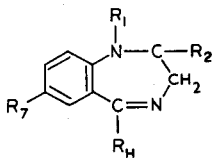

Designation	Substitutions			4,5-Azomethine		Nitro Peaks		pH	R_H
	R_1	R_2	R_7	E_p[a]	Slope ($\mu A/\mu g$)	E_p	Slope ($\mu A/\mu g$)		
IV-A	H	=O	Cl	−0.400	0.0881			3	
				−0.760	0.1121			7	
IV-B	H	=O	Cl	−0.915	0.0838			3	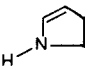
				−1.085	0.0122			7	
IV-C	H	=O	Cl	−0.400	0.0812			3	
				−0.650	0.0331			7	
IV-D	H	=O	Cl	−0.680	0.0797			3	
				−0.875	0.1109			7	
IV-E	CH_3	2H	NO_2	−0.270	0.0874	−0.215	0.1356	3	
				−0.600	0.1312	−0.510	0.1516	7	
IV-F	CH_3	2H	NO_2	−0.300	0.1265	−0.215	0.1738	3	
				−0.595	0.1218	−0.520	0.1940	7	
IV-G	CH_3	2H	NO_2	−0.450	0.0658	−0.240	0.1808	3	
				−0.750	0.1253	−0.540	0.1745	7	
IV-H	CH_3	2H	NO_2	−0.650	0.0818	−0.220	0.1526	3	
				−0.920	0.1371	−0.520	0.1761	7	
IV-I	CH_3	2H	NO_2	−0.320	0.0527	−0.260	0.1506	3	
				−0.650	0.0301	−0.535	0.0339	7	
IV-J	CH_3	2H	NO_2	−0.425	0.0810	−0.240	0.1764	3	
				−0.715	0.0465	−0.520	0.0521	7	
IV-K	CH_3	2H	NO_2	−0.590	0.0667	−0.210	0.1762	3	
				−0.975	0.0039	−0.520	0.0070	7	

[a] In V *vs.* SCE.

Compound [IV-F] showed additional polarographic peaks at both pH 3 and pH 7 due to the pyrimidinyl ring. A single peak was observed at pH 3, while a complicated series of peaks possibly indicating a more complex mechanism was recorded at pH 7. The sensitivity ($\mu A/\mu g$) increased with increasing pH, which is in contrast to the data for series I–III.

Compounds [IV-G] and [IV-H], which were methylimidazolyl- and methylpyrazolyl-substituted, respectively, yielded only those peaks reported in Table XI. As with [IV-F], sensitivity increased with increasing pH.

Compounds [IV-I] and [IV-J], both thiazolyl-substituted, yielded additional peaks in pH 3 solution at -1.130 V and -1.030 V, respectively; this may be attributed to a reduction in the heterocyclic system.

Compound [IV-K], thienyl-substituted, showed analytically useful polarographic activity only at pH 3. No additional peaks were observed.

In general, the pyridyl, pyrimidinyl, methylpyrazolyl and methylimidazolyl substitutions resulted in a higher current response ($\mu A/\mu g$) at pH 7 than pH 3, in contrast to series I–III. This may be due to increased electron induction effects of these moieties on the 1,4-benzodiazepine ring at higher pH than at pH 3, when these rings would tend to be protonated.

CONCLUSIONS

The type of polarographic data acquired in this study can be applied in the areas of mechanism studies, in the correlation of blood levels with pharmacological activities, for structural information and for the identification of unknown metabolites.

The high degree of resolution attained by differential pulse polarography yields information pertaining to the presence and identity of reducible groups on a molecule. The characteristic shifts of the E_p can be used to identify various substitutions on a parent compound. Using differential pulse polarography and thin-layer chromatography (t.l.c.), Hackman *et al.*[6] were able to identify and determine chlordiazepoxide (Librium) and its two major metabolites, desmethylchlordiazepoxide and demoxepam in serum. All three of these compounds possessed an N_4-oxide and a 4,5-azomethine, but owing to structural differences at the N_1–C_2 position all compounds are polarographically distinguishable. In another study[35], the same combination of techniques was used to differentiate and determine urinary trimethoprim and its structurally related N-1 and N-3 oxides in man, dog and rat.

By employing the Hammett relationship, it is also possible to identify unknown metabolites. The metabolic reduction of nitro substituents to acetamides and amines can be noted by loss of the nitro peak and characteristic shifts associated with the replacement group. The new group may often be identified by calculating the σ value from the Hammett plot and referring back to a tabulation of σ values. Likewise metabolic conversions of a carbonyl substituent to an acetal, N-oxidation, de-alkylation, hydroxylation and the formation of phenols may be investigated through the use of the Hammett relationship.

The authors thank Dr. R. I. Fryer, Department of Chemistry, Mrs. A. Sprules and Mrs. L. Lupi, Research Records Office of Hoffmann-La Roche Inc. for their

assistance in collecting the compounds used in this study. The authors also thank Mr. T. Daniels for the drawings of the figures presented.

SUMMARY

A differential pulse polarographic examination of 1,4-benzodiazepines structurally related to medazepam, chlordiazepoxide and N-desmethyldiazepam is presented. The data are used to correlate polarographic peak potentials (E_p) and Hammett substituent constants for the three series of compounds. Good correlations were found for the reduction of the 4,5-azomethine functional group for the three series of compounds in pH 3 and pH 7 supporting electrolyte. No correlation could be established for the reduction of the 1,2-azomethine and N_4-oxide in the series of compounds structurally related to chlordiazepoxide. Polarographic data are also presented for two groups of benzodiazepines structurally related to medazepam and N-desmethyldiazepam with heterocyclic substituents in the 5-position.

REFERENCES

1 H. Oelschlager, *Arch. Pharm. Weinheim*, 296 (1963) 396.
2 B. Z. Senkowski, M. S. Levin, J. R. Urbigkit and E. G. Wollish, *Anal. Chem.*, 36 (1964) 1991.
3 E. Jacobsen and T. V. Jacobsen, *Anal. Chim. Acta*, 55 (1971) 293.
4 G. Cimbura and R. C. Gupta, *J. Forensic Sci.*, 10 (1965) 228.
5 G. Caille, J. Brown and J. A. Mockle, *Can. J. Pharm. Sci.*, 5 (1970) 78.
6 M. R. Hackman, M. A. Brooks, J. A. F. de Silva and T. S. Ma, *Anal. Chem.*, 46 (1974) 1075.
7 E. Jacobsen and T. V. Jacobsen, *Anal. Chim. Acta*, 60 (1972) 472.
8 J. Fidelus, M. Zietek, A. M. Kolojek and Z. Grochowska, *Mikrochim. Acta*, (1972) 84.
9 H. Oelschlager, J. Volke and E. Kureck, *Arch. Pharm. Weinheim*, 297 (1964) 431.
10 M. A. Brooks, J. A. F. de Silva and M. R. Hackman, *Amer. Lab.*, 5 (9) (1973) 23.
11 D. J. Berry, *Clin. Chim. Acta*, 32 (1971) 235.
12 H. Oelschlager, J. Volke, T. Lim and R. Sprang, *Arch. Pharm. Weinheim*, 302 (1969) 946.
13 F. R. Fazzari and O. H. Riggleman, *J. Pharm. Sci.*, 58 (1969) 1530.
14 H. Oelschlager and H. P. Oehr, *Pharm. Acta Helv.*, 45 (1970) 708.
15 H. Oelschlager, J. Volke, G. T. Lim and V. Frank, *Arzneim.-Forsch.*, 16 (1966) 82.
16 S. Halvorsen and E. Jacobsen, *Anal. Chim. Acta*, 59 (1972) 127.
17 H. Oelschlager, J. Volke and G. T. Lim, *Arzneim-Forsch.*, 17 (1967) 637.
18 J. A. F. de Silva, I. Bekersky, M. A. Brooks, R. E. Weinfeld, W. Glover and C. V. Puglisi, *J. Pharm. Sci.*, 63 (1974) 1440.
19 J. A. F. de Silva, C. V. Puglisi and N. Munno, *J. Pharm. Sci.*, 63 (1974) 520.
20 L. F. Cullen, M. P. Brindle and G. J. Papariello, *J. Pharm. Sci.*, 62 (1973) 1708.
21 H. Oelschlager, J. Volke, H. Hoffmann and E. Kurek, *Arch. Pharm. Weinheim*, 300 (1967) 250.
22 H. Oelschlager, J. Volke and H. Hoffmann, *Collect. Czech. Chem. Comm.*, 31 (1966) 1264.
23 H. Oelschlager, J. Volke, G. T. Lim and U. Bremer, *Arch. Pharm. Weinheim*, 303 (1970) 364.
24 H. Oelschlager, J. Volke and G. T. Lim, *Arch. Pharm. Weinheim*, 302 (1969) 241.
25 E. S. Gould, *Mechanism and Structure in Organic Chemistry*, Holt, Rinehart and Winston, New York, 1959.
26 H. H. Jaffe, *Chem. Rev.*, 53 (1953) 191.
27 K. Muller and H. Meyer, F. Hoffmann-La Roche Co., Basle, (1971) private communication.
28 A. V. Bogatskii, S. A. Andronati, V. P. Gul'tyai, Y. I. Vikhlyaev, A. F. Galatin, Z. I. Zhilina and T. A. Klygul, *J. Gen. Chem. U.S.S.R.*, 41 (1971) 1364.
29 *Instruction Manual for PAR Model 171 (IV-31)*, Princeton Applied Research Corp., Princeton, N.J., 1970.

30 J. A. F. de Silva and M. R. Hackman, *Anal. Chem.*, 44 (1972) 1145.
31 M. A. Brooks, J. A. F. de Silva and L. M. D'Arconte, *Anal. Chem.*, 45 (1973) 263.
32 P. Zuman, *The Elucidation of Organic Electrode Processes*, Academic Press, New York, 1969, pp. 115–152.
33 P. Zuman, O. Exner, R. F. Rikker and W. Th. Nauta, *Collect. Czech. Chem. Comm.*, 33 (1968) 323.
34 C. L. Perrin in S. G. Cohen, A. Streitwieser, Jr. and R. W. Taft (Eds.), *Progress in Physical Organic Chemistry*, Volume III, Interscience, New York, 1965, pp. 165–316.
35 M. A. Brooks, J. A. F. de Silva and L. M. D'Arconte, *J. Pharm. Sci.*, 62 (1973) 1395.

Analytica Chimica Acta, 74 (1975) 387–393

THE CONVERSION OF LYNESTRENOL TO POLAROGRAPHICALLY ACTIVE SUBSTANCES BY MIXTURES OF SULFURIC ACID AND METHANOL

W. P. VAN BENNEKOM, H. J. E. M. REEUWIJK and J. B. SCHUTE

Gorlaeus Laboratoria, Department of Pharmaceutical Analysis and Analytical Chemistry, State University, Wassenaarseweg 76, Leiden (The Netherlands)

(Received 15th July 1974)

Lynestrenol (19-nor-17α-pregn-4-en-20-yn-17-ol) is a progestational agent[1] and is used alone (Orgametril and Exluton*) and in combination with mestranol (Lyndiol, Ovanon and Orgaluton) or ethynylestradiol (Pregnon 28) in oral contraceptives and other preparations. Lynestrenol in formulations can be determined by t.l.c.[2–11], followed by comparison of spot areas[10] or a spectrophotometric finish[2–9,11], by column chromatographic methods[12,13], by g.l.c.[14], by a radiochemical method[15], by i.r. spectrometry[16], and by titration[17].

In the work described here, a polarographic determination for lynestrenol was sought. Since the compound itself is not reducible at a dropping mercury electrode[18–20], as can be deduced from its structure, lynestrenol must be converted to a polarographically active substance by some chemical method. A variety of methods has been proposed for the polarographic determination of steroids by chemical derivatization[19,21–23], including nitrosation, oxidation, and formation of addition compounds. None of these methods seems to be adequate for lynestrenol. A new method of chemical modification was found for lynestrenol: the compound gives by treatment with concentrated sulfuric acid or mixtures of this acid with methanol, a number of reaction products, of which some are polarographically reducible. To establish if this conversion could form the basis of a quantitative method for lynestrenol, the influence of sulfuric acid concentration and time of treatment has been studied.

EXPERIMENTAL

Apparatus

The polarographic curves were run with a Princeton Applied Research Corporation Model 174 Polarographic Analyzer, with a drop timer and a Houston Omnigraphic Model 2200-3-3 X-Y Recorder. A thermostat (Tamson TX 9-100) was employed to keep the polarographic cell (Metrohm EA 876, volume 20 ml) at a temperature of 25°C.

* Orgametril, Exluton, Lyndiol and Orgaluton are registered trade names of Organon Nederland B.V., Oss (The Netherlands) and Pregnon 28 and Ovanon of Nourypharma, Oss (The Netherlands).

A three-electrode system was used, consisting of a dropping mercury working electrode, a platinum wire auxiliary electrode (Metrohm EA 202) and a saturated calomel reference electrode (SCE, Metrohm EA 404).

Reagents

The reagents were of analytical quality, unless stated otherwise and were used without further purification. Lynestrenol was of commercial quality*. The mercury used was of polarographic quality (Merck, Darmstadt). The nitrogen employed was deoxygenated previously by an alkaline solution of pyrogallol[24].

A 0.005% (w/v) Triton X-100 (Rohm & Haas, Philadelphia) solution in distilled water was used in order to suppress polarographic maxima.

Reaction solutions I to IV were prepared, consisting respectively of mixtures of 20, 40, 60 and 80% (v/v) concentrated sulfuric acid (Baker, Deventer) and methanol (Merck, Darmstadt). Reaction solution V consisted of concentrated sulfuric acid without any addition (95,7% (w/w) H_2SO_4, 4,3% (w/w) H_2O). The mixtures were prepared by dilution of the necessary volume of concentrated sulfuric acid with methanol to 250 ml. The volume of the acid was determined from the weight and the density.

Procedure

Approximately 10 mg of lynestrenol was weighed accurately, dissolved in one of the reaction solutions I–V and made up to 100 ml in a volumetric flask. Then the lynestrenol–sulfuric acid solution was transferred to a 50-ml buret.

The Triton X-100 solution (10 ml), 25 ml of methanol and a quantity (0–4 ml) of concentrated sulfuric acid depending on the reaction solution used, were pipetted into a 50-ml volumetric flask. At predetermined intervals, 5 ml of the lynestrenol–sulfuric acid solution were added from the buret into this mixture in order to stop the chemical reaction. After cooling to room temperature, the solution was made up to 50 ml with methanol. All polarographic solutions finally consisted of 10% (v/v) concentrated sulfuric acid and 20% (v/v) of the Triton X-100 solution in methanol and contained approximately 0.5 mg of modified lynestrenol.

Oxygen dissolved in the polarographic solution was removed by bubbling for 10 min with a nitrogen flow, which had been presaturated with vapors of a solution of the polarographic composition in a gas bubbler. Then the lynestrenol solution was polarographed. The polarographic curves were recorded from -350 to -1100 mV *vs.* SCE in the differential pulse mode at a sensitivity of 1, 2 or 5 μA full scale. The modulation amplitude was 100 mV, the scan-rate 2 mV s^{-1} and the drop time 1 s throughout the experiments. The height of the mercury column was kept constant at 70 cm.

RESULTS AND DISCUSSION

The experiments showed that at least three polarographically reducible derivatives can be formed from lynestrenol in the sulfuric acid–methanol mixtures, depending on acid concentration and time of reaction. The compounds A, B and

* Courteously supplied by Organon Nederland B.V., Oss (The Netherlands).

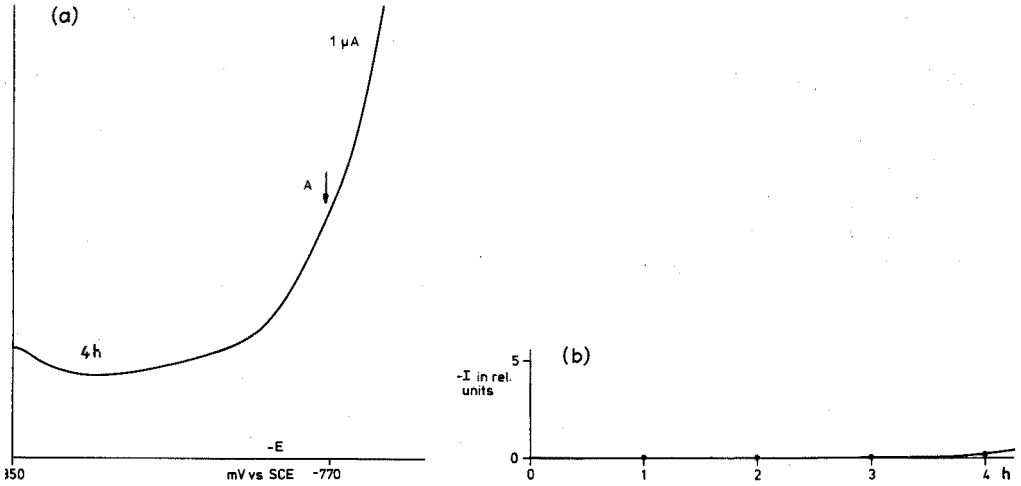

Fig. 1. (a) Polarographic curve of solution containing 20% sulfuric acid. (b) Peak current *vs.* time in 20% sulfuric acid. $E_p = -770$ mV *vs.* SCE.

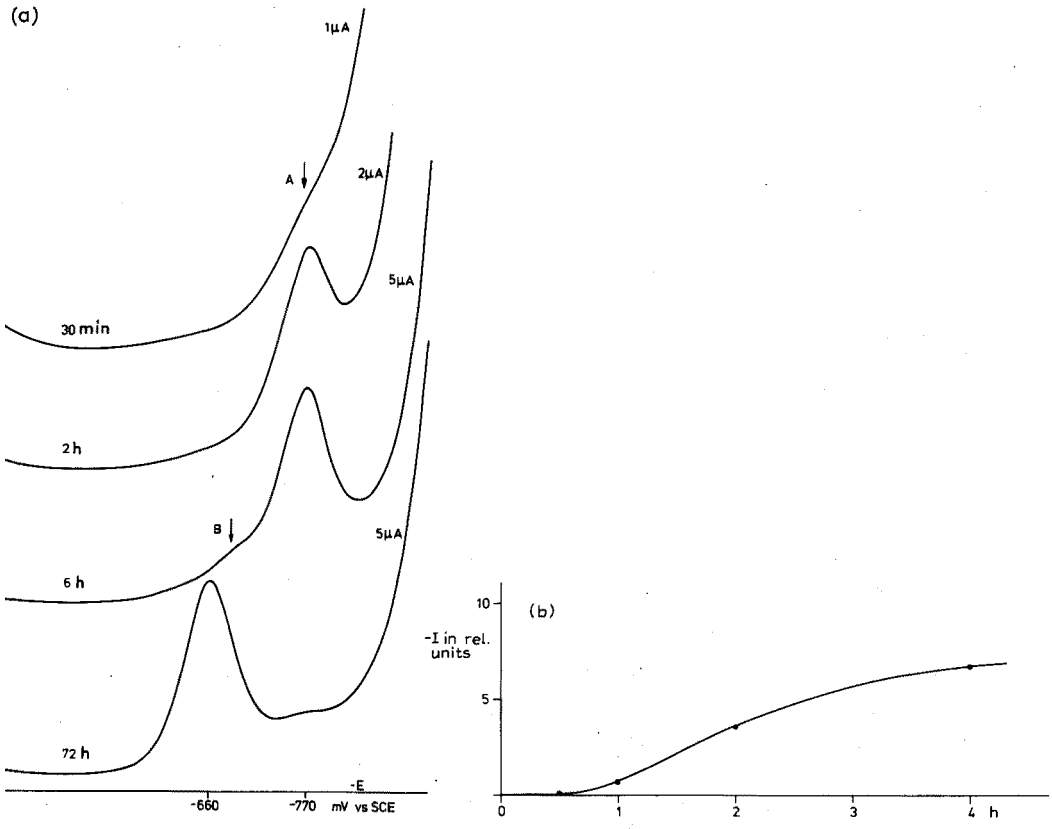

Fig. 2. (a) Conversion of compound A to compound B with time in 40% sulfuric acid. (b) Peak current *vs.* time in 40% sulfuric acid. $E_p = -770$ mV *vs.* SCE.

C have peak potentials (E_p) respectively at -770, -660 and -550 mV *vs.* SCE in the polarographic solutions used. After 4 h, the polarographic curve of solution I (20% H_2SO_4) started to show a minor wave, owing to the formation of compound A (Fig. 1a). The peak current (I_p) is plotted *vs.* time in Fig. 1b.

With increased acid concentration (solution II: 40% H_2SO_4), compound A is formed much sooner. After about 6 h, the polarographic curve shows a new compound B, which was not detectable before. After a reaction time of 72 h, compound A is almost completely converted into B (Fig. 2a). Figure 2b shows the peak current of compound A as a function of time for the first 4 h.

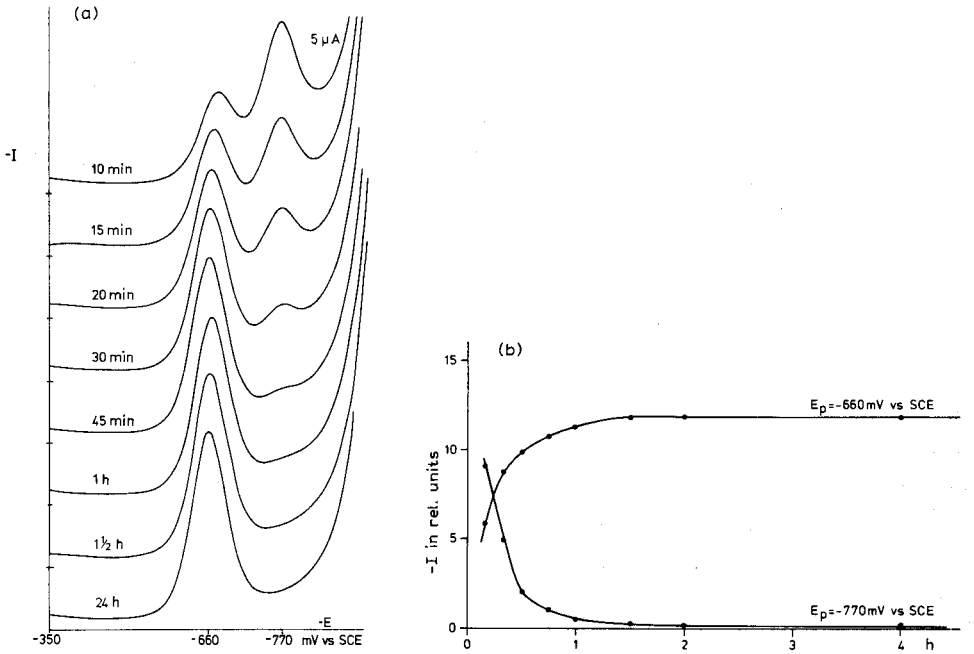

Fig. 3. (a) Development of compound B with time in 60% sulfuric acid. (b) Peak currents *vs.* time in 60% sulfuric acid.

In the first stage of the reaction in solution III (60% H_2SO_4), both compounds A and B are present. In this medium, A is converted into B much faster than in solution II. After about 1.5 h, only compound B is detectable (Fig. 3a). The peak currents of compounds A and B are plotted as a function of time in Fig. 3b.

In the polarographic curves of solution IV (80% H_2SO_4) only compound B appears (Fig. 4a). Compound A may be formed, but this compound is completely converted to B within 10 min. The peak current for compound B was found to be independent of time (Fig. 4b).

In solution V (undiluted concentrated sulfuric acid), compound B is initially the only detectable compound. However, after 4 h, a compound C appears in the polarographic curve (Fig. 5a). The peak current for compound B was plotted *vs.* time for the first 4 h, and was found to be independent of time (Fig. 5b).

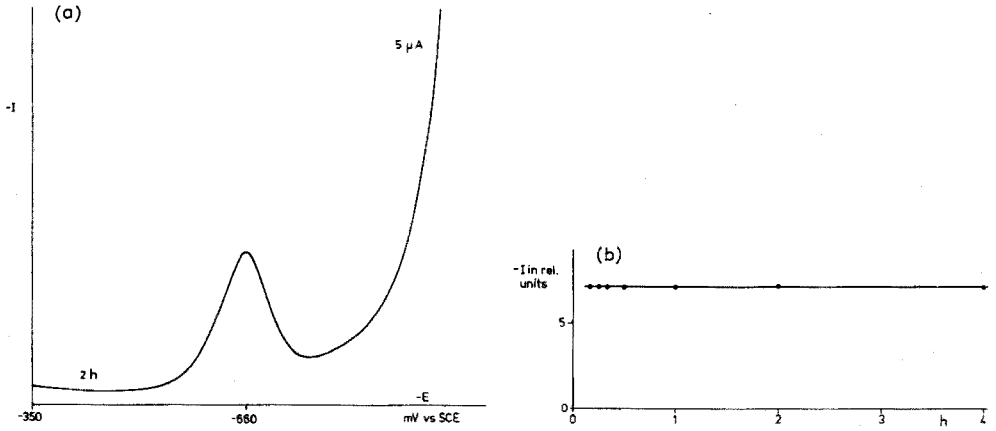

Fig. 4. (a) Development of compound B in 80% sulfuric acid. (b) Peak current *vs.* time in 80% sulfuric acid. $E_p = -660$ mV *vs.* SCE.

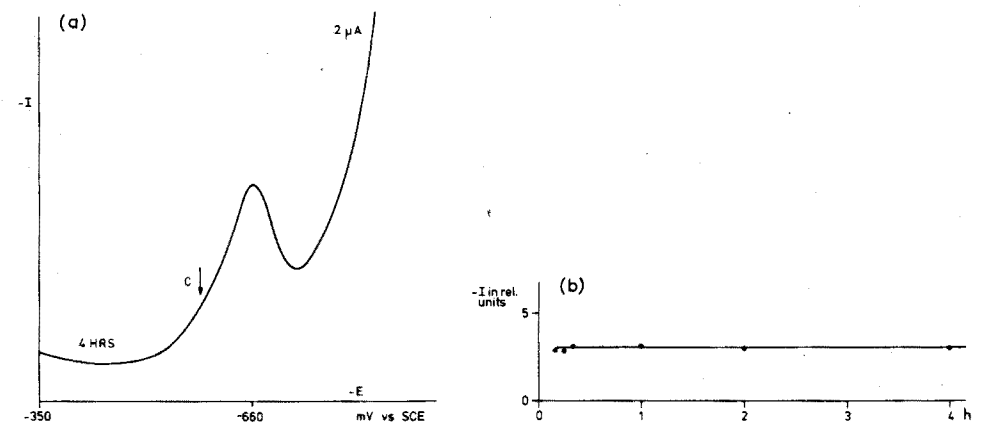

Fig. 5. (a) Development of compound B in 100% sulfuric acid. (b) Peak current *vs.* time in 100% sulfuric acid. $E_p = -660$ mV *vs.* SCE.

The results obtained with the five reaction solutions are presented in Fig. 6 as plots of peak current *vs.* time. For purposes of comparison, the peak currents were corrected for a polarographic blank, and calculated for an analytical concentration of 10 mg of lynestrenol in 100 ml of reaction solution and a current sensitivity of 5 μA full scale. Fig. 6 shows that the polarographic peak-current of compound B can serve for the determination of lynestrenol if solutions III–V are used. The I_p values for compound B are constant after 1.5 h or sooner. The sensitivity of the determination depends on the acid concentration of the reaction solution and decreases in the order III to V. When solution I or II is used, the I_p–time curves of compound A ($E_p = -770$ mV *vs* SCE) rise slowly at first. Among other things, this is caused by the slow rate of dissolution of the steroid in these media.

Work is now in progress to establish the chemical constitution of the polarographically reducible compounds and the reaction mechanism.

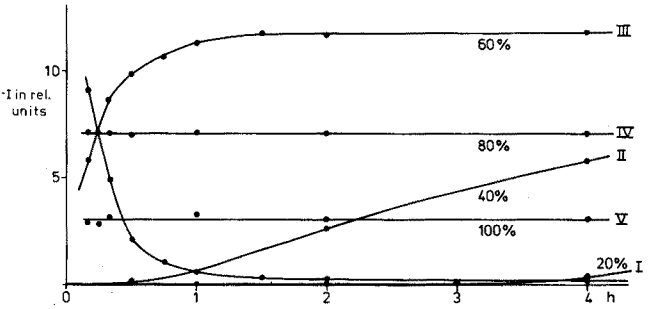

Fig. 6. Peak current *vs.* time for samples of lynestrenol in solutions I–V. $E_p = -770$ mV *vs.* SCE for curves I and II. $E_p = -660$ mV *vs.* SCE for curves III–V. Sensitivity 5 μA f.s.d.

Spectroscopic data (to be published) suggests that the structure of compound B is 19-nor-pregna-14,16- dien-20-one. The 17α-ethynylcarbinol group of the steroid is rearranged[25] to a Δ^{16}-20-one group and the double bond at C_4 is moved through the steroid backbone to C_{14}. The application of the method for the determination of lynestrenol in formulations is also being examined.

The influence of acids on other steroids containing a 17α-ethynyl-carbinol-group will also be investigated.

The authors are indebted to P. M. Hooymans and L. M. M. van Tetering, who made valuable experimental contributions to this work.

SUMMARY

Lynestrenol (19-nor-17α-preg-4-en-20-yn-17-ol) can be converted to polarographically active substances by treatment with sulfuric acid–methanol solutions. Maximal sensitivity is obtained in 60% sulfuric acid solutions but development of the active compound requires 1.5 h; slightly poorer sensitivity is found in 80% sulfuric acid solutions but the reaction requires only 10 min.

REFERENCES

1 M. S. de Winter, C. M. Siegmann and S. A. Szpilfogel, *Chem. Ind. (London)*, 37 (1959) 905.
2 H. G. Gaenshirt and J. Polderman, *J. Chromatogr.*, 16 (1964) 510.
3 D. Sonanini and L. Anker, *Pharm. Acta Helv.*, 42 (1967) 54.
4 E. Roeder, *Deut. Apoth. Ztg.*, 107 (1967) 1007.
5 G. R. Keay, *Analyst (London)*, 93 (1968) 28.
6 J. J. Thomas and L. L. Dryon, *Proc. Int. Symp. Chromatogr. Electrophor.*, V (1969) 405.
7 I. Szekacs and M. Klembala, *Z. Klin. Chem. Klin. Biochem.*, 8 (1970) 131.
8 M. B. Simard and B. A. Lodge, *J. Chromatogr.*, 51 (1970) 517.
9 A. Grochulski, *Acta Pol. Pharm.*, 28 (1971) 185.
10 S. Enache, *Chim. Anal. (Bucharest)*, 1 (1971) 244.
11 M. Kirchner, H. Holsen and K. Norpoth, *Zentralbl. Bakteriol., Parasitenk., Infektionskr. Hyg., Abt., 1: Orig., Reihe B*, 157 (1973) 44.
12 A. Alvarez Fernandez and N. Torre, *J. Pharm. Sci.*, 58 (1969) 740.
13 G. Cavina, G. Moretti, A. Mollica and R. Antonini, *J. Chromatogr.*, 60 (1971) 179.
14 R. Mestres and J. L. Berges, *Trav. Soc. Pharm. Montpellier*, 32 (1972) 313.

15 P. H. Cox, T. J. G. Ambaum and H. P. Wijnand, *J. Pharm. Pharmacol.*, 20 (1968) 238.
16 G. Bellomonte, *Ann. Ist. Super. Sanita*, 7 (1971) 102.
17 M. Risk, J. J. Vallon and A. Badinand, *Anal. Chim. Acta*, 70 (1974) 457.
18 M. Březina and P. Zuman, *Die Polarographie in der Medezin, Biochemie und Pharmazie*, Akad. Verlagsges. Geest & Portig K.-G., Leipzig, 1956, pp. 212.
19 M. Březina and P. Zuman, *Die Polarographie in der Medezin, Biochemie und Pharmazie*, Akad Verlagsges. Geest & Portig K.-G., Leipzig, 1956, p. 399–416.
20 I. M. Kolthoff and J. J. Lingane, *Polarography*, Vol. II, Interscience, New York, 1952, p. 634.
21 I. M. Kolthoff and J. J. Lingane, *Polarography*, Vol. II, Interscience, New York, 1952, p. 666–674.
22 A. F. Summa and J. H. Graham, *J. Pharm. Sci.*, 54 (1965) 612.
23 B. J. Forman and L. T. Grady, *J. Pharm. Sci.*, 58 (1969) 1262.
24 A. I. Vogel, *A Text-book of Quantitative Inorganic Analysis*, 3rd ed., Longmans, London, 1968, p. 1079.
25 T. F. Rutledge, *Acetylenes and Allenes*, Reinhold, New York, 1969, pp. 132–135.

Analytica Chimica Acta, 74 (1975) 395–410

AN EVALUATION OF SOME SODIUM ION-SELECTIVE GLASS ELECTRODES IN AQUEOUS SOLUTION

PART I. ELECTRODE CALIBRATION CHARACTERISTICS AND SELECTIVITY WITH RESPECT TO HYDROGEN IONS

MICHAEL F. WILSON, ESA HAIKALA and PEKKA KIVALO
Chemical Laboratory, Technical Research Centre of Finland, 02150 Otaniemi (Finland)
(Received 2nd August 1974)

Although the discovery of cation-responsive glass electrodes was one of the earliest of many new developments in the field of ion-selective electrodes[1], in recent years limited progress has been made in improving the performance of sodium ion-sensors. Much has yet to be attained in the performance of commercially available electrodes, especially from the point of view of response time and selectivity with respect to hydrogen ions.

After the notable work of Eisenman *et al.*[1], who examined the theoretical aspects of the glass electrode response behaviour, an early investigation into the behaviour of different sodium ion-selective electrodes was carried out by Mattock[2,3]. For this study, Mattock fabricated electrodes in the laboratory from the glasses EIL BH68, EIL BH104 and Corning NAS11–18, and electrode properties, including selectivities, were presented mostly in graphical form. Recently, Phang and Steel[4] noted that there is a disparity of information regarding the properties of commercial electrodes and these workers determined some properties including selectivity coefficients by the separate solution method.

In the present work, a technique of fixing the interfering hydrogen ion activity with solutions of Tris buffers was devised, in order to determine the selectivity coefficients of sodium ion-selective electrodes in mixed Na^+/H^+ solutions. Such buffer solutions also involve large organic cations, whose interference may be assumed to be negligible; the results showed that the selectivity coefficient with respect to hydrogen ion varies with change in pH of the solution.

Apart from the performance of various commercial electrodes, the present work is also concerned with the techniques involved in the use of sodium ion-sensors and improvements therein.

EXPERIMENTAL

Choice of electrode assembly

Although cells without liquid junction are considered the most reliable for precise work, the attack of the silver–silver chloride reference electrodes by the organic base used to buffer the sample solution, and subsequent liberation of silver ions, ruled out their use with sodium ion-selective electrodes. In using

conventional cells with potassium chloride salt bridge for the precise measurement of sodium ion activities to a low level, difficulties are caused by leakage of potassium ions, giving rise to e.m.f. transients. These problems were avoided by using the following cell:

double-junction reference half-cell

$$\overbrace{\mathrm{Ag} \mid \mathrm{AgCl}_{(s)},\ 0.70\ M\ \mathrm{KCl},\ 1.50\ M\ \mathrm{KNO_3} \parallel 2\ M\ \mathrm{RbCl}}\ \parallel \mathrm{Na^+}$$ sample | glass electrode (1)

For investigations of the deviation of the electrode response from Nernstian, a second arrangement (referred to as cell 2) was also used; here the Na^+ sample solution was also placed in the outer compartment of the double-junction reference electrode, replacing the 2 *M* rubidium chloride salt bridge.

The least interference was obtained with cell (2), because placing the sample solution in the outer compartment of the reference electrode served as a simple isolating system. This cell was convenient for simple calibration work but is obviously inconvenient for general use, for which a suitable salt bridge electrolyte is necessary. Rubidium chloride was chosen as bridge electrolyte since of several electrolytes investigated it gave the least interference; moreover, this electrolyte is even more equitransferent than potassium chloride.

A 3 *M* rubidium chloride bridge electrolyte solution has been used with success by Khuri[5] for *in vitro* and *in vivo* measurements of sodium ion activities in biological media. Khuri quoted the NAS 11-18 ion electrode glass as being 100 times less sensitive to Rb^+ than to K^+ ions and in general the selectivity coefficient with respect to the Rb^+ ion has been quoted in the order of 10^{-5} for most sodium ion electrode glasses.

Cell (1) gave linearity in calibration graphs down to better than 10^{-5} *M* and was considered suitable for the determination of selectivity coefficients and for general use.

Electrodes

A representative selection of commercially available sodium ion-selective electrodes was investigated. A total of twelve electrodes, four groups of three, were taken from distributors' stocks and were not specially chosen. The electrodes were designated as follows:

(i) three Beckman 39278 electrodes numbered 1, 2 and 3
(ii) three EIL GEA 33C electrodes numbered 4, 5 and 6
(iii) three Orion 94-11 electrodes numbered 7, 8 and 9
(iv) three Radiometer G502 Na electrodes numbered 10, 11 and 12.

EIL electrode number 6 was replaced after it was discovered that it gave erratic potential readings and drifting.

The glass electrodes were prepared for testing by soaking for at least 5 days in 10^{-1} *M* sodium chloride solution (where they were also stored when not in use) and then by "cycling" from 10^{-6} *M* to 10^{-1} *M* sodium chloride for 5 min. For certain tests, *e.g.* the determination of selectivity coefficients, the electrodes were soaked overnight in the initial test solution used.

A total of four Orion Double-Junction Reference Electrodes type 90-02-00

were used with internal filling solution 90-00-02 which contains approximately 0.70 *M* potassium chloride and 1.50 *M* potassium nitrate together with small amounts of sodium and silver ions[6].

Instrumentation

Measurements were made with a Keithley Instruments 630 electrometer and an Orion Ionalyser Model 801 digital potentiometer coupled with Honeywell Electronik 19 and Servogor RE 511 recorders, respectively. pH measurements were made with a Radiometer type PHM 4C meter fitted with a Radiometer G 202C glass electrode and Orion Double Junction Reference Electrode type 90-02-00 incorporating a 2 *M* rubidium chloride salt bridge. The assembly was calibrated with standard pH buffers. All measurements were made in thermostatted, earthed water baths at 25.0 °C in the absence of light; cell vessels were made of polyethylene and stirrers were of teflon. Pure nitrogen gas, which was pre-saturated with the sample solution, was bubbled through the cell and all solutions were made up from freshly distilled and de-ionized water.

Choice of buffer system for electrode calibration

Since hydrogen ion interferes seriously with sodium ion electrodes, particularly for low-level measurements, in most work the pH of the sample solution is raised to a suitable level by addition of a base, which is usually an organic base giving rise to large non-interfering cation. Eckfeldt and Proctor[7] claimed that for satisfactory measurement a hydrogen-to-sodium ion ratio of 1:1000 is needed; attempts have been made by some workers[8,9] to monitor sodium ion levels in boiler feed water in the range 10^{-6}–10^{-8} *M* with ammonia as the base for buffering to pH 11.0–11.6. However, measurement in these very low sodium ion concentration ranges is only practicable in flowing systems; under static conditions there is the possibility of contamination from the cation used in the salt bridge of the reference electrode, and in the flowing system the reference electrode is placed down-stream from the sodium ion sensor. Similarly another source of contamination is from the plastic material of the cell wall and this contamination is reduced significantly in the flowing system. In solutions of high alkalinity, attack of the electrode glass membrane as well as interference from ammonium ions may also occur with certain electrodes[7].

In this work, for calibration purposes under normal laboratory conditions, the lower level to be achieved was set at 10^{-6} *M* Na^+, and ethanolamine (pK_A 9.54[10]) was used as the base. The advantages of using this reagent are:

(a) it gives rise to the large ethanolammonium cation $\overset{+}{N}H_3CH_2CH_2OH$,

(b) it may be used as both a buffering agent and ionic strength adjustor giving a satisfactory intermediate pH between 9 and 10,

(c) by careful distillation it is obtainable in a high state of purity.

Hawthorn and Ray[8] have suggested that sodium impurities in the buffering agent may be responsible for departures from linearity in electrode calibration. However, the results obtained in this work—*i.e.* satisfactory calibration down to 10^{-6} *M* Na^+ for at least one electrode group—suggests that the method used for the purification of ethanolamine was satisfactory.

Experimental procedure

For the calibration of the electrodes, and the investigation of the deviation of their response from Nernstian and their effective linear molarity range, cell (2) was employed; 10^{-1}–10^{-6} *M* solutions of sodium chloride were prepared by the dilution method, and stored in plastic bottles. (Unfortunately, since no suitable complexing agent exists for sodium ions, solutions of metal buffers could not be used in electrode calibration[11].) The ionic strength of the solutions was adjusted to 0.10 *M* and maintained constant throughout by the formation in solution of equimolar quantities of pure ethanolamine base and ethanolammonium ions, the latter being generated by the addition of the calculated quantity of hydrochloric acid. By this means, it was ensured that the ionic activity was directly proportional to the concentration of sodium ions in the solution. Similarly, the pH of the buffered solution was maintained at 9.54, the latter being checked by direct measurement.

The electrode response as a function of pH was investigated with cell (1) by a titration method. Solutions whose ionic strengths were adjusted to 0.10 *M* with ethanolammonium chloride and containing an equimolar amount of ethanolamine and a fixed concentration of sodium ions, were titrated through the pH range with hydrochloric acid solution containing the same concentrations of sodium and chloride ions as in the initial test solution; hence the ionic strength and sodium ion concentration remained constant throughout. Readings of e.m.f. and pH were recorded for each addition and measurements were made in the range of sodium ion concentration 10^{-1}–10^{-4} *M*. The potential–pH diagrams were obtained by plotting the e.m.f. values recorded *vs.* pH.

Selectivity coefficients with respect to hydrogen ion were determined by a solution addition technique. Solutions of 10^{-5} *M* sodium chloride were made up to ionic strength 0.10 *M* with the buffer mixtures tris acetate/acetic acid (pH 4.60), tris maleate/tris base (pH 5.20) and bis-tris/HCl (pH 6.52). (For each buffer mixture the molar ratio of the acidic and basic components was found by calculation.) The electrodes were allowed to soak overnight in these solutions in order to reach equilibrium, and an aliquot of each solution served as an initial test solution in cell (1). A solution of 10^{-2} *M* sodium chloride in the same concentration of tris buffer was added in increments to the cell by means of a burette and hence the hydrogen ion activity remained constant in the presence of varying sodium ion activity and a constant background concentration of 0.10 *M* tris cation. Readings of volume added and e.m.f. were recorded for each addition, and since under these conditions the electrode response was slow, 10–15 min were allowed between additions to ensure that the system reached equilibrium (this was monitored by chart recorder). In these determinations it should be noted that changing the sodium ion activity from a low to high level was better from a practical standpoint, because the electrode response was then significantly faster. In all determinations the pH of the buffered solutions was checked by direct measurement.

Reagents

Sodium chloride was Suprapur grade (Merck). The pure buffers tris acetate (tris(hydroxymethyl)aminomethane acetate), tris maleate (mono-tris(hydroxy-

methyl)aminomethane maleate) and bis-tris (bis(2-hydroxyethyl)imino-tris(hydroxymethyl)methane) (obtained from Sigma Chemical Company, U.S.A.) were carefully desiccated before use. Ethanolamine (Fluka) was distilled twice under reduced pressure; it was found by titration with hydrochloric acid to be better than 99.98% pure. Sodium carbonate (*pro analysi;* Merck) was used as a primary standard, and was prepared by the method of Vogel[1,2]. Hydrochloric acid was from Titrisol ampoules which were checked by titration with standard carbonate. Rubidium chloride was *pro analysi* (Merck).

RESULTS AND DISCUSSION

Deviation of electrode response from Nernstian and overall sensitivity

The electrodes were calibrated by using cell (2) and the electromotive force E of this cell may be expressed in terms of the relationship

$$E = E^0_{ISE} + S \log c_{Na^+} \quad (3)$$

where S is the gradient of the calibration graph and at 25°C should be 59.2 mV/decade (*i.e.* 2.303 RT/F) if the response of the electrode is Nernstian; c_{Na^+} is the molar concentration of sodium ions in 0.10 M ethanolammonium buffer solution. Since the calibration solutions were made up to a constant ionic strength, the contribution from the activity coefficient of the sodium ion is constant and is incorporated in the E^0_{ISE} term, which also includes the potentials of the reference

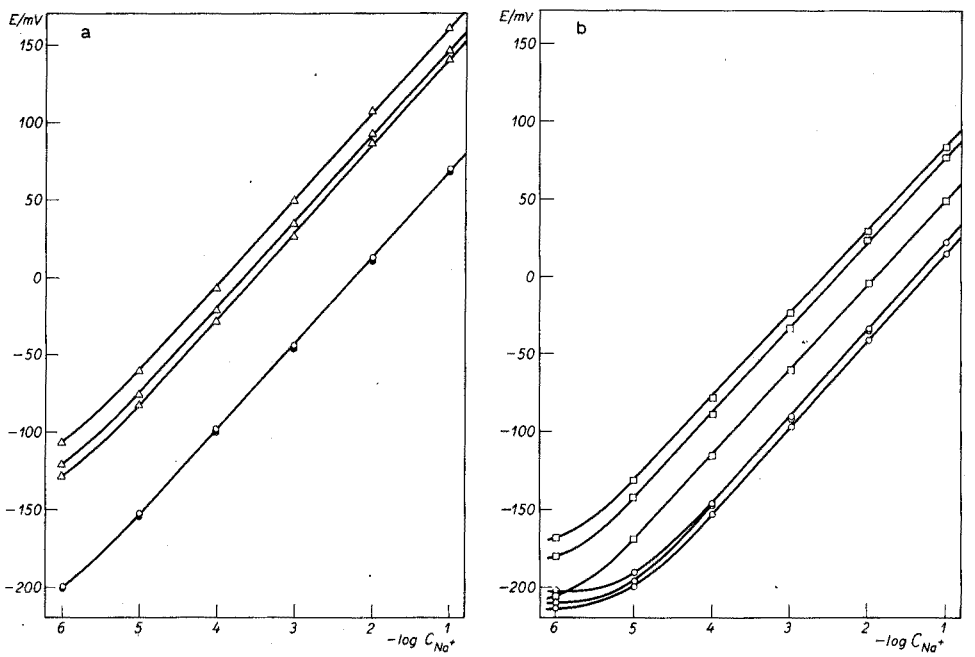

Fig. 1. Calibration plots for sodium ion-selective electrodes from potentiometric measurements in 0.10 M ethanolammonium buffer pH 9.54, temperature 25°C, (a): (○), Orion 94-11 electrodes; (△), Radiometer G502 Na electrodes. (b): (○), Beckman 39278 electrodes; (□), EIL GEA 33C electrodes.

electrodes together with the liquid junction potential of the double-junction reference electrode which is also assumed constant. The measured values of E were plotted as a function of log c_{Na^+}; Fig. 1 shows the calibration graphs for the new electrodes 1 to 12.

The gradients of the calibration graphs and values of E^0_{ISE} were calculated by regression analysis considering only the linear portions, and the values obtained are summarized in Table I. Also summarized are gradients and E^0_{ISE} values determined over the period of the investigation, the times between testing (in months) being an average value taken for all electrodes. Table I shows that, in most cases, aging causes the electrode response to become more Nernstian; moreover, new glass electrodes generally exhibit a gradient of 55–56 mV/decade.

TABLE I

GRADIENTS AND E^0_{ISE} VALUES FROM CALIBRATION GRAPHS FOR SODIUM ION-SELEC ELECTRODES DETERMINED IN 0.10 *M* ETHANOLAMMONIUM BUFFER OVER A PERIOI 3.5 MONTHS

(Temperature 25°C, pH 9.54.)

Electrode		*Initial values*		*After average of 2.5 months*		*After average of 3.5 months*	
		Gradient (mV/decade)	E^0_{ISE} *(mV)*	*Gradient (mV/decade)*	E^0_{ISE} *(mV)*	*Gradient (mV/decade)*	E (
Beckman	1	55.5	146.2	57.9	122.2	56.5	
39278	2	55.9	136.4	57.8	110.6	56.2	
	3	57.4	150.7	56.8	110.9	56.1	
	mean	56.3		57.5		56.3	
EIL	4	54.9	131.3	57.8	95.1	57.7	9
GEA 33C	5	54.7	102.8	57.6	67.4	57.5	6
	6	53.5	135.9	57.7	93.4	59.2	9
	mean	54.4		57.7		58.1	
Orion	7	55.4	122.0	56.7	121.0	57.8	1
94-11	8	55.4	123.6	57.1	123.3	58.1	1
	9	55.3	121.3	57.0	121.5	58.5	1
	mean	55.4		56.9		58.1	
Radiometer	10	55.6	217.0	57.2	168.9	59.2	1
G502 Na	11	55.7	202.4	57.0	162.8	59.6	1
	12	56.0	191.2	56.6	148.8	58.5	1
	mean	55.8		56.9		59.1	

After about 3.5 months, on average the Radiometer electrodes gave a Nernstian response, the gradients having increased by about 3 mV/decade. EIL and Orion electrodes gave somewhat less than Nernstian responses after this time, and the average maximum for Beckman electrodes was 57.5 mV/decade after about 2.5 months. However, even for new electrodes, the calibration gradients were found to be reproducible, at least within the same day.

The aging of glass electrodes has been investigated by Eisenman[13] who suggested that the principal factor may be the hydration of the membrane glass;

Moore[14] found that the selectivity of sodium glass electrodes improved with aging over long periods (*i.e.* in their experiments, 1 year), and proposed that before use in certain types of work, electrodes should be specially aged in solution.

It is also seen in Table I that, with the exception of the Orion electrodes, E^0_{ISE} values—and hence E^0 values for the glass membranes—decrease with aging. (It should be noted that slight fluctuations in the potentials of the reference electrodes also take place during long testing periods, but, by comparing the bias potentials of the reference electrodes, such fluctuations were found to be very small.) With the Orion electrodes the E^0_{ISE} values were almost identical for all three, unlike the other electrodes, and the values remained fairly constant throughout the testing period. This may be a consequence of the electrode design since the membrane consists of a specially cut plane-glass sheet, and construction involves no glass blowing or heat exposure. The phenomenon is probably a result of identical asymmetry potentials between electrodes and would seem to support the observation of Yoshimura[15] that plane-glass membranes have very small asymmetry potentials. This also suggests that the decrease in E^0_{ISE} values throughout the testing period for the other electrodes is a result of changing asymmetry potential with electrode use.

TABLE II

EFFECTIVE LINEAR MOLARITY RANGES OF SODIUM ION-SELECTIVE GLASS ELECTRODES DETERMINED IN ETHANOLAMMONIUM BUFFER AT 25°C

(pH 9.54, $I=0.1$.)

Electrode		*Effective linear molarity range*
Beckman 39278	1, 2 and 3	10^{-1}–10^{-4} M
EIL GEA 33C	4, 5 and 6	10^{-1}–$5\cdot10^{-5}$ M
Orion 94-11	7, 8 and 9	10^{-1}–10^{-6} M[a]
Radiometer G502 Na	10, 11 and 12	10^{-1}–$5\cdot10^{-5}$ M

[a] Orion electrodes exhibited slight but reproducible curvature between 10^{-5} and 10^{-6} M.

Table II summarizes the effective linear molarity ranges (often referred to as the range of overall sensitivity) of the glass electrodes, which were estimated from the calibration graphs (Fig. 1).

Electrode response as a function of pH

The potential–pH curves were plotted for electrodes 1–12; for any particular group all three electrodes were found to produce almost identical curves. For presentation, an electrode representative of each group was selected; Fig. 2 shows potential–pH curves for pH variation made in the presence of constant sodium ion concentrations from 10^{-1}–10^{-4} M inclusive.

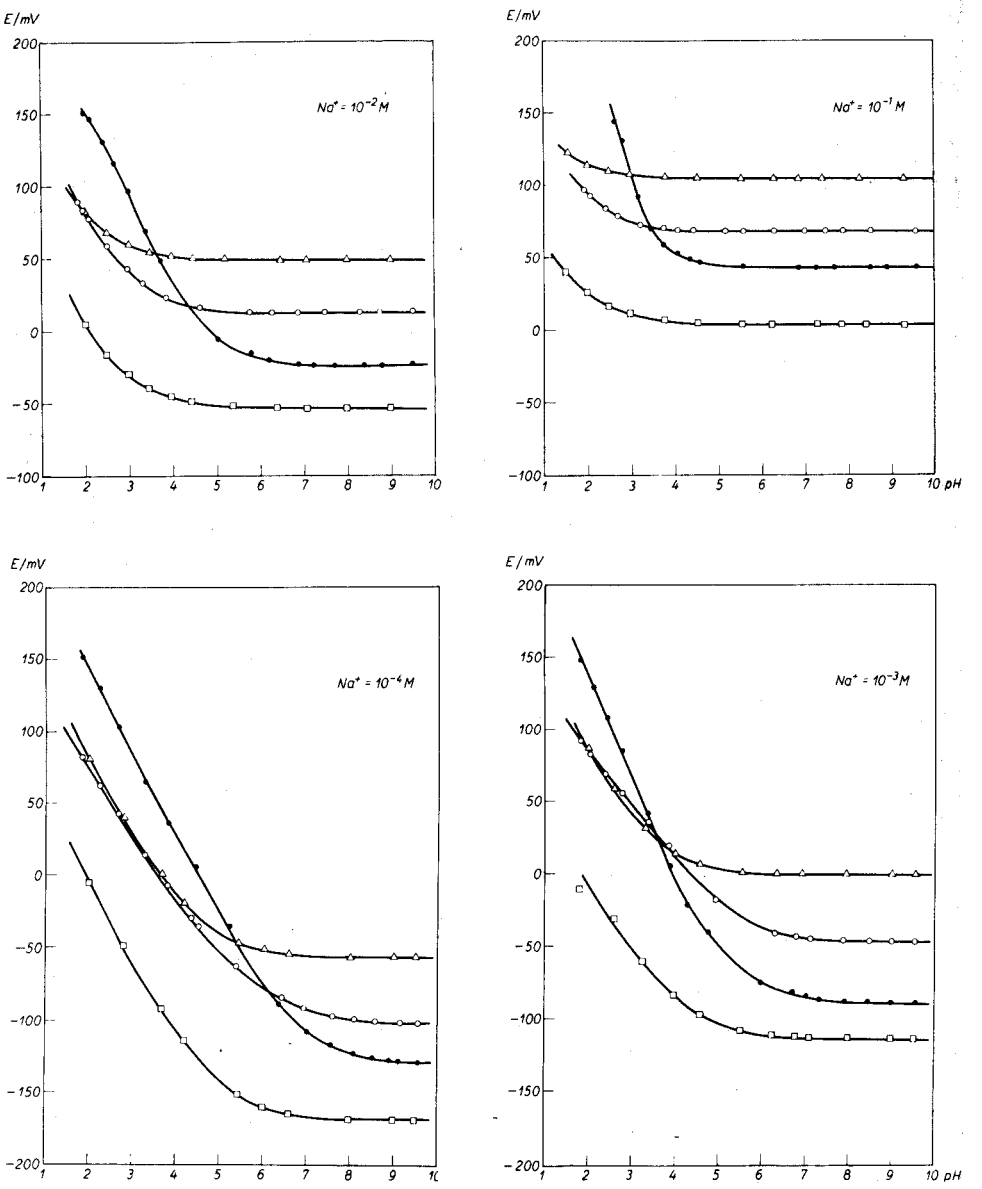

Fig. 2. Potential–pH curves for sodium ion-selective electrodes at constant sodium ion concentrations from 10^{-1} to 10^{-4} *M*. I=0.1 *M* adjusted with ethanolammonium chloride where necessary, temperature 25 °C. (●), Beckman 39278 electrodes; (□), EIL GEA 33C electrodes; (○), Orion 94-11 electrodes; (△), Radiometer G502 Na electrodes.

The potential–pH curves offer a useful visual guide in comparing the approximate operational pH ranges of the electrodes in aqueous solution within the pH scale. However, no reliable selectivity parameters can be determined from these curves as examination of the Figure shows, and since the critical ranges

in which interference begins to occur were unbuffered—as is usually the case with such curves—the results are not conclusive.

In carrying out work with sodium ion electrodes in aqueous solution, the electrode response is always complicated by the co-presence of hydrogen ions and these curves show that the interference from this ion may be very large and may also vary greatly from one electrode glass type to another depending on the composition of the hydrated layer of the glass membrane. It is also noteworthy that in those cases where the linear or so-called Nernstian section of the potential–pH curve is discernible (*i.e.* at low pH), the gradient for hydrogen ions is identical to that for sodium ions and hence S in eqn. (3) remains constant for both cations.

TABLE III

APPROXIMATE pH RANGES FREE FROM HYDROGEN ION INTERFERENCE[a]

(Temperature 25 C, $I = 0.1$ *M*.)

NaCl (M)	*Electrodes*			
	Beckman 39278 1, 2 and 3	*EIL GEA 33C 4, 5 and 6*	*Orion 94-11 7, 8 and 9*	*Radiometer G502 Na 10, 11 and 12*
10^{-1}	5.5–10.0	4.5–10.0	4.5–10.0	4.0–10.0
10^{-2}	7.0–10.0	5.0–10.0	5.5–10.0	4.5–10.0
10^{-3}	8.0–10.0	6.0–10.0	7.0–10.0	5.5–10.0
10^{-4}	9.0–10.0	7.0–10.0	8.0–10.0	6.5–10.0

[a] Average values estimated from potential–pH curves.

Table III summarizes the approximate ranges in which the electrodes are free from hydrogen ion interference, as determined from the curves for all electrodes.

Selectivity coefficients with respect to hydrogen ions

In considering the response of cation-selective glass electrodes in aqueous solution, the electrode potential in solutions containing a mixture of two univalent cations may be expressed in terms of the empirical equation of Eisenman *et al.*[16]:

$$E = E^0 + 2.303RT/nF \log \left[(a_{A^+})^{1/n_{AB}} + K_{AB}^{1/n_{AB}}(a_{B^+})^{1/n_{AB}}\right]^{n_{AB}} \quad (4)$$

where a_{A^+} and a_{B^+} are the activities of ions A^+ and B^+ respectively, and K_{AB} and n_{AB} are two adjustable parameters which are constant for a particular electrode and cation pair.

Eisenman *et al.* found that for Na^+–H^+ and Na^+–K^+ mixtures at a fixed pH, n_{AB} is approximately equal to unity. Hence eqn. (4), to a first approximation, reduces to the more general expression for the electrode potential, which for Na^+–H^+ mixtures may be written:

$$E = E_{ISE}^0 + S \log \left[a_{Na^+} + K_{Na-H}\, a_{H^+}\right] \quad (5)$$

where S will take the value 59.2 mV decade at 25°C if the electrode response is Nernstian under these conditions.

In general, for solid ion-exchangers, the selectivity between A^+ and B^+ is determined by the product of the mobility ratio of these species in the electrode membrane and the ion-exchange equilibrium constant for their exchange reaction at the membrane solution interface[17]. Thus it must be borne in mind that the selectivity coefficient, K_{AB}, is not a constant but depends on a particular set of experimental conditions, *i.e.* on such factors as the ratio of the primary to secondary ion in solution and on the ionic strength.

Moody and Thomas[18] have pointed out that the determination of selectivity coefficients by the separate solution method produces values which are not typical of operating systems, and determinations in mixed electrolyte solutions are of more practical value; thus K_{AB} values should be determined under solution conditions as close as possible to that of the sample and this is particularly true if K_{AB} is to be used for calibration purposes. The potential–pH curve is still used by some workers as a means of determining reciprocal selectivity coefficients *i.e.* K_{H-Na} values, but our investigations have shown that factors such as incomplete curves and poor functioning of the sodium ion electrode in the highly acidic solutions required produces poor results; apart from this, sodium ion electrodes are seldom used in such highly acidic solutions and the recommended procedure is to fix the interferent concentration and vary the acitivity of the primary ion.

No previous work seems to have been done in determining K_{Na-H} values by the mixed solution method given here. The interferent hydrogen ion activity was fixed with a series of tris buffers, and hence K_{Na-H} values were determined in mixed solutions—the large tris cation ($\overset{+}{N}H_3C(CH_2OH)_3$) exerting minimal interference. There are obvious advantages in using a buffered background level particularly in solutions where the interfering ion activity is very low, and this technique goes some way towards reproducing the conditions of the sample in the critical pH range. The method also proved useful in comparing the selectivity of different electrodes; by using a series of buffers, it was possible to investigate the variation of electrode selectivity with the ratio of the primary and secondary ion.

The methods of calculating selectivity coefficients have been dealt with by several workers[19, 20]. An additional method—a least squares curve fitting procedure—was also used here. The methods may be summarized as:

1. The method of breaking-point (method II A of Moody and Thomas[20])
2. Rechnitz method III[19]
3. Least-squares curve fitting

In applying the method of least squares, the parameters E^0_{ISE} and K_{Na-H} in eqn. (5) were determined by curve fitting, thus method 3 offers the advantage that the best fit to the experimental results is obtained.

Selectivity coefficients were determined by the experimental technique outlined above. Sodium ion activities in 0.1 *M* buffer solutions were determined from concentrations, based on a value of the activity coefficient calculated from Davies Equation[21] for an electrolyte in water at 25 °C:

$$-\log f = 0.511\, z^2 \left(\frac{(I)^{\frac{1}{2}}}{1+(I)^{\frac{1}{2}}} - 0.20\, I \right) \qquad (6)$$

The activity of the hydrogen ion was calculated in each case from the measured pH

TABLE IV

SELECTIVITY COEFFICIENTS OF SODIUM ION-SELECTIVE GLASS ELECTRODES K_{Na-H} MEASURED IN TRIS ACETATE BUFFER

(pH 4.60, $I=0.1$, temperature 25 °C.)

Electrode	*Method 1*		*Method 2*	*Electrode*	*Method 2*		*Method 3*
Beckman	1	118	124	EIL	4	5.29	6.61
39278	2	144	162	GEA 33C	5	8.10	8.46
	3	101	110		6	10.1	10.9
Orion	7	41.8	44.2	Radiometer	10	2.82	3.51
94-11	8	47.3	47.9	G502 Na	11	3.21	3.64
	9	47.4	45.4		12	3.09	4.06

and determinations were carried out for each of the buffer systems.

For the acetate system, the calculated selectivity coefficients for all the electrodes are presented in Table IV. Figure 3(a) shows e.m.f. *vs.* sodium ion activity plots for the different electrodes in the sodium ion activity range 10^{-5}–10^{-2} *M* (for this diagram an electrode representative of each group was chosen). The results show that the selectivity of the electrodes varies greatly from group to group and in all cases they are more selective to hydrogen ion. Furthermore, they may be divided into two groups, those that suffer high interference at this pH (4.60) (*i.e.* Beckman and Orion electrodes) and those suffering low interference (EIL and Radiometer electrodes). In calculating selectivity coefficients it was found that in those cases where interference was high, the least-squares method could not be applied since E^0_{ISE} was not constant over the complete range of sodium ion activity, and methods 1 and 2 were used, the value of E^0_{ISE} being taken from the Nernstian part of the curve.

The values determined in maleate buffer (pH 5.20) are given in Table V, and the e.m.f. *vs.* sodium ion activity plots are presented in Fig. 3(b). It is interesting to note, that at this pH, Beckman electrodes give a better relative selectivity and are on a par with Orion electrodes. The behaviour of Beckman electrodes may be understood more clearly by considering the potential–pH diagrams in Fig. 2 —in the pH range 4.5–6.5, the position of the Beckman electrode curve changes sharply in relation to the other electrodes as the sodium ion concentration is decreased.

In bis-tris buffer at pH 6.52 (Table VI), the Beckman electrodes have improved even more relative to Orion; Fig. 3(c) confirms this. At this pH Radiometer and EIL electrodes suffered such low interference that it was not possible to determine selectivity coefficients with any accuracy.

Over the range of pH investigated in this work, it is clear that, in general, selectivity coefficients are not constant but increase with increase in the sodium ion to hydrogen ion ratio (the exception being for Beckman electrodes) *i.e.* the selectivity coefficient is dependent on the solution pH as well as other factors. This fact was illustrated well by Buck *et al.*[22], who first determined the K_{H-Na} value of the Beckman 39278 electrode in solutions of fixed sodium ion concentration and variable pH. These workers quote a value for K_{Na-H} of $4 \cdot 10^3$ (obtained

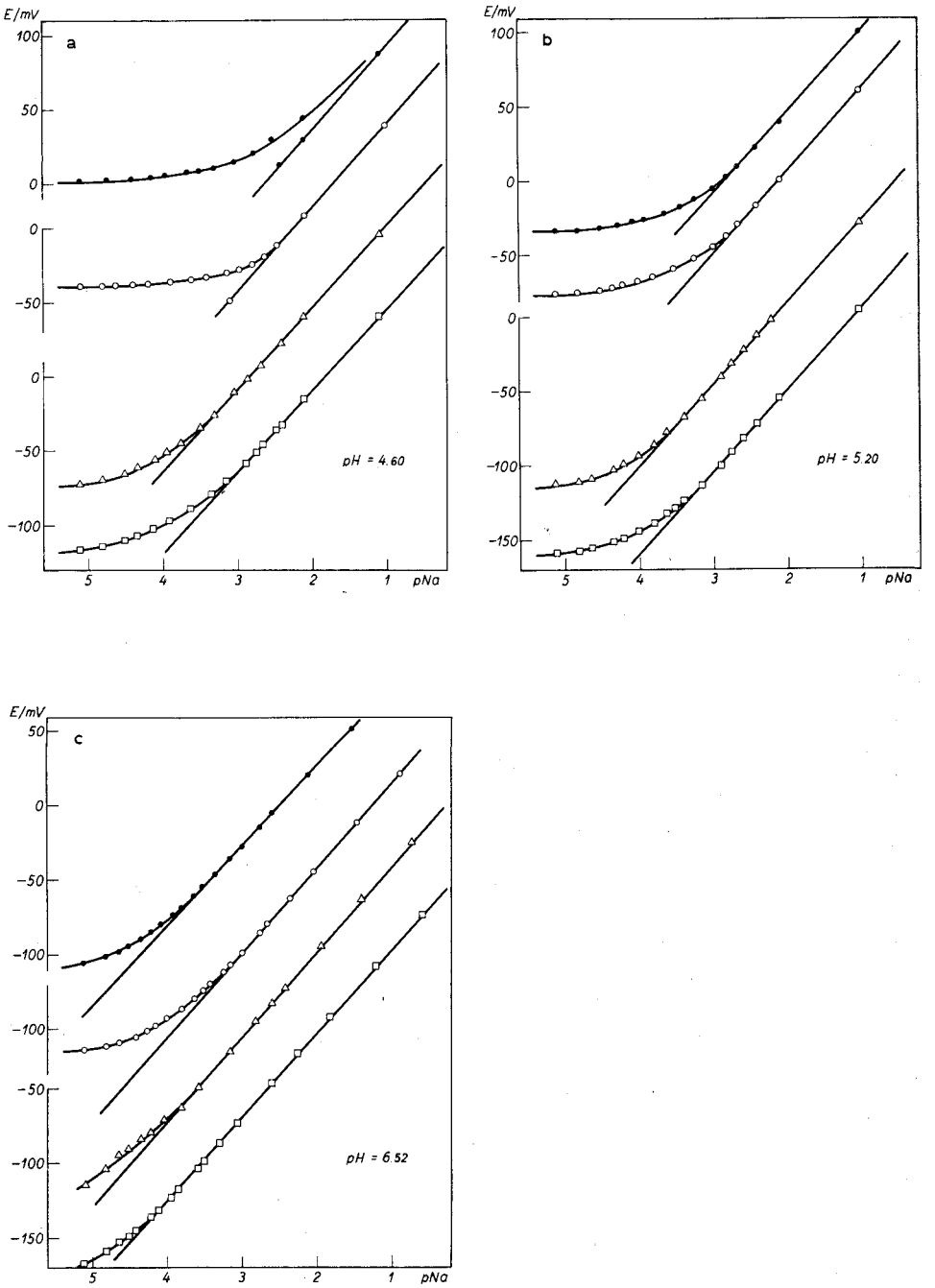

Fig. 3. Influence of hydrogen ion on the potential response of sodium ion-selective electrodes. $I=0.10$ M; temperature 25 °C. (●), Beckman 39278 electrode; (□), EIL GEA 33C electrode; (○), Orion 94-11 electrode; (△), Radiometer G502 Na electrode. (a) In acetic acid/tris buffer, pH = 4.60. (b) In tris maleate buffer, pH = 5.20. (c) In bis-tris buffer, pH = 6.52.

TABLE V

SELECTIVITY COEFFICIENTS OF SODIUM ION-SELECTIVE GLASS ELECTRODES K_{Na-H} MEASURED IN TRIS MALEATE BUFFER

(pH 5.20, $I=0.1$, temperature 25 °C.)

Electrode		*Method 2*	*Method 3*
Beckman	1	63.0	63.6
39278	2	59.1	61.5
	3	61.8	66.3
Orion	7	68.1	71.4
94-11	8	59.7	59.5
	9	62.0	60.1
EIL	4	27.3	21.7
GEA 33C	5	27.7	21.7
	6	34.0	24.6
Radiometer	10	10.6	9.98
G502 Na	11	10.3	9.79
	12	11.1	10.4

TABLE VI

SELECTIVITY COEFFICIENTS OF SODIUM ION-SELECTIVE GLASS ELECTRODES K_{Na-H} MEASURED IN BIS-TRIS BUFFER

(pH 6.52, $I=0.1$ *M*, temperature 25 °C.)

Electrode		*Method 2*	*Method 3*
Beckman	1	188	210
39278	2	153	156
	3	112	125
Orion	7	236	224
94-11	8	244	244
	9	233	242

by taking the reciprocal of the K_{H-Na} value) and this result is compared with the value of 36 given by the manufacturer[23]. Since the value of Buck *et al.* was also determined by means of a different equation from that of Eisenman[16], in our opinion it seems that both these values are possible and again it must be emphasized that the conditions of the determination be reported.

Table VII presents data taken from the literature for previous determinations of selectivity coefficients by separate solutions or by unspecified methods. Where necessary, K_{Na-H} values were estimated by taking the reciprocal of K_{H-Na}. The confusion in specifying the selectivity of sodium ion-selective electrodes is illustrated; thus, for example, three different values of the coefficients for the NAS 11-18 glass are found, all under unspecified conditions.

TABLE VII

LITERATURE VALUES OF SELECTIVITY COEFFICIENTS OF SODIUM ION-SELECTIVE ELECTRODES UNDER VARIOUS CONDITIONS

Electrode or glass type	*Conditions and method*	K_{H-Na}	K_{Na-H}[a]	*Reference*
Beckman 39278	Separate solutions 0.1 *M* NaCl/HCl, 25°C	0.034	29	4
Beckman 39278	Unspecified	0.028	36	22
Beckman 39278	Acid–base titration method with constant sodium ion activity, 25 °C	$2.5 \cdot 10^{-4}$	$4 \cdot 10^{3}$	23
Beckman 39137	Separate solutions 0.1 *M* NaCl/HCl, 25 °C	0.241	4.15	4
EIL GEA 33C	As above	0.546	1.83	4
NAS 11-18	Unspecified		≈ 10	5
NAS 11-18	Unspecified	0.06	17	14
NAS 11-18	Unspecified		30	24
Orion 94-11	Unspecified		≈ 100	25

[a] Where necessary K_{Na-H} values were calculated by taking $1/K_{H-Na}$

Calibration of electrodes for use at low pH

Light[24], in his work on industrial applications of ion-selective electrodes, has pointed out that, if sodium ion activities must be measured in acidic solution, then by measuring the pH with an additional glass electrode, the corrected sodium ion activity may be calculated from eqn. (5), provided that a reliable value of K_{Na-H} for the glass electrode is known. (It may be stated that the variation of K_{Na-H} with pH poses an additional problem—but a correction nomograph similar to that used to correct the sodium ion error of pH glass electrodes used in alkaline solution, may be envisaged.) Pommer[26], in his work on the measurement of sodium ion activity in acidic soil waters and pastes, has expressed a similar need for sodium ion measurement in these cases where it is impossible to suppress the hydrogen ion activity. Similarly, in biological work, *in vivo* and *in vitro* measurements may be required at low pH.

TABLE VIII

REPRODUCIBILITY OF K_{Na-H} VALUES.

(Determined for Radiometer G502 Na and EIL GEA 33C Sodium ion-selective electrodes in tris acetate buffer. Temperature 25 °C; pH 4.60, $I = 0.1$ *M*.)

	Radiometer G502 Na (Electrode 10)		*EIL GEA 33C (Electrode 4)*	
	2.86[a]	3.73[b]	5.50[a]	7.12[b]
	2.85[a]	3.44[b]	5.08[a]	5.76[b]
	2.74[a]	3.37[b]	5.28[a]	6.96[b]
Mean	2.82 ± 0.04[c]	3.51 ± 0.12[c]	5.29 ± 0.14[c]	6.61 ± 0.44[c]

[a] Method 2. [b] Method 3. [c] Standard deviation.

Table VIII shows the reproducibility of K_{Na-H} values determined for individual Radiometer and EIL electrodes in tris acetate buffer solution together with their standard deviations. The results indicate that by careful determination, the electrodes with low selectivity coefficients may be calibrated and used in acidic solutions.

Composition of the electrode membrane glasses

Eisenman *et al.*[1,16] were the first to demonstrate that the selectivity of electrode glass membranes is dependent in a systematic way on the glass composition. In particular, they showed that variations within the sodium aluminosilicate (Na_2O–Al_2O_3–SiO_2) glass system resulted in a wide range of selectivities for different cations.

Rechnitz[27] classified different glass types in terms of their selectivity characteristics and for sodium ion measurement two notable types were included:

A. 11% Na_2O–18% Al_2O_3–71% SiO_2. This composition is known generally as NAS 11-18; the figures specify the molecular percentages of Na_2O and Al_2O_3 in the glass.

B. 10.4% Li_2O–22.6% Al_2O_3–67% SiO_2. This glass is reported to be very selective towards sodium ions but is also reputed to show a large drift in e.m.f. readings[27].

In considering the composition of the glass membranes of electrodes investigated in this work, some information is available: EIL GEA 33C electrodes contain the glass type BH 104 which is a Li_2O–Al_2O_3–SiO_2 in which the ratio of aluminium to lithium oxides is not less than 1:3 [ref. 28]. The Orion 94-11 electrodes utilize the conventional NAS 11-18 glass (see above), the main difference being that plane-glass membranes are used. Radiometer G502 Na electrodes incorporate Jena Glass type 8245 (Jena Glaswerk, Scott und Gen., Mainz) but no information regarding this or the composition of the membrane glass of Beckman 39278 electrodes is available at the time of writing.

Comparison of at least two of the glasses, *i.e.* the NAS 11-18 and BH 104 types, indicates that the Li_2O-based glass does indeed have a lower selectivity coefficient with respect to hydrogen ions throughout the pH range studied; the BH 104 glass was also found to give stable e.m.f. readings.

The authors wish to thank Beckman Instruments Inc., Electronic Instruments Ltd., Radiometer A/S and Orion Research Inc. for providing the sodium ion-selective electrodes. We also wish to thank the Finnish Ministry of Education for a Grant.

SUMMARY

Some properties of a series of commercial sodium ion-selective electrodes have been investigated and the results compared. In general the potential response of the electrodes was found to approach Nernstian with aging.

An improved method for investigating the selectivity of ion-selective electrodes with respect to hydrogen ions is based on the mixed solution method utilizing tris buffers. The selectivity of the sodium ion electrodes with respect to hydrogen ions was also found to depend on the ratio of the primary to interfering ion activity. Some other improvements in technique are also reported.

REFERENCES

1 G. Eisenman, (Ed.), *Glass Electrodes for Hydrogen and Other Cations: Principles and Practice*, Marcel Dekker, New York, 1967.
2 G. Mattock, *Chimia*, 21 (1967) 209.
3 G. Mattock, *Analyst*, 87 (1962) 930.
4 S. Phang and B. J. Steel, *Anal. Chem.*, 44 (1972) 2230.
5 R. N. Khuri, in R. A. Durst (Ed.), *Ion-selective Electrodes*. N.B.S. Special Publication No. 314, U.S. Government Printing Office, Washington D.C., 1969, p. 287.
6 G. Johansson and K. Edström, *Talanta*, 19 (1972) 1623.
7 E. L. Eckfeldt and W. E. Proctor, *Anal. Chem.*, 43 (1971) 332.
8 D. Hawthorn and N. J. Ray, *Analyst*, 93 (1968) 158.
9 H. M. Webber and A. L. Wilson, *Analyst*, 94 (1969) 209.
10 L. G. Sillén and A. E. Martell, *Stability Constants of Metal-Ion Complexes*, Chem. Soc. Special Publications No. 17, London, 1964.
11 E. H. Hansen, C. G. Lamm and J. Růžička, *Anal. Chim. Acta*, 59 (1972) 403.
12 A. I. Vogel, *A Textbook of Quantitative Inorganic Analysis*, Longmans, London, 1961.
13 G. Eisenman, in C. N. Reilley (Ed.), *Advances in Analytical Chemistry and Instrumentation*, Vol. 4, Wiley–Interscience, New York, 1965.
14 E. W. Moore, in G. Eisenman (Ed.), *Glass Electrodes for Hydrogen and Other Cations: Principles and Practice*, Marcel Dekker, New York, 1967, p. 412.
15 H. Yoshimura, *Bull. Chem. Soc. Japan*, 12 (1937) 443.
16 G. Eisenman, D. O. Rudin and J. U. Casby, *Science*, 126 (1957) 831.
17 F. Conti and G. Eisenman, *Biophys. J.*, 5 (1965) 247.
18 G. J. Moody and J. D. R. Thomas, *Talanta*, 19 (1972) 623.
19 K. Srinivasan and G. A. Rechnitz, *Anal. Chem.*, 41 (1969) 1203.
20 G. J. Moody and J. D. R. Thomas, *Selective Ion Sensitive Electrodes*, Merrow, Watford, England, 1971.
21 C. W. Davies, *J. Chem. Soc.*, 2093 (1938).
22 R. P. Buck, J. H. Boles, R. D. Porter and J. A. Margolis, *Anal. Chem.*, 46 (1974) 255.
23 Beckman Instruments Inc., *Sodium-ion Electrode 39278*, Bulletin 7145, Fullerton, California 92634.
24 T. S. Light, in R. A. Durst, (Ed.), *Ion-selective Electrodes*, N.B.S. Special Publication No. 314, U.S. Government Printing Office, Washington D.C., 1969, p. 349.
25 *Orion Research Incorporated Newsletter*, 10 (1971) 111 (1, 2).
26 A. M. Pommer, in G. Eisenman (Ed.), *Glass Electrodes for Hydrogen and Other Cations: Principles and Practice*, Marcel Dekker, New York, 1967, p. 362.
27 G. A. Rechnitz, *Chem. Eng. News*, 45 (1967) 146.
28 Electronic Instruments Limited, Chertsey, Surrey, England, Private communication.

Analytica Chimica Acta, 74 (1975) 411–421

AN EVALUATION OF SOME SODIUM ION-SELECTIVE GLASS ELECTRODES IN AQUEOUS SOLUTION

PART II. ELECTRODE SELECTIVITY WITH RESPECT TO POTASSIUM, SILVER AND AMMONIUM IONS—MEASUREMENT AND COMPARISON OF RESPONSE TIMES

MICHAEL F. WILSON, ESA HAIKALA and PEKKA KIVALO
Chemical Laboratory, Technical Research Centre of Finland, 02150 Otaniemi (Finland)
(Received 2nd August 1974)

Part I[1] of this investigation was concerned with the calibration characteristics and hydrogen ion interference of different commercially available sodium ion-selective electrodes; their performance with respect to these factors was compared. The techniques involved in the measurement of sodium ions in solution by means of sodium ion-sensors were also investigated and some improvements introduced.

This section of the work is concerned with the interference of other common monovalent cations; for use in different ionic environments—apart from hydrogen ion interference, which must always be considered—interferences from a third ionic component may be significant. This is particularly true for potassium ion in biological work where, in certain cases, the concentration of the latter may greatly exceed that of sodium[2].

Silver ion interference is high even at low concentrations, a factor which requires attention if silver–silver chloride reference electrodes are used in cells without liquid junction. The interference of ammonium ions must also be assessed if ammonia is used as a buffer in sodium ion samples of very low concentration[3].

The response time of sodium ion-sensors is an important factor to be considered in practice. The effect of temperature change on the response time may also be significant for certain sodium ion glass electrodes and this has also been investigated.

EXPERIMENTAL

Electrodes and instrumentation

The instrumentation and the same total number and series of electrodes were used as in Part I. (Before the determinations reported here, the electrodes were in use for about 12 weeks which covered the first part of the investigation).

The method of preparation of the electrodes for testing was as reported previously[1] and their designation was as follows:

Electrode type	Beckman 39278	EIL GEA 33 C	Orion 94-11	Radiometer G502 Na
Electrode number	1, 2, 3	4, 5, 6	7, 8, 9	10, 11, 12

Orion Double Junction Reference Electrodes type 90-02-00 with internal filling solution 90-00-02 were also used to make up the cell assembly.

Electrode assemblies

The precautions required in choosing a suitable electrochemical cell assembly for work with sodium ion-selective electrodes have been discussed previously[1]. For general use of the electrodes, rubidium chloride was favoured as the most reliable salt bridge electrolyte and the need to exclude silver ions (present in the reference electrode internal filling solution) from the test solution is apparent from the silver ion interference studies reported below.

For the determination of selectivity coefficients, two different electrode assemblies were used. For the study of potassium ion interference, the following cell (1) was used:

$$\mathrm{Ag}\,\big|\,\mathrm{AgCl(s)},\ 0.70\,M\,\mathrm{KCl},\ 1.50\,M\,\mathrm{KNO_3}\,\big\|\,2\,M\,\mathrm{RbCl}\,\big\|\begin{matrix}\mathrm{Na^+\ sample}\\ 0.1\,M\,\mathrm{KCl}\\ \text{or}\\ 0.5\,M\,\mathrm{KCl}\end{matrix}\,\big|\,\text{glass electrode}\quad(1)$$

For the determination of selectivity coefficients with respect to silver ion, cell (2) was utilized, the salt bridge and test solution being necessarily chloride-free:

$$\mathrm{Ag}\,\big|\,\mathrm{AgCl(s)},\ 0.70\ M\ \mathrm{KCl},\ 1.50\ M\ \mathrm{KNO_3}$$

$$\big\|\begin{matrix}\text{Satd.}\\ \mathrm{NH_4NO_3}\end{matrix}\big\|\begin{matrix}\mathrm{Na^+\ sample}\\ 10^{-6}\ M\ \mathrm{AgNO_3}\\ I=0.1\,(\mathrm{Ca(NO_3)_2})\end{matrix}\big|\,\text{glass electrode}\qquad(2)$$

In the latter case the ionic strength of the test solutions was adjusted to 0.1 with calcium nitrate, the calcium ion being safely assumed to have a negligible effect on the electrode potential of the sodium glass electrode compared to that of sodium and silver ions[4]. The investigation of the ammonium ion interference (see below) showed that its interference is sufficiently small that leakage of ammonium nitrate from the salt bridge during measurements with silver solutions had an insignificant effect. It may also be stated that in this connection no transient effects were observed.

For the determination of selectivity coefficients with respect to ammonium ions, cell (1) was also used, with 1 *M* ammonium chloride replacing the potassium chloride interferent in the sample solution.

For the measurement of response times, the electrode assembly used was similar to cell (1), the test solution consisting of sodium ion concentrations made up in ethanolammonium buffer to a pH of 9.54 and ionic strength of 0.1 at 25°C.

Experimental procedure

Selectivity coefficients with respect to K^+, Ag^+ and NH_4^+ ions were determined by the mixed solution method with an addition technique. In all cases the electrodes were allowed to stand overnight in the initial cell solution which consisted of 10^{-5} *M* sodium chloride (or nitrate in the case of the silver ion interference determinations) made up with the appropriate interfering ion concentration level

and any required buffer and ionic strength adjuster. A solution 10^{-2} *M* in sodium ion concentration and containing the same background composition was added in increments to the cell by means of a burette and readings of volume and e.m.f. were recorded.

In the case of the potassium ion interference studies, initially all electrodes were investigated at the 0.10 *M* potassium chloride level; subsequently, the Radiometer G 502 Na and EIL GEA 33 C electrodes were found to suffer low interference at this level, and selectivity coefficients for these electrodes were also determined in 0.50 *M* potassium chloride background concentrations.

Selectivity coefficients with respect to silver ions were determined with 10^{-6} *M* silver nitrate; the ionic strength was adjusted to 0.10 with calcium nitrate.

For the potassium and silver ion interference studies, the pH of all solutions was checked and in all cases found to be greater than 8, the deionized water from the ion-exchange column being slightly alkaline. Hence there was no possibility of hydrogen ion interference in these solutions, and the pH level was also sufficiently low to exclude any possibility of silver ion hydrolysis.

Ammonium ion selectivity coefficients were determined in a background of 1 *M* ammonium chloride; it was then necessary to suppress the dissociation of the NH_4^+ ion, but also to maintain a high enough pH in order to avoid hydrogen ion interference. Part I[1] showed that, for the electrodes tested, the interference of hydrogen ion in sodium ion concentrations of 10^{-4} *M* was only detectable below pH 7.0 at 25°C. For this reason the sodium ion test solutions containing the ammonium chloride interferent were buffered with a small amount of tris base/HCl buffer to give a solution pH of 7.60. The temperature for these studies was also lowered to 20°C. Under these conditions, it was calculated that any dissociation of NH_4^+ would be negligible.

The dynamic response times of the electrodes were determined by exposing them to rapid changes in sodium ion concentration and recording the change in e.m.f. with time (chart recorder). The concentration changes were effected by injection with a syringe, and mixing was achieved by rapid mechanical stirring. (This method was considered suitable for sodium ion glass electrodes since these sensors are amenable to slower measurement techniques than other electrode systems where more sophisticated methods are required for effecting very rapid concentration changes[5].)

Electrodes were allowed to equilibrate overnight in the initial test solution, which in all cases consisted of 10^{-4} *M* sodium chloride made up to an ionic strength of 0.10 *M* with ethanolammonium buffer and at a pH of 9.54. Measurements were made at 25°C for two-fold (10^{-4} *M* → $2 \cdot 10^{-4}$ *M*), ten-fold (10^{-4} *M* → 10^{-3} *M*) and 100-fold (10^{-4} *M* → 10^{-2} *M*) concentration changes. The response times for a ten-fold change at 10°C were also determined. The changes in e.m.f. produced were recorded by means of a Keithley Instruments 630 electrometer coupled with a Honeywell Electronik 19 recorder. The response time of the instruments and mixing time were assumed constant and in all cases the resulting e.m.f. *vs.* time curves were smooth after the initial mixing. The response time was defined as the time required to obtain a 95% response for all the step-changes made.

Reagents

Sodium chloride and potassium chloride were Suprapur grade (Merck). Sodium nitrate, silver nitrate, calcium nitrate, ammonium chloride and rubidium chloride were *pro analysi* (Merck). Ethanolamine (Fluka) was purified as in Part I. Tris buffer was obtained from the Sigma Chemical Company, U.S.A. and hydrochloric acid solutions were made up from Titrisol ampoules.

RESULTS AND DISCUSSION

Selectivity coefficients with respect to potassium, silver and ammonium ions

The full equation of Eisenman *et al.*[6] for the e.m.f., E, of an appropriate electrode assembly in an aqueous solution containing two univalent cations, A^+ and B^+, was given in Part I (eqn. 4)[1]. For most univalent cation mixtures at fixed[6] pH, this equation reduces to the simpler expression of Nicolsky *et al.*[7] which may be derived from simple ion-exchange considerations:

$$E = E^0_{ISE} + S \log [a_{Na^+} + K_{Na-X} a_{X^+}] \quad (3)$$

where K_{Na-X} represents the selectivity coefficient of the electrode in $Na^+ - X^+$ univalent ion mixtures in aqueous solution, and a_{X^+} is the activity of the interfering ion X^+. The constant E^0_{ISE} incorporates the constant reference electrode potentials and the liquid junction potentials in the system which are also assumed to be constant. If the response of the glass electrode is Nernstian under these conditions, the constant S will take the value 59.2 mV/decade at 25°C. Part I showed that most sodium ion-selective electrodes give a value of S of 55–56 mV/decade and the electrode response approaches Nernstian with aging.

The need for determining the selectivity coefficients of ion-selective electrodes by the mixed solution method has been discussed in Part I; the recommended procedure is to fix the interfering ion concentration and vary the activity of the primary ion[8]. It is also important to make determinations under realistic conditions, *i.e.* under solution conditions as close as possible to that of the sample. This, however, is not always possible if K_{AB} values are very small; in this work, for example, in investigating the ammonium ion interference, a background level of 1 M ammonium chloride was necessary. The results obtained in this case may still be considered to be a useful guide, and the performance of different electrode types may at least be compared.

The methods used here for the calculation of selectivity coefficients are the same as used previously[1]; they are designated in the text as methods 1, 2 and 3 and are the method of breaking-point[1], method III of Rechnitz[9] and a least-squares, curve-fitting method, respectively[1]. In applying the latter method, the parameters E^0_{ISE} and K_{Na-X} in eqn. (3) were determined by curve fitting.

For the determination of selectivity coefficients with respect to K^+ ion, the mean ionic activity coefficients of NaCl ($\gamma\pm$) in the presence of the second interfering 1:1 electrolyte were determined by means of Harned's Rule[10]. For a series of binary mixed electrolytes in aqueous solutions having a constant total ionic strength, Harned's Rule may be stated as:

$$\log \gamma_{12} = \log \gamma_{10} - \alpha_{12} x_2 I \quad (4)$$

where, for the present example, γ_{12} is the mean ionic activity coefficient of NaCl in the mixture, γ_{10} is the mean ionic activity coefficient in pure NaCl of the same ionic strength, α_{12} is the Harned's Rule coefficient (usually obtained from isopiestic data), I is the total ionic strength and x_2 the mole fraction of the second (interfering) 1:1 electrolyte. For the determination of selectivity coefficients with respect to K^+ ion in this work, the sodium ion concentration in the 1:1 binary electrolyte mixtures varied in the concentration range 10^{-5}–$10^{-2.5}$, hence to a very good approximation it was possible to take x_2 as unity and assume I constant for 0.1 M and 0.5 M background interferent levels.

For work in a background interferent level of 0.1 M KCl, α_{12} was estimated from the results of Robinson[11] to be 0.030, and for work in 0.50 M KCl the value was 0.025.

The estimation of mean ionic activity coefficients in NaCl–KCl mixtures has also been dealt with by Moore[2], who devised a simple empirical method of calculation for mixtures in the lower concentration range. Moore's method was also used in this work for calculation of the $\gamma\pm$ value for NaCl–KCl mixtures at ionic strength 0.10 M, and the results were found to be in good agreement with that calculated by Harned's Rule.

For the investigation of silver ion interference, the ionic strength of the solution was fixed at 0.10 M with calcium nitrate as a swamping background electrolyte; the mean ionic activity coefficient of the medium was calculated by means of the Davies Equation[12] (see eqn. 6, Part, I) for an electrolyte in water at 25°C.

In the case of the determinations of the selectivity coefficients in 1 M ammonium chloride, the mean ionic activity coefficient of the medium was assumed constant throughout and the value was obtained from Robinson and Stokes[13].

Table I presents values of the selectivity coefficients for the sodium ion-selective glass electrodes with respect to potassium ions determined in a background interferent concentration of 0.10 M potassium chloride. The trend in selectivity for different electrode types is the same as that found for hydrogen ion interference at a pH of 4.60 (see Table IV, Part I). Figure 1 shows plots of e.m.f. *vs.* sodium ion activity, and the interference of the different electrodes may be compared.

Moore[2] has stated that the NAS 11-18 glass (used in Orion electrodes) gives a value of K_{Na-K} in the range from about 10^{-2} to $4 \cdot 10^{-3}$, and the three Orion electrodes investigated are in good agreement with this.

Table I also shows values for the EIL and Radiometer electrodes determined in a background interferent concentration of 0.50 M potassium chloride solution. By comparing the results at the different background concentrations, it can be seen that the value of K_{Na-K} decreases with increasing background interferent level. This observation coincides with the fall in values of K_{Na-H} with pH given in Part I.

The results for silver ion interference are presented in Table II. Again the trend is the same for all the electrodes, the Radiometer giving the lowest values of about 100. The silver response of some sodium–aluminium–silicate glass electrodes has been investigated by Covington and Lilley[14]. Electrodes which respond to sodium ions usually have a large silver ion error, which is attributed to the similarity of the ionic radii of these species. Covington and Lilley determined no selectivity coefficients in their work, but the value given by Orion Research[15] of K_{Na-Ag} 350 is in good agreement with the values found for the Orion Electrodes here.

TABLE I

SELECTIVITY COEFFICIENTS OF SODIUM ION-SELECTIVE GLASS ELECTRODES FOR POTASSIUM IONS, K_{Na-K}

(Measured in 0.1 *M* or 0.5 *M* KCl; temperature 25°C. In all cases the solution pH exceeded 8.)

Electrode		*Method 1*	*Method 2*
		Measured in 0.1 M KCl	
Beckman	1	$2.05 \cdot 10^{-2}$	$1.95 \cdot 10^{-2}$
39278	2	$2.46 \cdot 10^{-2}$	$2.20 \cdot 10^{-2}$
	3	$1.89 \cdot 10^{-2}$	$1.78 \cdot 10^{-2}$
Orion	7	$1.30 \cdot 10^{-2}$	$1.28 \cdot 10^{-2}$
94-11	8	$6.96 \cdot 10^{-3}$	$6.98 \cdot 10^{-3}$
	9	$7.63 \cdot 10^{-3}$	$7.65 \cdot 10^{-3}$

Electrode		*Method 2*	*Method 3*	*Method 2*	*Method 3*
		Measured in 0.1 M KCl		*Measured in 0.5 M KCl*	
EIL	4	$9.71 \cdot 10^{-4}$	$8.38 \cdot 10^{-4}$	$2.45 \cdot 10^{-4}$	$2.84 \cdot 10^{-4}$
GEA 33 C	5	$9.75 \cdot 10^{-4}$	$9.54 \cdot 10^{-4}$	$2.38 \cdot 10^{-4}$	$2.44 \cdot 10^{-4}$
	6	$9.68 \cdot 10^{-4}$	$1.01 \cdot 10^{-3}$	$1.55 \cdot 10^{-4}$	$1.49 \cdot 10^{-4}$
Radiometer	10	$1.76 \cdot 10^{-4}$	$2.28 \cdot 10^{-4}$	$1.12 \cdot 10^{-4}$	$1.52 \cdot 10^{-4}$
G502 Na	11	$1.99 \cdot 10^{-4}$	$2.47 \cdot 10^{-4}$	$5.88 \cdot 10^{-5}$	$9.41 \cdot 10^{-5}$
	12	$3.03 \cdot 10^{-4}$	$4.73 \cdot 10^{-4}$	$1.01 \cdot 10^{-4}$	$1.20 \cdot 10^{-4}$

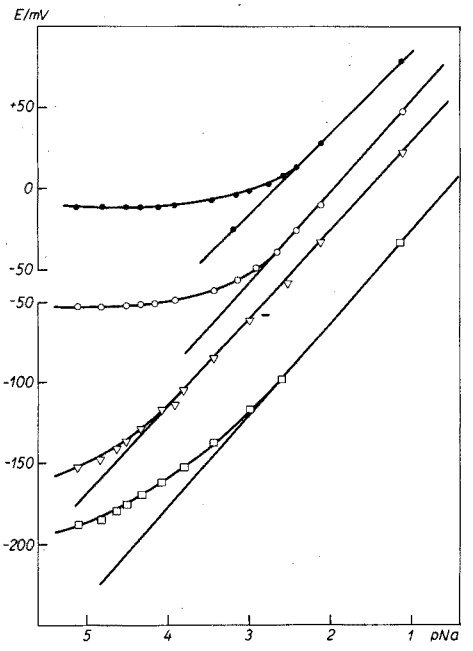

Fig. 1. Influence of potassium ion on the potential response of sodium ion-selective electrodes in 0.1 *M* potassium chloride, temperature 25°C. (●) Beckman 39278 electrodes, (□) EIL GEA 33C electrodes, (○) Orion 94-11 electrodes, (△) Radiometer G502 Na electrodes.

TABLE II

SELECTIVITY COEFFICIENTS OF SODIUM ION-SELECTIVE GLASS ELECTRODES FOR SILVER IONS, K_{Na-Ag}

(Measured in 10^{-6} *M* $AgNO_3$, $I=0.1$ with respect to $Ca(NO_3)_2$. Temperature 25°C. Solution pH 7.8.)

Electrode		*Method 2*	*Method 3*	*Electrode*		*Method 2*	*Method 3*
Beckman	1	—	389	EIL GEA	4	257	216
39278	2	386	352	33 C	5	242	213
	3	381	369		6	248	197
Orion	7	397	395	Radiometer	10	108	113
94-11	8	356	347	G502 Na	11	107	121
	9	434	394		12	69.4	86.8

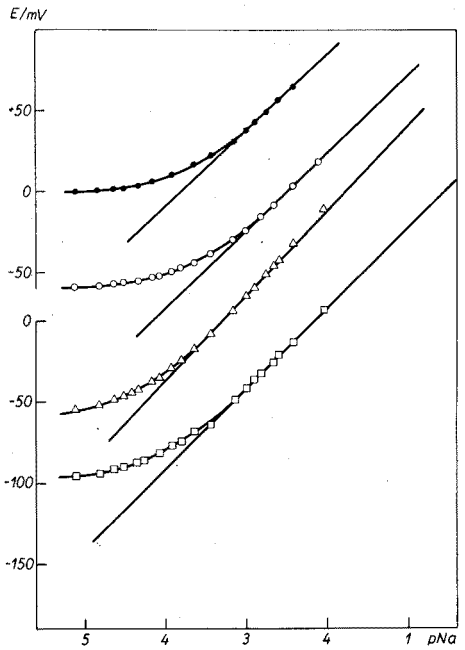

Fig. 2. Influence of silver ion on the potential response of sodium ion-selective electrodes. Silver concentration 10^{-6} *M*, ionic strength 0.1 *M* with respect to $Ca(NO_3)_2$, temperature 25°C. (●) Beckman 39278 electrodes, (□) EIL GEA 33C electrodes, (○) Orion 94-11 electrodes, (△) Radiometer G502 Na electrodes.

The interference by silver ion in solution is high, even for interfering concentrations as low as 10^{-6} *M*. This indicates the danger of interference in cells without liquid junction utilising silver–silver chloride electrodes. Figure 2 shows how the e.m.f. of the cell varies in the presence of 10^{-6} *M* Ag^+.

Results for interference studies with ammonium ion are presented in Table III; the interfering level of NH_4^+ ions seems excessively high, but such levels were required in order to measure effectively the K_{Na-NH_4} values. With the exception of the

TABLE III

SELECTIVITY COEFFICIENTS OF SODIUM ION-SELECTIVE GLASS ELECTRODES FOR AMMONIUM IONS, K_{Na-NH_4}

(Measured in 1 *M* NH_4Cl, pH 7.60. Temperature 20°C.)

Electrode		*Method 2*	*Method 3*	*Electrode*		*Method 2*	*Method 3*
Beckman	1	$1.29 \cdot 10^{-4}$	$1.30 \cdot 10^{-4}$	EIL	4	$3.35 \cdot 10^{-5}$	$4.25 \cdot 10^{-5}$
39278	2	$1.75 \cdot 10^{-4}$	$1.62 \cdot 10^{-4}$	GEA 33 C	5	$4.12 \cdot 10^{-5}$	$5.37 \cdot 10^{-5}$
	3	$1.60 \cdot 10^{-4}$	$1.56 \cdot 10^{-4}$		6	$4.62 \cdot 10^{-5}$	$5.81 \cdot 10^{-5}$
Orion	7	$6.86 \cdot 10^{-5}$	$6.85 \cdot 10^{-5}$	Radiometer	10	$2.91 \cdot 10^{-5}$	$3.47 \cdot 10^{-5}$
94-11	8	$4.87 \cdot 10^{-5}$	$5.40 \cdot 10^{-5}$	G502 Na	11	$3.25 \cdot 10^{-5}$	$3.53 \cdot 10^{-5}$
	9	$5.76 \cdot 10^{-5}$	$6.17 \cdot 10^{-5}$		12	$2.87 \cdot 10^{-5}$	$3.93 \cdot 10^{-5}$

Beckman 39278 electrodes—which gave an average K_{Na-NH_4} value of *ca.* $1.5 \cdot 10^{-4}$, the other electrodes all gave values within the range $3 \cdot 10^{-5}$–$7 \cdot 10^{-5}$. The results are a useful guide in comparing the behaviour of different electrodes; this type of medium is unlikely to be encountered in normal experimental work, and lower ammonium ion levels would be expected—judging by the performance of the electrodes in other media—to give higher K_{Na-NH_4} values as the background interferent concentration is lowered.

Electrode response times

A theoretical study of the time dependence of the electrode potential of cation-sensitive glass electrodes has been made by Rechnitz and Hameka[16] who devised a theoretical expression to describe the time course of potential changes. Previously, Wynne-Jones *et al.*[17] had studied the slow changes in "asymmetry" potentials arising from structural modifications of the hydrated glass layer as a function of time. The time taken for glass electrodes to attain steady values is often very long. Savage and Isard[18] have suggested that the slow response is associated with changes in the glass membrane hydration. The importance of studying the response times of sodium-sensitive glass electrodes becomes apparent when one considers their use in monitoring sodium ion levels[3].

Table IV compares the dynamic response of the electrodes tested by subjecting them to two-fold, ten-fold and one hundred-fold changes in sodium ion concentration at 25°C. The response times were calculated from the recorder traces; 95% of the steady value was taken for the response of all the electrodes. In this respect, the results are comparable, since it may be assumed that the response time of the instruments and time of mixing were constant. These results indicate that, in general, the electrode response is faster the greater the concentration change, the final concentration being attained more quickly the higher it is set. (It may be noted that all response times were obtained in going from lower to higher sodium ion levels; no dilution tests were performed). The results also show that the Beckman 39278 and EIL GEA 33 C electrodes have a faster response than the Radiometer G502. Na electrodes, which were slowest. Hence, although the Beckman 39278 electrode shows poor selectivity compared to that of the Radiometer G502 Na electrode, the former has the advantage of an appreciably faster response. Figure 3

compares the average response curves obtained for the different electrode types.

Table V compares the effect of temperature on the electrode dynamic response time; in all cases the lowering of the temperature has a significant effect.

TABLE IV

ELECTRODE RESPONSE TIMES FOR SODIUM ION-SELECTIVE GLASS ELECTRODES IN ETHANOL–AMMONIUM BUFFER

(pH 9.54, $I = 0.1$. Temperature 25°C. Response times are for 95% of the steady value and are quoted in s.)

Electrode		*Concn. change*		
		10^{-4} $M \rightarrow 2 \cdot 10^{-4}$ M	10^{-4} $M \rightarrow 10^{-3}$ M	10^{-4} $M \rightarrow 10^{-2}M$
Beckman	1	13.5	16	6
39278	2	13	14	5
	3	9	13	6
EIL GEA	4	20	12	7
33 C	5	23	9.5	7
	6	15	7.5	6
Orion	7	25	30	14
94-11	8	39	33	17
	9	18	27	12.5
Raadiometer	10	60.5	46.5	19.5
G502 Na	11	66	41.5	24
	12	82	58	44

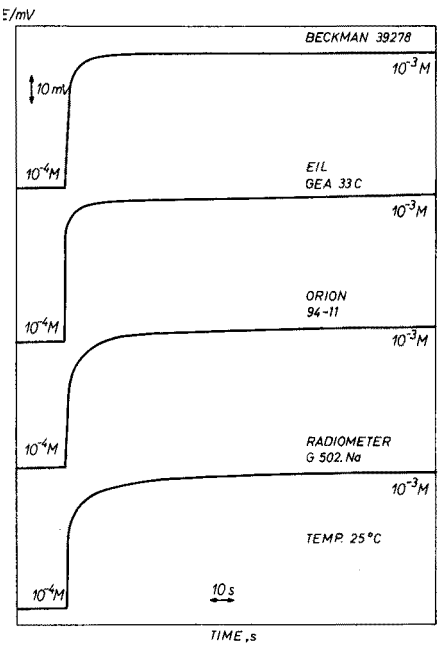

Fig. 3. Dynamic response behaviour of sodium ion-selective electrodes, temperature 25°C.

At 10°C, the resistance of the glass membrane has probably increased significantly. Nevertheless, both Beckman 39278 and EIL GEA 33 C electrodes reach 95% of the steady value in *ca.* 1 min at this lower temperature. Radiometer electrodes are

TABLE V

EFFECT OF TEMPERATURE ON THE ELECTRODE RESPONSE TIMES OF SODIUM ION-SELECTIVE ELECTRODES

(The concentration change is for 10^{-4} $M \rightarrow 10^{-3}$ M NaCl in ethanol–ammonium buffer, pH 9.54, $I = 0.1$. Response times are for 95% of the steady value obtained and times are quoted in s.)

Temperature		*10°C*	*25°C*
Beckman	1	72	16
39278	2	53	14
	3	68	13
EIL GEA	4	84	12
33 C	5	63	10
	6	64	7.5
Orion	7	208	30
94-11	8	278	33
	9	249	27
Radiometer	10	284	46.5
G502 Na	11	275	41.5
	12	302	58

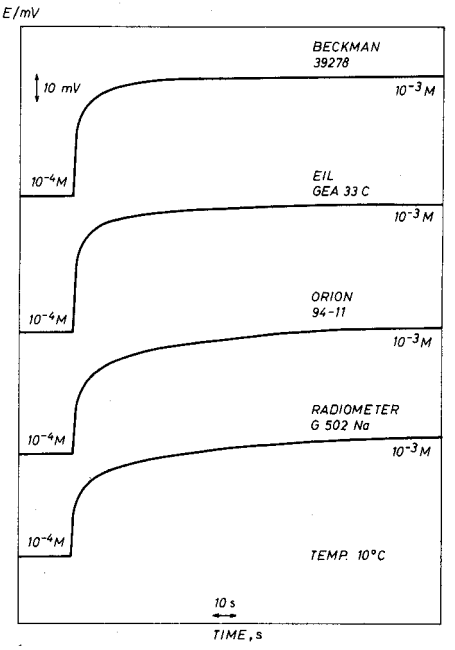

Fig. 4. Dynamic response behaviour of sodium ion-selective electrodes, temperature 10°C.

not suitable for monitoring at this temperature, and the limit in temperature set by the manufacturers[19] is 20°C. The comparison between electrodes at these temperatures may be seen in Fig. 4.

The authors wish to thank Beckman Instruments Inc., Electronic Instruments Ltd., Radiometer A/S and Orion Research Inc. for providing the sodium ion-selective electrodes. We also wish to thank the Finnish Ministry of Education for a grant.

SUMMARY

Selectivity coefficients for a series of commercial sodium ion-selective electrodes were determined with respect to potassium, silver and ammonium ions by means of the mixed solution method. In general, the order of the selectivity performance of the electrodes was the same for all the interferences tested. Response times were determined by the injection method, and the results for different electrodes are compared. The effect of temperature on the electrode response time was also investigated.

REFERENCES

1 M. F. Wilson, E. Haikala and P. Kivalo, *Anal. Chim. Acta*, 00 (1975) 000.
2 E. W. Moore, in G. Eisenman (Ed.), *Glass Electrodes for Hydrogen and Other Cations: Principles and Practice*, Marcel Dekker, New York, 1967, p. 412.
3 H. M. Webber and A. L. Wilson, *Analyst*, 94 (1969) 209.
4 *Orion Research Incorporated Newsletter*, 10 (1971) 111 (1, 2).
5 K. Tóth and E. Pungor, *Anal. Chim. Acta*, 64 (1973) 417.
6 G. Eisenman, D. O. Rudin and J. U. Casby, *Science*, 126 (1957) 831.
7 O. K. Stephanova, M. M. Schultz, E. A. Materova and B. P. Nicolsky, *Vestn. Leningrad Univ.*, 4 (1963) 93.
8 G. J. Moody and J. D. R. Thomas, *Talanta*, 19 (1972) 623.
9 K. Srinivasan and G. A. Rechnitz, *Anal. Chem.*, 41 (1969) 1203.
10 H. S. Harned and B. B. Owen, *The Physical Chemistry of Electrolytic Solutions*, 3rd edn., Reinhold, New York, 1958, Ch. 14, p. 585.
11 R. A. Robinson, *J. Phys. Chem.*, 65 (1961) 662.
12 C. W. Davies, *J. Chem. Soc.*, (1938) 2093.
13 R. A. Robinson and R. H. Stokes, *Electrolyte Solutions*, 2nd edn., Butterworths, London, 1959, p. 495.
14 A. K. Covington and T. H. Lilley, *Phys. Chem. Glasses*, 8 (1967) 88.
15 Orion Research Inc., *Analytical Methods Guide*, 6th ed., August 1973.
16 G. A. Rechnitz and H. F. Hameka, *Z. Anal. Chem.*, 214 (1965) 252.
17 W. H. Beck, J. Candle, A. K. Covington and W. F. K. Wynne-Jones, *Proc. Chem. Soc.*, April, (1963) 110.
18 J. A. Savage and J. O. Isard, *Phys. Chem. Glasses*, 7 (1966) 60.
19 *Instructions for Sodium Glass Electrode Type G502 Na*, Radiometer A9S, Copenhagen NV., Denmark.

Analytica Chimica Acta, 74 (1975) 423–435

MEASUREMENTS OF CARBON DIOXIDE WITH THE AIR-GAP ELECTRODE

DETERMINATION OF THE TOTAL INORGANIC AND THE TOTAL ORGANIC CARBON CONTENTS IN WATERS

ULLA FIEDLER

Department of Analytical Chemistry, Chemical Center, University of Lund, S-220 07 Lund 7 (Sweden)

ELO H. HANSEN and JAROMIR RŮŽIČKA

Chemistry Department A, The Technical University of Denmark, Building 207, DK-2800 Lyngby (Denmark)

(Received 10th July 1974)

The renewed interest in gas-sensing electrodes[1] is undoubtedly the most important recent development in the field of ion-selective electrodes. The high selectivity of these sensors, which is a result of the combined selectivities of the gas volatilization and of the actual sensing process, makes the electrodes valuable tools in analytical practice. The range of possible applications is far from being recognized yet, as it is not only the gas (NH_3, SO_2, H_2S, NO_2, etc.) which can be estimated, but also a number of species in solutions, or even in solid samples, which can be selectively and quantitatively converted to a gas to be sensed. For example, ammonia electrodes have been used for determinations of ammonia[2], urea[3] or amino acids in serum or blood, and for the determination of nitrate[4] or ammonium sulphate in airborne particulates[5].

The construction of the currently available[6,7] gas sensors is in principle identical with that of the original carbon dioxide sensor of Stow *et al.*[8], in which a glass pH-sensing electrode and a reference electrode are joined by a diluted solution of an electrolyte (sodium hydrogencarbonate). The gas to be sensed (carbon dioxide) diffuses through a thin, gas-permeable membrane and changes the pH in a film of electrolyte, until equilibrium has been established. The novelty of the most recent development is two-fold. First, a new gas-permeable membrane material has been developed[9], which, in addition to CO_2, also allows a fast diffusion of NH_3, SO_2, H_2S and other gases, yet still prevents undesirable penetration of sample solution into the electrolyte layer. The second development is a conceptual one, and reflects the purpose for which the new sensors have been developed. The carbon dioxide electrode is mainly used for estimation of the acid-base status of blood, which characterizes various respiratory and excretion disorders. This is done by measuring the equilibrium pCO_2 and pH values and relating them to a certain standard state of blood[10]. The new gas sensors, on the other hand, are used in quantitative analysis for certain species, and for that reason the measurement conditions (such as pH of the sample solution) are always adjusted so that the species to be determined are totally converted into a gas to be measured.

The most recent development in gas-sensing probes is the introduction of the

air-gap electrode[11]. The concept of this sensor is a logical continuation of the thoughts which led to the development of the previously mentioned new membrane materials. While the original carbon dioxide electrodes were furnished with a gas-permeable membrane made of silicone rubber or polyethylene, the newly developed membrane material, a microporous Teflon[1,9], is made in such a way that up to 60% of its area consists of narrow pores filled with air. Thus, the actual transport of gas from the sample to the inner electrolyte solution occurs through air rather than via solid material as was the case in the original membranes. The result is a much faster electrode response, as, according to Ross[1], the ratios of the *Dk* values between air and dimethylsilicone rubber are: O_2, $3.6 \cdot 10^4$; CO_2, $5.5 \cdot 10^3$; H_2S, $2.3 \cdot 10^3$; SO_2, $9.7 \cdot 10^2$; NO_2, $2.2 \cdot 10^3$; NH_3, $5.4 \cdot 10^3$ and H_2O, 26 (*D* is the diffusion coefficient and *k* is the partition coefficient of the gas between the membrane material and the aqueous sample).

The next factor influencing the speed of response, is the electrode geometry, described by the thicknesses of the electrolyte layer *l* and the membrane material *m* as well as by the effective electrode area *A*[1]. The latter two values are different from the actual membrane dimensions, as the effective open area (*ca.* 60%) and especially the tortuosity of the diffusion path prolong the time necessary for establishing the equilibrium. By removing the porous Teflon membrane entirely, these hindrances are avoided, but the electrode has to be situated above the sample solution, so that it becomes separated from it by an air gap[3,11-13]. Although the width of the air gap is larger (min. *ca.* 3 mm) than the thickness of the hydrophobic membrane, the speed of response of the air-gap electrode is faster, because (a) the diffusion of gas across the air gap is not hindered, (b) not only the aqueous sample, but also the air in the gap is mixed during measurement, and (c) the layer of electrolyte *l* is kept very thin. Other advantages of the air-gap electrode, such as the ready and easy renewability of the electrolyte layer (resulting in a rapid return of the signal to a baseline level and therefore in negligible hysteresis) and the indifference of the sensor towards surfactants, solvents and particulate matter present in the sample (the electrode never touches the sample solution) have been stressed previously[3,11-13].

In connection with the carbon dioxide measurements, however, another important feature of the air-gap construction has to be emphasized: the sample solution and the volume of the air (constituting the air gap) are contained in a chamber, hermetically closed during the measurements by the electrode body. This approach, which does not seem to be necessary in *e.g.* the case of ammonia measurements—where a dip-type sensor is immersed into a well-mixed sample solution, placed in an open beaker[1,5-7]—is imperative in carbon dioxide measurements, as otherwise a great deal of gas would escape from the sample long before equilibrium has been reached ($k_{NH_3} = 1.5 \cdot 10^{-3}$ while $k_{CO_2} = 1.2$ at 23°C). Thus the measurements of carbon dioxide carried out here stress the importance of this often neglected problem, which would also arise if NO_2 ($k = 22.4$), H_2S ($k = 0.42$) and perhaps also SO_2 ($k = 2.8 \cdot 10^{-2}$) were to be measured.

The practical utility of the air-gap carbon dioxide electrode has been tested on measurements of a very important water pollution parameter, namely the concentration of organic matter. Ecological concern has created a demand for fast and accurate measurements of this parameter. Two general approaches have been used in assessing the value.

The classical Biological Oxygen Demand (BOD) test is a standard five-day test. It relies on conversion of oxidizable matter to stable compounds by the biological activity present, and is determined by the amount of oxygen consumed. In the analogous 2-h Chemical Oxygen Demand (COD) test, the oxidation is performed by a powerful oxidizing agent, potassium dichromate. Because of the vastly different methods of oxidizing the organic matter, there is no inherent correlation between these two analyses.'

The second approach used to evaluate the degree of organic pollution is to determine the total organic carbon (TOC) content. This is one of the most frequently determined parameters in sea water; its measurement enables workers to estimate the amount of organic matter collectively contained in living organisms and detritus[14,15]. The determination is usually accomplished by wet chemical oxidation with potassium persulphate in acid solution after the sample has been freed of total inorganic carbon (TIC) by purging with nitrogen. The sample, contained in a sealed ampoule, is boiled under pressure[16] for 30 min; the carbon dioxide formed is then measured with an i.r.-analyzer. Analyzing an unpurged sample gives the total carbon (TC) content; thus the parameters are related according to:

$$TOC + TIC = TC \tag{1}$$

The TOC method has been compared with BOD and COD tests. Both these methods are affected by certain oxidizable inorganic compounds, while TOC is unaffected by the inorganics normally found in water. Furthermore, it is obvious that there can be no inherent correlation of TOC to either BOD or COD, although they often show the same trend[17]. Where wastes are relatively uniform, there is also a fairly constant correlation between TOC and BOD or between TOC and COD. Once the relationship between the parameters has been established, the TOC method is the fastest method and should be favoured for monitoring.

Based on the principle of wet chemical oxidation or dry combustion of the sample, many different commercial instruments have been marketed[18-20], all of which claim to measure quickly and precisely two of the interesting parameters, the third being obtained by difference; their main drawback is their high cost and complicated technical handling.

The purpose of the present work is to utilize the selectivity, simplicity and speed of response of a new gas sensor in this type of studies and thus introduce the air-gap electrode into the field of water analysis.

THEORY

Electrode sensitivity and choice of electrolyte

It has previously been shown[11] that the air-gap electrode responds to hydrogencarbonate concentrations according to the equation:

$$pH_e = -\log [HCO_3^-]_s + \log [HCO_3^-]_e + pH_s + \text{const.} \tag{2}$$

from which it follows, that the response of the electrode (pH_e) is a linear function of the logarithmic value of the hydrogencarbonate content of the sample, $[HCO_3^-]_s$, provided that the electrolyte concentration on the electrode surface, $[HCO_3^-]_e$, the pH of the sample solution, pH_s, and the conditions during a series of experiments

are kept constant (combined in the "const." term). Thus, in order to obtain optimal measuring conditions these parameters should be chosen in the most favourable way. The const. term in eqn. (2) comprises the influences of the geometry of the experimental set-up, the temperature, the ionic strength of the sample, and the atmospheric pressure[3]; thus, this term does not influence the slope of the calibration curve, but does affect its relative position. As to pH_s, there are two possibilities: the hydrogencarbonate ions in the sample can be either totally or partially converted to carbon dioxide. For a given concentration of hydrogencarbonate in the electrolyte, $[HCO_3^-]_e$, quantitative conversion, *i.e.*, a 99% or better liberation of the total latent gas content, is obtained at $pH_s \leqslant 4.4$ (Fig. 1A, shaded area), and a calibration curve encompassing the largest possible $[HCO_3^-]_s$ range will be obtained (Fig. 1B, curve c; $[HCO_3^-]_e = 10^{-2}$ *M*).

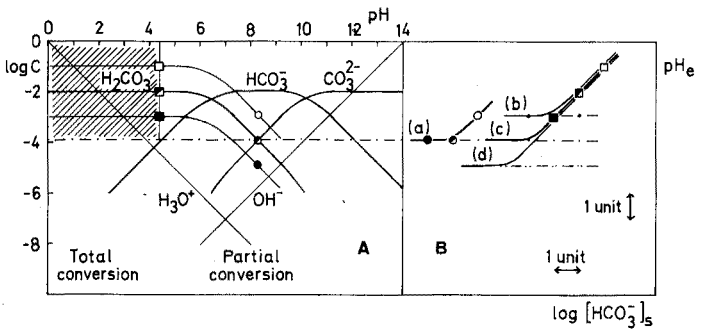

Fig. 1. (A) Logarithmic diagram (Hägg diagram) for the carbonate system: $pK_1 = 6.37$; $pK_2 = 10.25$. (B) Calibration curves for a carbon dioxide electrode with an electrolyte solution of $[HCO_3^-]$ of 10^{-2} *M*, operated by (a) the partial conversion method, and (c) the total conversion method. Curves (b) and (d) depict the calibration curves obtained by the total conversion method for electrolyte solution concentrations of 10^{-1} and 10^{-3} *M*, respectively.

Furthermore, in this region changes in pH_s will not affect pH_e. At higher pH_s values, partial conversion and thus lower sensitivity are obtained. This also requires a good buffering of the sample, since changes in pH_s within this range are directly reflected in pH_e. In almost neutral solutions the measuring range is further restricted (Fig. 1B, curve a; $[HCO_3^-]_e = 10^{-2}$ *M* and $pH_s = 8.3$). This is so not only because just a small fraction of the total carbonate content is volatilized as carbon dioxide, but also because on the electrode surface already a significant amount of CO_2 is present, originating from hydrolysis of the electrolyte (Fig. 1, point ◐). The hydrogencarbonate content of the electrolyte will thus influence the response of the electrode

In Fig. 1B calibration curves are shown for total conversion, the hydrogencarbonate concentration of the electrolyte solution being varied from 0.10 *M* (curve b) to 0.001 *M* (curve d). The part of the calibration curve near the sensitivity limit cannot be used in practice; only the linear part (one log-unit above the sensitivity limit) provides sufficient precision.

A more detailed evaluation of the range within which a carbon dioxide sensor (*e.g.*, the air-gap electrode) based on an electrolyte may be applicable, can be obtained from Fig. 2, which shows pH_e as a function of $\log [CO_2]_e$ for various selected values of electrolyte concentrations. As the principal equilibrium in the electrolyte solution, hopefully[1], is:

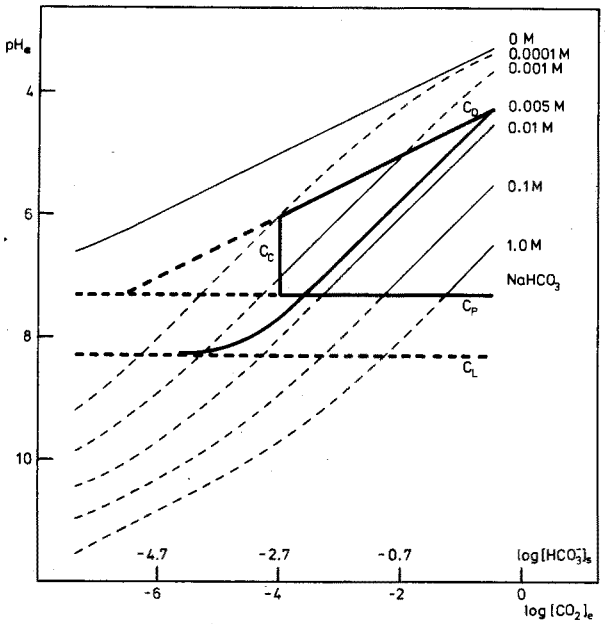

Fig. 2. Calculated CO_2-electrode response curves for various hydrogencarbonate electrolyte concentrations. The area confined by lines c_P, c_C and c_D denotes the region within which the electrode response will be Nernstian. For details, see text.

$$CO_2 + H_2O \rightleftharpoons HCO_3^- + H^+ \tag{3}$$

the glass indicator electrode will ideally yield a Nernstian response to changes in carbon dioxide. For the general case, however, the effect of carbonate formation ($HCO_3^- \rightleftharpoons H^+ + CO_3^{2-}$) must also be considered, as this can become important at low carbon dioxide levels. Additionally, the possibility of hydrogencarbonate increasing above its initial value at high concentrations (*cf.* sulphur dioxide measurements[12]) must be taken into account. The equilibrium equations are:

$$[CO_2] = [H^+] \cdot [HCO_3^-]/K_1 \tag{4}$$

$$[HCO_3^-] = [H^+] \cdot [CO_3^{2-}]/K_2 \tag{5}$$

$$[H^+] \cdot [OH^-] = K_W \tag{6}$$

If the concentration of the sodium hydrogencarbonate electrolyte solution is denoted as c, the electrical neutrality condition gives:

$$c + [H^+] = [HCO_3^-] + 2[CO_3^{2-}] + [OH^-] \tag{7}$$

Elimination of variables then yields $[H^+]$ as a function of $[CO_2]$. The computed values of this relationship (pH_e as a function of $\log [CO_2]_e$ for various values of c) are shown in Fig. 2. Depending on the value of c and $[CO_2]$, the slope (electrode sensitivity) will thus theoretically vary from a maximum of 1.0 to a minimum of 0.5 pH units per decade change in $[CO_2]$.

A condition for Nernstian response of the carbon dioxide sensor is, however,

that $[HCO_3^-]_e$ remains constant, which restriction imposes lower and upper limits for the measuring range. Theoretically, the sensitivity limit (c_L) is, for any value of c, given by the concentration of CO_2 originating from the electrolyte, *i.e.*, by $\log [CO_2]$ at pH 8.3. But the practical limit of sensitivity, c_p, is at best equal to $\log c_L + 1$ (Fig. 2, line c_p). The upper limit is given by the restriction that the $[HCO_3^-]$ generated by hydrolysis in the electrolyte layer by the CO_2 from the sample solution must be insignificant compared to the original hydrogen carbonate concentration of the electrolyte. This condition is illustrated graphically by line c_D in Fig. 2, the line being drawn 1 pH unit below the line corresponding to 0 *M* electrolyte concentration.

A further quite general restriction is imposed by the carbon dioxide content in the air; the CO_2 content of water in equilibrium with air is *ca.* $1–3 \cdot 10^{-5}$ *M*[21], so that a practical lower limit of measurable CO_2 is about 10^{-4} *M* (Fig. 2, line c_C). This limit may, however, increase if care is not taken with chemicals and solutions.

Thus, a Nernstian response of the carbon dioxide sensor will be obtained only over a fairly limited measuring range (confined by lines c_p, c_C and c_D). In practice, this is not a serious restriction, since concentrated samples may be diluted, and diluted samples preconcentrated as described below.

Figure 2 shows that an electrolyte solution 0.01–0.001 *M* in hydrogencarbonate will give a linear response over the greatest range; it was found most advantageous to use a 0.005 *M* solution. The actual calibration curve recorded for this electrolyte solution is incorporated in Fig. 2, *i.e.*, pH_e *vs.* $\log [HCO_3^-]_s$. With the measuring geometry used here, the $\log [CO_2]_e$ axis was experimentally found to be displaced 1.3 log units from the $\log [HCO_3^-]_s$ axis. This corresponds very well with the calculated value, computed on the basis of the *k*-value (1.2) and the ratio of the total sample solution volume to the gas volume (1 : 7.5).

Preconcentration of carbonate solutions

Among the different methods available for preconcentration, precipitation seemed the most suitable one for carbonate.

For quantitative precipitation of carbonate, the very slightly soluble lead carbonate was chosen; the solubility product is $3.3 \cdot 10^{-14}$ at 18°C[22]. Moreover, if the reaction is done in an alkaline medium, hydroxide will coprecipitate, forming lead hydroxocarbonate[23], thereby securing quantitative recovery. The equilibrium reaction:

$$3Pb^{2+} + 2OH^- + 2CO_3^{2-} \rightleftharpoons 2PbCO_3 \cdot Pb(OH)_2 \qquad (8)$$

is obviously pH-dependent; the hydroxide content must suffice for coprecipitation, but in too alkaline solutions the precipitate redissolves, owing to formation of $Pb(OH)_3^-$. Within a certain pH range, the recovery should be 100%.

The first prerequisite is that the hydroxide concentration should equal or exceed the carbonate concentration. This is fulfilled at various pH values as can be seen from Fig. 3A, which shows part of a Hägg diagram. Secondly, all hydrogencarbonate ions must be converted to carbonate ions (at least to 90%); this occurs for $pH \geqslant pK_2 + 1$, *i.e.* $pH \geqslant 11.25$, independent of total carbonate concentration. The higher of these two limiting pH values will determine the lower limit of pH, pH_l. For 10 m*M* CO_3^{2-}, it is 12.00; and for 1.0 and 0.10 m*M* CO_3^{2-}, it is 11.25. The upper limit, pH_u, determined by dissolution of lead hydroxide, depends on the amount of

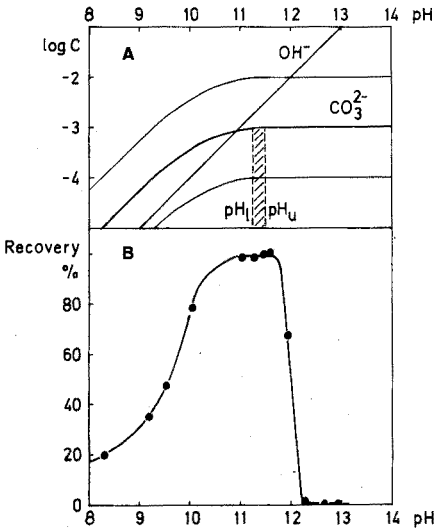

Fig. 3. (A) Part of a Hägg diagram for the carbonate system. The shaded area indicates the expected pH range for 100% recovery, when precipitating 10 ml of 10^{-3} *M* sample solution with 20 μmoles of Pb^{2+} ions. (B) The experimentally recorded recovery curve.

lead ions added. For the preconcentration of solutions maximally 1.0 m*M* with respect to carbonate, 20 μmoles of lead ions are added to 10 ml of sample. The upper limit is then $pH_u = 11.48$ (corresponding to 30 μmoles of hydroxide in the sample). Smaller carbonate contents give higher pH_u limits, *e.g.* $pH_u = 11.76$ for a 0.10 m*M* sample. In Fig. 3A the shaded area thus indicates the calculated pH range for quantitative precipitation.

When preconcentrating by means of precipitation, attention must be paid to possible interferences from other ions. In the final measurement, such ions have no effect because of the selective release of CO_2 from the sample; however, care should be taken that the content of those ions (mainly phosphate), which form less soluble lead complexes than carbonate, is low.

EXPERIMENTAL

Apparatus

The apparatus and the air-gap electrode have been described previously[3]. The microchamber, having a total volume of about 1 ml, was used throughout. The electrolyte layer on the surface of the glass electrode was renewed after each measurement, by letting the electrode rest on a Perspex holder containing a cone-shaped sponge, which was well soaked with the electrolyte solution and accommodated so that the glass electrode just touched its surface. When not in use, the electrode was similarly stored in the electrode holder.

Reagents

All solutions were prepared from analytical-reagent grade chemicals and demineralized, freshly redistilled water.

The electrolyte solution was $5.0 \cdot 10^{-3}$ *M* $NaHCO_3$, containing $5.0 \cdot 10^{-2}$ *M* NaCl (saturated with AgCl) as a reference solution and 0.1% wetting agent. Standard solutions in the range 0.10–1000 m*M* sodium hydrogencarbonate were prepared. Two acid solutions, 1.0 *M* sodium hydrogensulphate and 0.10 *M* hydrochloric acid, respectively, and an alkaline solution, 0.10 *M* sodium hydroxide, were prepared, the latter being carefully protected against CO_2 in the air.

Water samples

The analyses for TIC were performed on waste waters and lake waters within 1 day after collection. Analysis of the oxidized samples for TOC and TC could be made at a later time, provided that the samples were stored at 4°C.

Wet chemical oxidation of water samples

Mix 10.0 ml of water sample with 15.0 ml of oxidation solution (0.025 *M* potassium persulphate–0.075 *M* sodium hydroxide) in a stoppered glass bottle. Boil the mixture under pressure for 30 min. Determine the total carbonate content of this mixture to obtain a value of TC. Obtain the TOC value by oxidation of 10.0 ml of sample, which has been pretreated by acidification with hydrochloric acid and then purged with nitrogen under heating to remove CO_2.

Measuring technique for carbon dioxide

Pipette an aliquot (100 μl) of sample solution into the microchamber containing a Teflon-covered magnetic stirring bar. Acidify the sample with 100 μl of 1.0 *M* sodium hydrogensulphate. Immediately close the chamber by the body of the air-gap electrode, and start the magnetic stirrer. Take readings of the electrode, pH_e, when equilibrium has been reached, within 1–2 min, and read to 0.001 pH.

Preconcentration technique

Adjust 10.0 ml of sample, containing at most 1.0 m*M* total carbonate, to *ca.* pH 11.3 (indicator: alizarin yellow R, aqueous 0.01% (w/v) solution) by addition of 0.10 *M* sodium hydroxide or 0.10 *M* hydrochloric acid. Add 200 μl of 0.10 *M* lead nitrate solution to the agitated sample, and collect the precipitate formed on a Millipore filter (cellulose acetate no. EAWP 01300, 13 mm diameter, 1.0 μm pore size) placed in a Millipore Analytical 13-mm filter holder. For measuring, place the filter paper upside down on the bottom of the microchamber, and add the stirring bar. Dissolve the precipitate and expel the CO_2 by adding 200 μl of 1.0 *M* sodium hydrogensulphate. The electrode response reaches a stable value within 2–3 min. This technique yields a preconcentration of 100 times. Samples in the range 1–5 m*M* total carbonate were preconcentrated $10 \cdot a$ times ($10 \cdot a = 100$–20) by taking *a* ml of sample and $10 - a$ ml of water.

RESULTS AND DISCUSSION

Electrode standardization

In choosing an appropriate electrolyte for a series of measurements, a compromise has to be made between fast time response at low sample concentrations and linearity at high concentrations. An electrolyte, $5 \cdot 10^{-3}$ *M* in hydrogencarbonate

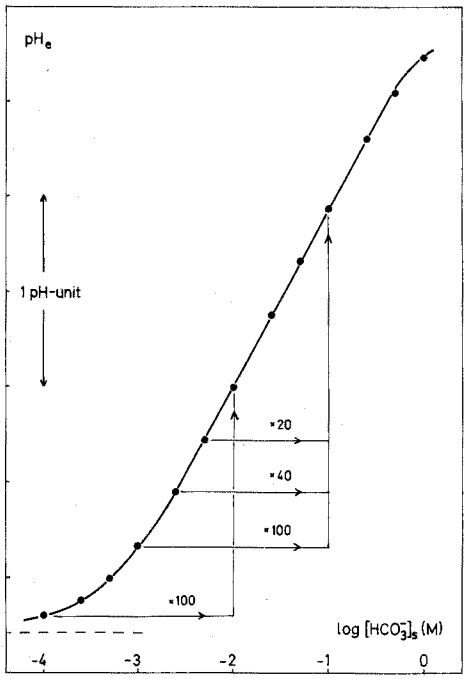

Fig. 4. Calibration curve recorded with standards of sodium hydrogencarbonate. The figure also indicates the preconcentration of samples in the range 0.1–5.0 m*M*.

proved to be most suitable. A higher electrolyte concentration ($5 \cdot 10^{-2}$ *M*) resulted in a slower response time, while lower concentrations ($5 \cdot 10^{-4}$ *M*) gave a noisy signal. The calibration curve at 23°C obtained for standard samples in the range 0.10–1000 m*M* hydrogencarbonate is shown in Fig. 4; each point represents the mean value of three determinations. The curve is linear between 2 and 500 m*M* HCO_3^-, with a regression line:

$$pH_e = a \cdot \log [HCO_3^-]_s + \text{const.} \quad (9)$$

where the slope $a = -0.9222$. The correlation coefficient is 0.9998 and the standard deviation around the line is 0.0126 pH-units, corresponding to 2.9 %. The non-linearity at high concentrations is due to slightly incomplete conversion with the acid used; discrepancies at low concentrations are due to the inherent lower sensitivity limit (see Theory). The calibration curve can be used with sufficient precision only within the linear range. Thus, in order to extend the optimal range of the CO_2 electrode, a preconcentration technique must be applied.

Preconcentration

The preconcentration of carbonate was achieved by precipitation with lead(II) ions. The reaction is, however, quite pH-dependent. Therefore the recovery of coprecipitation as a function of pH was investigated: 10-ml samples, containing 10 μmoles of total carbonate and various amounts of hydroxide ions (thereby establishing the starting pH), were allowed to react with 20 μmoles of lead ions. The results

obtained, which are shown in Fig. 3B, compare well with the theoretical calculations (Fig. 3A). By choosing pH 11.3, almost quantitative recovery will be obtained for 10-ml samples containing at the most 10 μmoles of total carbonate. An indicator (*e.g.* alizarin yellow R) with a colour change in this range can be used for routine pH adjustment. A 100-fold preconcentration of standard samples (0.10, 0.25, 0.50 and 1.00 m*M*), performed as described above, confirmed the good recovery. After correction for the blank value, corresponding to 0.040 m*M* carbonate solution (from the ever-present CO_2 content of water and the minute carbonate content of the hydroxide added), the recovery was 98.6% with a relative standard deviation of 3.2% for 5 determinations. Standard samples, ranging from 1 to 5 m*M* hydrogencarbonate, were also analysed (preconcentrated 100 to 20 times) in order to investigate the consistency of results obtained by these two techniques. It can be concluded that samples more dilute than 2 m*M* should be preconcentrated, because of the non-linear calibration curve, whereas more concentrated solutions can be analysed directly.

Water analysis: TIC

The total inorganic carbon (TIC) content of waters is composed of dissolved carbon dioxide and hydrogencarbonate and carbonate ions. Without any sample pretreatment, the TIC of water samples thus can be determined directly (or after preconcentration).

Table I shows the results obtained for various samples, which were all evaluated from a linearized calibration curve. All samples were analysed for TIC directly, except the lake water sample, for which the comparative results shown were obtained by preconcentration.

TABLE I

THE TIC CONTENT OF VARIOUS WATER SAMPLES

Water sample	*TIC content Mean value of 6 determinations*		
	mM HCO_3^-	*mg C* l^{-1}	s_r %
Waste water, untreated	7.73	92.8	2.0
Waste water, after biological purification	5.98	71.8	2.1
Tap water	4.47	53.6	2.2
Lake water; directly	2.53	30.4	2.6
Lake water; preconcentrated · 40	2.54	30.5	2.3

An extensive investigation was further performed on two series of water samples: waste water and lake water. In order to study the carbon balance, all three parameters were determined. The TIC content was obtained as described above. The results are shown in Table II, where the stated TIC values as well as the TC and TOC values are the mean of three determinations.

Water analysis: TC and TOC

For the determination of the total carbon and the total organic carbon content

TABLE II

THE TIC, TOC AND TC CONTENTS OF VARIOUS WATER SAMPLES

Water sample	*Content in mg C l^{-1}*			
	TIC	*TOC*	*TIC+TOC*	*TC*
Waste water, untreated	170	170	340	341
Waste water, after biological purification	79	28	107	114
Waste water, after denitrification	51	43	94	99
Lake Esrum, inlet I	39	19	58	62
Lake Esrum, inlet II	48	13	61	67
Lake Esrum, outlet I	29	13	42	47

of waters, a wet oxidation method was applied, based on the oxidation by persulphate in alkaline solution according to the reaction:

$$C + 2S_2O_8^{2-} + 6OH^- \rightleftharpoons CO_3^{2-} + 4SO_4^{2-} + 3H_2O \quad (10)$$

The carbonate content of the oxidized solution was determined as described previously, either directly or after preconcentration. Testing of the method by a standard substance, sodium oxalate, showed an efficiency of 99.1%. Further measurements and calculations were then based on the assumption that all organic substances present in the water samples were oxidized to that same degree. This, however, remains to be investigated further, as a quantitative wet oxidation of low concentrations of organic matter is difficult to achieve[15].

Table II shows the results on TC and TOC for some different water samples. While the waste water samples as a rule could be analysed without application of the preconcentration technique, this was obviously not the case for the less polluted lake waters. The Table also contains the calculated value of TIC+TOC, which theoretically should be equal to TC. The lower value of the sum, which has been observed also by other methods[24], is probably caused by the loss of volatile organic compounds in purging the acidified sample, before the TOC analysis.

CONCLUSION

The successful development of the method for TIC determination and the results obtained in TOC measurements confirm the usefulness of the air-gap electrode for this type of water pollution study, and indicate that this sensor might find useful applications also in other assays, where CO_2 can be released by or from the species to be determined. The very good reproducibility is due to the well established measurement conditions, which not only involve properly chosen chemistry of the sample solutions and their pretreatment, but are also based on well defined geometry of measurement, both aqueous and gaseous phases being contained in a closed system during measurement. For these reasons, the present work can be regarded as a starting point for carbon balance studies by means of gas sensors, and as providing a reliable way of measuring gases, which are, like carbon dioxide, only slightly soluble in water. In this respect, a study should be undertaken to elucidate the effects of mixing speed,

sample volume, sample surface area and depth of immersion of a dip-type gas sensor (furnished with a gas-permeable membrane) on the reproducibility of the measurements. The data obtained should further be compared with similar data obtained in closed systems. As the Ostwald absorption coefficient in water decreases in the order $NH_3 > SO_2 > H_2S > CO_2 > NO_2$, it would be interesting to find at which point the use of open sample containers is still tolerable and when a hermetically closed sample container becomes a necessity.

The preconcentration technique based on coprecipitation is a simple way of adjusting the sample concentration to the optimal range of electrode performance. The good results obtained indicate that analysis of airborne particles retained on filters, analysis of spots in paper chromatography or rings obtained by the ring-oven technique, might be simplified by placing these samples directly into the microchamber of the air-gap electrode.

The authors wish to express their sincere thanks to J. P. Jørgensen of the Department of Sanitary Engineering, Technical University of Denmark, for introducing us to this analytical problem in water analysis. His help in providing water samples and his participation in critical discussions is gratefully acknowledged.

SUMMARY

The newly developed air-gap electrode has been used in water analysis for a study of the carbon balance in waste waters and lake waters. The total inorganic carbon (TIC) content is determined directly; the total carbon (TC) and the total organic carbon (TOC) content are determined after wet chemical oxidation of the sample, directly or after acidification, by an alkaline potassium persulphate solution. The resulting total carbonate content can be determined directly if the concentration exceeds 2 m*M*. In order to cover the range down to 0.1 m*M* total carbonate, a preconcentration technique was developed, based on precipitation of very slightly soluble lead carbonate in alkaline solution. The analysis can be done quickly and reliably in this way. The relative standard deviation is less than 3% and the method is highly selective, as only carbonate is sensed after selective release as CO_2 The peculiarities of carbon dioxide measurements with gas-sensing electrodes are indicated. Optimal measuring parameters for the air-gap carbon dioxide sensor are suggested.

REFERENCES

1 J. W. Ross, J. H. Riseman and J. A. Krueger, *IUPAC Selective Ion-Sensitive Electrodes, Cardiff, 1973*, Butterworths, London, 1973, p. 473.
2 H. F. Proelss and B. W. Wright, *Clin. Chem.*, 19 (1973) 1162.
3 E. H. Hansen and J. Růžička, *Anal. Chim. Acta*, 72 (1974) 353.
4 Orion Research Inc., *Instruction Manual for Ammonia Electrode Model 95-10*; Orion Research Inc., *Newslett.*, 5 (1973) 7.
5 M. L. Eagan and L. Dubois, *Anal. Chim. Acta*, 70 (1974) 157.
6 Orion Research Inc., *Analytical Methods Guide*, Massachusetts, U.S.A., 6th edn., 1973, p. 3.
7 Electronic Instruments Limited, *Leaflet No. 8002-2/3*, p. 1.
8 R. W. Stow, R. F. Baer and B. F. Randall, *Arch. Phys. Med. Rehabil.*, 38 (1957) 646.
9 A. Strickler and C. H. Beebe, *U. S. Patent No. 3, 649, 505*, Mar. 14, 1972.
10 O. Siggaard-Andersen, *The Acid–Base Status of Blood*, Munksgaard, Copenhagen, 1972, p. 30.

11 J. Růžička and E. H. Hansen, *Anal. Chim. Acta*, 69 (1974) 129.
12 E. H. Hansen, H. Bergamin Filho and J. Růžička, *Anal. Chim. Acta*, 71 (1974) 225.
13 J. Růžička, E. H. Hansen, P. Bisgaard and E. Reymann, *Anal. Chim. Acta*, 72 (1974) 215.
14 C. Copin-Montegut and G. Copin-Montegut, *Mar. Chem.*, 1 (1972) 151.
15 J. H. Sharp, *Mar. Chem.*, 1 (1973) 211.
16 D. W. Menzel and R. F. Vaccaro, *Limnol. Oceanog.*, 9 (1964) 138.
17 Beckman Instruments Inc., *Application Data, No. 4375.*
18 Beckman Instruments Inc., *Bulletin No. 4082-A.*
19 Dohrmann Division, *Manual for Total Organic Carbon Analyzer, Model DC-50*, Envirotech Corporation.
20 Oceanography International Corporation, *Manual for Total Carbon System.*
21 *Gmelin Handbuch der anorganischen Chemie*, 8. Auflage 1973, *Kohlenstoff*, Teil C3, pp. 42, 43.
22 *Handbook of Chemistry and Physics*, 50th Edn., Chemical Rubber Co., 1970, p. 252.
23 G. Hägg, *Allmän och Oorganisk Kemi*, AWE, Sweden, p. 590–592.
24 C. E. Van Hall and V. A. Stenger, *Anal. Chem.*, 39 (1967) 503.

Analytica Chimica Acta, 74 (1975) 437–440

SHORT COMMUNICATION

Application de la spectrométrie par réflexion totale atténuée dans l'infrarouge et de la spectrométrie dans le visible a l'étude des residus d'antigerminatifs (propham et chlorpropham) sur les tubercules de pommes de terre

A. COPIN et P. H. MARTENS

Laboratoire de Chimie Analytique

R. KETTMANN, J. L. CLOSSET et C. DUCULOT

Laboratoire de Physique et de Chimie physique, Faculté des Sciences Agronomiques de l'Etat, 5800 Gembloux (Belgium)

(Reçu le 8 juillet 1974)

Comme Kettmann *et al.*[1] l'ont déjà signalé, la polarographie, la chromatographie en phase gazeuse et la spectrométrie visible sont essentiellement des méthodes de dosage. Leur efficacité quant à l'identification du produit à doser est beaucoup plus aléatoire.

Les faibles quantités de substances inconnues mises en oeuvre lors d'une analyse de résidus de pesticides (de l'ordre du microgramme) obligent à recourir aux microtechniques d'identification. Nous avons choisi la spectrométrie par réflexion totale atténuée multiple dans l'infrarouge (Multi-ATR ou M-ATR).

L'application de cette technique requiert parfois une rigoureuse purification de l'extrait végétal[1–2]. Dans cette étude, au contraire, nous abordons un cas où l'identification des composantes d'un mélange de pesticides n'est précédée d'aucune purification.

Partie expérimentale

L'enregistrement des spectres infrarouges est réalisé au moyen du spectrophotomètre Leitz III G à réseaux équipé d'un accessoire "Multi-ATR-Leitz" permettant de réaliser treize réflexions dans un cristal de KRS-5.

Un spectrophotomètre Zeiss PMQ II est utilisé pour les analyses dans la région visible du spectre.

Mode et doses d'application des antigerminatifs. L'essai a été réalisé sur des tubercules de pomme de terre (*Solanum Tuberosum L.*) de la variété alpha. Sur un premier lot de celles-ci on a appliqué une première formule poudreuse (formulation A) contenant 0,07% de Propham (isopropyl-N-phénylcarbamate, ou IPC) et 1,27% de Chlorpropham (isopropyl-N-3-chlorophénylcarbamate, ou CIPC).

À un deuxième lot on a appliqué par poudrage une seconde formulation (formulation B) à base de 0,98% de Propham (IPC) et de 1,32% de Chlorpropham (CIPC). Le dosage de la formule pulvérulente est conforme aux spécifications commerciales, à savoir 150 g de produit formulé par 100 kg de pommes de terre.

Un troisième lot n'ayant subi aucune application d'antigerminatifs sert de témoin.

Avant d'être soumis à l'analyse, les tubercules sont conservés pendant un mois à basse température (8 à 10°C) et à l'obscurité.

Au laboratoire les échantillons sont soigneusement lavés puis pelés; les parties (pelures et tubercules pelés) ont été pesées, puis découpées. Chaque prélèvement de 100 g est soumis pendant 2 h à une agitation mécanique en présence de 200 ml d'éther de pétrole (40–60°C) et de 50 g environ de sulfate sodique anhydre; après 12 h de repos, on récupère par filtration la couche d'éther de pétrole.

L'analyse spectrophotométrique par multi-ATR

Mode opératoire. Une aliquote, 30 ml de l'extrait de pelure, est évaporée jusqu'à environ 100 µl. Ceux-ci sont transférés quantitativement sur le cristal de

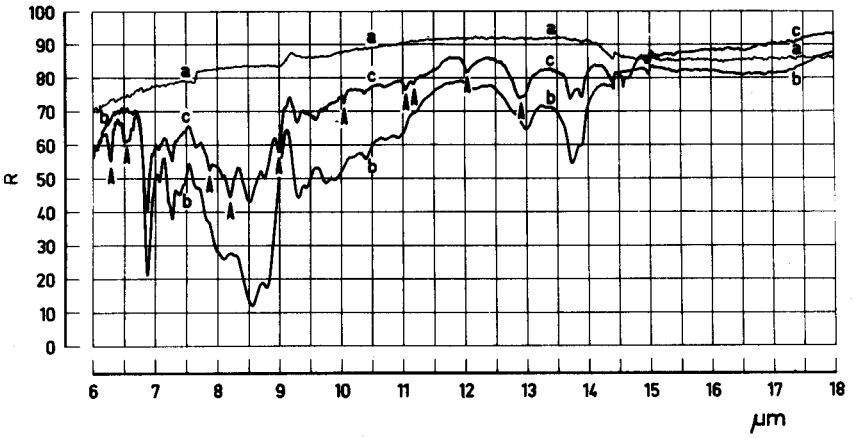

Fig. 1. Spectrométrie par réflexion totale atténuée multiple dans l'infrarouge du chlorpropham (formulation A) sur pelures de pommes de terre: (a) spectre du cristal de KRS-5; (b) spectre de l'extrait pelure témoin; (c) spectre de l'extrait pelure traité.

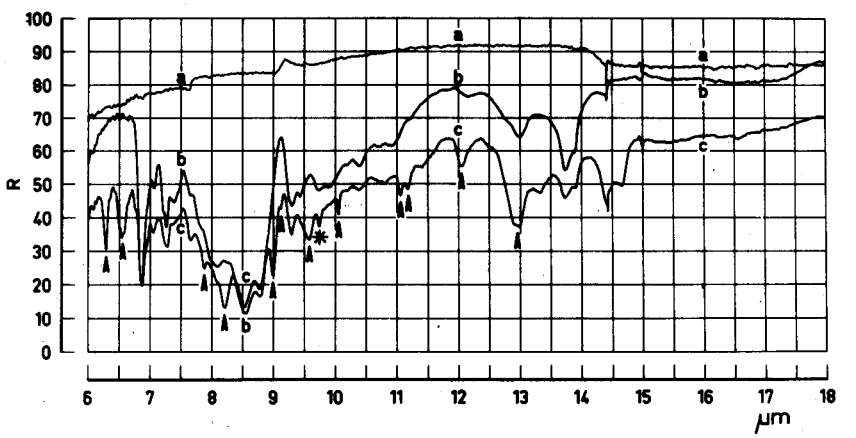

Fig. 2. Spectrométrie par réflexion totale atténuée multiple dans l'infrarouge du mélange propham–chlorpropham (formulation B) sur pelures de pommes de terre: (a) spectre du cristal de KRS-5; (b) spectre de l'extrait pelure témoin; (c) spectre de l'extrait pelure traité.

KRS-5 maintenu à basse température par réfrigération de son support. Après évaporation du solvant, l'enregistrement du spectre s'effectue à la vitesse de 0,48 min μm^{-1}. Nous obtenons ainsi les spectres repris dans les Figs. 1 et 2.

Résultats. Les bandes d'absorption des antigerminatifs sont annotées par un flèche. La présence d'IPC dans le mélange est mise en évidence par son absorption propre à 9,75 μm. Elle ne se remarque que pour la formulation B où la concentration en IPC atteint une valeur proche de celle du CIPC. Elle est indiquée dans le spectre (c) de la Fig. 2 par *. Une manipulation identique sur une aliquote de 100 ml de l'extrait pulpe de l'échantillon traité donne un spectre identique à celui de l'échantillon non traité.

L'analyse spectrophotométrique dans le visible

Mode opératoire. Après l'évaporation du solvant d'une aliquote de l'extrait, l'IPC et (ou) le CIPC subissent une hydrolyse alcaline en aniline et (ou) chloraniline. Celles-ci sont distillées et recueillies dans l'acide chlorhydrique. Après diazotation par le nitrite sodique, l'aniline est copulée au moyen du naphtyléthylénediamine[3]. L'intensité de la coloration est mesurée à 540 nm sans possibilité de distinction entre la coloration provenant de l'aniline et celle de la chloraniline.

TABLEAU I

RÉSULTATS DE CIPC

Poudrage	*Pelure*[a] *(p.p.m.)*	*Chair (p.p.m.)*
Formulation A	4,6	*[b]
Formulation B	14,3	0,2

[a] Moyenne de deux dosages.
[b] Non décelé c.à.d. inférieur à 0,1 p.p.m.

Résultats. Les résultats exprimés en parts par million (p.p.m.) de CIPC sont repris dans le Tableau 1.

Discussion

Les spectres de l'IPC et du CIPC repris dans les Figs. 1 et 2 correspondent aux spectres de référence retrouvés dans la littérature[4].

La spectrophotométrie dans le visible dose le radical amine aromatique primaire; une distinction entre la chloraniline et l'aniline est impossible; les spectres d'absorption des dérivés formés étant trop semblables. La valeur donnée représente un résultat global exprimé en l'une des deux matières.

Par contre, la bande située dans la région infrarouge du spectre, à la longueur d'onde de 9,75 μm permet de déceler l'IPC en mélange avec le CIPC. On a pu montrer par la technique de l'enrichissement des extraits témoins qu'il est possible de mettre en évidence des doses n'excédant pas 0,5 p.p.m. en l'un ou l'autre des deux antigerminatifs aussi bien dans la pulpe que dans la pelure[5].

Les bandes d'absorption de l'extrait végétal masquent peu celles des deux antigerminatifs. La purification de l'extrait s'avère dès lors superflue.

Les auteurs ont grandement apprécié l'aide technique apportée par Mrs. M. Cus, J. Delmarcelle, E. Massaux et M. Yernaux.

REFERENCES

1 R. Kettmann, J.-L. Closset, A. Copin, C. Duculot et P. H. Martens, *Anal. Lett.*, 6 (1973) 1013.
2 R. Kettmann, J.-L. Closset, A. Copin, C. Duculot et P. H. Martens, *C.R. Acad. Sci. Paris*, 277 (1973) 967.
3 L. N. Gard et C. E. Ferguson dans G. Zweig (Éd.), *Analytical Methods for Pesticides, Plant Growth Regulators and Food Additives*, Vol. IV, Academic Press, New York, London, 1964, p. 49–65.
4 J. Y. T. Chen et W. R. Benson, *J. Ass. Off. Agr. Chem.*, 49 (1966) 417.
5 R. Kettmann, Étude non publiée, Faculté des Sciences Agronomiques de l'État, Gembloux, 1973.

Analytica Chimica Acta, 74 (1975) 441–445

SHORT COMMUNICATION

Spectrophotometric determination of selenium(IV) with diaminochrysazine

R. S. BROWN
Department of Chemistry, University of Guelph, Guelph (Canada)
(Received 6th August 1973)

It has been shown[1] that selenium reacts with the organic reagent 1,1′-dianthrimide; the color of the selenium–1,1′-dianthrimide complex was developed in concentrated sulfuric acid by heating. Further investigation[2] indicated that by varying the concentrations of reactants, it was possible to form either a 1:1 or a 2:1 selenium(IV)–1,1′-dianthrimide complex. Similar investigations[3] with 2,2′-dianthrimide showed that with this reagent selenium(IV) formed a 1:1 complex and a dimer of this complex. Diaminochrysazine (4,5-diamino-1,8-dihydroxy-anthraquinone) has an amine group adjacent to the quinone oxygen and might be expected to react with selenium(IV) in a manner similar to the dianthrimides. The present communication describes a spectrophotometric study of the complex formation between diaminochrysazine and selenium(IV) in a concentration range of analytical interest.

Experimental

Equipment. Absorbance measurements were made with a Bausch and Lomb Spectronic 505 recording spectrophotometer. The silica cells used had path lengths of 0.1, 0.5, 1.0, and 5.0 cm. For all except the 5-cm cells, the cell compartment of the instrument contained a jacket through which water, maintained thermostatically at 25°C, was circulated. For the 5-cm cells, the room temperature was constant at 22°C.

All glassware used for storage of acidic solutions was Corning alkali-resistant ("boron-free") glass No. 7280. Solutions for heating were contained in 50-ml Pyrex bottles with standard taper stoppers. The solutions were heated in thermostatically controlled drying ovens.

Reagents and standard solutions. Diaminochrysazine ("Boran"; Lamotte Chemical Products Co.) and selenious acid (Specpure, Johnson Matthey and Co. Ltd.) were used. The concentrated sulfuric acid and the fuming sulfuric acid were reagent grade.

The standard solutions ($1 \cdot 10^{-3}$ *M*) were prepared by weighing the required amounts of selenious acid or diaminochrysazine and dissolving in sulfuric acid. On ageing for a few days, the selenious acid solutions acquired a slight yellow color. The solutions of diaminochrysazine are somewhat light-sensitive and should be stored away from light if they are to be retained over a period of months.

For both the reactants, solutions of other concentrations were prepared by dilution of the standard solutions with sulfuric acid.

After preliminary experiments, the concentration of the sulfuric acid was always 99.8–100.0%. This concentration was obtained by mixing 95–97% acid with 20% fuming sulfuric acid. The exact concentration was determined by titration with alkali solution.

Results and discussion

Concentration of sulfuric acid, heating time, heating temperature. It was found that selenious acid reacts with diaminochrysazine at room temperature when the reactants are dissolved in 100% sulfuric acid and have stood for about ten days. The reaction was much faster on heating, but heating at temperatures over 100°C resulted in some destruction of the diaminochrysazine and a general darkening of the solution. When the temperature was held at 90°C, the color development was complete in 21 h. When the sulfuric acid concentration was reduced to 98%, full color development required at least 60 h at 90°C. Concentrations of sulfuric acid greater than 100.0% resulted in some destruction of the diaminochrysazine even on standing at room temperatures for a few weeks. The conditions adopted were solution in 99.8–100.0% sulfuric acid and heating for 21 h in a 90°C oven.

Absorption curves. Solutions of diaminochrysazine in 100% sulfuric acid which had been heated for 21 h at 90°C exhibited maximum absorbance around 440 nm and low absorbance above 550 nm. When solutions of selenium(IV) and diaminochrysazine reacted, the most prominent feature in the visible spectrum was a broad peak around 610 nm. This peak was present in all solutions at total concentrations in the range $3.3 \cdot 10^{-5}$–$1 \cdot 10^{-3}$ *M* except where the Se: diaminochrysazine ratio was either extremely large or extremely small. When the Se:diaminochrysazine ratio was 1, a much weaker peak appeared at 395 nm, and as the ratio became greater, this peak moved up to 410 nm. At a total concentration of $3.3 \cdot 10^{-5}$ *M* and a Se:diaminochrysazine ratio of 9, the peak at 610 nm disappeared although the absorbance still exceeded that of the blank. However, with a total concentration of $1 \cdot 10^{-3}$ *M*, even at a Se:diaminochrysazine ratio of 50, the peak at 610 nm was still stronger than the one at 410 nm. From these observations it is evident that there are different complexes formed in different concentration ranges, and in this respect the diaminochrysazine reacts with selenium(IV) in a similar manner to the reaction of selenium with the dianthrimides[2,3].

The continuous variations method. With diaminochrysazine (L) and selenium(IV) concentrations of $1 \cdot 10^{-3}$ *M*, the continuous variations curves were plotted for 610, 560, 525, 455, and 395 nm. The maximum at each wavelength was in the range 0.63–0.66 mole fraction of diaminochrysazine. The curves showed no inflections. Detailed curves were plotted for a series of solutions with mole fractions near zero and near one. Both sides were straight, and long extrapolations of each from the origin intersected at 0.66 mole fraction of diaminochrysazine. At this concentration only one complex was present; its simplest formula is SeL_2.

At a total concentration of $1 \cdot 10^{-4}$ *M*, the continuous variations curves gave a maximum around 0.66 mole fraction of diaminochrysazine when measured

at 610 and 455 nm, but the maximum at 410 nm was at 0.2 mole fraction of diaminochrysazine.

At a total concentration of $3.3 \cdot 10^{-5}$ *M*, the absorbances at 610 nm gave a maximum in the continuous variations curves at a mole fraction of 0.5. At 410 nm, the maximum occurred at 0.2 mole fraction of diaminochrysazine.

The mole ratio method. The mole ratio method was used with the Se:L ratio varying from 0.1:1.0 to 2.0:1.0. From the absorbance readings at 610 nm, the intersection point occurred at a mole ratio of 0.5:1.0. This result was obtained in each of three series in which the diaminochrysazine ligand concentration was $3.3 \cdot 10^{-4}$, $0.66 \cdot 10^{-4}$ and $3.3 \cdot 10^{-5}$ *M*. In each series, there was an isosbestic point close to 500 nm, the point occurring at a wavelength slightly above 500 nm in the most dilute of the three series.

When the ligand concentration was $1.66 \cdot 10^{-5}$ *M*, the point of intersection occurred at a mole ratio of 1:1. For the spectra of this series the isosbestic point was at 515 nm but the spectra of solutions with selenium in excess of the diaminochrysazine did not go through the isosbestic point.

The straight-line method. The straight-line method of Asmus[4] as modified by Klausen and Langmyhr[5] was used with diaminochrysazine in excess and constant to determine the selenium index. These conditions are essentially the same as the starting concentrations for the mole ratio method, and data from this method may be used. The following concentrations and ranges were used: the diaminochrysazine was held constant at $6.6 \cdot 10^{-4}$ *M*, $1.33 \cdot 10^{-4}$ *M* or $1.66 \cdot 10^{-5}$ *M* while the selenium concentration was varied in the ranges $1.67 \cdot 10^{-4}$–$3.3 \cdot 10^{-4}$ *M*, $0.33 \cdot 10^{-4}$–$0.66 \cdot 10^{-4}$ *M*, or $0.16 \cdot 10^{-5}$–$1.66 \cdot 10^{-5}$ *M*, respectively. The absorbances were measured at 610 nm. In all cases the straight line obtained indicated the selenium index as 1.

When selenium was in excess, a peak at about 400 nm appeared. When the straight-line method was applied with selenium in excess and constant, and with varying concentrations of diaminochrysazine, the results were as shown in Table I.

TABLE I

THE STRAIGHT-LINE METHOD WITH SELENIUM IN EXCESS

Se·concn. ($\cdot 10^{-4}$ *M*)	*Diaminochrysazine concn.* ($\cdot 10^{-4}$ *M*)	*Diaminochrysazine index*	
		610 nm	*400 nm*
6.6	6.6–3.3	2	2
1.33	0.66–0.33	1	1
0.80	0.66–0.33	1	1
0.166	0.066–0.022	1	1

Stability constants. Of the two complexes which are indicated by the continuous variations and the mole ratio methods, SeL_2 is the only one present when the ligand is in excess, and is $3 \cdot 10^{-4}$ *M* or greater. To obtain the stability constant for SeL_2, the method of Rose and Drago[6] was used. These authors developed an equation which can be used for 1:1 complexes, but they indicated

that similar equations could be derived for other stoichiometry. When their method was applied to the reaction

$$Se + 2L \rightleftharpoons SeL_2$$

the following equation was derived

$$\frac{1}{K} = \frac{c_{Se}\, c_B^2(\varepsilon_C - 2\varepsilon_B)}{A - A_0} - 4c_B\, c_{Se} - c_B^2 + \frac{4(A - A_0)(c_{Se} + c_B)}{\varepsilon_C - 2\varepsilon_B} - 4\left(\frac{A - A_0}{\varepsilon_C - 2\varepsilon_B}\right)^2$$

where c_{Se} is the analytical concentration of selenium, c_B is the analytical concentration of diaminochrysazine, A is the measured absorbance (1-cm path), A_0 is $\varepsilon_B c_B$, ε_C is molar absorptivity of the complex, and ε_B is molar absorptivity of the diaminochrysazine.

The value of ε_C is not known but its approximate value may be obtained from the maximum absorbance on the mole ratio plots where it is assumed that all the available diaminochrysazine has been converted to complex. By substituting chosen values of ε_C into the equation and solving for $1/K$, a plot can be made of ε_C *vs.* $1/K$ which is treated as a straight line over a small range of ε_C. This treatment was applied to a set of six solutions, in all of which the diaminochrysazine concentration was constant at $6.6 \cdot 10^{-4}$ *M*. The selenium concentrations ranged from $1.66 \cdot 10^{-4}$ to $3.3 \cdot 10^{-4}$ *M*. The resulting intersections of the lines led to a value of $1/K$ of $0.57 \cdot 10^{-8}$ ($s = 0.12 \cdot 10^{-8}$). Thus the stability constant is $1.75 \cdot 10^{8}$ ($s = 0.37 \cdot 10^{8}$). The value of ε_C obtained is $2.20 \cdot 10^{4}$ ($s = 0.027 \cdot 10^{4}$).

TABLE II

STABILITY CONSTANT OF THE COMPLEX SeL_2

Solution	*Ligand*[a] *concentration* ($\cdot 10^{-4}$ *M*)	*Absorbance*[b] *at 610 nm*	*Stability constant* ($\cdot 10^{8}$)
1	5.66	0.339	1.25
2	6.00	0.354	1.46
3	6.66	0.368	1.60
4	7.33	0.378	1.81
5	8.00	0.382	1.66

[a] Se concentration constant at $2 \cdot 10^{-4}$ *M*.
[b] Solutions were read in 0.1-cm cells and values have been corrected for the blank from diaminochrysazine.

Method II of Holme and Langmyhr[7] can be used for complexes of the type A_mB_n to obtain the ratio m/n. When the method was used with diaminochrysazine in excess and varied, the changes in absorbance were small and there was some uncertainty in deciding on the best straight line. If m/n is known, the method can be used to calculate the stability constant by the use of Holme and Langmyhr's equation. With $m/n = 0.5$, results of one set of solutions are shown in Table II. The value of E_0 was 0.395. The average of K was $1.56 \cdot 10^{8}$ ($s = 0.21 \cdot 10^{8}$). This result is in reasonable agreement with the value obtained by the method of Rose and Drago. When the total concentration was $3.3 \cdot 10^{-5}$ *M* or lower, the complex indicated by the continuous variations and mole ratio methods was SeL.

While the maximal absorbance was still a broad peak around 610 nm, the isosbestic point for the mole ratio method was moved to about 515 nm.

To obtain a value for ε_C and the stability constant for the SeL complex, the original method of Rose and Drago[6] was used. A set of 6 solutions in which the ligand concentration varied from $2.66 \cdot 10^{-5}$ to $1.0 \cdot 10^{-5}$ M and the selenium concentration from $1.66 \cdot 10^{-5}$ to $0.44 \cdot 10^{-5}$ M, was used; selenium was never present in excess. The values obtained were $\varepsilon_C = 1.45 \cdot 10^4$ ($s = 0.06 \cdot 10^4$) and $K = 2.32 \cdot 10^5$ ($s = 0.39 \cdot 10^5$).

Attempts to obtain a solid complex. Attempts to isolate the SeL_2 compound as a solid were unsuccessful. With 1,1'-dianthrimide, Langmyhr and Myhrstad[2] used a 10:1 excess of selenium with a 0.25 M selenium solution; the 1:1 compound was formed. After heating for the usual period the solution was transferred slowly into a mixture of water and ice. The resulting precipitate, when washed, dried, and then redissolved in sulfuric acid, gave a spectrum which was identical with the spectrum identified as that of the 1:1 compound. With diaminochrysazine the use of a 10:1 excess of selenium at a concentration of 0.14 M, produced a spectrum which differed from that of the SeL_2 complex; the peak at 610 nm was missing and a weaker peak at about 525 nm formed. With the ligand and selenium in the ratio of 2:1 and a 0.14 M selenium concentration, the solution after heating gave the characteristic spectrum of SeL_2 with the major peak at 610 nm. When this concentrated solution was poured over ice, the precipitate recovered was the ligand only. Thus the compound SeL_2 is decomposed by water.

Calibration curve. To obtain a calibration curve, varying volumes of $1 \cdot 10^{-3}$ M selenium solution were measured into a series of 50-ml glass-stoppered bottles. Aliquots (5.00 ml) of $1 \cdot 10^{-3}$ M ligand solution were measured into each bottle and also into a bottle with no selenium solution. The final volume of solution in each bottle was brought to 15.0 ml by addition of 100% sulfuric acid. The bottles were heated at 90°C for 21 h. After cooling, the absorbances were measured at 610 nm against the blank solution. The calibration data showed that Beer's law was obeyed up to a selenium concentration of $1 \cdot 10^{-4}$ M (in the sulfuric acid solution, 4.3 p.p.m.).

The sensitivity[8] of the reaction calculated from the calibration data was 0.00068 μg Se cm^{-2} at 610 nm for absorbance $= 0.001$. This sensitivity is similar to that obtained with 1,1-dianthrimide[1] in 100% sulfuric acid. However, diaminochrysazine has the advantage over 1,1-dianthrimide in that Beer's law is followed up to a selenium concentration of $1 \cdot 10^{-4}$ M, while the 1,1-dianthrimide reaction deviates from Beer's law.

REFERENCES

1 F. J. Langmyhr and S. H. Omang, *Anal. Chim. Acta*, 23 (1960) 565.
2 F. J. Langmyhr and J. A. Myhrstad, *Anal. Chim. Acta*, 35 (1966) 212.
3 I. Dahl and F. J. Langmyhr, *Anal. Chim. Acta*, 35 (1966) 24.
4 E. Asmus, *Z. Anal. Chem.*, 178 (1960) 104.
5 K. S. Klausen and F. J. Langmyhr, *Anal. Chim. Acta*, 28 (1963) 501.
6 N. J. Rose and R. S. Drago, *J. Amer. Chem. Soc.*, 81 (1959) 6138.
7 A. Holme and F. J. Langmyhr, *Anal. Chim. Acta*, 36 (1966) 383.
8 E. B. Sandell, *Colorimetric Metal Analysis*, Interscience, New York, 3rd edn., 1959, p. 83.

Analytica Chimica Acta, 74 (1975) 446–448

SHORT COMMUNICATION

Response of the specific fluoride ion electrode in the presence of monofluorophosphate Ion

ALAN F. BERNDT
Chemistry Department, University of Missouri-St. Louis, St. Louis, Missouri 63121 (U.S.A.)
ROBERT I. STEARNS
Lorvic Corporation, St. Louis, Missouri 63134 (U.S.A.)
(Received 15th January 1974)

Spurious results were obtained with a specific fluoride ion electrode (Orion model 94-09A) in attempts to study the hydrolysis of the monofluorophosphate ion to orthophosphate and fluoride. The data indicated that the response of this electrode is affected by monofluorophosphate ion.

To test this hypothesis, solutions of ammonium monofluorophosphate monohydrate were prepared at various concentrations in a pH 5.9 acetate buffer at 27°C. The ammonium monofluorophosphate monohydrate used was purified by recrystallization from aqueous solution and was of sufficient purity to provide single crystal specimens for an x-ray crystal structure determination[1]. No evidence of a second phase was observed in the x-ray powder pattern.

Figure 1 illustrates the relationship between total concentration and potential for these solutions, as measured by the fluoride electrode with a saturated calomel electrode as the reference electrode. For comparison, the calibration curve for solutions of pure hydrofluoric acid in the same buffer is also illustrated. The curve for the monofluorophosphate solutions is parallel to the curve for fluoride solutions but is displaced to higher potentials. The slopes of these two curves indicate that both correspond to a one-electron transfer process.

If these data are interpreted to represent the actual fluoride concentrations in the solutions, then it must be concluded that the ammonium monofluorophosphate monohydrate contains 16 mole % fluoride impurity or is 16% hydrolyzed at all concentrations. The latter is impossible at equilibrium and the former is inconsistent with the x-ray observations.

Devonshire and Rowley[2] studied the first-order kinetics of the hydrolysis of monofluorophosphate ion to form fluoride and orthophosphate ions. The reaction is slow and the kinetics are pH-dependent. At pH 5.9 the half-life is several years. The monofluorophosphate ion could not have hydrolyzed to a measurable extent under the conditions of the experiment. Therefore, the above calculation (16% F^-) cannot be explained on the basis of slow hydrolysis.

It must be concluded that fluoride analysis by use of the specific fluoride ion electrode is unreliable in the presence of the monofluorophosphate ion.

Further experiments were performed with solutions of commercial sodium

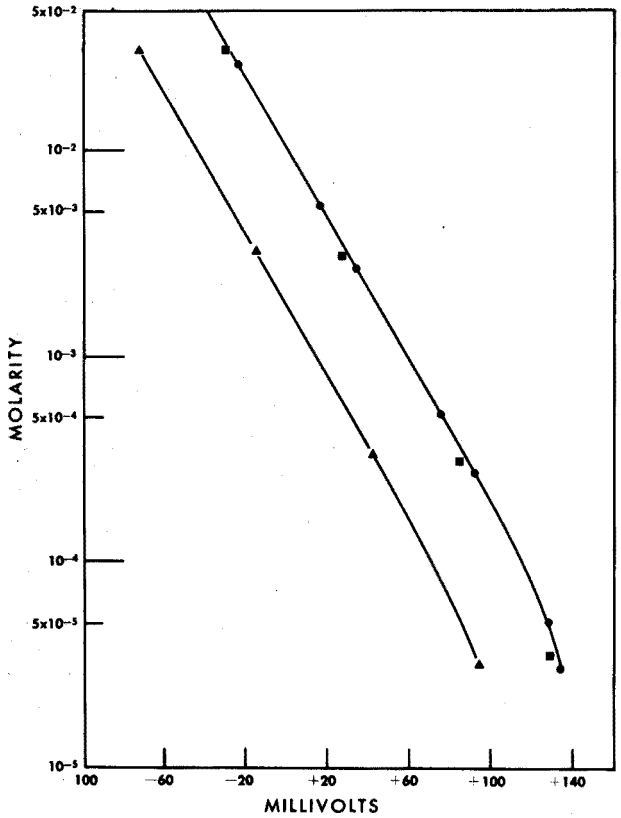

Fig. 1. Response of the specific fluoride ion electrode to solutions of monofluorophosphate ion and fluoride ion at pH 5.9. (●), $(NH_4)_2PO_3F \cdot H_2O$; (■), Na_2PO_3F; (▲), HF.

monofluorophosphate; the results are also illustrated in Fig. 1 and are seen to be consistent with those obtained with ammonium monofluorophosphate monohydrate.

Analysis of the sodium monofluorophosphate (Galbraith Labs, Knoxville, Tenn.) gave the following results: found, 32,12% Na, 21.30% P, 12.95% F; calculated for Na_2PO_3F, 31.94% Na, 21.52% P, 13.19% F. This analysis is inconsistent with the existence of 16 mole % fluoride impurity, although a much smaller amount could be present. In fact, since the data for sodium monofluorophosphate fall slightly below the curve for ammonium monofluorophosphate monohydrate it is suggested that the commercial salt contains some slight amount of fluoride.

Although there is no apparent theoretical reason to believe that monofluorophosphate should interfere with the specific fluoride ion electrode, the above results indicate the contrary. The reasons for this are perhaps a fruitful area of research, but it is suggested, that in the meantime, care be exercised in the use of the specific fluoride ion electrode in solutions where monofluorophosphate may be present.

One of us (A.F.B.) wishes to thank N.I.H. for financial support through grant DE 03143-03.

REFERENCES

1 A. F. Berndt and J. M. Sylvester, *Acta Crystallogr., Sect. B*, 28 (1972) 2191.
2 L. N. Devonshire and H. H. Rowley, *Inorg. Chem.*, 1 (1962) 680.

Analytica Chimica Acta, 74 (1975) 449–451

SHORT COMMUNICATION

Direct non-aqueous titration of N,N′-diacylhydrazines

S. EHRLICH-ROGOZINSKI and M. WILCHEK
Department of Biophysics, The Weizmann Institute of Science, Rehovoth (Israel)
(Received 16th May 1974)

Bis-acetylated hydrazines have come into increased use during the coupling of ligands to a solid support for the technique of affinity chromatography[1–3]. The determination of the bis-acylated hydrazines formed before the rearrangement to the peptide hydrazides in the "insertion method" of peptide synthesis[4–7] is also very useful. A direct method has been worked out to ascertain the purity of these compounds.

It is known that the monoacylhydrazide group loses its basic character on acylation[8]. Moreover, the nitrogen linked to the acyl group is weakly acidic and N,N′-diacylhydrazines dissolve in bases and are capable of forming salts[5,9]. Potentiometric titrations of bis-acylated hydrazines and α-amino-diacylhydrazine peptides give pK values from 9.5 to 10.7 (ref. 6), which confirms the postulated weakly acidic properties of this proton.

Indeed, titrations of a series of these compounds in dimethylformamide (DMF) with strong non-aqueous bases such as tetrabutylammonium hydroxide[10] or potassium tert-butoxide[11] in the presence of 2-nitrodiphenylamine as the indicator gave quantitative results.

Experimental

Apparatus. Automatic burets (10 ml) were equipped with 1-l reservoirs and tubes to protect the contents from atmospheric carbon dioxide and water.

Reagents. The monoacylhydrazines were prepared by the hydrazinolysis of the corresponding methyl or ethyl esters. The 1,2-diacylhydrazines were prepared by acylation of the monohydrazines. Elemental analysis and thin-layer chromatography of the compounds showed that they were pure. Dimethylformamide, analytical grade, and tetrabutylammonium hydroxide (TBAH; 40% in water) were purchased from Fluka, Switzerland. For preparation of titrant (*ca.* 0.05 *M*), 55 ml of the aqueous TBAH was evaporated on an evaporator and then washed several times with tert-butanol to expel the vapors of water. The residual 20 ml was dissolved in 180 ml of tert-butanol; 400 ml of isopropanol and 400 ml of benzene were later added. The solution was standardized against benzoic acid in dimethylformamide solvent with *o*-nitroaniline as indicator. The indicators were *o*-nitroaniline and 2-nitrodiphenylamine used as 0.2% (w/v) solutions in benzene. All other reagents used were analytical grade.

Procedure. Introduce 50–150 μmoles of substance into a 50-ml Erlenmeyer flask and dissolve in 3 ml of dimethylformamide. Neutralize the DMF initially with the titrant to the color change of the indicator (yellow to red for *o*-nitroaniline, or yellow to violet for 2-nitrodiphenylamine). Titrate to the end-point of the chosen indicator with the tip of the buret dipping into the solution. Protect the contents from atmospheric carbon dioxide by a Parafilm sheet.

Results and discussion

A series of hydrazine compounds was titrated as indicated; the results are presented in Table I. The dibenzoylhydrazine is very acidic, owing to the aromatic substitution, and could be titrated with a less basic titrant such as sodium methoxide in benzene–methanol[12]. The diacylhydrazine, which does not possess the aromatic ring, is less acidic and was quantitatively titrated only by the strong titrants. The strongly basic titrants were therefore used as a general method. Recoveries within the acceptable errors were obtained.

TABLE I

DETERMINATION OF N,N'-DIACYLHYDRAZINES

Compound	*Neutral equivalent*[a]		*Recovery (%)*
	Calculated	*Found*	
Ac–NHNHAc	116.1	118.8	97.7
		116.7	99.5
Bz–NHNHBz	240.3	238.6	100.7
		242.4	99.1
		239.9	100.2
Z–Cys(Bzl)NHNHAc	401.5	403.3	99.6
		383.0	104.8
		404.4	99.3
		398.4	100.8
Z–Ala–Leu–NHNHAc	392.5	375.1	104.6
		373.2	105.2
		388.0	101.2
Z–Lys(Z)–NHNHAc	470.5	473.6	99.3
		480.1	97.9
		462.7	101.7
		465.0	101.2
Biotin–NHNHCOCH$_2$Br	379.2	370.5	102.3
		368.3	103.0

[a] Mean value of two titrations performed with tetrabutylammonium hydroxide or potassium tert-butoxide using one of the indicators as given in the procedure. Ac, Acetyl; Z, carbobenzyloxy; Bz, benzoyl; Bzl, benzyl; Cys, cysteine; Ala, alanine; Leu, leucine; Lys, lysine.

The method presented here, together with the method for titration of monoacylhydrazines[13] can be used to follow peptide synthesis by the "insertion method"[5]. The monoacylhydrazides are first titrated as bases with perchloric acid in acetic acid[14]. After substitution with protected amino acids, the diacylhydrazine formed is titrated as an acid by the method presented here. After rearrangement, the newly

formed hydrazide is again titrated as a base. Thus the whole cycle of synthesis can be followed.

REFERENCES

1 M. Wilchek, *Proc. 9th Int. Cong. Biochemistry, Stockholm, 1973*, p. 9.
2 M. Wilchek and T. Miron, *Methods in Enzymology*, Vol. 34B, in press.
3 J. K. Inman and H. M. Dintzis, *Biochemistry*, 8 (1969) 4074.
4 M. Brenner and W. Hofer, *Helv. Chim. Acta*, 44 (215) (1961) 1794.
5 M. Brenner and W. Hofer, *Helv. Chim. Acta*, 44 (216) (1961) 1798.
6 R. Weber, W. Hofer, W. Heer and M. Brenner, *Helv. Chim. Acta*, 44 (267) (1961) 2154.
7 E. Schröder and K. Lübke, *The Peptides, Vol. 1*, Academic Press, New York, 1965, p. 128.
8 J. Kucharský and L. Safařik, *Titration in Nonaqueous Solvents*, Elsevier, Amsterdam, 1965, p. 199.
9 H. Paulsen and D. Stoye in J. Zabicky (Ed.), *The Chemistry of Amides*, Wiley–Interscience, London, 1970, p. 547.
10 J. Gyenes, *Titration in Nonaqueous Media*, Iliffe Books Ltd., London, 1967, p. 163.
11 S. Ehrlich-Rogozinski and H. R. Bosshard, *Anal. Chem.*, 45 (1973) 2436.
12 A. Patchornik and S. Ehrlich-Rogozinski, *Anal. Chem.*, 31 (1959) 985.
13 M. Fridkin and H. J. Goren, *Experientia* 26 (1970) 561.
14 J. S. Fritz, *Anal. Chem.*, 22 (1950) 578.

Analytica Chimica Acta, 74 (1975) 452–456

SHORT COMMUNICATION

Potassium nitrosodisulfonate as a reagent for oxidimetric titrations of inorganic cations in basic solutions

MARIO COSPITO
CAMEN, S. Piero a Grado, Pisa (Italy)
and GIORGIO RASPI
Istituto di Chimica Generale, Università di Siena, 53100-Siena (Italy) and Academia Navale, Livorno (Italy)
(Received 1st July 1974)

Potassium nitrosodisulfonate or Fremy's reagent[1] is widely used as a selective oxidizing agent for organic compounds. A comprehensive and detailed review of such applications in the field of organic chemistry has been recently published by Zimmer *et al.*[2].

The present work evaluates the analytical application of potassium nitrosodisulfonate as a reagent for the oxidimetric determination of some inorganic cations in slightly alkaline solutions in the presence of suitable complexing agents. Preliminary experiments indicate that it is possible to titrate iron(II), cobalt(II), manganese(II), tin(II), cerium(III) and uranium(IV), with potentiometric or biamperometric methods for end-point detection.

Experimental

Instrumentation. Potentiometric measurements were made with an Orion Research Ionalyzer, model 801, and smooth platinum wire and saturated calomel electrodes.

Two identical platinum spheres of surface area of about 0.05 cm^2, across which a constant voltage of 50 mV was applied, were used as indicating system for the biamperometric end-points.

All titrations were done at room temperature (22 ± 2°C).

Potassium nitrosodisulfonate. Potassium nitrosodisulfonate was prepared by electrochemical oxidation of basic solutions of potassium hydroxylamine disulfonate at a platinum anode. This is a well known method[3,4], but some simplifications are reported below. The procedure was as follows. Prepare potassium hydroxylamine disulfonate by bubbling sulfur dioxide gas through a mixture of potassium nitrite and potassium acetate (molar ratio 1:1.2) in ice water, following the method of Rollefson and Oldershaw[5]. Filter the precipitate and wash many times with ice water and then with purified methanol and ether. This material can be stored indefinitely at -5°C in a desiccator.

Prepare solutions of potassium nitrosodisulfonate by dissolving aliquots of potassium hydroxylamine disulfonate in concentrated borate buffer solutions, pH 9.8,

and placing the solutions obtained in a coulometric cell; as generator anode use a platinum foil of surface area about 40 cm^2, and as cathode use a platinum wire, separated from the solution to be oxidized by immersion in a glass tube closed by a sintered glass disk and filled to the level of the anolyte with the same borate buffer. Efficient stirring is provided by a magnetic stirrer.

Take aliquots containing about 3 g of potassium hydroxylamine disulfonate (m.w. 269.3), and apply a current intensity of 20 mA across the electrodes. If a total current efficiency of $\geq 95\%$ is assumed, a time of electrolysis of about 6 h suffices to obtain 0.2 l of *ca.* 0.02 *M* potassium nitrosodisulfonate solution.

The solutions obtained by this method always contained unoxidized potassium hydroxylamine disulfonate. The titre of these solutions was checked potentiometrically with a standard 0.02 *N* solution of vanadyl sulfate in the same buffer solutions[6] or by measurement of absorbance at 545 nm as suggested by Gehlen and Cermak[7].

The stability of solutions of potassium nitrosodisulfonate in concentrated borate buffer solution is satisfactory if they are stored at 0°C. The normality of a typical stock solution over a period of 3 weeks is given in Table I.

TABLE I

STABILITY OF STOCK SOLUTIONS OF POTASSIUM NITROSODISULFONATE IN BORATE BUFFER SOLUTION, pH 9.8, AT 0°C

Days of storage	0	7	14	21
Normality	$1.775 \cdot 10^{-2}$	$1.763 \cdot 10^{-2}$	$1.747 \cdot 10^{-2}$	$1.730 \cdot 10^{-2}$

For accurate work, daily standardization with vanadyl sulfate is recommended.

Other reagents. Borate buffer solutions were *ca.* 0.5 *M* in boric acid and 0.4 *M* in sodium hydroxide.

Carbonate–hydrogen carbonate buffer solutions were *ca.* 1 *M* in the respective potassium salts.

Tartrate solutions (2 *M*) were prepared from Seignette's salt and 1 *M* cyanide solutions from potassium cyanide.

Iron(II) solutions were prepared by dissolution of Mohr's salt in 0.025 *M* sulfuric acid and standardized with potassium permanganate.

Tin(II) solutions were prepared by dissolution of the chloride dihydrate in 1 *M* hydrochloric acid and standardized with cerium(IV) sulfate, with iron(III) as an intermediate.

Cerium(III) solutions were prepared by dissolution of the sulfate monohydrate in 0.025 *M* sulfuric acid and standardized by means of the silver-catalyzed peroxydisulfate oxidation to cerium(IV).

Uranium(IV) solutions were obtained by electrochemical reduction on a mercury pool of uranium(VI) sulfate solution in 0.05 *M* sulfuric acid, and standardized with potassium permanganate.

Cobalt(II) and manganese(II) solutions were obtained by dissolution of the respective sulfate salts, after ignition at 450°C, in 0.025 *M* sulfuric acid.

All chemicals used were of reagent grade.

Determination of iron(II), tin(II) and uranium(IV). Place 20–25 ml of borate buffer and 2 ml of 2 *M* tartrate solution in the titration cell. Deaerate completely by bubbling pure nitrogen. Add the solution of the cation to be determined, previously completely deaerated. Titrate with a standard solution of potassium nitrosodisulfonate, detecting the end-point by the potentiometric or biamperometric method.

Determination of cobalt(II). Place 20–25 ml of borate buffer and 2 ml of 1 *M* potassium cyanide solution in the titration cell. Deaerate thoroughly and proceed as described above, titrating with a deaerated standard solution of potassium nitrosodisulfonate.

Because of the ready oxidation of the cyanide complex of cobalt(II) by dissolved oxygen, cobalt(II) might be more conveniently determined by an indirect method as follows: place an excess of a standard solution of Fremy's reagent together with borate buffer and cyanide solutions in the titration cell, deaerate thoroughly, add the solution of cobalt(II) and titrate the excess of potassium nitrosodisulfonate with standard vanadyl sulfate.

Determination of manganese(II). Place 20–25 ml of 1 *M* sodium hydroxide and 2 ml of 2 *M* tartrate solution in the titration cell and proceed as described for iron(II), etc.

Determination of cerium(III). Place 20–25 ml of carbonate–hydrogencarbonate buffer solution in the titration cell and proceed as described for iron(II), etc.

Results and discussion

Potassium nitrosodisulfonate in solution can be represented by the structure $2K^+(SO_3^-)_2NO$. Because of its radical nature, this is a rather unstable compound which is generally very sensitive towards reduction. Alkaline solutions in the pH range 8–12 are the most stable but they also undergo decomposition[8,9]. The stability of solutions in carbonate–hydrogencarbonate[3] or in ammonia–ammonium chloride buffers is not great. Concentrated borate buffer solutions of Fremy's radical show adequate stability in the pH range 9.6–10.0, especially when stored at 0°C.

When potassium nitrosodisulfonate is used as an oxidant for the cations used, it is reduced to potassium hydroxylamine disulfonate, as checked by voltammetric investigation. The potential of the nitrosodisulfonate–hydroxylamine disulfonate couple in the pH range 9.6–10.0 is 0.24 V (*vs.* SCE)[10]; Fremy's reagent in alkaline solution is thus comparable in oxidizing power to potassium hexacyanoferrate(III).

Typical results of titrations are presented in Table II.

Tartrate ions were very effective as a complexing agent to keep the cations cited in an alkaline solution. Cyanide was chosen as complexing agent for cobalt(II) instead of tartrate because the cobalt(III) tartrate–cobalt(II) tartrate couple has a potential very close to that of the nitrosodisulfonate–hydroxylamine disulfonate couple in borate buffer medium, so that the potentiometric and biamperometric end-points were poorly defined.

Cerium(III) was oxidized very smoothly by potassium nitrosodisulfonate in

E II

ATIONS WITH POTASSIUM NITROSODISULFONATE

	Product	*Medium*[a]	*Taken (mmol)*	*Found*[b] *(mmol)*	*Fremy's reagent (equiv.) per mole reductant*	*Error (%)*	*End-point detection method*[c]
	Fe(III)	B,T	0.0540	0.0539	0.998	−0.2	P
			0.0540	0.0538	0.996	−0.4	BA
			0.1080	0.1080	1.000	0.0	P
			0.1080	0.1074	0.994	−0.5	BA
[d]	Co(III)	B,CN	0.0520	0.0512	0.985	−1.6	P
			0.1040	0.1028	0.988	−1.1	P
[e]	Co(III)	B,CN	0.0520	0.0523	1.006	+0.6	P
			0.0520	0.0520	1.000	0.0	BA
			0.1040	0.1038	0.998	−0.2	P
			0.1040	0.1041	1.001	+0.1	BA
)	Mn(III)	OH,T	0.0480	0.0485	1.010	+1.0	P
			0.0480	0.0482	1.004	+0.4	BA
			0.0672	0.0665	0.990	−1.0	P
			0.0672	0.0670	0.997	−0.3	BA
			0.0960	0.0950	0.990	−1.0	P
			0.0960	0.0952	0.992	−0.8	BA
	Sn(IV)	B,T	0.0190	0.0191	2.010	+0.5	P
			0.0190	0.0188	1.978	−1.0	BA
			0.0390	0.0389	1.994	−0.3	P
			0.0390	0.0390	2.000	0.0	BA
)	Ce(IV)	CH	0.0432	0.0432	1.000	0.0	P
			0.0432	0.0430	0.996	−0.5	BA
			0.0648	0.0652	1.006	+0.6	P
			0.0648	0.0650	1.003	+0.3	BA
			0.1080	0.1080	1.000	0.0	P
			0.1080	0.1079	0.999	−0.1	BA
	U(VI)	B,T	0.0196	0.0197	2.010	+0.5	P
			0.0196	0.0195	1.990	−0.5	BA
			0.0294	0.0298	2.028	+1.3	P
			0.0294	0.0296	2.014	+0.7	BA
			0.0490	0.0491	2.004	+0.2	P
			0.0490	0.0490	2.000	0.0	BA

ium: B, borate buffer; CH, carbonate–hydrogencarbonate buffer; OH, sodium hydroxide; T, tartrate; CN cyanide.
age of three determinations.
point detection: P, potentiometric; BA, biamperometric.
ct method.
ect method.

borate buffer and in presence of tartrate ions, but the resulting cerium(IV) oxidized tartrate; the carbonate–hydrogencarbonate buffer provided a suitable medium for this titration.

Titration of manganese(II) in borate buffer gave a poorly defined potentiometric curve and the biamperometric method also did not show the equivalence point correctly. A 1 *M* sodium hydroxide medium was chosen, although the use of potassium nitrosodisulfonate at so high a pH is not strictly correct owing to a

lack of stability[8]. However, because of the rapid reaction rate, the results were good.

The end-points were obtained from potentiometric curves and/or biamperometric plots. A few minutes sufficed for attainment of equilibrium near the equivalence point. The potential breaks observed for an addition of 0.1 ml of 0.02 *N* titrant solution around the equivalence point were about 650 mV for iron, manganese and tin, 400 mV for cobalt and uranium, and 200 mV for cerium.

The reversibility of the nitrosodisulfonate–hydroxylamine disulfonate system proved useful in the biamperometric method. The graphs obtained were V-shaped for titrations of iron, manganese and cerium, reverse L-shaped for titrations of tin and uranium, and L-shaped for the indirect titration of cobalt, where the reaction between nitrosodisulfonate and vanadyl ions was involved. In direct titrations of cobalt in the presence of cyanide, the biamperometric method was unsatisfactory.

We are grateful to the Consiglio Nazionale delle Ricerche of Italy for financial support (contract no. CT73.01082.03) to one of us (G.R.).

REFERENCES

1 E. Fremy, *Ann. Chim. Phys.*, 15 (1845) 408.
2 H. Zimmer, D. C. Lankin and S. W. Horgan, *Chem. Rev.*, 71 (1971) 229.
3 W. P. Wehrli and F. L. Pigott, *Inorg. Chem.*, 9 (1970) 2614.
4 W. R. T. Cottrell and J. Farrar, *J. Chem. Soc. A*, (1970) 1418.
5 G. K. Rollefson and C. E. Oldershaw, *J. Amer. Chem. Soc.*, 54 (1932) 977.
6 G. Raspi, A. Cinquantini and M. Cospito, unpublished data.
7 H. Gehlen and J. Cermak, *Z. Anorg. Allg. Chem.*, 275 (1954) 113.
8 J. H. Murib and D. M. Ritter, *J. Amer. Chem. Soc.*, 74 (1952) 3394.
9 B. J. Wilson and D. M. Ritter, *Inorg. Chem.*, 2 (1963) 974.
10 S. Aoyagui and F. Kato, *J. Electroanal. Chem. Interfacial Electrochem.*, 38 (1972) 243.

Analytica Chimica Acta, 74 (1975) 457–458

BOOK REVIEWS

B. Kakáč und Z. J. Vejdělek, *Handbuch der photometrischen Analyse organische Verbindungen*, Band 1 u. 2, Verlag Chemie, Weinheim/Bergstrasse, 1974. Band 1, viii+718 S, Band 2, vi+598 S, Ladenpreis DM320,—.

The authors present their information according to the compound class determined, arranged in the order found in Beilstein. The sole exceptions to this sequence are the last three chapters which deal with: saccharides and their compounds; amino acids, peptides and proteins; steroids and structurally related compounds. Each of the 18 chapters is divided into compound classes in a narrower sense (over 200 altogether), for which photometric methods are given; the selected methods are mostly based on reactions of known chemistry. A statement of the principle is followed by comments on selectivity with brief but adequate practical details of a suggested concrete procedure or procedures. The magnitude of the work is shown by the fact that papers by over 8000 authors on more than 6000 compounds are classified in 671 tables! Some typical examples of the collation of the vast amount of information are the determinations of phenols with diazonium salts (*ca.* 200 references), of oxo compounds with 2,4-dinitrophenylhydrazine (over 100), and of amino acids with ninhydrin (*ca.* 125). Those consulting the book will surely be delighted to find such exhaustive—and quite up-to-date—coverage. Valuable also are the three indexes at the end of the book (Vol. 2). In the index of some 500 reagents, each reagent entry is accompanied by a list of the compound classes determined with its help. This permits rapid assessment of the field of application and likely usefulness of any reaction. Indexes of all compounds determined and of authors are also provided.

The only real criticism is that values of molar absorptivities might have been given, where available; these would have helped in deciding between otherwise equally favourably sounding procedures.

Few errors were found, and then only of the type scarcely avoidable in a book of this size. "Tetrathiocyanokobaltat" on p. 77 ought to be "Tetrathiocyanatokobaltat"; "Perjodate" on p. 416 should be "Perjodide"; in the foreword, p. VI, an inadvertent "nicht" has led to the remarkable assertion of a "lack of not strictly specific reagents and colour reactions...". None of these errors is likely to mislead the reader, however.

Altogether, the impression is excellent and the handbook can be recommended for every organic–analytical laboratory. A final word for those readers whose German is perhaps not so strong; even they should have little difficulty in mastering the clearly displayed contents.

M. R. F. Ashworth (Saarbrücken)

Annual Reports on NMR Spectroscopy, Vol. 5B, Edited by E. F. Mooney, Academic Press, London, 1973, xi+441 pp., price £11.20.

Volume 5 in this series departs from previous practice in that it has been divided into two parts. Part A has been reviewed separately (*Anal. Chim. Acta*, 68 (1974) 250) and contains seven short reviews on various diverse aspects of n.m.r. spectroscopy. Part B consists of a single review by G. Mavel entitled *N.m.r. Studies of Phosphorus Compounds (1965–1969)*. This specialist review will probably appeal almost exclusively to those working in the area of phosphorus chemistry, and in view of the length of the article, this reviewer welcomes the editorial decision to publish it separately. The literature coverage appears to be very thorough and a large amount of data is presented in tabular form. A very useful formula index is also provided. Topics considered include ^{31}P, ^{1}H, ^{19}F, ^{13}C, and ^{11}B chemical shifts and coupling constants.

It is regrettable that it has taken until late 1973 for this review to be published. Considering that it only covers the literature until the end of 1969, one might reasonably conclude that it is now seriously out of date. It is unfortunate that this delay detracts somewhat from the utility of this otherwise excellent review.

W. B. Jennings (Birmingham)

ANALYTICA CHIMICA ACTA, VOL. 74 (1975)

AUTHOR INDEX

ANALYTICA CHIMICA ACTA, VOL. 74 (1975)

SUBJECT INDEX

Continued from page 4 of cover)

CONTENTS

(Continued on inside